Investigating the molecular mechanisms of meiotic recombination

A thesis submitted for the degree of Doctor of Philosophy in Biochemistry

Stephen Gray

MRC Genome Damage and Stability Centre

University of Sussex

September 2012

Declaration

I hereby declare that this thesis has not been and will not be, submitted in whole or in part to another university for the award of any other degree.

Signature:……

“A journey of a thousand miles begins with a single step.”

Lao-Tzu

Acknowledgements

First and foremost I would like to thank my supervisor, Dr. Matt Neale. Matt has always provided a challenging, enjoyable and friendly scientific environment with which to work in, providing constant expertise, support and motivation. I have learnt an enormous amount from interacting with such an incredible scientific mind and am extremely privileged.

I am also grateful to all other members of the Neale, Hoffman and Downs laboratories, especially Valerie Garcia, Louise Newnham, Alice Copsey, Anna Chambers and Eva Hoffman. Their support and friendship throughout has been invaluable. In addition, I owe thanks to numerous members of the GDSC for the incredible diverse skills, ways of thinking and friendship that has enabled me to carry out my research.

I would also like to thank the Medical Research Council and Royal Society for funding my PhD studentship. Without this financial support, I would not have been able to carry out this research project.

I also wish to thank the incredible friends that I have. Thank you Emma, Simon, Mike, Paul, Mel, Gaz, Nathan, Neal, Debbie and Bernie. This list is nowhere near exhaustive but you helped me through the tough times when experiments weren't working well, or when motivation was low, or when I just needed a distraction to help think about a problem differently. Without your support and friendship I couldn't have done this.

Finally, very special thanks go to my Mum, my sister, Lin and other members of my family. Without your love, support and guidance I would have given up long ago! I am extremely thankful for everything, not just through my Ph.D. but for all the things before. They set me on this path and enabled me to get to this point. I am eternally grateful.

And now for the science,

Summary

University of Sussex

Stephen Gray

Ph.D. Biochemistry

Investigating the molecular mechanisms of meiotic recombination

Meiotic recombination is initiated by DNA double-strand breaks (DSBs) created by the topoisomerase-like protein Spo11. During DSB formation, Spo11 becomes covalently attached to the 5' DSB ends. Removal of Spo11 is essential to repair the DSB by homologous recombination. Spo11 is removed endonucleolytically creating short-lived Spo11-oligonucleotide products. Here I demonstrate that:

1. Spo11-oligonucleotide products are not detected in recombination mutants believed to be defective in meiotic DSB formation.
2. When DSB repair is delayed, Spo11-oligonucleotides persist for longer.
3. Processing of Spo11-DSB ends to create Spo11-oligonucleotides is largely dependent on Mec1 and Tel1 activity.

In the process of investigating Spo11-oligonucleotide degradation, it was observed that a mutant defective in both the meiotic recombination checkpoint and in DSB repair failed to accumulate the expected level of DSBs. Work described here leads to the proposal of a DSB feedback mechanism that functions though the Mec1 (ATR) pathway to increase the efficiency of DSB formation. By contrast, Tel1 (ATM) functions to inhibit DSB formation, agreeing with recently published data. However, the data presented also suggests that Tel1 acts alongside the Mec1 pathway to promote DSB formation. It is therefore proposed that such positive and negative regulation creates a homeostatic mechanism to ensure that an optimum frequency of DSBs is formed.

In wildtype cells, single –stranded DNA resection relies only on the Exo1 nuclease. In checkpoint defective cells resection length is increased. Results described here demonstrate that in a checkpoint defective strain, resection functions through Exo1, Sgs1/Dna2 and a third currently untested resection mechanism, likely to be Mre11 dependent.

Table of Contents

List of Figures

Abbreviations List

Amp	Ampicilin
APC/C	Anaphase promoting complex / cyclosome
BSA	Bovine serum albumin
CDK	Cyclin dependent kinase
ChIP	Chromatin immunoprecipitation
CO	Crossover
DAPI	4',6-diamidino-2-phenylindole
DDA	DNA damaging agent
dHJ	Double Holliday junction
D-Loop	Displacement Loop
DNA	Deoxyribonucleic acid
DSB	Double-strand break
DSBR	Double-strand break repair
ECL	Enhanced chemiluminescence
EDTA	Ethylenediaminetetraacetic acid
FACS	Fluorescence-activated cell sorting
HR	Homologous recombination
IP	Immunoprecipitate
Kb	Kilobases
LB	Luria-bertani Broth
M	Molar
mBq	mega bequerels
ml	milli litre
mM	milli Molar

mn	Meiotic null
MRX	Mre11-Rad50-Xrs2
NCO	Non-crossover
ng	Nano gram
PCNA	Proliferating cell nuclear antigen
rpm	revolutions per minute
SDS	sodium dodecyl sulphate
SDSA	Synthesis dependent strand annealing
SDS-PAGE	sodium dodecyl sulphate polyacylamide gel electrophoresis
SEI	Single end invasion
ssDNA	Single-stranded DNA
TBST	Tris-buffered saline and tween-20
TCA	Trichloroacetic acid
TdT	Terminal deoxynucleotidyl transferase
uCi	micro Curies
ug	micro Gram
ul	micro litre
uM	micro Molar

CHAPTER 1:

Introduction

1: Introduction

1.1: Mitosis and Meiosis

In order for organisms to survive, they must continue to create new cells to replace damaged, dying or lost cells by means of a process called mitosis. In mitosis the cells undergo a cycle consisting of one round of DNA replication followed by one round of chromosome segregation (figure 1.1). The product of mitosis is two diploid daughter cells identical to the starting parent cell. In situations that require the chromosome complement to be halved however, such as in the formation of gamete cells, mitosis is unable to produce the required cells and so a specialised cellular process known as meiosis is adopted. In meiosis one round of DNA replication occurs followed by two rounds of chromosome segregation. First a reductional division (meiosis I) takes place segregating homologous chromosomes followed by an equational division (meiosis II) segregating sister chromatids (figure 1.1). The two meiotic divisions lead to the formation of haploid cells with half the starting DNA complement. The products of meiosis are used in sexual reproduction producing genetically diverse organisms. The new organism created by this process contains two copies of each chromosome (the homologous chromosomes) in every cell.

Mitotic division

At the beginning of the mitotic cell cycle DNA replication takes place forming sister chromatids and laying down cohesin complexes. In *Saccharomyces cerevisiae* mitotic cohesin consists of four subunits: Smc1, Smc3, Scc1 and Scc3 (Stoop-Myer and Amon 1999; Petronczki, Siomos et al. 2003). These subunits form a ring around the two sisters, linking the chromatids (Gruber, Haering et al. 2003). It is still unknown as to how cohesin wraps around the chromatids but

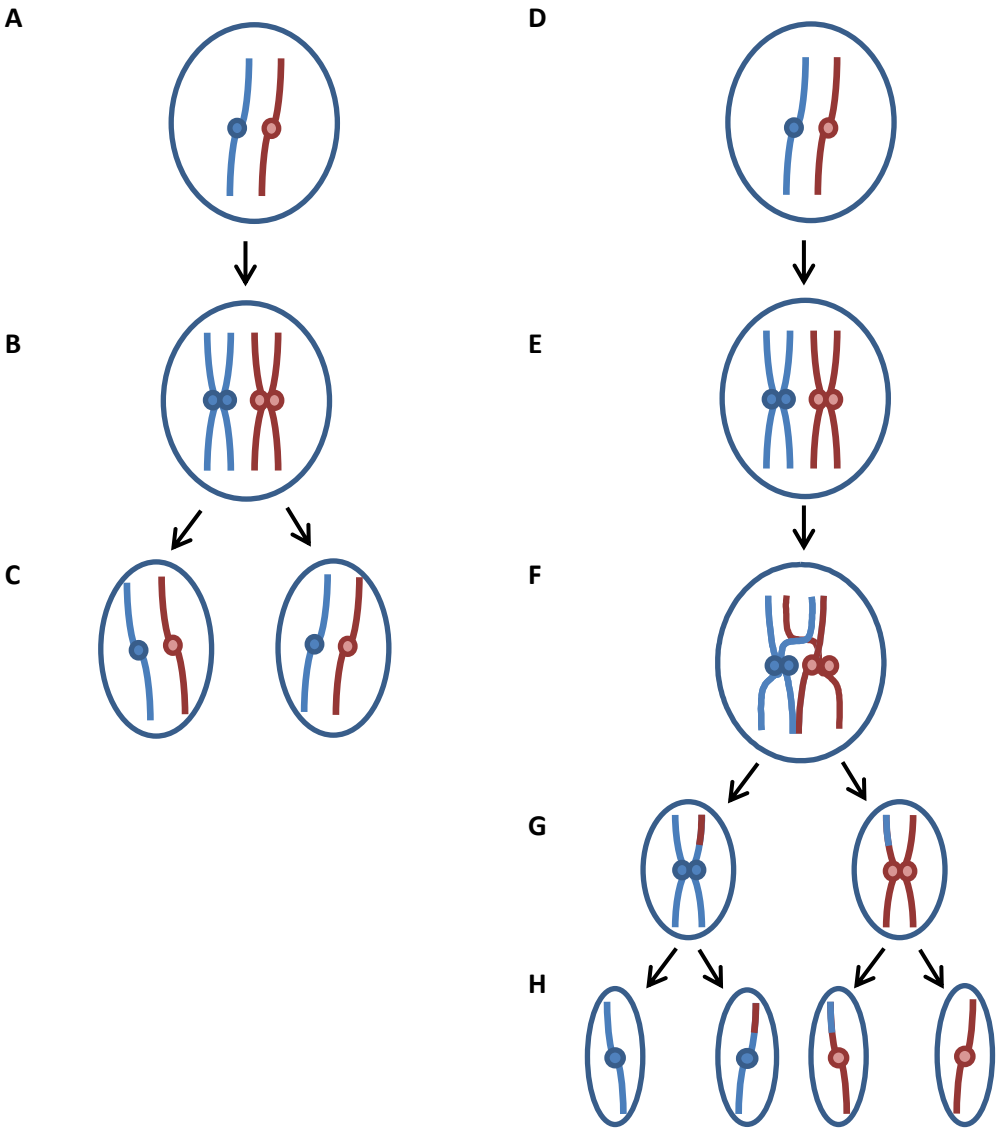

Figure 1.1: Mitosis and Meiosis. In cells undergoing mitosis, a diploid cell **(A)** undergoes replication producing sister chromatids **(B).** The sister chromatids are then segregated during division producing two diploid cells **(C).** In meiosis, the starting diploid cell **(D)** undergoes one round of replication producing sister chromatids **(E).** DSBs are then introduced throughout the genome and repaired from the homologous chromosomes creating connections between homologs **(F).** The connections allow for tension to form and correct segregation at the first meiotic division **(G)** followed by segregation of the sister chromatids at the second division. The products of meiosis are four haploid cells **(H).**

different models have been proposed, such as the monomeric cohesin ring, the dimeric cohesin ring and the handcuff model (Nasmyth 2011).

The aim of mitosis is to segregate the sister chromatids. In order to accurately achieve this, microtubules attach to kinetochores (protein structures that assemble at the centromere)(Kline-Smith, Sandall et al. 2005). Microtubules originate from centrosomes (spindle pole bodies in yeast) at either side of the cell (Pereira and Schiebel 1997; Adams and Kilmartin 2000). When microtubules from one centrosome attach to the kinetochore of one sister chromatid and microtubules from the other centrosome attach to the kinetochore of the other sister, this is known as amphitelic attachment (figure 1.2) (Petronczki, Siomos et al. 2003). The amphitelic attachment allows the chromatids to be pulled towards the centrosome but because of the cohesin complexes around the centromere linking the sister chromatids, tension is formed (Ishiguro and Watanabe 2007). The equal force from the spindles causes the chromosomes to align at the midpoint between both centrosomes.

The formation of tension between the sister chromatids are monitored by the spindle checkpoint (Amon 1999; Pinsky and Biggins 2005; May and Hardwick 2006). When all chromosomes have the correct attachment and formed tension, the spindle checkpoint is relieved leading to activation of the anaphase promoting complex/cyclosome (APC/C) (King, Deshaies et al. 1996; Amon 1999). This causes degradation of Pds1/Securin which inhibits the action of Esp1/Separase (Ciosk, Zachariae et al. 1998). When no longer inhibited, Separase causes cleavage of Scc1, one of the mitotic cohesin subunits, causing loss of cohesin (Uhlmann, Lottspeich et al. 1999). The sister chromatids can then be separated, pulled towards the centrosomes and packaged into new daughter cells.

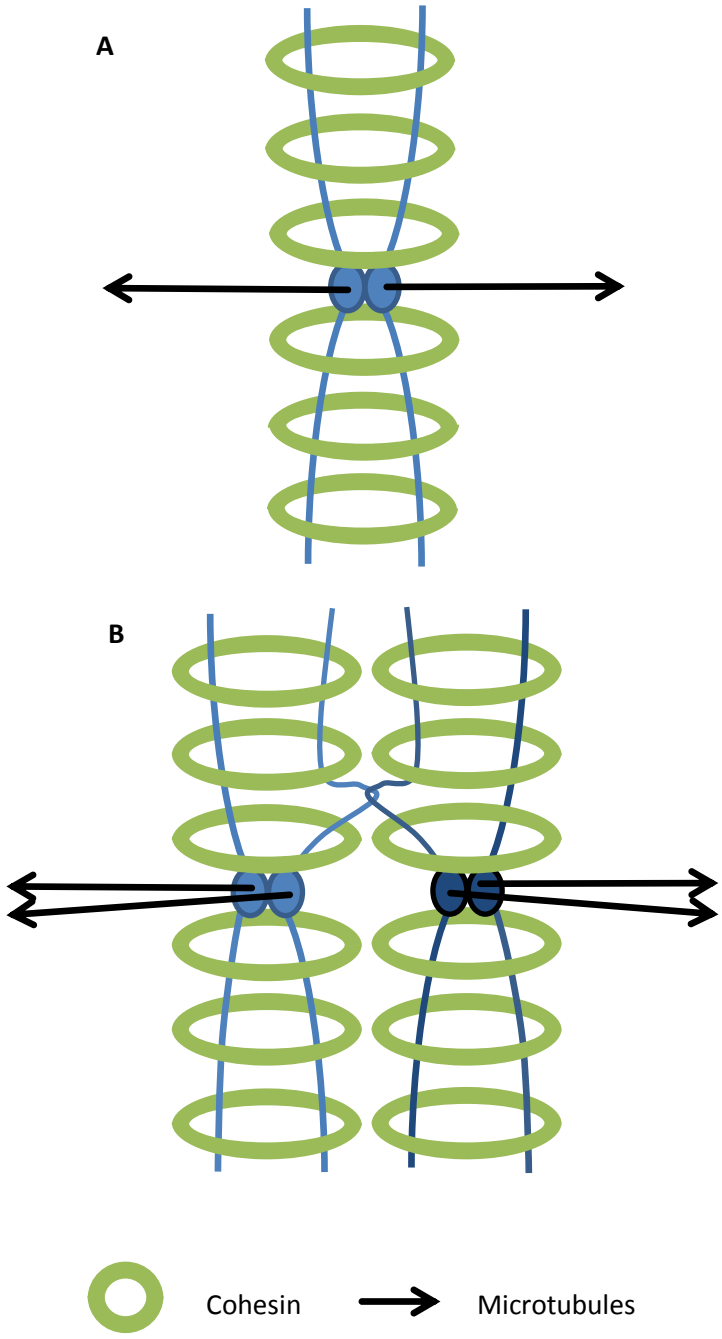

Figure 1.2: Cohesin loading and microtubule attachment. (A) In mitosis, when microtubules from one centrosome attaches to one kinetochore and microtubules attach from the other centrosome to the other kinetochore (amphitelic attachment) then tension can form due to the cohesin surrounding the sister chromatids. **(B)** In the first meiotic division, the meiotic cohesin remains along the chromosome arms. When crossovers occur, the two homologous chromosomes become linked allow tension to form between the two homologs when pulled in opposite directions.

Meiotic nuclear division

As in mitosis, in order for meiosis to take place, the cell first undergoes one round of DNA replication. Cohesin is also laid down but in meiosis it differs by the cleavable subunit, using Rec8 instead of Scc1 (Klein, Mahr et al. 1999; Stoop-Myer and Amon 1999; Watanabe and Nurse 1999). In contrast to the mitotic division, the first meiotic division segregates homologous chromosomes. Correct homologous chromosome segregation relies upon the homologous chromosomes being paired and linked together which is achieved by undertaking meiotic recombination. In meiotic recombination DNA double-stranded breaks (DSBs) are introduced throughout the genome (Szostak, Orr-Weaver et al. 1983; Sun, Treco et al. 1989; Cao, Alani et al. 1990; Keeney, Giroux et al. 1997; Keeney 2001). Left unrepaired these DSBs are catastrophic to the cell. Instead the DSBs are repaired by homologous recombination (HR) using the homologous chromosome and sister chromatid as a template for repair in a 3:1 ratio (Schwacha and Kleckner 1995; Carballo, Johnson et al. 2008; Heyer, Ehmsen et al. 2010). In the process of repair some of the DSBs form chiasmata: crossover events that physically link the homologous chromosomes (Carpenter 1994).

As with mitosis, during meiosis cohesin is laid down during DNA replication (figure 1.2). The cohesin along the chromosome normally links the sister chromatids of one homolog but when a crossover event has occurred, the cohesin distal from the event links the two homologs (Petronczki, Siomos et al. 2003). This means that when microtubules from different centrosomes attach to the kinetochores of different homologs, tension is formed. Spindle attachment is monitored by the spindle checkpoint and when tension is formed between all pairs of homologous chromosomes, the checkpoint is relieved (Shonn, McCarroll et al. 2000). At this stage the resolution of the crossover events can take place allowing for segregation of the homologous chromosomes (Stoop-Myer and Amon 1999). The checkpoint relief leads to

activation of the APC/C which degrades securin leading to activation of separase (King, Deshaies et al. 1996; Ciosk, Zachariae et al. 1998). Separase functions to cleave Rec8 (Buonomo, Clyne et al. 2000) targeting cohesin along the arm; however the cohesin at the centromere is protected from degradation by shugoshins (Clift, Bizzari et al. 2009). Following the first meiotic division, meiosis II segregates the sister chromatids (Allshire 2004). This is achieved in a similar manner to the mitotic division.

Meiotic Variations

In the process of oogenesis, the female equivalent to spermatogenesis, the meiotic process is slightly different. The oocyte produced provides all of the cellular material that the zygote needs, with the spermatocyte only providing the other half of the genetic information. Because of this, instead of producing four haploid cells from a starting diploid cell, oogenesis produces one viable haploid oocyte and two polar bodies (which are discarded), one from the first meiotic division and one from the second division (Brunet and Verlhac 2011).

The process of meiosis is not always successful in segregating chromosomes to form haploid cells. When unsuccessful this can leads to aneuploidy in the form of monosomic or trisomic conditions. In humans most monosomies are aborted spontaneously, but trisomic events are viable such as Edwards syndrome (trisomic chromosome 18), Downs syndrome (trisomic chromosome 21) and Klinefelter's syndrome (XXY) (Hassold and Sherman 2000; Thomas and Hassold 2003; Hassold, Hall et al. 2007). Most trisomic conditions are linked to errors in the first meiotic division during oogenesis with prevelance increasing with the age of the female (Hassold and Hunt 2001; Hassold, Hall et al. 2007). This increase is likely due to the start of oogenesis taking place in the fetal ovary and remaining dormant, only completing the first division at ovulation (Hassold, Hall et al. 2007; Nagaoka, Hassold et al. 2012).

Other mechanisms for segregating homologs

Not all organisms require meiotic recombination to pair the homologous chromsomses. In *Caenorhabditis elegans*, meiotic recombination occurs but pairing of homologous chromosomes is successful due to pairing centres found on each chromosome which pair and synapse homologous chromosomes (Tsai and McKee 2011). *Drosophila melanogaster* males also succeed in accurate chromosome segregation by the use of pairing centres but without chromosome exchange. It is thought that the male fruit flies, that do not form a synaptonemal complex (a proteinaceous structure that forms between homologs [more detail can be found in section 1.9]), manage accurate chromosome segregation by pairing the homologs early before meiosis. The pairing persists throughout meiosis and homologous chromosomes are sequestered to particular regions within the nucleus, enabling accurate segregation (Hawley 2002). Another example of an organism that does not undertake meiotic recombination is the *Bombyx mori* females. This silk worm does not have genetic exchange and instead forms a synaptonemal complex that exists longer throughout meiosis, suggesting that the prolonged synaptonemal complex helps accurately segregate the homologs (Hawley 2002; Tsai and McKee 2011).

1.2: Controlling the cell cycle

The processes of meiosis and mitosis are complex cellular events that require one stage to be completed before another begins, and for the correct stages to follow each other. In order to achieve correct progression the cell uses a series of cyclins and cyclin dependent kinases (CDK). The pairing of a particular cyclin with CDK causes activation of a particular cell cycle stage. In *S.cerevisiae*, just one CDK exists (Cdk1 / Cdc28) (DeCesare and Stuart 2012). In G1 phase Cln1,

Cln2 and Cln3 sequentially interact with Cdk1, followed by Clb5 and Clb6 during S phase and Clb1, Clb2, Clb3 and Clb4 in mitosis (Nasmyth 1996).

The meiotic programme uses many of the same cyclins but with a number of differences. The mitotic programme can still take place adequately in the absence of Clb5, however, in contrast to mitosis, Clb5 is crucial to the pre-meiotic S phase (Dirick, Goetsch et al. 1998; Stuart and Wittenberg 1998; DeCesare and Stuart 2012) and to the initiation of meiotic recombination (Smith, Penkner et al. 2001; Henderson, Kee et al. 2006). In work examining Clb1, Clb2, Clb3 and Clb4 expression, it was identified that Clb2 is expressed during mitosis, however, it is not expressed during meiosis (Grandin and Reed 1993). The lack of Clb2 expression during meiosis has enabled researchers to utilise the Clb2 promoter to conditionally express proteins and prevent expression during meiosis (Jessop, Rockmill et al. 2006). The method of preventing expression during meiosis is known as a meiotic null (mn) mutation. The advantage of meiotic null mutations is that it allows the investigation of a protein's function in meiosis without removing its expression during the rest of the cell cycle. This allows investigation of mutants which, for example, may not be viable if completely deleted.

Control of meiotic entry in *S.cerevisiae*

Yeast cells enter into meiosis, part of sporulation, as a starvation response due to lack of a nitrogen source and non-fermentable carbon source (Freese, Chu et al. 1982; Mitchell 1994). The entry into meiosis is initiated by increased transcription expression of the 'master regulator of meiosis': Ime1 (Mitchell 1994). Meiosis genes can be separated into three different categories: early, middle and late genes (Mitchell 1994). Ime1 transcription leads to the expression of early meiosis genes. Some of the genes within this early group are the proteins involved in meiotic recombination initiation (for example Spo11, Rec102, Rec104,

Rec114 and Mei4) and subsequent repair of the DSBs, such as the meiosis specific recombinase Dmc1 (Mitchell 1994). Also within the early group are proteins involved in formation of the synaptonemal complex (Zip1, Hop1 and Red1). Genes categorised within the middle group are proteins that function during the first and second meiotic divisions such as Ndt80 (Mitchell 1994; Xu, Ajimura et al. 1995; Hepworth, Friesen et al. 1998; Winter 2012). Ndt80 is a meiotic transcription factor that is required for entry into the meiotic divisions (Xu, Ajimura et al. 1995; Hepworth, Friesen et al. 1998). Late genes function to develop spore packaging (Mitchell 1994; Guttmann-Raviv, Martin et al. 2002).

1.3: Models of meiotic recombination

As previously mentioned, meiotic recombination is important to create the physical linkages between homologs for accurate segregation at the first meiotic division. The idea of physical links being formed between homologous chromosomes was first described by Thomas Hunt Morgan (Hunt Morgan 1916) and the first cytological visualisation of chiasmata between "chromosome knobs" was observed by McClintock and Creighton (Creighton and McClintock 1931).

The first model to explain how these chiasma were formed was presented by Robin Holliday (Holliday 1964) (figure 1.3). The Holliday model suggested that single-stranded nicks formed at the same position on homologous chromatids which then swap, become ligated and form a Holliday junction. The Holliday junction is then resolved forming either crossovers or non-crossovers (Holliday 1964). The final molecules produced in this model have regions of heteroduplex DNA which is present in both chromosomes (see figure 1.3A). The expected genetic segregation pattern from heteroduplex DNA existing on both chromosomes would be an aberrant 4:4 ratio (Meselson and Radding 1975; Stahl 1994). Spores of *Saccharomyces*

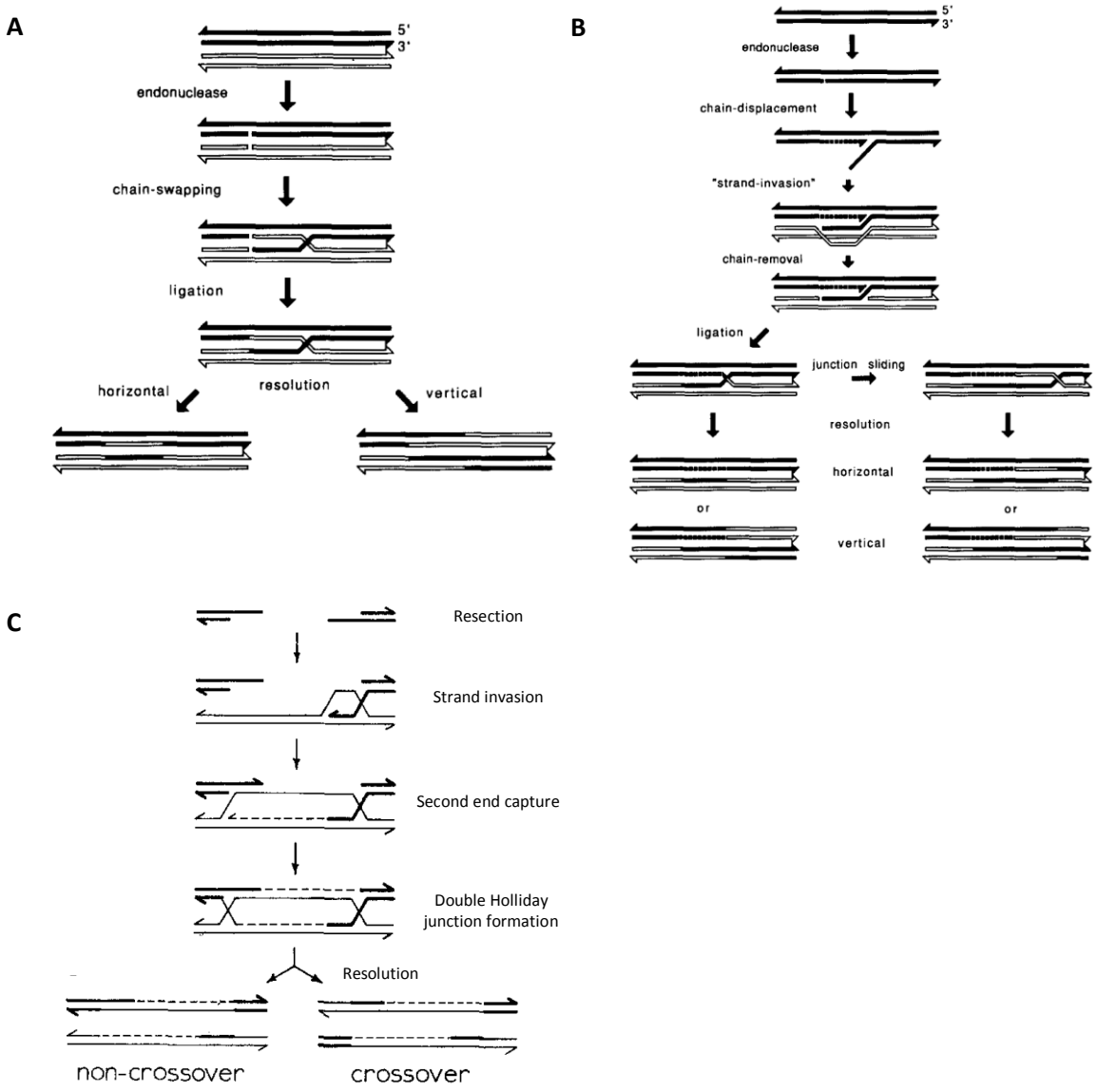

Figure 1.3: Models of recombination. (A) Holliday presented a model of recombination consisting of a single stranded nick occuring on different homolgous chromosomes which then exchanged, forming a Holliday junctions. The ends then ligated together and the Holliday junction resolved forming either crossovers or non-crossovers. **(B)** In the Meselson- Radding model, the single stranded nick was displaced from the template and invaded a homolgous template, creating a D-loop. The loop was then removed and DNA ends ligated forming a Holliday junction. The junction could then slide along the DNA. Once resolved, and depending upon the way in which the resolution took place, crossovers or non-crossovers could form. **(C)** In the Szostak model of double strand break repair, a DSB forms and DNA end are resected forming a 3' single-stranded DNA overhang. Strand invasion takes place creating a D-loop which allows for replication of DNA. Following this, second end capture can occur creating a double Holliday junction. Dependent upon either symmetric or asymmetric resolution, crossovers and non-crossovers can form. Images taken from Stahl, 1994 (**A** and **B**)and Szostak, Orr-Weaver et al. 1983 (**C**).

cerevisiae (produced as products of meiosis) had lower than predicted heteroduplex exchanges at the *arg4* locus (Fogel and Mortimer 1970) meaning that the Holliday model was unable to explain the observed results (Meselson and Radding 1975; Stahl 1994).

An advancement of Holliday's model was presented by Meselson and Radding which helped to explain the decreased 4:4 genetic segregation pattern (Meselson and Radding 1975; Stahl 1994). In the Meselson-Radding Model a single-stranded nick causes a DNA polymerase to extend, causing a strand displacement (figure 1.3B). The displacement can then invade a homologous template, which in turn causes displacement of the strand whose place it has taken. This displaced strand is enzymatically digested, the two ends ligated and a Holliday junction is formed. The Holliday junction then has the potential to slide along the DNA or remain where it is formed. The Holliday junction is then resolved forming crossovers or non-crossovers and different patterning dependent upon the migration of the Holliday junction (Stahl 1994).

As with the Holliday model however, the Meselson-Radding model was also unable to stand up to the genetic information, with a larger number of 6:2 genetic products observed than the predicted 5:3 ratio (Stahl 1994). In contrast to Holliday and Meselson-Radding models, Szostak's model (the double-strand break repair model [DSBR]) proposed that double-strand breaks (DSBs) were the events that initiated recombination, instead of single strand nicks (Szostak, Orr-Weaver et al. 1983) (figure 1.3C). In the model, DSB formation is followed by formation of single stranded DNA by exonucleases (a process known as resection). The next stage involves the 3' single stranded DNA end invading homologous template creating a displacement (D)-loop. Following this, DNA synthesis takes place using the homolog as a template causing extension of the invading strand. As the invading strand extends, the D-Loop gets longer, until the displaced strand can anneal with the other end of the DSB in a process

known as second end capture. The extended invading strand can then re-join the other end of the DSB forming a second Holliday junction. Finally it was proposed that resolution of the double Holliday junctions leads to either crossover or non-crossover events (Szostak, Orr-Weaver et al. 1983) (figure 1.3C). The DSBR model is the basis of research but has undergone additional revisions, as detailed below.

Physical analysis of meiotic recombination

The first physical evidence to support the DSBR model was provided by analysis of the migration of a plasmid. A plasmid with a sequence that had been identified as being an initiation site for gene conversion (Nicolas, Treco et al. 1989), was transformed into *Saccharomyces cerevisiae* cells. When the cells are put through meiosis, the migration of the plasmid changes to a linear form concomitantly with meiotic recombination taking place (Sun, Treco et al. 1989). The change in migration indicated the formation of a DSB. One of the predictions of the Szostak model was that following DSB formation, single stranded DNA is formed by resection. To test if ssDNA tails existed, meiotic samples at the peak of DSB formation (4 hours) were treated with a single-stranded specific nuclease (S1 nuclease) which removes single-stranded DNA tails. When treated, the probed DSB bands migrated at a position consistent with a smaller DNA molecule (Sun, Treco et al. 1989). This indicates that the DSB molecules have single-stranded DNA tails. The reduction in DSB molecule size, along with the formation of a linear DNA fragment at meiotic recombination initiation supports the DSBR model at the initiation stage and at the resection stage (Szostak, Orr-Weaver et al. 1983; Sun, Treco et al. 1989). The mechanisms that resect DSBs are discussed later in section 1.10.

Following the resection stage in the DSBR model, it is predicted that the single-stranded DNA tail can invade the homologous chromosomes. Using a modified meiotic DSB locus (the

HIS4LEU2 locus), DNA samples were treated with psoralen and then crosslinked by exposure to UV light. This treatment causes stabilisation of the joint molecule events. Following crosslinking, the DNA samples are run on a 2D gel, first separating the molecule according to mass (in the first dimension) and then separating the molecule according to the shape of the molecule (in the second dimension) (Schwacha and Kleckner 1995). Using Southern blotting technique, the locus was probed revealing the presence of single end invasion events (Hunter and Kleckner 2001). The DSBR model also predicts that double Holliday junctions would form following single end invasion. The double Holliday junction molecules were observed by using similar 2D gel analysis as was used to discover the single end invasion molecules (Schwacha and Kleckner 1995).

The final stage proposed in of the DSBR model is that resolution of the double Holliday junctions leads to either crossover or non-crossover events. However, more recent observations indicate that crossover / non-crossover decision is more complex than this. In contrast to the DSBR model, another mechanism repairing DSBs is synthesis-dependent strand-annealing (SDSA) (figure 1.4). Taking place after single end invasion, synthesis takes place after D-loop formation and the extended strand disassociates from the invaded homolog, re-annealing with the original partner strand (McMahill, Sham et al. 2007). The product of SDSA is a non-crossover event (Paques and Haber 1999; Krogh and Symington 2004; McMahill, Sham et al. 2007; Mimitou and Symington 2009; Martini, Borde et al. 2011). It was observed that in an *ndt80Δ* mutation, where double Holliday junctions are unable to be resolved (more information in section 1.8), non-crossovers formed with normal timing and levels (Allers and Lichten 2001). This observation indicated that non-crossovers are not formed by double Holliday junction resolution (Allers and Lichten 2001). In addition, the crossover / non-crossover differentiation occurs early, after DSB formation and before single end invasion (Borner, Kleckner et al. 2004). Therefore crossovers are formed in a double Holliday junction

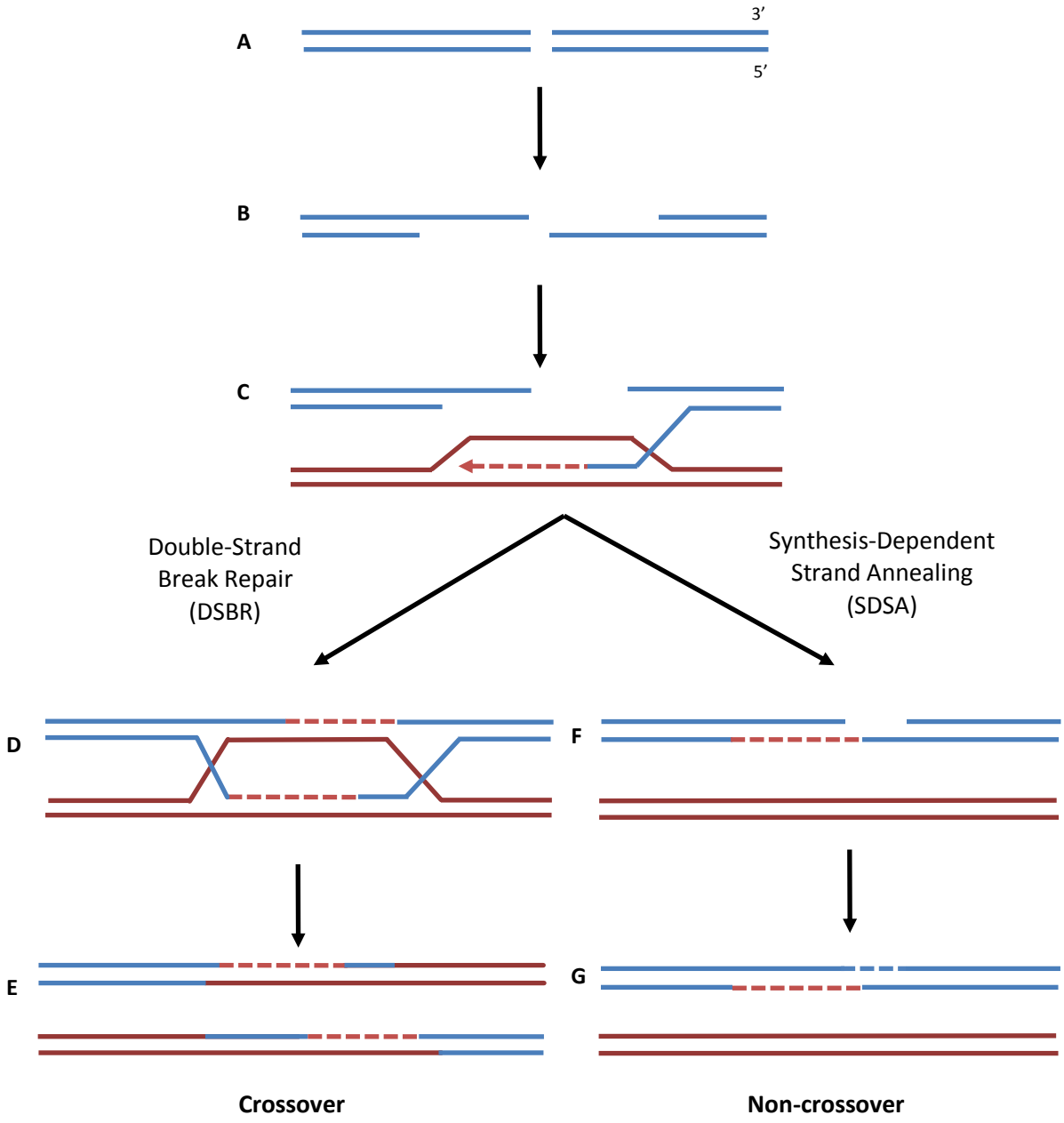

Figure 1.4: Double-strand break repair and synthesis dependent strand annealing repair pathways. A) Double stranded DNA has DSBs introduced. **(B)** 5'-3' resection is carried out forming single stranded DNA. **(C)** Strand invasion occurs in order to find homologous templates and replication of the template takes place. Repair can take place by different mechanisms. At the strand invasion step, DSBs can be repaired by double-strand break repair (DSBR) or synthesis-dependent strand annealing (SDSA). In DSBR **(D)** DNA synthesis continues until the displacement (D)-loop captures the second end of the DSB creating a second Holliday junction. **(E)** The asymmetric resolution of the double Holliday junction creates a crossover event. In SDSA, the invaded strand replicates the template synthesizing the DNA required to fill the gap. **(F)** The DNA then dissociates from the template and re-anneals with the original strand. **(G)** The remaining gap is filled in and repair is completed.

formation pathway and non-crossovers are produced from SDSA repair, in contrast to the DSBR model.

1.4: Investigating factors required for meiosis

Saccharomyces cerevisiae was used in a screen to detect mutants defective in spore formation (Esposito and Esposito 1969). Spo13 was one of the mutants that was discovered from this screen (Esposito and Esposito 1969). The *spo13* mutation does not undertake the first meiotic division and instead just completes the second meiotic division (segregating the sister chromatids) (Klapholz and Esposito 1980; Klapholz and Esposito 1980; Shonn, McCarroll et al. 2002). Although this division is like a mitotic division, meiotic recombination still occurs, generating links between homologous chromosomes which impedes chromosomes segregation leading to a reduction in spore viability. Removing components that are required for meiotic recombination causes a rescue of the spore inviability observed in the *spo13* mutant.

Rad52 is required for repair, but not formation, of meiotic DSBs (Game, Zamb et al. 1980; Borts, Lichten et al. 1986). Using the combination of *rad52Δ* and *spo13Δ* mutations, proteins required for DSB formation were discovered. In total, ten proteins have been identified: Spo11 (Klapholz, Waddell et al. 1985), Ski8 (Malone, Bullard et al. 1991), Mre11 (Ajimura, Leem et al. 1993), Rad50 (Game, Zamb et al. 1980; Malone and Esposito 1981), Xrs2 (Ivanov, Korolev et al. 1992), Rec102 (Malone, Bullard et al. 1991), Rec104 (Malone, Bullard et al. 1991), Rec114 (Malone, Bullard et al. 1991), Mei4 (Menees and Roeder 1989) and Mer2 (Malone, Bullard et al. 1991) (Keeney 2001). Nam8 (Ogawa, Johzuka et al. 1995) and Mer1 (Engebrecht and Roeder 1989; Engebrecht and Roeder 1990; Engebrecht, Voelkel-Meiman et al. 1991) were also identified in the process of investigating mutants defective in meiotic DSB formation. These

genes have indirect roles in meiotic DSB formation and function to splice an intron from Mer2 leading to a functionally active protein (Engebrecht, Voelkel-Meiman et al. 1991; Nakagawa and Ogawa 1997; Keeney 2001). In the absence of any of these ten proteins, meiotic DSBs do not form and the *spo13Δ* spore viability is rescued.

DSB formation proteins

Yeast two hybrid experiments identified that the DSB formation proteins form four sub-complexes. Interactions identified a Spo11-Ski8 complex, Rec102-Rec104 complex, Rec114-Mei4-Mer2 complex and the previously characterised Mre11-Rad50-Xrs2 complex (Petrini 1999; Uetz, Giot et al. 2000; Arora, Kee et al. 2004; Maleki, Neale et al. 2007). Two hybrid interactions also identified meiosis specific interactions between all of the sub-complexes (Arora, Kee et al. 2004; Maleki, Neale et al. 2007). Co-immunoprecipitation experiments support the interaction between Spo11 and Rec102 (Kee and Keeney 2002) and the complex formation of Rec102-Rec104 (Jiao, Salem et al. 2003). Immunofluorescence supports the formation of the Rec114-Mei4-Mer2 complex (Li, Hooker et al. 2006). In addition, immunofluorescence also revealed that Ski8, Rec114 and Mei4 localise to the chromosome at, or before DSB formation and Ski8 aids to stabilise Spo11 (Arora, Kee et al. 2004; Maleki, Neale et al. 2007).

Spo11 protein is highly conserved between organisms and homologs have been discovered in mouse and human (Romanienko and Camerini-Otero 1999; Romanienko and Camerini-Otero 2000), in *Schizosaccharomyces pombe* (as Rec12) (Lin and Smith 1994), in *Drosophila melanogaster* (as *mei-W68*) (McKim and Hayashi-Hagihara 1998), in *Caenorhabditis elegans* (as *spo-11*) (Dernburg, McDonald et al. 1998) and in *Arabidopsis thaliana* (as SPO11-1, SPO11-2 and SPO11-3) (Shingu, Tokai et al. 2012). Interestingly, in contrast to *Saccharomyces cerevisiae,*

Schizosaccharomyces pombe, Caenorhabditis elegans and *Drosophila melanogaster*, *Spo11* is essential in mouse meiosis as *spo11*$^{-/-}$ mutants gametes arrest during meiosis and undergo apoptosis (Baudat, Manova et al. 2000). Both Mei4 and Rec114 homologs have also been discovered in mice (as Mei4 and Rec114) and *Schizosaccharomyces pombe* (as Rec24 and Rec7 respectively) (Molnar, Parisi et al. 2001; Kumar, Bourbon et al. 2010). Homologs to Mre11 and Rad50 have also been discovered from organisms such as *Escherichia coli* (as SbcC and SbcD) (Leach, Lloyd et al. 1992; Keeney 2001) up to Humans (Stewart, Maser et al. 1999; Stracker and Petrini 2011)

In contrast to *Saccharomyces cerevisiae*, not all organisms require the same proteins for DSB formation. In *Drosophila melanogaster*, *mei-P22*, a chromosome-associated protein that interacts with meiosis specific proteins facilitating DSB formation, is required for DSB formation (Liu, Jang et al. 2002). Also in contrast to *Saccharomyces cerevisiae,* in *Arabidopsis thaliana* PRD1 (a homolog of the mammalian Mei1, a protein required for DSB induction in mouse spermatocytes (Libby, Reinholdt et al. 2003)) is required for meiotic DSB formation and meiotic DSB repair (De Muyt, Vezon et al. 2007). Although homologs of both Ski8 and the MRX complex have been found in *Arabidopsis thaliana* neither are required for meiotic DSB formation (Jolivet, Vezon et al. 2006; Shingu, Tokai et al. 2012). In *Schizosaccharomyces pombe*, Rad32 (the homolog of Mre11) and Rad50 are not required for meiotic DSB formation (Young, Hyppa et al. 2004).

The differences observed between organisms highlight the evolutionary change in proteins that play a role in regulating DSB formation. However, the conservation of Spo11 indicates that the catalytic mechanism for DSB formation remains similar.

1.5: Initiating meiotic DSB formation

Before meiotic DSBs are introduced into a chromosomal location, DNA replication must first be completed within that region (Simchen, Idar et al. 1976; Stuart and Wittenberg 1998). Under conditions where replication origins have been deleted, and therefore DNA replication is delayed in certain chromosomal locations, DSB formation is also delayed within those regions (Borde, Goldman et al. 2000). This emphasises the regulation between these two processes. Two components that are important in the regulation of these two processes are Cdc7 (Murakami and Keeney 2008; Lo, Kunz et al. 2012) and Cdc28 (Henderson, Kee et al. 2006). Cdc7 is similar to cyclin dependent kinases requiring an active catalytic subunit (Cdc7) and a regulatory subunit (Dbf4), together referred to as DDK (Lo, Kunz et al. 2012). Both Cdc28-Clb5 and Cdc7-Dbf4 are crucial to meiotic recombination initiation (Sasanuma, Hirota et al. 2008; Wan, Niu et al. 2008). Mer2, a component of the DSB formation complex is phosphorylated at serine 30 and 271 by Cdc28-Clb5 and at up to eight sites by Cdc7-Dbf4 (Henderson, Kee et al. 2006; Murakami and Keeney 2008; Wan, Niu et al. 2008). Critical to the initiation of meiotic recombination are phosphorylation on serine 30 by Cdc28-Clb5 which primes phosphorylation on serine 29 by Cdc7-Dbf4 (Wan, Niu et al. 2008).

Making the DSB

Isolation of ten Rad50 mutations that were competent in meiotic DSB formation but defective in the formation of resected ends provided a separation of function mutation: *rad50S* (Alani, Padmore et al. 1990; Keeney 2001). In the *rad50S* mutation DSBs accumulated with protein attachments (Alani, Padmore et al. 1990; Keeney and Kleckner 1995; Liu, Wu et al. 1995). One explanation for this was that the catalytic component of the DSB formation complex remained attached to the DSB end (Keeney, Giroux et al. 1997). Purification of protein from *rad50S* DNA

and mass spectrometry identified Spo11 as the protein attached to the end of the DSB (Keeney, Giroux et al. 1997).

Spo11 has structural similarity to Top6a and is a type II topoisomerase like protein (Bergerat, de Massy et al. 1997; Shannon, Richardson et al. 1999; Keeney 2001). Topoisomerases break DNA to relieve super helical tension and catenation within DNA. Type I topoisomerases make single-stranded breaks whilst type II topoisomerases make double-stranded breaks. Top6a, a type II topoisomerase is from the archaeon *Sulfolobus shibatae* and shares similarity with Spo11 and *S.pombe* Spo11 homolog Rec12 (Bergerat, de Massy et al. 1997). Key to the catalytic activity of Top6a as a topoisomerase is a tyrosine residue (Bergerat, de Massy et al. 1997). The DSB is created by the tyrosyl group attacking the phosphate group of the DNA backbone in a transesterification reaction (Wang 1996). This creates a linkage between the DNA phosphate backbone and the tyrosine of the topoisomerase (Wang 1996). Consistent with Spo11 functioning like this topoisomerase, a tyrosine residue at position 135 was identified as being crucial to DSB formation (Bergerat, de Massy et al. 1997) and highly conserved between organisms (Keeney, Giroux et al. 1997). Mutations of tyrosine to phenylalanine allows for production of Spo11 that is catalytically dead and therefore unable to make DSBs (Bergerat, de Massy et al. 1997; Diaz, Alcid et al. 2002).

Double strand break repair: Spo11-processing

The use of the *rad50S* mutant to determine that Spo11 was the protein attached to the DNA end indicated that the *rad50S* mutant was deficient at processing Spo11 (Keeney, Giroux et al. 1997). It was proposed by Keeney et al, that one of two possible mechanisms existed for removal of Spo11, either endonucleolytic cleavage which would lead to Spo11 with a short oligonucleotide attachment or direct hydrolysis, which would not have the oligonucleotide

attachment (Keeney, Giroux et al. 1997). Detection of the Spo11-oligonucleotide complex clarified that the processing event is by endonucleolytic cleavage.

Because DSB resection was inhibited in the *rad50S* (Alani, Padmore et al. 1990; Keeney and Kleckner 1995; Liu, Wu et al. 1995) and *mre11* nuclease mutants (Moreau, Ferguson et al. 1999), and Mre11 has endonuclease function (Moreau, Ferguson et al. 1999), it was suggested that this was the mechanism for processing Spo11. In addition, the lack of Spo11-oligonucleotides in the *sae2Δ* background and due to the similar phenotype observed in the *rad50S* (McKee and Kleckner 1997) suggests that Sae2 interacts with the MRX complex to process Spo11 (Neale, Pan et al. 2005)

The discovery of the mechanism of Spo11 DSB formation leading to its attachment at the DSB end, and the processing event that leads to Spo11-oligonucleotide formation, has further clarified the mechanism of meiotic DSB formation. This has led to the addition of two steps in the double-strand break repair model compared with the model previously described by Szostak (figure 1.5) (Szostak, Orr-Weaver et al. 1983; Neale, Pan et al. 2005).

Detection of the Spo11-oligonucleotides involves immunoprecipitation of Spo11 followed by end labelling of the oligonucleotide with radio-nucleotides (Neale and Keeney 2009). In order to perform the immunoprecipitation stage, a tagged form of Spo11 consisting of three copies of the hemagglutinin epitope and six copies of histidine repeats was used (known from this point onwards as *spo11-HA* due to the recessive phenotype it confers). Interestingly, in *Saccharomyces cerevisiae* the detected Spo11-oligonucletide complexes exist as two forms having either a short (10-15 nucleotides) or long (24-40 nucleotides) DNA attachment. In a *spo11-HA* background, approximately 50% of the Spo11-oligonucleotide complexes that are

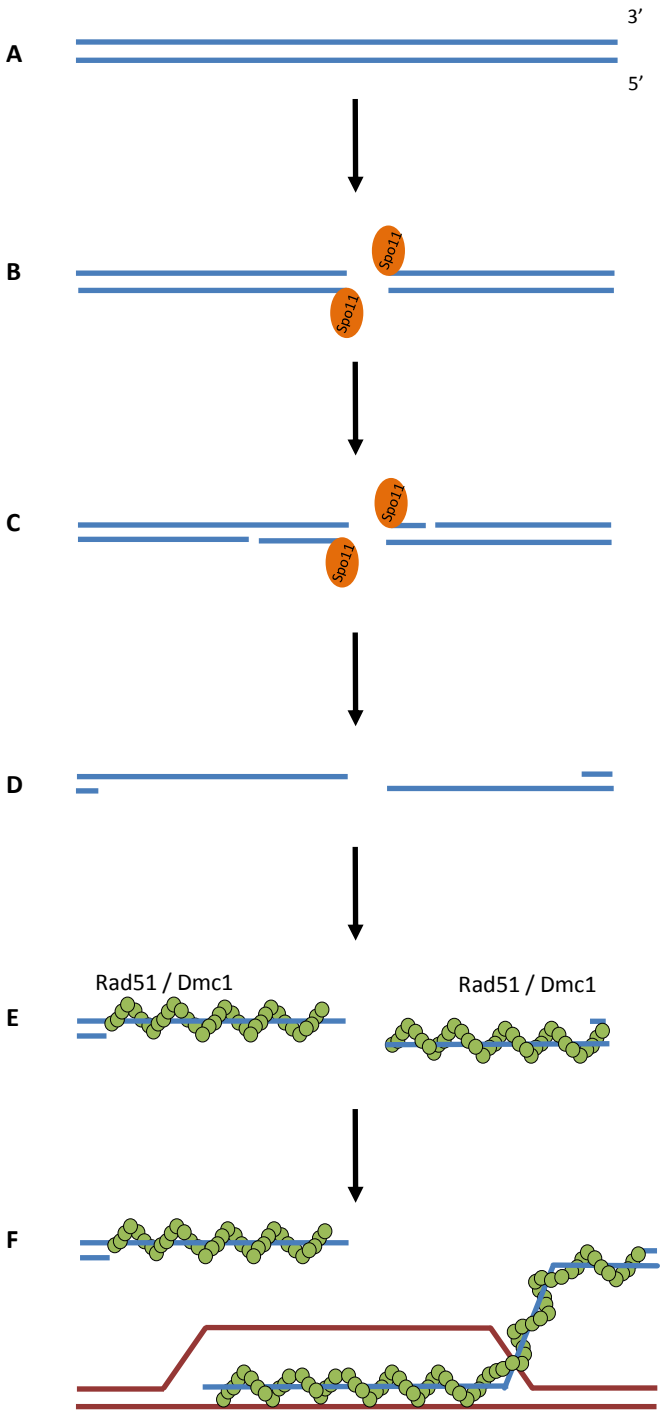

Figure 1.5: Revised double-strand break repair model. (A) Double stranded DNA. **(B)** Spo11 and accessory proteins introduce DSBs throughout the genome and Spo11 becomes covalently attached the DSB ends. **(C)** MRX-Sae2 functions to remove Spo11 by endonucleolytic cleavage creating Spo11-oligonucleotides. **(D)** Resection takes place creating single-stranded DNA overhangs which are coated with Rad51 and Dmc1 **(E). (F)** The single-stranded DNA end invades the homologous template searching for homology.

seen have short DNA attachment and the remaining approximate 50% have long DNA attachments. One hypothesis for this equal distribution of Spo11-oligonucleotide species is that each break formed is processed asymmetrically creating both a short and long Spo11-oligonucleotide from each processed DSB. Analysis of one DSB hotspot in Spo11-oligonucleotide mapping experiments, where long Spo11-oligonucleotides were enriched for and sequenced, observed that one side preferentially forms long Spo11-oligonucleotides (Pan, Sasaki et al. 2011). This observation supports the idea that asymmetric processing takes place.

One interesting question that has been raised from the discovery of two classes of Spo11-oligonucleotide size is what determines the length of the Spo11-oligonucleotides? Experiments aimed at answering this question focused on the nuclease functions of Mre11 (Moreau, Ferguson et al. 1999). Of the MRX-Sae2 complex that processes Spo11, Mre11 has both endonuclease and exonuclease function (Moreau, Ferguson et al. 1999; Stracker and Petrini 2011). Characterisation of the *mre11-H125N* mutant identified that it was defective in both functions and therefore did not produce Spo11-oligonucleotides (Moreau, Ferguson et al. 1999; Garcia, Phelps et al. 2011).

An interesting breakthrough was made when investigating the *mre11-H59S* mutation (Garcia, Phelps et al. 2011). Using structural observations from *Pyrococcus furiosus* Mre11 (Williams, Moncalian et al. 2008), mutants were made that were exonuclease deficient and endonuclease proficient. The corresponding mutation in *Saccharomyces cerevisiae* is the *mre11-H59S* mutation. In the *mre11-H59S* background meiotic DSBs are formed and processed, creating Spo11-oligonucleotides, but the resection function of Mre11 is defective (Garcia, Phelps et al. 2011). The *mre11-H59S* mutant saw a change in the distribution of Spo11-oligonucleotides with an increase in the larger Spo11-oligonucleotide forms in addition to Spo11-oligonucleotides with even larger DNA attachments (Garcia, Phelps et al. 2011). The *mre11-*

H59S data supports the hypothesis that the Spo11-oligonucleotides are created after an endonucleolytic cleavage between 200 and 300 nucleotides away from the DSB. Mre11 exonuclease function then resects towards the break in a 3'-5' direction creating the Spo11-oligonucleotides. As to why the Spo11-oligonucleotide complexes are the size that they are is still unknown but one hypothesis is that the footprint of the DSB forming complexes dictates the size of the Spo11-oligonucleotides. Additional observations to support this hypothesis come from DNAse treatments, where Spo11-oligonucleotides do not degrade in the presence of DNAse, but DNA of the same length as the oligonucleotides are degraded. This indicates that the oligonucleotide attachment is protected from nuclease activity.

Co-ordinating Spo11 processing

Investigations into the co-ordination of Spo11 processing by the MRX-Sae2 complex focused on Sae2. Sae2, homologue of the human CtIP (Sartori, Lukas et al. 2007), was discovered in a screen of mutants that sporulated in the absence of Spo11 (McKee and Kleckner 1997; Prinz, Amon et al. 1997; Keeney 2001). In mitosis, Sae2 functions to process DSB ends independently of, and in conjunction with the MRX complex enabling resection to take place (Huertas, Cortes-Ledesma et al. 2008) (Clerici, Mantiero et al. 2005; Lengsfeld, Rattray et al. 2007). Phosphorylation by CDK at serine 267 regulates that activity of Sae2 at the DSB, with phosphomutants exhibiting increased sensitivity to DNA damaging agents, impaired DNA end processing and defective sporulation (Huertas, Cortes-Ledesma et al. 2008). Phosphomimic of serine 267 relieve the phenotypes observed in the phosphomutant and remove the need for CDK (Huertas, Cortes-Ledesma et al. 2008). In response to DNA damage, Sae2 is also phosphorylated at multiple sites by the DNA damage kinases Mec1 and Tel1 (Baroni, Viscardi et al. 2004).

In meiosis, Sae2 is also phosphorylated by CDK at serine 267 (Manfrini, Guerini et al. 2010) and by Mec1 and Tel1 (Cartagena-Lirola, Guerini et al. 2006; Terasawa, Ogawa et al. 2008) which increases the cooperation with Mre11 (Terasawa, Ogawa et al. 2008). In Sae2 phosphomutants meiotic DSBs form but remain unprocessed (Cartagena-Lirola, Guerini et al. 2006; Terasawa, Ogawa et al. 2008; Manfrini, Guerini et al. 2010). A similar phenotype is observed in a *mec1Δ tel1Δ* mutant (Cartagena-Lirola, Guerini et al. 2006). These observations therefore highlight the requirement of Mec1, Tel1 and CDK phosphorylation in controlling Spo11 processing by Sae2.

1.6: Resecting the DSB

Following Spo11 processing DSBs are resected (Sun, Treco et al. 1989). In order for the detected 3' single-stranded DNA tails to form, resection mechanisms must exist. Originally discovered in *Schizosaccharomyces pombe,* Exo1 was identified as a protein up-regulated during meiosis (Szankasi and Smith 1992). The homolog was identified in *Saccharomyces cerevisiae* by homology to both the *Schizosaccharomyces pombe* Exo1 and Rad27 (another exonuclease (Harrington and Lieber 1994)) in *Saccharomyces cerevisiae* (Fiorentini, Huang et al. 1997). Exo1 was shown to resect in a 5' to 3' direction (Fiorentini, Huang et al. 1997). In vitro experiments demonstrated that Exo1 activity promotes recombination (Fiorentini, Huang et al. 1997). In vivo experiments demonstrated that removal of Exo1 caused a reduction in recombination between two markers(Fiorentini, Huang et al. 1997). These observations implicated Exo1's role in mitotic recombination (Fiorentini, Huang et al. 1997). In addition to the role in mitotic recombination, Exo1 was known to interact with the repair protein Msh2 (Tishkoff, Boerger et al. 1997). Removal of Exo1 caused not only a reduction in resection but also a mutator phenotype consistent with a defect in the Msh2 mismatch repair pathway (Tishkoff, Boerger et al. 1997).

With Exo1 shown to have a role in mitotic recombination, and its up-regulation seen in meiosis, it was likely that Exo1 functioned as the exonuclease resecting during meiotic recombination. When DNA is run on an agarose gel, is separates according to its size. If a DNA molecule is resected, creating a ssDNA tail as opposed to the unresected souble-stranded molecule, this will then run at a different location due to the decrease in its size. As more resection occurs, the molecule decreases in size, causing it to migrate at a different position. A diploid strain with the modified meiotic recombination hotspot inserted at the *LEU2* locus (*HIS4::LEU2*), was used to measure resection at a meiotic DSB due to its high likelihood of breaking (Zakharyevich, Ma et al. 2010). The DNA samples were separated using 2D gel electrophoresis, which first separated the molecule according to size (under native conditions) in the first dimension, and then separated the DNA strands under denaturing conditions in the second dimension (Zakharyevich, Ma et al. 2010). This allowed the top and bottom strands of the DSB to be separated and distance migrated measured, to determine the amount of resection that occurs (Zakharyevich, Ma et al. 2010). The observations from this analysis indicated that Exo1 was responsible for at minimum approximately 350 nucleotides of resection and up to approximately 1550 nucleotides during meiosis. In the *dmc1Δ* background, DSBs that form continue to be resected, more than in wildtype. Exo1 was identified as a mechanism that causes the continued resection, with *exo1Δ dmc1Δ* having reduced resection compared with *dmc1Δ* (Tsubouchi and Ogawa 2000).

In addition to Exo1, two other resection mechanisms have been observed in processing DSBs (Mimitou and Symington 2008). The Sae2-MRX complex, previously described as having a function in Spo11-processing (Neale, Pan et al. 2005), has endonuclease function along (Neale, Pan et al. 2005; Lengsfeld, Rattray et al. 2007) with Mre11 exhibiting 3’ to 5’ exonuclease function (Paull and Gellert 1998; Garcia, Phelps et al. 2011). At mitotic DSBs endonucleolytic functions to process DSB ends allowing for exonuclease action by Exo1 and another

independent resection mechanism: Sgs1/Dna2 (Mimitou and Symington 2008). Sgs1/Dna2 is a helicase/nuclease resection mechanism (Watt, Louis et al. 1995; Mimitou and Symington 2008; Zhu, Chung et al. 2008; Mimitou and Symington 2009). Sgs1/Dna2 functions in alternative resection pathway to Exo1 in repairing mitotic DSBs (Mimitou and Symington 2008; Zhu, Chung et al. 2008). Interestingly, Sgs1 mutants have little or no reduction on the amount of resection that occurs at *HIS4::LEU2* in meiosis (Zakharyevich, Ma et al. 2010). The reason for this intriguing difference is unclear.

Resection of telomeres is prevented by action of the Cdc13 protein (Nugent, Hughes et al. 1996). This caps the end of the telomere stopping nucleolytic degradation (Nugent, Hughes et al. 1996). In *cdc13-1* mutants, when the telomere is uncapped, Exo1 resection takes place forming ssDNA (Morin, Ngo et al. 2008). The presence of the uncapped telomere and the ssDNA causes activation of the checkpoint which phosphorylates Exo1 (Morin, Ngo et al. 2008). This phosphorylation inhibits Exo1 (Morin, Ngo et al. 2008). The control of resection at meiotic DSBs still remains to be elucidated but checkpoint defective strains have hyper resected DSBs (Grushcow, Holzen et al. 1999; Shinohara, Sakai et al. 2003) consistent with a lack of resection control.

1.7: Finding the partner

Not all DSBs formed during meiosis create crossovers. In mouse, there is a ten-fold excess in recombination markers than recombination products (Moens, Kolas et al. 2002). This observation indicates that the majority of DSBs form non-crossover events which aid in finding the homologous partner. After formation of a 3' single-stranded DNA overhang by resection, a homologous template must be found for strand invasion to occur. Once formed, the single-stranded DNA is coated with RPA, a protein complex that binds the single-stranded DNA (Sung,

Krejci et al. 2003). The binding of RPA prevents the single-stranded DNA from forming secondary structures and allows the recombinases that carry out strand exchange to bind (Sung, Krejci et al. 2003; Neale and Keeney 2006). Rad51, a protein homologous to the *E.coli* RecA (Shinohara, Ogawa et al. 1992), was discovered in the same radiation sensitive screen as Rad50 and is part of the Rad52 epistasis group (Game and Mortimer 1974). Identified as being required for mitotic and meiotic recombination, the function of Rad51 was predicted because of its sequence similarity to RecA (Shinohara, Ogawa et al. 1992). In In vitro experiments using a single-stranded plasmid and a double stranded DNA fragment with homology it was observed that Rad51 was able to undertake homologous pairing and strand exchange (Sung 1994).

In addition to Rad51 being capable of carrying out the strand invasion steps, an additional RecA homologue, Dmc1, was identified in *Saccharomyces cerevisiae* (Bishop, Park et al. 1992). Dmc1 was identified in a screen that enriched for cDNA expressed during meiosis (Bishop, Park et al. 1992). Mutants in Dmc1 displayed an inability to form normal synaptonemal complex and arrest in meiotic prophase (Bishop, Park et al. 1992). Both Rad51 and Dmc1 mutants caused an accumulation of resected DSBs (Bishop, Park et al. 1992; Shinohara, Ogawa et al. 1992). The Dmc1 function as a strand exchange mechanism was implied due to the similar homology to RecA (Bishop, Park et al. 1992). Further structural analysis and filament formation comparison with Rad51 highlighted the ability for Dmc1 to function as a strand exchange mechanism (Sheridan, Yu et al. 2008).

The functional difference that Rad51 or Dmc1 provides compared to each other is unknown. One possible difference between the two recombinases is suggested by the difference in repair partner that is required in meiosis. In mitosis, repair can occur using a homologous template provided by the homologous chromosome or (if after S phase) the sister chromatid.

In meiotic recombination, the important event is the formation of at least one crossover per homologous chromosome (Jones 1984). In order to achieve this, repair must take place using the homologous chromosome as the template for repair, as opposed to the sister chromatid. Thus, it is possible that Dmc1 helps catalyse the repair towards the homologous chromosomes. One difference between Rad51 and Dmc1 has been observed in immunofluorescence microscopy experiments. In the absence of Rad51, Dmc1 is not able to form foci but Rad51 is able to form foci in the absence of Dmc1 (Dresser, Ewing et al. 1997). This suggests that Rad51 may be able to function in the absence of Dmc1, although in a limited manner as Dmc1 mutants cause an accumulation of DSBs (Bishop, Park et al. 1992). Another possibility is that Rad51 helps create the Dmc1 filaments for strand invasion to take place, but in the absence of Dmc1, Rad51 is inhibited from carrying out repair due to the enforcement towards homologous chromosomes as repair templates (Dresser, Ewing et al. 1997).

Rad51 and Dmc1 do not work alone and have a number of different accessory proteins to enable filament formation and strand exchange. Rdh54, a Rad54 homologue (Klein 1997), interacts with Dmc1 and helps promote D loop formation, the stage that occurs due to strand exchange (Shinohara, Shita-Yamaguchi et al. 1997; Neale and Keeney 2006). Rdh54 also interacts with Rad51 during mitotic homologous recombination (Petukhova, Stratton et al. 1998). In addition to Rdh54, Rad54 also interacts with Rad51 (Clever, Interthal et al. 1997) to help promote filament formation (Petukhova, Stratton et al. 1998). Mek1, a meiosis specific kinase that is a Rad53/Chk2 paralogue (Perez-Hidalgo, Moreno et al. 2003; Carballo, Johnson et al. 2008), phosphorylates Rad54 during meiosis preventing its interaction with Rad51, thereby preventing Rad51 activity (Niu, Wan et al. 2009). Another inhibitor of Rad54 is Hed1, a protein identified in a screen where high copies supressed *red1* mutants, which prevents accessibility of Rad54, thereby preventing Rad51 filament formation (Tsubouchi and Roeder 2006).

Other accessory proteins identified are Mei5 and Sae3. These co-localise and interact with Dmc1 as well as interacting with RPA (Hayase, Takagi et al. 2004; Okada and Keeney 2005; Ferrari, Grubb et al. 2009). In mutants defective in Mei5 or Sae3, Dmc1 filaments are unable to form (Hayase, Takagi et al. 2004). In order for Dmc1 to carry out its function, it must be loaded onto the single-stranded DNA in exchange for RPA. Mei5 and Sae3 have been identified as the proteins responsible for carrying out the RPA unload and Dmc1 loading (Ferrari, Grubb et al. 2009). In addition to Mei5 and Sae3, Hop2 and Mnd1 have also been identified as being important in the strand invasion step (Leu, Chua et al. 1998; Gerton and DeRisi 2002; Chen, Leng et al. 2004). Work carried out has so far highlighted their role in DNA condensation as opposed to direct functions on Dmc1 and Rad51 observed in Mei5 and Sae3 (Pezza, Camerini-Otero et al. 2010).

1.8: Resolving the DSBs

Once strand invasion has occurred, a displacement loop (D-loop) forms. As synthesis takes place, the D-loop extends until second end capture can take place. Once captured, double Holliday junctions form (Schwacha and Kleckner 1995) and the final stage of DSB repair is resolution of the junctions. Dependent upon the mechanism used or the way in which the junctions are resolved can lead to non-crossover or crossover products. Previous observations in *Sacchromyces cerevisiae* have highlighted that SDSA repair leads to non-crossovers and double Holliday junction resolution leads to crossovers (Allers and Lichten 2001). However, crossover and non-crossover formation may not be exclusive to SDSA and double Holliday junction resolution.

In order to produce the crossover events which are important for correct segregation of the homologues, different resolution mechanisms must be used. Yen1, a Holliday junction resolvase, is capable of resolving Holliday junctions in vitro (Ip, Rass et al. 2008). If the Holliday junctions are resolved symmetrically then non-crossover events are formed and if the Holliday junctions are resolved asymmetrically then crossover events are formed (figure 1.6A-E). At present however, Yen1 has only been observed to process double Holliday junctions symmetrically, thereby producing non-crossover events (Ip, Rass et al. 2008).

Recent observations from the Hunter lab have indicated an additional role for Exo1 in the resolution of double Holliday junctions into crossover events (Zakharyevich, Tang et al. 2012). *exo1Δ* mutants were seen to have normal levels of double Holliday junction formation but a decrease in crossover events (Zakharyevich, Ma et al. 2010). In addition it was demonstrated that an Exo1 pathway, in cooperation with Sgs1 and Mlh1-Mlh3 (part of the mismatch repair pathway), were responsible for the majority of double Holliday junction resolution into crossover events (Zakharyevich, Tang et al. 2012).

Two other mechanisms of resolution have been identified, one by the Sgs1/Top3/Rmi1 complex and the other by Mus81-Mms4 / Slx1-Slx4 (Symington and Holloman 2008; Cejka, Plank et al. 2010; Zakharyevich, Tang et al. 2012). In the Sgs1/Top3/Rmi1 complex, Sgs1 and Rmi1 are both helicases which unwind the DNA whilst Top3, a topoisomerase, decatenates the DNA molecules (Cejka, Plank et al. 2010). The output from the Sgs1/Top3/Rmi1 processing is a non-crossover event (figure 1.6) (Symington and Holloman 2008; Ashton, Mankouri et al. 2011). In contrast, the Mus81-Mms4 and Slx1-Slx4 can function at the stage where a single Holliday junction forms. These structure specific endonuclease complexes are capable of cleaving the molecule to produce a crossover event (figure 1.6G) (Symington and Holloman 2008; Martini, Borde et al. 2011).

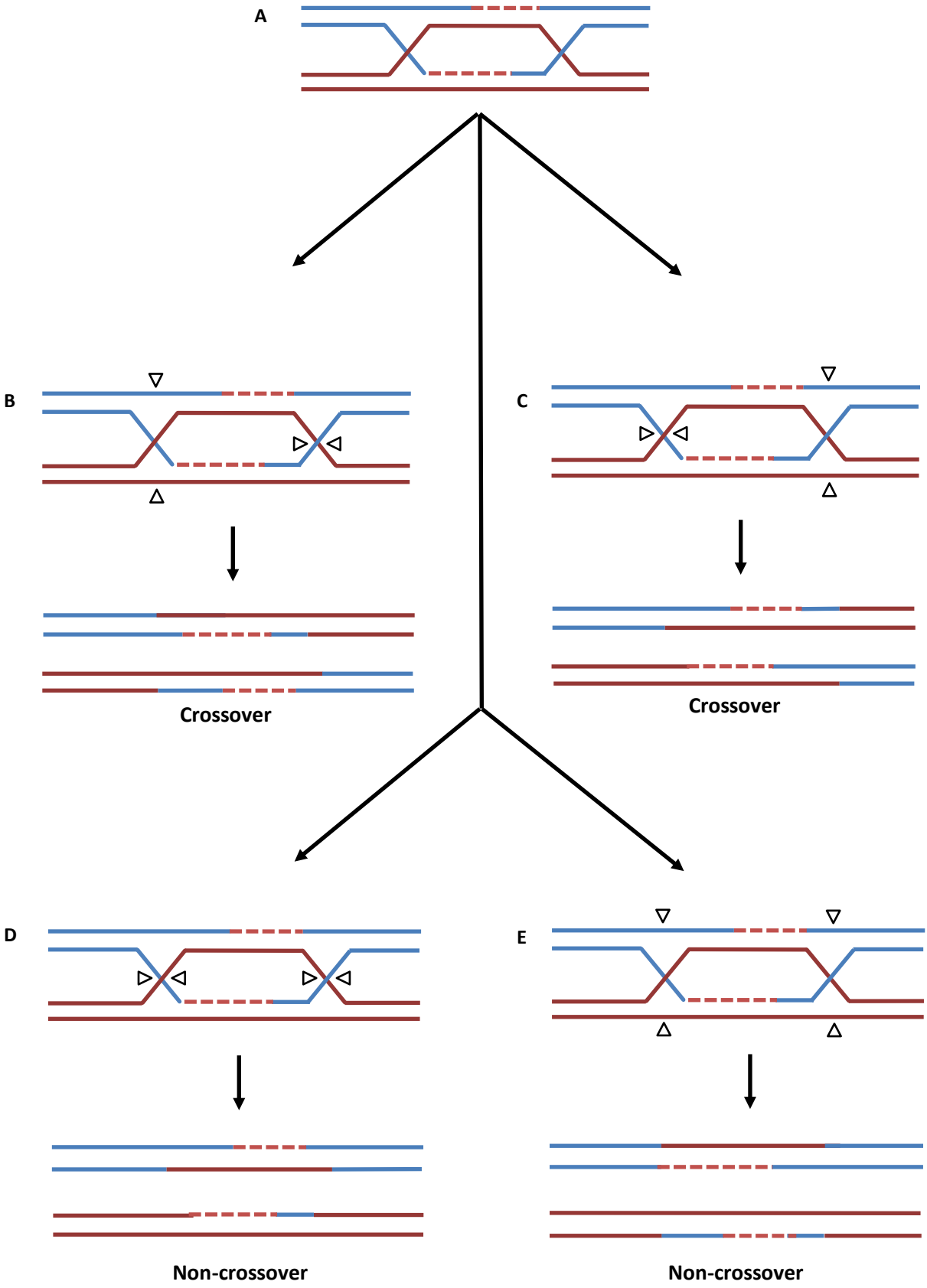
A
B
C
Crossover
Crossover
D
E
Non-crossover
Non-crossover

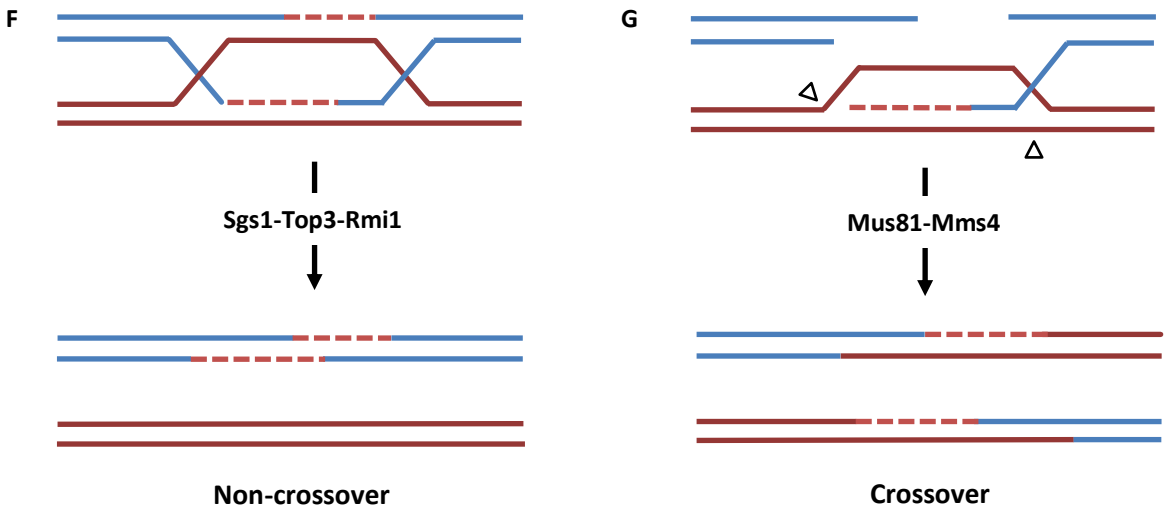

Figure 1.6: Resolving Holliday Junctions. (A) Double Holliday junctions form in the process of DSB repair. Double Holliday junctions can be resolved in different ways either asymmetrically (in the case of **B** and **C**) forming crossovers or symmetrically (in the case of **D** and **E**) forming non-crossovers. The actions of Yen1 and Exo1-Mlh1-Mlh3-Sgs1 are capable of resolving double Holliday junctions in this manner. **(F)** Sgs1-Top3-Rmi1 can unwind and decatenate double Holliday junctions forming non-crossover events. **(G)** In a pre-cursor to double Holliday junction, endonuclease function of Mus81-Mms4 can cut the DNA creating crossover events. (Images reproduced from Symington and Holoman, 2008 and Martini, Borde et al. 2011)

1.9: Providing the environment for crossovers: forming the synaptonemal complex

The synaptonemal complex is a proteinaceous structure that forms between homologous chromosomes. The state of synaptonemal complex has been used to stage meiotic progression of cells. The beginnings of the synaptonemal complex are seen in the forming axial elements, consisting of Hop1 and Red1, forming along the homologous chromosomes (figure 1.7) (Rockmill and Roeder 1988; Hollingsworth and Byers 1989; Hollingsworth, Goetsch et al. 1990; Roeder 1997). After DSB formation, at zygotene, the axial elements are connected by transverse filaments, Zip1, causing synapsis of the homologs (Sym, Engebrecht et al. 1993). In the mature synaptonemal complex axial elements are referred to as lateral elements with the Zip1 transverse filaments forming the central element of the synaptonemal complex (figure 1.7) (Sym, Engebrecht et al. 1993; Roeder 1997).

Functions of the synaptonemal complex were thought to provide an environment for DSB formation and homologous chromosome pairing (Roeder 1997). However, in Zip1 mutants, where the mature synaptonemal complex is not formed, both homolog pairing and DSB formation occurred ruling out these ideas (Sym, Engebrecht et al. 1993; Henderson and Keeney 2005). Work in yeast has demonstrated that components of the axial elements are required for normal meiotic DBS levels. Mutants in Hop1 and Red1, proteins that make up the axial element, have been shown to have only approximately 10% of the normal level of meiotic DSBs (Mao-Draayer, Galbraith et al. 1996). Insight into the function of the synaptonemal complex was gained through mutations of the ZMM proteins. The ZMM proteins consist of Zip1, Zip2, Zip3, Zip4, Msh4, Msh5 and Mer3 and are proteins that, when mutated, have reductions in crossovers (Roeder 1997). The synaptonemal complex therefore functions to promote crossover formation between homologous chromosomes.

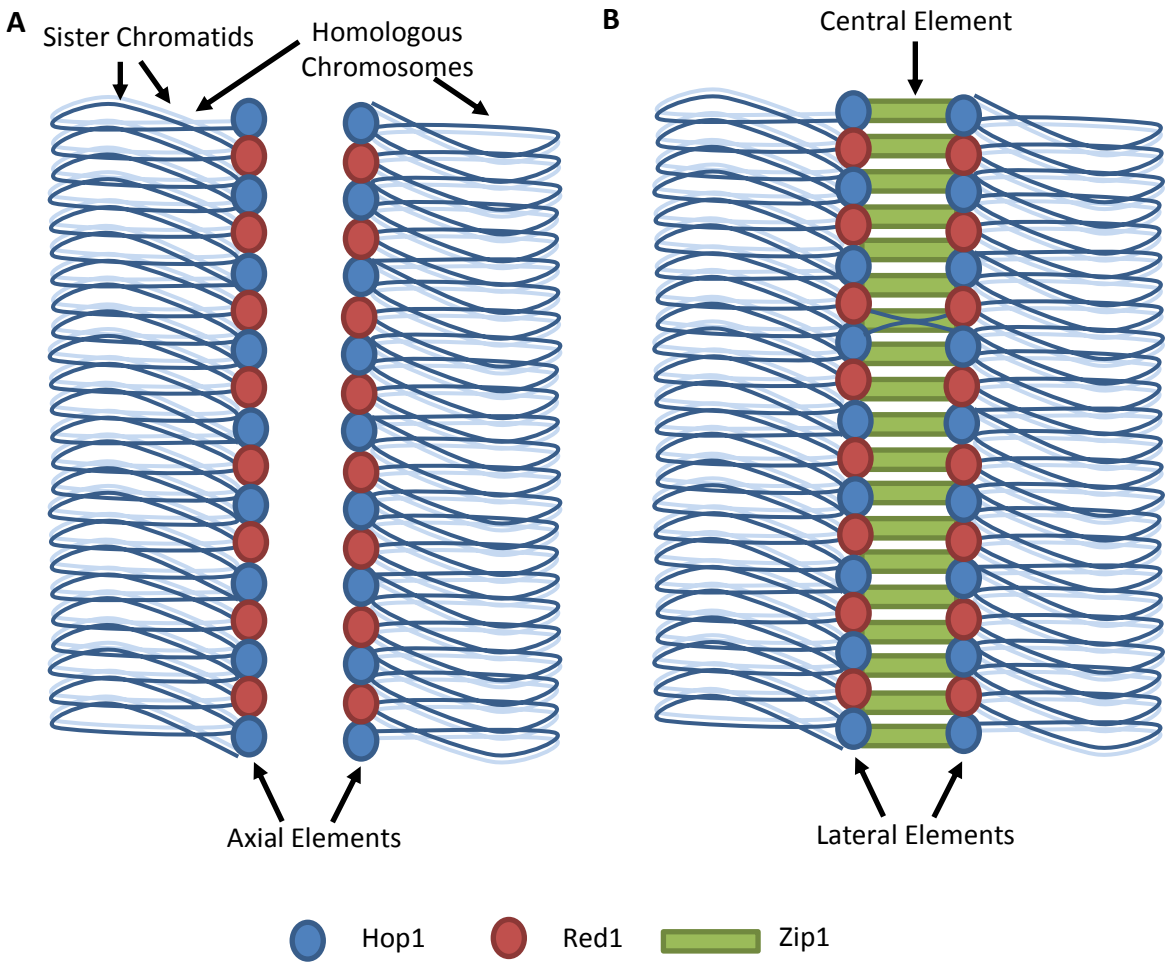

Figure 1.7: Synaptonemal Complex formation. **(A)** In leptotene, axial elements start to appear consisting of Hop1 and Red1. **(B)** By pachytene, full synaptonemal complex formation has occurred and synapsis has taken place between the two homologous chomosomes. The axial elements become lateral elements and are linked by transverse filaments that form the central element. The synaptonemal complex provides an environment for crossovers to take place.

The synaptonemal complex that forms in mammals consists of additional proteins forming the central element. The lateral element is formed of SYCP2, which has sequence similarity to Red1 (Offenberg, Schalk et al. 1998) and SYCP3 (Page and Hawley 2004). The central element consists of the transverse filament SYCP1 (Meuwissen, Offenberg et al. 1992), and four additional proteins required for central synaptonemal complex formation: SYCE1 (Costa, Speed et al. 2005), SYCE2 (Costa, Speed et al. 2005), SYCE3 (Schramm, Fraune et al. 2011) and TEX12 (Hamer, Gell et al. 2006).

During meiosis it is important that the DSBs that are formed repair by means of the homologous chromosome as opposed to the sister chromatid. Characterisation of the axial element protein Hop1 has revealed a function for ensuring inter-homologue bias (Carballo, Johnson et al. 2008). This inter-homologue bias ensures that some of the DSBs go on to produce the crossover events which ensure accurate chromosome segregation at the first division. The Hop1 protein is phosphorylated by checkpoint proteins Mec1 and Tel1. The phosphorylation of threonine 318 is crucial to enforcing Dmc1 dependent repair towards the homologous chromosome (Carballo, Johnson et al. 2008). In phosphomutants of threonine 318, spore viability was very low. In addition, in a *hop1*^{SCD} mutant, where three residues within an SQ/TQ cluster domain (where three or more SQ or TQ residues exist within 100 residues (Traven and Heierhorst 2005; Carballo, Johnson et al. 2008)) were mutated, repair occurred via Rad51 inter-sister repair (Carballo, Johnson et al. 2008). Hop1 has also been demonstrated to be upstream of Mek1, a protein also demonstrated to be involved in the inter-homologue repair bias (Niu, Wan et al. 2005; Niu, Li et al. 2007).

1.10: The meiotic recombination checkpoint

DSBs created through meiosis activate the meiotic recombination checkpoint. The checkpoint functions to prevent the progression to the first meiotic division until all DSB are repaired. The checkpoint uses many of the same proteins involved in mitotic checkpoints (Lydall, Nikolsky et al. 1996). The two main kinases in budding yeast that recognise DNA damage are Mec1 and Tel1. The human homologues are ATR and ATM (Greenwell, Kronmal et al. 1995; Cimprich, Shin et al. 1996). The two kinases differ by the types of damage that they recognise. Tel1 is activated in the presence of unprocessed DSBs with protein attachments (Fukunaga, Kwon et al. 2011). By contrast, Mec1 is activated in the presence of ssDNA.

The formation of meiotic DSBs involves Spo11, the MRX complex, Ski8, Rec102, Rec104, Rec114, Mei4 and Mer2 (Game, Zamb et al. 1980; Klapholz and Esposito 1980; Malone and Esposito 1981; Menees and Roeder 1989; Malone, Bullard et al. 1991; Ivanov, Korolev et al. 1992; Ajimura, Leem et al. 1993). In the DSB formation reaction Spo11 becomes attached the end of the DSB (Bergerat, de Massy et al. 1997; Keeney, Giroux et al. 1997). The MRX complex, which is required in both the DSB formation reaction and Spo11 processing reaction (Neale, Pan et al. 2005), is the first proteins involved in the checkpoint response (Lisby, Barlow et al. 2004). MRX recruits Tel1 by an interaction with Xrs2 (Nakada, Matsumoto et al. 2003). The presence of MRX and Spo11 bound at DNA ends causes activation of Tel1 (Fukunaga, Kwon et al. 2011) leading to phosphorylation of Mre11, Xrs2 and Sae2 (Usui, Ogawa et al. 2001; Cartagena-Lirola, Guerini et al. 2006). In backgrounds where Spo11 is not processed and removed from the end of the DSB (such as *rad50S* or *sae2Δ*), Tel1 becomes hyperactivated (Usui, Ogawa et al. 2001; Clerici, Mantiero et al. 2006).

Following Spo11 processing, the 5' to 3' resection by Exo1 creates a 3' ssDNA tail (Zakharyevich, Ma et al. 2010). RPA coats ssDNA preventing secondary structures from forming and protecting the DNA (Sung, Krejci et al. 2003; Neale and Keeney 2006). The DNA damage kinase Mec1 associates with its accessory protein Ddc2 and binds to the RPA (Zou and Elledge 2003). Rad51 and Dmc1 compete with RPA and form filaments for homology searching and strand exchange to take place (Sung, Krejci et al. 2003; Keeney and Neale 2006). In the *dmc1Δ* mutant, where repair does not take place and resection continues forming more ssDNA, Mec1 remains active (Zou and Elledge 2003).

The PCNA–like clamp consisting of Rad17, Ddc1 and Mec3 (also as the 9-1-1 complex) is recruited to DSBs independently of the recruitment of Mec1 (Kondo, Wakayama et al. 2001; Melo, Cohen et al. 2001; Majka and Burgers 2003). The Rad17-Ddc1-Mec3 DNA clamp is loaded onto the ssDNA by the Rad24 clamp loader, which consists of Rad24 and components of the replication factor C complex (Kondo, Wakayama et al. 2001; Melo, Cohen et al. 2001). The meiotic recombination checkpoint functions to phosphorylate the synaptonemal complex protein Hop1 (Carballo, Johnson et al. 2008). Phosphorylation of Hop1 causes phosphorylation of the Rad53 paralogue Mek1 (Carballo, Johnson et al. 2008). Both Hop1 and Mek1 phosphorylation are required to establish the inter-homologue repair required during meiosis (Niu, Wan et al. 2005; Niu, Li et al. 2007; Carballo, Johnson et al. 2008).

One target of Mek1 is the kinase Swe1, which is phosphorylated (Leu and Roeder 1999; Perez-Hidalgo, Moreno et al. 2003). Once phosphorylated, Swe1 in turn phsophsorylated Cdc28 at tyrosine 19 (Leu and Roeder 1999). This phosphorylation causes Cdc28 to become inactive. In addition to Swe1, another target of the meiotic recombination checkpoint is the transcription factor Ndt80 (Hepworth, Friesen et al. 1998). When active, the checkpoint prevents Ndt80 phosphorylation (Tung, Hong et al. 2000; Shubassi, Luca et al. 2003). In turn this prevents

Ndt80 from causing transcription of multiple genes required for the first meiotic division, one of which is clb1 which normally interacts with Cdc28 (Chu and Herskowitz 1998; Hepworth, Friesen et al. 1998). In *ndt80Δ* mutants it was observed that cells arrested at pachytene (Xu, Ajimura et al. 1995). DSB formation is normal in the *ndt80Δ* mutant but unable to repair with double Holliday junctions persisting (Allers and Lichten 2001). Another target of the meiotic recombination checkpoint is the transcriptional repressor Sum1 (Lindgren, Bungard et al. 2000). When the checkpoint is active Sum1 prevents transcription of Ndt80 (Lindgren, Bungard et al. 2000; Pak and Segall 2002).

1.11: Distribution of DSBs across the genome: recombination hotspots

Initial work carried out in the Szostak, localised a meiotic DSB site to a specific locus (Sun, Treco et al. 1989). Genetic observations of recombination between markers placed on different chromosomes also identified a preference for DSBs to form (Goldman and Lichten 1996). DSB distribution analysis of chromosome III highlighted regions within the chromosome that have a preference for meiotic DSB formation, termed meiotic hotspots (Baudat and Nicolas 1997). The analysis provided evidence of the meiotic hotspots identifying the uneven distribution along the chromosome and finding most hotspots within intergenic promoter containing regions (Baudat and Nicolas 1997). As Spo11 is covalently attached to the end of the DSB, it provides a marker for where DSB formation has occurred. Using the *rad50S* background, where DSBs accumulate in an unprocessed state (Alani, Padmore et al. 1990; Keeney and Kleckner 1995), after DNA shearing by sonication Spo11 was immunoprecipitated. By ligation of a primer and subsequent PCR, this template was a sequence specific map for DSB formation. Hybridisation to a microarray of 6,500 genes provided a profile of meiotic DSBs across the whole genome, supporting the observations seen at chromosome III (Gerton, DeRisi et al. 2000). In their review of meiotic recombination mapping, Pan and Keeney highlighted the

main problem with the southern blot and micro-array data: the use of the *rad50S* mutation (Pan and Keeney 2007). Although the *rad50S* mutation accumulated DSBs that are unprocessed and not resected, allowing accurate mapping of meiotic DSBs, observations from Dmc1 chromatin immunoprecipitation experiments identified additional regions where recombination was occurring but was not identified in the *rad50S* microarray data (Blat, Protacio et al. 2002; Pan and Keeney 2007). In addition, the *rad50S* microarray data was did not identify sites where recombination occurred in wildtype situations along chromosome III previously identified in the whole chromosome observations (Baudat and Nicolas 1997). The *dmc1Δ* background was used to perform a method to enrich for ssDNA (Blitzblau, Bell et al. 2007; Buhler, Borde et al. 2007). This ssDNA was then hybridised against a whole genome microarray, providing a map of genome wide DSBs. The *dmc1Δ* microarray data provided a more accurate representation of DSBs compared to the chromosome III data and identified DSB sites near the centromere and telomere that were previously absent in the *rad50S* background (Blitzblau, Bell et al. 2007; Buhler, Borde et al. 2007). Although the *dmc1Δ* mutation may provide more accurate meiotic DSB map, the use of the Spo11-oligonucleotide as a marker for meiotic DSB location is performed under otherwise wildtype conditions. This thereby removes problems created by using either the *rad50S/sae2Δ* or *dmc1Δ* backgrounds.

The Spo11-oligonucleotide complexes provide a molecular barcode of meiotic DSB formation within the oligonucleotide attachment. The Spo11-oligonucleotide is formed from the processing of the Spo11 protein and the DNA attachment is the specific sequence of the location where the DSB formed. Using the Spo11-oligonucleotides as a template, PCR amplification followed by next generation sequencing was used to provide a map for DSB formation (Pan, Sasaki et al. 2011). The map produced from the Spo11-oligonucleotide data indicated that a most meiotic DSBs form in promoter regions but Spo11-oligonucleotide signal was also detected from DSBs within open reading frames (Pan, Sasaki et al. 2011).

The obligate crossover, crossover homeostasis and crossover interference

Meiotic DSBs are repaired to form both non-crossover and crossover events. Crossovers are the important event in meiotic recombination to create a physical link between homologs. This physical link enables the accurate segregation of the homologs at the first meiotic division. It is therefore important to ensure that a crossover occurs between each homolog pair, known as the obligate crossover (Jones 1984). One model suggested to ensure that an obligate crossover occurs is the stress model (Kleckner, Zickler et al. 2004). In this model, it is suggested that mechanical stress is placed on a pair of sister chromatids which is relieved by the formation of a crossover (Kleckner, Zickler et al. 2004).

Tension allowing for correct segregation of the homologs, is formed by the crossover events that cause a link between two homologs. Although a crossover is required between a homolog pair, if another crossover event occurs, the tension is then reduced to form between the two crossover events. The mechanism of crossover interference means that when a crossover has formed, another crossover is prevented from forming in close proximity (Jones 1984). In *Saccharomyces cerevisiae* it has been observed that Dmc1 and Tid1 are required to ensure crossover interference (Shinohara, Sakai et al. 2003; Bishop and Zickler 2004). How crossover interference is determined is unknown, however in the stress model that ensures the obligate crossover occurs, it would suggest that the lack of stress caused by the formation of the obligate crossover therefore prevents an additional crossover from forming (Kleckner, Zickler et al. 2004).

The effect of crossover and non-crossover levels was investigated in hypomorphic versions of Spo11. Using a series of Spo11 hypomorphs which caused a reduction in DSB levels, both the

levels of crossovers and non-crossovers were measured (Martini, Diaz et al. 2006). Interestingly, in situations where total DSB formation is decreased, crossovers are maintained but the non-crossovers decrease. This mechanism termed crossover homeostasis has been proposed to ensure that the obligate crossover event occurs when DSB levels are reduced (Martini, Diaz et al. 2006).

1.12: Future questions

The ability to detect the Spo11-oligionucleotide complexes provides a new mechanism for determining DSB levels. Previously, DSB levels are determined by either DSB signal on southern blots or by genetic data looking at segregation of markers. With the Spo11-oligonucleotide complexes created proportional to the amount of DSBs that have formed and have been processed, the detected levels can be used as an indicator for DSB levels. To this extent, the Spo11-oligonucelotide assay can be used to determine whether Spo11 dependent DSBs form in DSB formation mutants, where previous assays have detected no DSBs.

Comparisons between the Spo11-oligonucleotide and DSB levels at points throughout meiosis were made and both the DSB and Spo11-oligonucleotides peaked at the same time (Neale, Pan et al. 2005). Although this might be expected, as the first appearance of a DSB is in a resected state with Spo11 having been endonucleolytically removed thereby forming the Spo11-oligonucleotides, the degradation of the Spo11-oligonucleotide complexes also matched the repair kinetics of the DSB. The similar kinetics of Spo11-oligonucleotide degradation and the repair of the DSB therefore suggested a mechanistic link between these processes. The ability to detect DSBs and the Spo11-oligonucleotide complexes allows investigations to occur to attempt to answer whether the observed correlation between DSB repair and Spo11-oligonucleotide complex degradation is co-incidental or mechanistic.

When comparing backgrounds that are unable to resect, such as a *rad50S* background, and a resection proficient background, DSBs signal migrates at different places on a southern blot. The difference in migration is due to the resection that has taken place and the decrease in size of the DNA molecule. Interestingly, in a wildtype background, DSBs migrate a certain distance which does not change over time. This observation suggests that there is some form

of resection control that functions to limit the amount of resection that takes place. The resection control may be due to a limitation in the amount of resection proteins available, physical barriers to resection or a mechanism that controls the exonucleases. Exo1 has been implicated as the resection mechanism during meiosis (Zakharyevich, Ma et al. 2010). One possible control mechanism may be inhibition of Exo1 by checkpoint machinery, due to hyper-resected DSBs being observed in checkpoint defective strains (Grushcow, Holzen et al. 1999; Shinohara, Sakai et al. 2003). If this is the case, this would be similar to resection control observed at telomeres (Morin, Ngo et al. 2008).

In this thesis I will investigate these questions.

CHAPTER 2:

Materials and methods

Chapter 2: Materials and methods

2.1.1: Bacterial growth

Luria Broth (LB): 1% Bacto-tryptone, 0.5% Yeast Extract, 1% NaCl pH 7.0

For LB plates, 2% Bacto Agar is added before autoclaving.

In order to make LB-Amp for selection of bacteria that have ampicillin resistance, ampicillin is added to a final concentration of 100µg/ml.

Bacteria is usually woken from -80°C storage and streaked onto LB/LB-Amp plates and grown at 37°C. After overnight growth, single colonies are inoculated into 1.5 ml LB/LB-Amp and grown overnight (16 hours) at 37°C.

2.1.2: Preparation of chemically competent DH5α cells

Bacteria is grown overnight in 5 ml LB at 37°C then inoculated into 600 ml LB and grown at 37°C until the OD_{600} is between 0.3 and 0.4. Cells are then chilled on ice for 15 minutes, pelleted for 5 minutes at 6,000 rpm at 4°C then supernatant is removed. Pellet is resuspended in 6 ml ice cold 1xTSS (10% PEG 3350, 5% DMSO, 20 mM $MgCl_2$), transferred into cold 1.5 ml tubes, flash frozen in liquid nitrogen and stored at -80°C.

2.1.3: Bacterial transformation

An aliquot of bacterial DH5α cells are removed from -80°C storage and put on ice to defrost for 20 minutes. Between 20 and 40µl are transferred to a 1.5 ml tube and the plasmid that is required to be transformed is added to the tube. The tube is flicked and then put on ice for 15

minutes. The mix is then heat shocked at 42°C for 90 seconds and then put on ice for between 5 and 15 minutes. The mix is then plated onto LB-Amp plates for selection of bacteria that has gained the plasmid.

2.1.4: Alkaline Isolation of plasmids from bacteria (Miniprep)

Starting with an overnight culture of 4 ml bacterial growth is spun down in 1.5 ml tubes for 1 minute at top speed. Supernatant is removed and resuspended in 100 µl TEG (0.9% Glucose, 25 mM Tris Base·HCl pH 7.5, 10 mM EDTA pH 8.0) (ice-cold) and left at room temperature for 5 minutes. 200 µl alkaline SDS (0.2 M NaOH, 1% SDS) is added and mixed then the tubes are left on ice for 5 minutes. 150 µl Potassium Acetate (3 M Potassium Acetate, 11.5% Glacial Acetic Acid) mix is added (ice-cold), the sample vortex and left on ice for a further 5 minutes. Tubes are spun down for 10 minutes at 4°C and 400 µl supernatant transferred to a new 1.5 ml tube. 300 µl 100% isopropanol is added to the tubes and inverted then left at room temperature for 5 minutes. Tubes are spun at top speed for 15 minutes at 4°C. Supernatant is aspirated then pellet is washed in 1 ml 70% ethanol. Tubes are spun for 10 minutes at 4°C then supernatant removed. The pellet is air dried for 15 minutes after which the pellet is resuspended in 40 µl TE RNAse (0.02 mg/ml RNAse A in 1xTE [10 mM Tris Base·HCl pH 8.0, 1 mM EDTA pH 8.0]).

2.2.1: Yeast growth

YPDAU*:* 1% BD Bacto Yeast Extract, 2% BD Bacto Peptone, 0.5 mM Adenine, 0.4 mM Uracil 20% D-Glucose

Yeast extract, peptone, adenine and uracil are added to 90% volume double distilled water and autoclaved. D-Glucose is added to a final concentration of 2% bringing the total final volume to

100%. For YPDAU plates, 2% Bacto Agar is added before autoclaving and the addition of D-glucose.

For genotyping strains and selecting for relevant markers, drop-out liquids and plates are made as follows:

0.675% Yeast Nitrogen Base with ammonium sulphate

2% Glucose

Addition of relevant amino acids to the final concentrations as listed below. For plates, 2% Bacto Agar is added before autoclaving.

Amino Acid	Final Concentration
Adenine Sulphate	0.02%
Arginine	0.02%
Aspartic Acid	0.1%
Histidine	0.02%
Leucine	0.06%
Lysine	0.03%
Methionine	0.02%
Phenylalanine	0.05%
Threonine	0.2%
Tryptophan	0.02%
Tyrosine	0.03%
Uracil	0.02%

For drug selection, YPDAU is prepared as documented and drugs are added to the final concentration as listed below. For plates, 2% Bacto Agar is added before autoclaving

Drug	Final Concentration
5-Fluoroorotic Acid Monohydrate (5-FOA)	1 mg/ml
Copper Sulphate	0.1 mM
Cycloheximide	1 µg/ml
G418-200	200 µg/ml
G418-400	400 µg/ml
Hygromycin	300 µg/ml
Nourseothricin-dihydrogen sulfate (Nat)	100 µg/ml

YPA: 1% BD Bacto Yeast Extract, 2% BD Bacto Peptone, 1% Potassium Acetate, 0.001% Sigma Antifoam 204

Sporulation Media: 2% Potassium Acetate, 5 µg/ml Adenine, 5 µg/ml Arginine, 5 µg/ml Histidine, 15 µg/ml Leucine, 5 µg/ml Tryptophan, 5 µg/ml Uracil, 0.001% Sigma Antifoam 204

2.2.2: Standard Yeast Meiosis Culture

Strains were woken up from -80°C storage, streaked onto YPDAU plates and incubated at 30°C for 2 days. A single colony was inoculated into 4 ml YPDAU, incubated at 30°C at 250 rpm for 24 hours. Cell density was measured and inoculated to a density of (OD_{600}) 0.2 into 250 ml YPA. The culture is incubated at 250 rpm at 30°C for between 13 ½ and 15 hours. Culture is then spun at 4°C at 6,000 g for 5 minutes, resuspended in 250 ml double distilled water, re-spun and then resuspended in 250 ml pre-warmed sporulation media. The culture is then incubated

at 30°C at 250 rpm for the duration of the time course with samples taken at relevant time points.

For usual meiotic time courses, 10 ml sample is used for genomic DNA preparation, 10 ml sample for TCA protein extraction, 1 ml for FACS analysis, 100 µl for DAPI nuclei staining and 100 µl for sporulation efficiency.

2.2.3: Yeast Transformation

4 ml of YPD is inoculated with cells and grown overnight. 50 ml of YPD is inoculated to a cell density (OD_{600}) of $5x10^6$ cells/ml and grown for 3 to 5 hours to a cell density of $2x10^7$ cells/ml. Cells are spun down for 5 minutes at 3,000g. Supernatant is poured off and pellet is resuspended in 25 ml water and spun again for 5 minutes at 3,000g. Water is poured off and pellet is resuspended in 1 ml of 100 mM lithium acetate, transferred to 1.5 ml tubes and spun for 1 minute. Lithium acetate is removed by aspiration and pellet is resuspended in 50 µl of 100 mM lithium acetate per transformation and 50 µl of mix is moved into 1.5 ml tubes. Tubes are spun down for 1 minute at top speed, lithium acetate removed and 360 µl transformation mix (33.3% PEG, 100 mM Lithium Acetate, 0.28 mg/ml single stranded DNA (salmon sperm), between 0.1-10 µg transformation DNA fragment) added to each tube. Tubes are vortex until pellet is fully resuspended then incubated at 30°C for 30 minutes. Tubes are transferred to 42°C for 30 minutes to heat shock cells then spun for 15-30 seconds at 6-8,000 rpm and transformation mix removed by aspiration. Pellets are resuspended in YPD and incubated for 1 hour to allow recovery. Cells are then spun down for 1 minute at 13,000 rpm, YPD aspirated and pellet resuspended in 100 µl water. Cells are then plated onto selection plates and grown for 2-4 days to allow recovery of transformants.

2.3: DAPI Nuclei Staining

100 µl of meiotic cell culture has 500 µl of 100% Methanol added to it and stored at -20°C until use. When ready for analysis, 10 µl of mix is dropped on a slide, allowed to dry and then 1 µl of 20 µg/ml DAPI dropped on. A cover slide is placed on top and cells are scored on a fluorescent microscope according to number of nuclei. A minimum of 200 cells are scored for each sample.

2.4: Fluorescent Activated Cell Sorting (FACS) Analysis

1 ml of meiotic culture is spun down and resuspended in 1 ml 70% ethanol then stored at -20°C until ready to process. Sample is spun down for 1 minute at 20,000g, supernatant aspirated and resuspended in 0.5 ml RNAse A (1 mg/ml RNAse A in 50 mM Tris Base·HCl pH7 .5). Sample is incubated at 37°C for 4 hours or overnight. Sample is spun down for 1 minute at 20,000g, aspirated, and resuspended in 0.5 ml proteinase K (2 mg/ml Proteinase K in 50 mM Tris Base·HCl pH 7.5). Sample is incubated for 1 hour at 60°C, spun down for 1 minute at 20,000g, aspirated and resuspended in 0.5 ml FACS storage buffer (200 mM Tris Base·HCl pH7 .5, 200 mM NaCl, 78 mM $MgCl_2$) and stored at 4°C indefinitely. On the day of processing, 5 ml BD FACS tubes have 1 ml propidium iodide (50 µg/ml Propidium Iodide in 50 mM Tris Base·HCl pH 7.5) added and 25 µl of cells stored in FACS storage buffer then sonicated at 20% amplitude for 7-10 seconds per sample. Samples are then processed on BD FACS Canto and FACS analysis carried out using BD FACS DIVA and WinMDI.

2.5: Genomic DNA Preparation

10 ml of meiotic culture is transferred to 1.5 ml tubes and resuspended in 0.5 ml spheroplasting buffer (1 M Sorbitol, 100 mM Sodium Phosphate Buffer pH 7.5, 100 mM EDTA,

1% 2-Mercaptoethanol, 0.25 mg/ml Zymolyase 100T). The mix is then incubated at 37°C for 30 minutes, 100 µl lysis buffer (3% SDS, 0.1 M EDTA, 1 mg/ml Proteinase K) added, mixed, and incubated at 60°C for 1 hour. Samples are cooled to room temperature and then 500 µl Phenol/Chloroform/Isoamyl alcohol (25:24:1) is added, vigorously mixed and then left to settle for 5 minutes. Samples are then re-mixed and then spun at 20,000 g for 5 minutes. 450 µl of the top aqueous phase is removed using a cut P1000 tip and pipette into a new 1.5 ml tube. 45 µl 3 M NaAc pH 5.2 is added, mixed and then 500 µl 100% Ethanol is added, mixed and spun for 1 minute at 20,000 g. Supernatant is aspirated, 1 ml 70% Ethanol is added to wash the pellet, spun for 1 minute, aspirated and air dried for 10 minutes. The pellet is then dissolved in 450 µl 1xTE (10 mM Tris Base·HCl pH 8.0, 1 mM EDTA pH 8.0) and incubated at 37°C for 1 hour to aid in dissolution. 50 µl 1 mg/ml RNAse A in 1xTE is added, mixed and incubated at 37°C for 1 hour. DNA is re-precipitated by adding 50 µl 3 M NaAc pH 5.2, mixing adding 1 ml 100% ethanol then mixing. Tube is spun for 1 minute at 20,000 g, supernatant aspirated and pellet washed in 70% ethanol then spun again for 1 minute at 20,000g. Pellet is air dried for 10 minutes and then dissolved in 100 µl 1xTE. To aid dissolution tube is incubated overnight at 4°C or at 37°C for 1 hour. For additional purification, 400 µl stop solution (0.5% SDS, 100 mM Tris Base·HCl pH 8.0, 10 mM EDTA) is added, mixed, and then incubated at 60°C for 30 minutes. 500 µl Phenol/Chloroform/Isoamyl alcohol is added, vigorously mixed and then left to settle for 5 minutes. Samples are then re-mixed and then spun at 20,000 g for 5 minutes. 450 µl of the top aqueous phase is removed using a cut P1000 tip and pipette into a new 1.5 ml tube. 45 µl 3 M NaAc pH 5.2 is added, mixed and then 800 µl 100% Ethanol is added, mixed and spun for 1 minute at 20,000g. Supernatant is aspirated, 1 ml 70% Ethanol is added to wash the pellet, spun for 1 minute, aspirated and air dried for 10 minutes. Pellet is air dried for 10 minutes and then dissolved in 100 µl 1xTE.

2.6: Southern Blot

Approximately 10 ng of DNA was digested overnight using enzyme as detailed in figure Additional enzyme was added and incubated at appropriate temperature for 4 hours.
A 0.7% 1xTAE (40 mM Tris Base, 20 mM glacial acetic acid, 1 mM EDTA pH 8.0) agarose gel with 50 µg/ml ethidium bromide was cast and 6x DNA loading dye (15% Ficoll 400, 0.25% Bromophenol Blue) was added to digested DNA, loaded into the gel and run with 1xTAE buffer at between 55 and 65 volts for varying times to best resolve the DNA fragments. Gel was then imaged using Syngene InGenius bioimaging system to check migration and then exposed to 1800J/m^2 UV in the Stratalinker. The gel was then soaked in three times its volume of denaturation solution (0.5 M Sodium Hydroxide, 1.5 M Sodium Chloride) for 30 minutes and then transferred to Bio-rad zetaprobe membrane by means of a vacuum at 50mBar for 2-3 hours. 50 ml of hybridisation mix (0.5 M Sodium Phosphate Buffer pH 7.2, 7% SDS, 1 mM EDTA, 1% BSA) was made up and incubated at 65°C. After transfer the membrane was washed in water three times and then crosslinked by exposing the membrane to 1200 J/m^2 UV in the Stratalinker. The membrane was then incubated at 65°C with 35 ml of hybridisation mix for 1 hour or more whilst the probe was made.
The probe was created from 50 ng of template DNA, 0.1 ng of NEB Lambda DNA digest with BstEII and water which was denatured by incubating at 100°C for five minutes then put on ice. Roche High Prime was added in addition to 0.5-3 mBq of α-^{32}P dCTP and incubated at 37°C for 15 minutes. 30 µl 1xTE (10 mM Tris Base·HCl pH 8.0, 1 mM EDTA pH 8.0) was added to the probe and then spun through a GE Healthcare G-50 spin column at 2,000 rpm for 2 minutes. The probe was then denatured by incubating at 100°C for five minutes and then put on ice. The probe was then added to the remaining 15 ml hybridisation mixture, the original 35 ml hybridisation mixture discarded off and the 15 ml containing the probe was added to the membrane and incubated at 65°C overnight.

After incubation, the membrane was washed five times with 100 ml pre-warmed southern wash buffer (1% SDS, 40 mM Sodium Phosphate Buffer, 1 mM EDTA) and exposed to phosphorscreen.

2.7: Spo11-oligonucleotide assay

After TCA extraction, 300 µl of SDS Extract has 300 µl 2x IP Buffer (2% TritonX100, 300 mM Sodium Chloride, 30 mM Tris Base·HCl pH 8.1, 2 mM EDTA) added to it in a 1.5 ml tube and mixed. 600 µl 1x IP Buffer is added to each tube along with 40 µl protein-G-agarose and 4 µl anti-HA antibody. Tubes are mixed and incubate at 4°C overnight (14 hours). Samples are then spun down for 30 seconds at 500g. Supernatant is aspirated and pellet washed in 1 ml 1x IP Buffer. Samples are spun down for 30 seconds at 1,000 g and supernatant removed and the wash and spin are repeated. Supernatant is aspirated and pellet resuspended in 1 ml 1x TKAc (20 mM Tris Acetate pH 7.9, 50 mM Potassium Acetate). Tubes are spun down for 30 seconds at 2,000 g and supernatant removed. The wash and spin is repeated and supernatant removed. 25 µl of radio-labeling mix (1x New England Biolabs Buffer 4, 0.25 mM $CoCl_2$, 0.4 Units/µl Fermentas TdT, 0.2 µCi/µl ^{32}P-alpha dCTP) is added per tube and incubated at 37°C for 2 hours. 1 ml of 1x IP Buffer is added to each tube and mixed to stop the reaction. Tubes are spun down for 15 seconds and supernatant removed. Pellets are resuspended in 50 µl 2x LB buffer (4% SDS, 100 mM Tris Base·HCl pH 6.8, 20% Glycerol, 1 mM EDTA, 0.05% Bromophenol Blue, 5% β-mercaptoethonal).

2.8: Sporulation Efficiency

100 µl meiotic culture taken at 24 hours and added to 500 µl 100% Methanol then stored at -20°C until ready to score. 6 µl of mix is added to a slide, cover slip placed on top, and then

scored under a microscope for cells that have not formed tetrads and those that have formed tetrads. Percentages are then calculated to form the sporulation efficiency.

2.9: TCA Protein Extraction

10 ml of meiotic cell culture pellet has approximately 300 µl 10% TCA added along with zirconium/silica beads up to the meniscus of the TCA. Three rounds of 30 seconds beat beating at 6,500 rpm with 2 minutes of chilling in an ice bath in between each round. Tubes are pierced using a flamed 25G needle, a 1.5 ml tube attached to the bottom of the lysis tube and spun for 1 minute at 500 g, separating the lysate and beads. Lysate is spun for 10 minutes at 20,000 g at 4°C. Supernatant is aspirated and pellet is resuspended in 300 µl 2x SDS extraction buffer (2% SDS, 0.5 M Tris Base·HCl pH 8.1, 10 mM EDTA, 0.005% Bromophenol Blue), fully mixed and an additional 300 µl SDS extraction buffer added and mixed. Sample is spun for 1 minute at 20,000 g and supernatant poured into new 1.5 ml tubes. Samples boiled at 95°C for 5 minutes then chilled on ice and finally stored at either -20°C or -80°C until use. When ready to use, samples are defrosted, mixed and then boiled at 95°C for 5 minutes and chilled on ice.

2.10: Tetrad Dissection

50 µl of sporulated cells in sporulation media is added to 150 µl 200 mM sodium phosphate buffer in a 1.5 ml tube. 1 µl of a 1 mg/ml zymolyase 100T (10 mM Sucrose, 0.7% Glucose, 1 mM HEPES pH 7.5, 1 mg Zymolyase 100T) dilution is added, tube flicked to resuspend and incubated at 37°C for 10-15 minutes. 10 µl of mix is then pipette on a YPD plate and left to dry before tetrads are dissect.

2.11: Western Blot

Make up the appropriate resolving gel using the acrylamide to the correct final percentage (gels are usually 7.5%), resolving buffer to a final concentration of 1x (375 mM Tris Base·HCl pH 8.8, 0.1% SDS), 0.1% ammonium persulfate and 0.01% TEMED. Pour into SDS PAGE casting kit and add 100% Isopropanol on top. Allow to set (approximately 30 minutes) and then pour off isopropanol and wash with distilled water. Make up appropriate stacking gel using the acrylamide, stacking buffer to a final concentration of 1x (125 mM Tris Base·HCl pH 6.8, 0.1% SDS), 0.1% ammonium persulfate and 0.02% TEMED. Place the comb in and allow the gel to set (approximately 15 minutes). Once set, remove the comb and wash the wells out with distilled water. Clamp the gel kit into the running apparatus and fill the chambers with 1x SDS Running Buffer (25 mM Tris Base, 200 mM Glycine, 0.5% SDS). Protein samples (in SDS Extraction Buffer [see 2.9]) should be added to 2x LB Buffer (4% SDS, 100 mM Tris Base·HCl pH 6.8, 20% Glycerol, 1 mM EDTA, 0.05% Bromophenol Blue, 5% β-mercaptoethonal) to end with a final concentration of 1x LB Buffer. Samples are boiled at 95°C for 5 minutes and then chilled on ice. Once chilled, samples can be added to the wells of the gel. The gel is then run until samples have migrated far enough. The apparatus is then disassembled and the gel is soaked in 1x CAPS transfer buffer (10 mM CAPS·NaOH pH 11, 10% Methanol). PVDF is activated in 100% methanol and then soaked in 1x CAPS Transfer buffer for 5 minutes. The gel is then 'captured' using the PVDF, placed in between Whatmann paper and setup within a wet transfer tank along with 1x CAPS transfer buffer. Protein transfer is setup and is run for approximately 1 hour at 100V (time and voltage can be adjusted for different proteins). The transfer apparatus is then dismantled and the PVDF washed in 1xTBST (25 mM Tris Base·HCl pH 7.5, 150 mM NaCl, 0.1% Tween-20). Membrane is then blocked by rotating in 5% non-fat dried milk in 1xTBST for 30 minutes. The milk is then poured off and exchanged for the primary antibody (at appropriate concentration) in 1xTBST for the appropriate amount of time. Afterwards, the

membrane is washed in 1xTBST for 5 minutes and then poured off. This is repeated for two more times. The secondary antibody (at appropriate concentration) in 1xTBST is then poured on the membrane and rotated for the appropriate amount of time. The antibody is then poured off and membrane is washed in 1xTBST for 5 minutes. This is then poured off and the wash repeated two more times. The ECL is then pipette over the membrane, left to incubate for 1 minute and then wrapped in saran and exposed to film for varying times (dependent upon signal).

2.12: Strain List

Strain Name	Strain Number	Genotype
wildtype	MJ6	ho::LYS2/', lys2/', ura3/', arg4-nsp/', leu2::hisG/', his4X::LEU2/', nuc1::LEU2/'
spo11-HA	MJ13	ho::LYS2/', lys2/', ura3/', arg4-nsp/', leu2::hisG/', his4X::LEU2/', nuc1::LEU2/', SPO11-HA3His6::KanMX4/'
spo11-Y135F-HA	MJ16	ho::LYS2/', lys2/', ura3/', arg4-nsp/', leu2::hisG/', his4X::LEU2/', nuc1::LEU2/', spo11(Y135F)-HA3His6::KanMX4/'
rec102Δ	SKY245	ho::LYS2/', ura3::hisG/', lys2/', leu2::hisG/', HIS4/', rec102Δ::URA3/', SPO11-HA3His6::KanMX4/'
rec104Δ	SKY398	ho::LYS2/', lys2/', ura3/', leu2::hisG/', rec104Δ/', SPO11-HA3His6::KanMX4/'
rec114Δ	SKY2300	ho::LYS2, ura3, lys2, leu2::hisG, SPO11-HA3His6::KanMX4, rec114Δ::KanMX4
mei4Δ	SKY389	ho::LYS2/', lys2/', ura3/', leu2-?/', nuc1Δ::LEU2/', mei4:: URA3/', SPO11-HA3His6::KanMX4/'
exo1Δ spo11-HA	MJ145	ho::LYS2/', lys2/', arg4-nsp/', leu2::hisG/', trp1::hisG/', his4X::LEU2/', nuc1::LEU2/', ura3::PGPD1GAL4(848)-ER::URA3/', SPO11-HA3His6::KanMX4/', exo1Δ::KanMX4/'
dmc1Δ spo11-HA	SG32	ho::LYS2/', lys2/', ura3/', leu2::hisG/', his4X::LEU2/', arg4-Nsp/', nuc1::LEU2/', dmc1Δ::LEU2/', SPO11-HA3His6::kanMX4/'

Strain Name	Strain Number	Genotype
rad24Δ dmc1Δ spo11-HA	SG29	ho::LYS2/', lys2/', ura3/', arg4-nsp/', leu2::hisG/', his4X::LEU2/', nuc1::LEU2/', dmc1Δ::LEU2/', rad24Δ::Hyg/', SPO11-HA3His6::KanMX4/'
mec1-mn spo11-HA	SG261	ho::LYS2/', lys2/', ura3/', arg4-nsp/', leu2::hisG/', his4X::LEU2/', nuc1::LEU2/', ade2-Bgl/ADE2', clb2-MEC1::KanMX4/', SPO11-HA3His6::KanMX4/',
tel1Δ spo11-HA	SG345	ho::LYS2/', lys2/', ura3/', arg4-nsp/', leu2::hisG/', his4X::LEU2/', nuc1::LEU2/', SPO11-HA3HIS6::KanMX4/', tel1Δ::HphMX4
mec1-mn tel1Δ spo11-HA	VG260	ho::LYS2/', lys2/', ura3/', arg4-nsp/', leu2::hisG/', his4X::LEU2/', nuc1::LEU2/', clb2-MEC1::KanMX4/', tel1Δ::Hyg/', SPO11-HA3His6::KanMX4/',
rad24Δ tel1Δ spo11-HA	SG199	ho::LYS2/', lys2/', ura3/', arg4-nsp/', leu2::hisG/', his4X::LEU2/', nuc1::LEU2/', rad24Δ::Hyg/', tel1Δ::Hyg/', SPO11-HA3His6::KanMX4/',
rad24Δ spo11-HA	SG69	ho::LYS2/', lys2/', ura3/', arg4-nsp/', leu2::hisG/', his4X::LEU2/', nuc1::LEU2/', SPO11-HA3His6::KanMX4/', rad24Δ::Hyg/'
dmc1Δ	SG147	ho::LYS2/', lys2/', ura3/', arg4-nsp/', leu2::hisG/', his4X::LEU2/', nuc1::LEU2/', dmc1Δ::LEU2/'
rad24Δ	SG150	ho::LYS2/', lys2/', ura3/', arg4-nsp/', leu2::hisG/', his4X::LEU2/', nuc1::LEU2/', rad24Δ::Hyg/'

Strain Name	Strain Number	Genotype
rad24Δ dmc1Δ	SG146	ho::LYS2/', lys2/', ura3/', arg4-nsp/', leu2::hisG/', his4X::LEU2/', nuc1::LEU2/', dmc1Δ::LEU2/', rad24Δ::Hyg/'
rad24Δ dmc1Δ spo11-HA isolate 2	SG263	ho::LYS2/', lys2/', ura3/', arg4-nsp/', leu2::hisG/', his4X::LEU2/', nuc1::LEU2/', dmc1Δ::LEU2/', rad24Δ::Hyg/', SPO11-HA3His6::KanMX4
rad24Δ dmc1Δ spo11-HA isolate 3	SG274	ho::LYS2/', lys2/', ura3/', arg4-nsp/', leu2::hisG/', his4X::LEU2/', nuc1::LEU2/', dmc1Δ::LEU2/', rad24Δ::Hyg/', MEK1-3HA::URA3/', SPO11-HA3His6::KanMX4/'
rad17Δ	SG181	ho::LYS2/', lys2/', ura3/', leu2::hisG/', his3::hisG?/', his4X::LEU2/', nuc1Δ::LEU2/', rad17Δ::natMX/'
rad17Δ spo11-HA	SG187	ho::LYS2/', lys2/', ura3/', arg4-nsp/ARG4, leu2::hisG/', his3::hisG?/', his4X::LEU2/', nuc1::LEU2/', rad17Δ::natMX/', SPO11-HA3His6::KanMX4/',
rad17Δ dmc1Δ	SG177	ho::LYS2/', lys2/', ura3/', ARG4/arg4-nsp, his3::hisG?/', his4X::LEU2/', nuc1::LEU2/', rad17Δ::natMX/', dmc1Δ::LEU2/',
rad17Δ dmc1Δ spo11-HA	SG180	ho::LYS2/', lys2/', ura3/', arg4-nsp/', leu2::hisG/', his3::hisG?/', his4X::LEU2/', nuc1::LEU2/', rad17Δ::natMX/', dmc1Δ::LEU2/', SPO11-HA3His6::KanMX4/'
mec1-mn	SG286	ho::LYS2/', lys2/', ura3/', arg4-nsp/', leu2::hisG/', his4X::LEU2/', nuc1::LEU2/', ade2-Bgl/ADE2, clb2-MEC1::KanMX/'

Strain Name	Strain Number	Genotype
mec1-mn dmc1Δ	SG283	ho::LYS2/', lys2/', ura3/', arg4-nsp/', leu2::hisG/', his4X::LEU2/', nuc1::LEU2/', dmc1Δ::HphMX/', clb2-MEC1::KanMX/'
mec1-mn dmc1Δ spo11-HA	SG258	ho::LYS2/', lys2/', ura3/', arg4-nsp/', leu2::hisG/', his4X::LEU2/', nuc1::LEU2/', clb2-MEC1::KanMX4/', SPO11-HA3His6::KanMX4/', dmc1Δ::HphMX/'
rad24Δ rad51Δ dmc1Δ	SG243	ho::hisG/', lys2/', ura3/', arg4-nsp/', leu2::hisG/', his4X::LEU2/', nuc1::LEU2/', dmc1Δ::LEU2/', rad24Δ::Hyg/', rad51Δ::hisG-URA3-hisG/',
rad24Δ rad51Δ dmc1Δ spo11-HA	SG242	ho::LYS2/', lys2/', ura3/', arg4-nsp/', leu2::hisG/', his4X::LEU2/', nuc1::LEU2/', dmc1Δ::LEU2/', rad24Δ::Hyg/', rad51Δ::hisG-URA3-hisG/', SPO11-HA3His6::KanMX4/',
sae2Δ	MJ315	ho::LYS2/', lys2/', ura3/', arg4-nsp/', leu2::hisG/', his4X::LEU2/', nuc1::LEU2/', sae2Δ::KanMX6/'
sae2Δ spo11-HA	MJ10	ho::LYS2/', lys2/', ura3/', arg4-nsp/', leu2::hisG/', his4X::LEU2/', nuc1::LEU2/', sae2Δ::KanMX6/', SPO11-HA3His6::KanMX4/'
sae2Δ rad24Δ	SG103	ho::LYS2/', lys2/', ura3/', arg4-nsp/', leu2::hisG/', his4X::LEU2/', nuc1::LEU2/', rad24Δ::Hyg/', sae2Δ::KanMX/',
sae2Δ rad24Δ spo11-HA	SG237	ho::LYS2/', lys2/', ura3/', arg4-nsp/', leu2::hisG/', his4X::LEU2/', nuc1::LEU2/', SPO11-HA3His6::KanMX4/', rad24Δ::Hyg/', sae2Δ::KanMX/',

Strain Name	Strain Number	Genotype
rad51Δ dmc1Δ spo11-HA	SG268	ho::LYS2/', lys2/', ura3/', arg4-nsp?ARG4?/', leu2::hisG/', his4X::LEU2/', nuc1::LEU2/', rad51Δ::hisG-URA3-hisG/', dmc1Δ::HphMX/', SPO11-HA3His6::KanMX4/'
mek1Δ rad51Δ dmc1Δ spo11-HA	SG291	ho::LYS2/', lys2/', ura3/', arg4-nsp?ARG4?/', leu2::hisG/', his4X::LEU2/', nuc1::LEU2/', rad51Δ::hisG-URA3-hisG/', dmc1Δ::HphMX/', mek1Δ::URA3/', SPO11-HA3His6::KanMX4/',
ndt80Δ rad24Δ rad51Δ dmc1Δ spo11-HA	SG350	ho::LYS2/', lys2/', ura3/', leu2::hisG/', his3::hisG? HIS3?/', his4X::LEU2/', nuc1::LEU2/', ndt80Δ::HphMX4/', rad24Δ::HpHMX4/', dmcΔ::LEU2/', rad51Δ::hisG-URA3-hisG/', SPO11-HA3His6::KanMX4/',
sae2Δ spo11-D290A-HA	MJ482	ho::LYS2/', lys2/', ura3/', ARG4/arg4-nsp, leu2-?/', his4-?::LEU2/', nuc1::LEU2/', sae2Δ::KanMX6/', spo11(D290A)-HA3His6::KanMX4/'
dmc1Δ spo11-D290A-HA	SG297	ho::LYS2/', lys2/', ura3/', arg4-nsp/', leu2-? or leu2::hisG/', his4X(or B)::LEU2/', spo11(D290A)-HA3His6::KanMX/', dmc1Δ::HphMX/'
rad24Δ dmc1Δ spo11-D290A-HA	SG300	ho::LYS2/', lys2/', ura3/', arg4-nsp/', leu2-? or leu2::hisG/', his4X(or B)::LEU2/', spo11(D290A)-HA3His6::KanMX/', rad24Δ::HphMX/', dmc1Δ::LEU2/'

Strain Name	Strain Number	Genotype
sae2Δ spo11-Y135F-HA/spo11-HA	SG483	ho::LYS2/', lys2/', ura3/', ARG4/arg4-nsp, leu2-?/leu2::hisG, his4-?::LEU2/his4X::LEU2, nuc1::LEU2/', sae2Δ::KanMX6/', spo11(D290A)-HA3His6::KanMX4/spo11(Y135F)-HA3His6::KanMX4
dmc1Δ spo11-Y135F-HA/spo11-HA	SG306	ho::LYS2/', lys2/', ura3/', arg4-nsp/', leu2::hisG/', his4X::LEU2/', nuc1::LEU2/', SPO11-HA3His6::kanMX4/spo11(Y135F)-HA3His6::KanMX, dmc1Δ::HphMX/dmc1Δ::LEU2,
rad24Δ dmc1Δ spo11-Y135F-HA/spo11-HA	SG307	ho::LYS2/', lys2/', ura3/', arg4-nsp/', leu2::hisG/', his4X::LEU2/', nuc1::LEU2/', SPO11-HA3His6::kanMX4/spo11(Y135F)-HA3His6::KanMX, dmc1Δ::LEU2/', rad24Δ::HphMX/'
tel1Δ sae2Δ	SG346	ho::LYS2/', lys2/', ura3/', arg4-nsp or bgl?/', leu2::hisG or leu2Δ?/', his4X::LEU2/', nuc1::LEU2/', tel1Δ::HphMX4/', sae2Δ::KanMX6/'
tel1Δ sae2Δ spo11-HA	SG347	ho::LYS2/', lys2/', ura3/', arg4-nsp/', leu2::hisG/', his4X::LEU2/', nuc1::LEU2/', SPO11-HA3HIS6::KanMX4/', sae2Δ::KanMX6/', tel1Δ::HphMX4/'
tel1Δ	SG344	ho::LYS2/', lys2/', ura3/', arg4-nsp/', leu2::hisG/', his4X::LEU2/', nuc1::LEU2/', tel1Δ::HphMX4
tel1Δ dmc1Δ	SG343	ho::LYS2/', lys2/', ura3/', arg4-nsp/', leu2::hisG/', his4X::LEU2/', nuc1::LEU2/', dmc1Δ::HphMX/', tel1Δ::HphMX/',

Strain Name	Strain Number	Genotype
tel1Δ dmc1Δ spo11-HA	SG340	ho::LYS2/', lys2/', ura3/', arg4-nsp/', leu2::hisG/', his4X::LEU2/', nuc1::LEU2/', dmc1Δ::HphMX/', tel1Δ::HphMX/', SPO11-HA3His6::KanMX4/',
rad24Δ tel1Δ	SG386	ho::LYS2/', lys2/', ura3/', arg4-nsp/', leu2::hisG/', his4X::LEU2/', nuc1::LEU2/', rad24Δ::Hyg/', tel1Δ::Hyg/',
sae2Δ rad24Δ tel1Δ	SG355	ho::LYS2/', lys2/', ura3/', arg4-nsp/', leu2::hisG/', his4X::LEU2/', nuc1::LEU2/', rad24Δ::Hyg/', tel1Δ::Hyg/', sae2Δ::KanMX4/',
sae2Δ rad24Δ tel1Δ spo11-HA	SG358	ho::LYS2/', lys2/', ura3/', arg4-nsp/', leu2::hisG/', his4X::LEU2/', nuc1::LEU2/', rad24Δ::Hyg/', tel1Δ::Hyg/', sae2Δ::KanMX4/', SPO11-HA3His6::KanMX4/'
sae2Δ mek1Δ	SG370	ho::LYS2/', lys2/', ura3/', arg4-nsp/', leu2::hisG/', his4X::LEU2/', nuc1::LEU2/', mek1Δ::URA3/', sae2Δ::KanMX/',
sae2Δ mek1Δ spo11-HA	SG373	ho::LYS2/', lys2/', ura3/', arg4-nsp/', leu2::hisG/', his4X::LEU2/', nuc1::LEU2/', mek1Δ::URA3/', sae2Δ::KanMX/', SPO11-HA3His6::KanMX4/'
sae2Δ mek1Δ tel1Δ	SG385	ho::LYS2/', lys2/', ura3/', arg4-nsp/', leu2::hisG/', his4X::LEU2/', nuc1::LEU2/', mek1Δ::URA3/', sae2Δ::KanMX/', tel1Δ::Hyg/',
sae2Δ mek1Δ tel1Δ spo11-HA	SG382	ho::LYS2/', lys2/', ura3/', arg4-nsp/', leu2::hisG/', his4X::LEU2/', nuc1::LEU2/', mek1Δ::URA3/', sae2Δ::KanMX/', tel1Δ::Hyg/', SPO11-HA3His6::KanMX4/'

Strain Name	Strain Number	Genotype
exo1Δ	SG190	ho::LYS2/', lys2/', ura3/', arg4-nsp?Δ?/', leu2::hisG/', his4X::LEU2/', nuc1::LEU2/', exo1Δ::KanMX4/'
sgs1-mn	SG193	ho::LYS2/', lys2/', ura3/', arg4-nsp?Δ?/', leu2::hisG/', his4X::LEU2/', nuc1::LEU2/', natMX::pCLB2::3HA::SGS1/',
exo1Δ sgs1-mn	SG196	ho::LYS2/', lys2/', ura3/', arg4-nsp?Δ?/', leu2::hisG/', his4X::LEU2/', nuc1::LEU2/', exo1Δ::KanMX4/', natMX::pCLB2::3HA::SGS1/',
rad24Δ exo1Δ spo11-HA	SG72	ho::LYS2/', lys2/', ura3/', arg4-nsp/', leu2::hisG/', his4X::LEU2/', nuc1::LEU2/', SPO11-HA3His6::KanMX4/', exo1Δ::KanMX4/', rad24Δ::Hyg/'
rad24Δ exo1Δ	SG173	ho::LYS2/', lys2/', ura3/', arg-nsp?Δ?/', leu2::hisG/', his4X::LEU2/', nuc1Δ::LEU2/', rad24Δ::Hyg/', exo1Δ::KanMX4/'
rad24Δ sgs1-mn	SG153	ho::LYS2/', lys2/', ura3/', arg-nsp?Δ?/', leu2::hisG/', his4X::LEU2/', nuc1Δ::LEU2/', rad24Δ::Hyg/', natMX::pCLB2::3HA::SGS1/'
rad24Δ exo1Δ sgs1-mn	SG185	ho::LYS2/', lys2/', ura3/', arg-nsp?Δ?/', leu2::hisG/', his4X::LEU2/', nuc1Δ::LEU2/', rad24Δ::Hyg/', exo1Δ::KanMX4/', natMX::pCLB2::3HA::SGS1/'

CHAPTER 3:

Investigating the formation and processing of meiotic double-strand breaks using the Spo11-oligonucleotide repair product

3.1: Investigating DSB formation using Spo11-oligonucleotides

3.1.1: Introduction

Ten proteins are required for formation of meiotic DSBs in *Saccharomyces cerevisiae*: Spo11 (Klapholz, Waddell et al. 1985), Ski8 (Malone, Bullard et al. 1991), Mre11 (Ajimura, Leem et al. 1993), Rad50 (Game, Zamb et al. 1980; Malone and Esposito 1981), Xrs2 (Ivanov, Korolev et al. 1992), Rec102 (Malone, Bullard et al. 1991), Rec104 (Malone, Bullard et al. 1991), Rec114 (Malone, Bullard et al. 1991), Mei4 (Menees and Roeder 1989) and Mer2 (Malone, Bullard et al. 1991) (Keeney 2001). These proteins were identified by focusing on mutants that allowed rescue of the *spo13Δ* spore inviability (Malone and Esposito 1981; Klapholz, Waddell et al. 1985), sometimes in the presence of the *rad52Δ* mutation (Game, Zamb et al. 1980; Menees and Roeder 1989; Malone, Bullard et al. 1991; Ivanov, Korolev et al. 1992). The ability to rescue the *spo13Δ* mutation was due to a lack of meiotic recombination and this observation was supported by a lack of recombination occurring between genetic markers. Meiotic DSB levels as measured by southern blot also indicated a lack of meiotic DSB formation (Ivanov, Korolev et al. 1992). The assays mentioned all provide evidence that meiotic recombination is defective in the meiotic DSB formation mutant strains, but are not able to determine whether the strains are completely deficient in DSB formation. For example, although the s*po13Δ* spore viability increased when combined with a DSB formation protein, the viability levels did not return to wildtype levels (Malone and Esposito 1981; Klapholz, Waddell et al. 1985; Menees and Roeder 1989; Malone, Bullard et al. 1991; Ivanov, Korolev et al. 1992). This indicates that either Spo13 has another function during meiosis which causes a secondary decrease in spore viability, or that meiotic recombination is still occurring at a low, (currently undetected) level. The reduction in recombination between genetic markers also indicated a decrease in meiotic recombination but due to the relatively low abundance of markers throughout the genome, a

low level of recombination may remain undetected. DSBs detected by southern blotting are limited by the detection ability of the assay and DSBs under approximately 10% of wildtype signal are difficult to detect. It is therefore possible that meiotic DSBs form in meiotic DSB formation mutants, but at a low, currently undetected, level.

Discovery of Spo11-oligonucleotides has provided an independent assay for measuring processed meiotic DSBs. Spo11-oligonucleotides are created as a by-product of repair and are produced proportionally to the amount of DSBs that are formed (Neale, Pan et al. 2005). Therefore detection of Spo11-oligonucleotide levels can be used to measure the number of meiotic DSBs that form. Preliminary investigations in the Neale lab have illustrated that the Spo11-oligonucleotide assay has an extremely sensitive detection capability.

Using whole cell lysate preparations, different titrations of *spo11-HA* whole cell lysate was spiked in to s*po11-Y135F-HA* lysate. *Spo11-Y135F-HA* is defective in DSB formation (Bergerat, de Massy et al. 1997; Diaz, Alcid et al. 2002) therefore only the *spo11-HA* spiked in is capable of producing Spo11-oligonucleotide signal. The results from the titration experiment identified the ability to detect just 0.1% of *spo11-HA* spiked into the *spo11-Y135F-HA* lysate. With the ability to detect a signal 1,000-fold lower than wildtype, it means that even if DSB levels were reduced to one DSB per cell (approximately 200 fold lower than wildtype) this would still be detected. The Spo11-oligonucleotide assay is therefore capable of detecting a much lower DSB level than previously described assays and can be used to determine if any meiotic DSBs form in the meiotic DSB formation mutants. In order to carry out the Spo11-oligonucelotide assay, the spo11-HA tagged form was crossed into DSB formation mutants.

3.1.2: Spo11-oligonucleotides levels are below 0.5% of wildtype in DSB formation proteins.

To perform the assay, strains were woken from -80°C storage and allowed to grow on YPDAU agar plates. Following two days growth, one colony of each strain was inoculated into YPDAU and grown overnight. Strains were then inoculated into large scale pre-sporulation YPA cultures (200ml) to the same cell density. After overnight growth, cultures were washed and transferred to sporulation media (2% potassium acetate) causing the cells to begin meiosis. Samples were taken at 4 hours, the peak of DSB signal and Spo11-oligonucleotide signal (Neale, Pan et al. 2005). Following TCA protein extraction (see section 2.9), immunoprecipitation of HA tagged proteins was performed. The samples were then treated with terminal transferase and radioactive nucleotides causing the addition of detectable signal onto the 3' end of any DNA molecules. Labeled samples were washed to remove residual unincorporated nucleotides and then run on an SDS-PAGE gel causing separation of the Spo11-oligonucleotides according to size. Finally transfer to PVDF membrane (for western blotting) and exposure to a phosphor-screen allows detection of the Spo11-oligonucleotide signal.

Spo11-oligonucleotide levels were measured in the *rec102Δ*, *rec104Δ*, *rec114Δ* and *mei4Δ* mutants. The amount of signal in the mutants was compared to wildtype control (*spo11-HA*) and a standard containing *spo11-Y135F-HA* lysate with 0.5% *spo11-HA* lysate spiked in. In the *spo11-HA* lanes, two strong bands of equal intensity migrating at the correct position for Spo11-oligonucleotides were detected (figure 3.1.1). In the *spo11-Y135F-HA* with 0.5% *spo11-HA* lysate spiked in, two bands consistent with Spo11-oligonucleotides were detected at a lower intensity. These observations indicate that 0.5% of *spo11-HA* signal spiked into the *spo11-Y135F-HA* strain is detectable in these gels. In contrast to the *spo11-HA* and the *spo11-Y135F-HA* with 0.5% *spo11-HA* lysate spiked in, the *rec102Δ spo11-HA, rec104Δ spo11-HA, rec114Δ spo11-HA* and *mei4Δ spo11-HA* strains did not produce any detectable signal in any

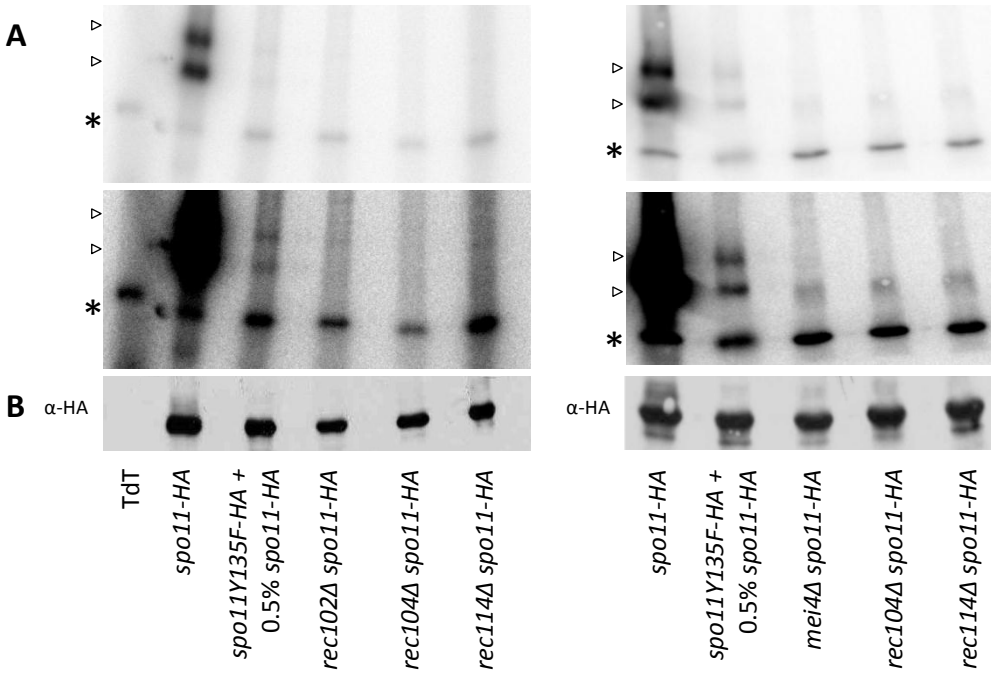

Figure 3.1.1: Spo11-oligonucleotides are not detected in DSB formation mutants. A) Spo11-oligonucleotide blots. TCA Extracts from meiotic cultures were immuno-precipitated (IP) and end labelled according to the Spo11-oliognucleotide assay (see materials and methods section 2.7). Samples were run on a 7.5% SDS PAGE for 1 hour 30 minutes at 150 volts, transferred to PVDF at 0.65 amps for 1 hour and exposed to phosphor screens. Light and darker contrast images are displayed. Open triangles (▹) mark upper and lower Spo11-oligonucleotide species. Asterisk (*) marks non-specific terminal transferase (TdT) band. **B)** Western blot of the Spo11-oligonucleotide blot. 1:10,000 Santa Cruz antibody with HRP conjugate was used against the HA epitope attached to Spo11 and exposed to film.

lane consistent with Spo11-oligonucleotides. These observations suggest that, if Spo11-oligonucleotides are produced in these mutants, it is at a level lower than 0.5% of wildtype.

An alternative explanation for the lack of Spo11-oligonucleotide signal in the *rec102Δ spo11-HA, rec104Δ spo11-HA, rec114Δ spo11-HA* and *mei4Δ spo11-HA* strains is that there was a problem with the cultures and that Spo11 was not expressed. To ensure that this was not the case, Spo11-HA levels were detected by western blotting the Spo11-oligonucleotide membrane. Spo11-HA was detected in all lanes (figure 3.1.1B) indicating that this is not the case.

3.1.3: Discussion

Previous analysis of mutants defective in meiotic DSB formation has relied upon assays which do not have the detection ability to rule out low levels of DSB formation. The Spo11-oligonucleotide assay is a genome wide measure of meiotic DSB formation events which has an exquisitely low detection capability, with the ability to detect as low as 0.1%, or in these gels 0.5% of *spo11-HA* signal. With approximately 200 meiotic DSBs forming within each wildtype cell, this assay potentially provides the capability to detect events as rare as one DSB per cell.

The experiments within this section have demonstrated that the *rec102Δ, rec104Δ, rec114Δ* and *mei4Δ* mutants do not produce 0.5% of wildtype Spo11-oligonucleotides or greater. Further experiments to develop these findings would be to perform the Spo11-oligonucleotide assay on the remaining DSB formation mutants (excluding the *spo11Δ* mutant). The results from these experiments would give insight as to whether all DSB formation proteins are completely required for DSB formation.

Spo11-oligonucleotide complexes are created proportional to the number of DSBs formed. In mutants that are have a reduction in DSBs, the level of recombination between genetic markers and southern blotting techniques have been used to determine the actual levels of DSBs formed. In *hop1Δ* and *red1Δ* mutants for example, the DSB levels are estimated to be approximately 10% of wildtype DSBs (Hollingsworth and Byers 1989; Mao-Draayer, Galbraith et al. 1996). This level of DSBs is at the extreme of detection by southern blotting and the observed DSB level focused on one meiotic recombination locus. The detection of Spo11-oligonucleotides in *hop1Δ* and *red1Δ* in comparison to wildtype could therefore enable a more accurate determination of genome wide DSB levels for these mutants.

The ability to detect Spo11-oligonucleotides in *Saccharomyces cerevisiae* has also enabled investigations into whether similar molecules exist in other organisms. So far, Spo11-oligonucleotide complexes have been discovered in *Schizosaccharomyces pombe* (as Rec12-oligonucleotides) (Milman, Higuchi et al. 2009) and mouse (Neale, Pan et al. 2005). This assay therefore provides the basis for detecting Spo11-oligonucleotide complexes in different organisms and enables investigations into the similarities and differences.

The ability to detect and measure levels of Spo11-oligonucleotide complexes therefore provides a wide range of scope for investigations both within *Saccharomyces cerevisiae* and across organisms.

3.2: What is the relationship between Spo11-oligonucleotide degradation and DSB repair?

3.2.1: Introduction

DSBs are formed by Spo11, which becomes covalently attached to the 5' DSB ends (Keeney, Giroux et al. 1997) (figure 3.2.1D). For repair to take place, Spo11 must be removed from the DSB end. Spo11 is removed by Mre11-dependent endonucleolytic cleavage creating Spo11-oligonucleotide complexes (Neale, Pan et al. 2005).

Spo11-oligonucleotide signals peak when DSB signals are maximal (Neale, Pan et al. 2005) (figure 3.2.1C). This may be expected as Spo11-oligonucleotides are formed as a by-product of DSB repair. Interestingly the degradation of the Spo11-oligonucleotide matched the kinetics of DSB repair. This observation led to the hypothesis that the repair of DSBs and the degradation of Spo11-oligonucleotides are mechanistically linked (figure 3.2.1). If the hypothesis is true, delaying DSB repair might be expected to affect the rate of Spo11-oligonucleotide degradation. However, if the rate of Spo11-oligonucleotide degradation and DSB repair is merely co-incidental, delaying repair will have no effect on Spo11-oligonucleotide degradation.

Following the removal of Spo11, the DSB ends are resected (Szostak, Orr-Weaver et al. 1983; Sun, Treco et al. 1989). Exo1 is the main exonuclease that resects the 5' DSB end during meiosis, creating single-stranded DNA (ssDNA) overhangs of 500-1500 nucleotides in length (Zakharyevich, Ma et al. 2010). When *EXO1* function is removed, DSB repair is delayed (Zakharyevich, Ma et al. 2010). The ssDNA created by resection is bound by the meiosis-specific recombinase, Dmc1, which catalyses strand invasion with homologous DNA sequences on the homologous chromosome (Bishop, Park et al. 1992). Mutating Dmc1 prevents repair

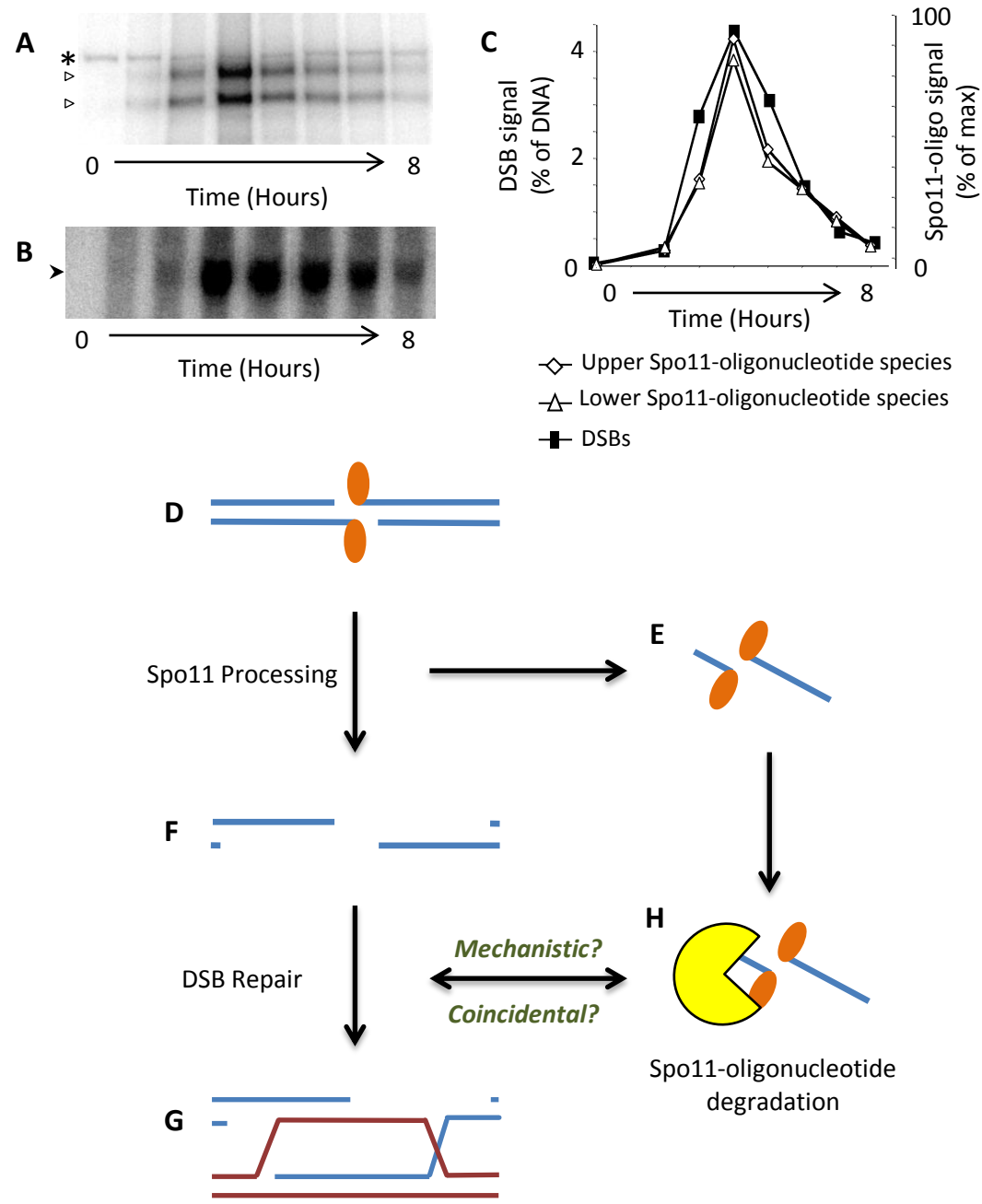

Figure 3.2.1: DSB repair and Spo11-oligonucleotide degradation may be mechanistically linked because of similar kinetics. A) Spo11-oligonucleotide blot from Neale, Pan et al. 2005 demonstrating Spo11-oligonucleotide signal over time. The asterisk (⁎)marks non-specific TdT band. Spo11-oligonucleotide species are indicated by the open arrow heads (▹). **B)** A southern blot of signal at the DSB1 site at the *HIS4::LEU2* hotspot. **C)** From Neale, Pan et al. 2005. A plot of DSB signal and Spo11-oligonucleotide against time indicating the similar formation and degradation kinetics. **D)** DSBs are formed by Spo11 which become covalently attached to the DSB end. Endonucleolytic cleavage of Spo11 forms Spo11-oligonucleotides **(E).** The processed DSB end can undergo resection **(F)** and strand invasion **(G)**, creating crossover and non-crossover events. As DSB repair occurs, Spo11-oligonucleotide degradation takes place, highlighting the possibility of a mechanistic link between DSB repair and Spo11-oligonucleotide degradation.

causing DSBs to accumulate with long ssDNA ends (Bishop, Park et al. 1992; Tsubouchi and Ogawa 2000). Because *exo1Δ* and *dmc1Δ* mutations cause a defect in DSB repair, they delay or halt the repair process. Therefore if the degradation of Spo11-oligonucleotides is mechanistically linked to the DSB repair process, then delaying repair by introducing the *exo1Δ* or *dmc1Δ* mutations will also cause a delay in Spo11-oligonucleotide degradation. If however the *exo1Δ* and *dmc1Δ* mutations have no effect on Spo11-oligonucleotide degradation, then the observed link with DSB repair is co-incidental.

3.2.2: Spo11-oligonucleotide kinetics were altered in *exo1Δ spo11-HA* compared to *spo11-HA*

In the Spo11-oligonucleotide assay Spo11 is immuno-precipitated. This stage can be carried out by using the *spo11-HA* tagged form. Therefore the *exo1Δ* mutation was introduced into the *spo11-HA* background. Hourly samples were taken from synchronised meiotic cultures. Samples were used for genomic DNA preparation and southern blotting enabling DSB levels to be measured at the *HIS4::LEU2* locus. *HIS4::LEU2* is a recombination hotspot with two DSB sites separated with 2.4Kb that has high likelihood of forming DSBs during meiosis. In *spo11-HA*, DSB signals first appear at 2 hours and peak at 4 hours (figure 3.2.2A and C). By contrast in *exo1Δ spo11-HA*, DSB signals were increased at 3 hours and from 5-11 hours (figure 3.2.2A and C). The increased signal suggests that DSBs persist for longer in the *exo1Δ spo11-HA* background, consistent with published data regarding *exo1Δ* (Zakharyevich, Ma et al. 2010).

The Spo11-oligonucleotide assay was performed using total protein samples from the meiotic time course used for genomic DNA preparation and *HIS4::LEU2* analysis. To compensate for small differences in cell density between cultures, the cell density of each strain was measured and adjusted to give approximately the same number of cells in each sample. The Spo11-oligonucleotide assay requires a radio-labelling stage. To control for potential variations at this step *spo11-HA* and *exo1Δ spo11-HA* samples were processed on the same day using the same reagents and directly compared. In s*po11-HA*, the Spo11-oligonucleotides signal first appeared at 2 hours and peaked at 4 hours (figure 3.2.2B and D). By contrast, in *exo1Δ spo11-HA* the abundance of Spo11-oligonucleotides were greater than *spo11-HA* from 2 hours to 9 hours (figure 3.2.2B and D). Furthermore, the curve of the Spo11-oligonucleotide peak was less sharp and lasted longer in the *exo1Δ spo11-HA* strain. The increased Spo11-oligonucleotide signal suggests that either more Spo11-oligonucleotides are formed or Spo11-oligonucleotides persist for longer in the *exo1Δ spo11-HA* mutant. The DSBs formed in the *exo1Δ spo11-HA*

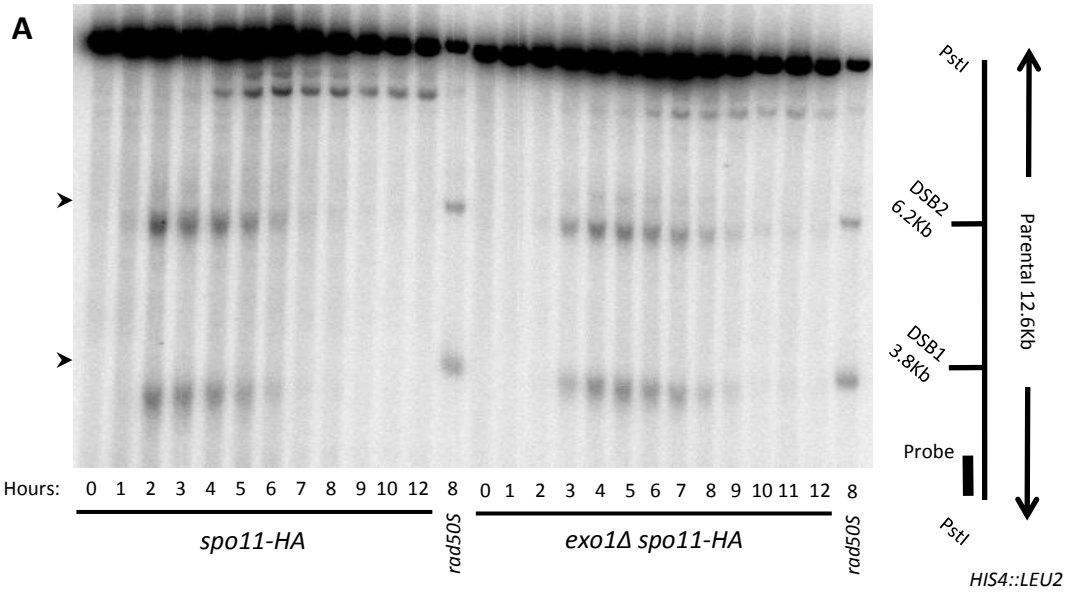
A
PstI
DSB2
6.2Kb
DSB1
3.8Kb
Parental 12.6Kb
Probe
PstI
HIS4::LEU2
Hours: 0 1 2 3 4 5 6 7 8 9 10 12 8 0 1 2 3 4 5 6 7 8 9 10 11 12 8
spo11-HA
rad50S
exo1Δ spo11-HA
rad50S

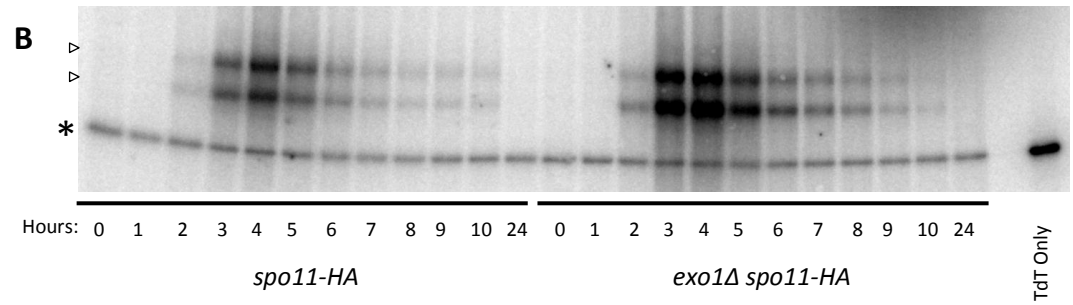
B
Hours: 0 1 2 3 4 5 6 7 8 9 10 24 0 1 2 3 4 5 6 7 8 9 10 24
spo11-HA
exo1Δ spo11-HA
AlwNI DTL

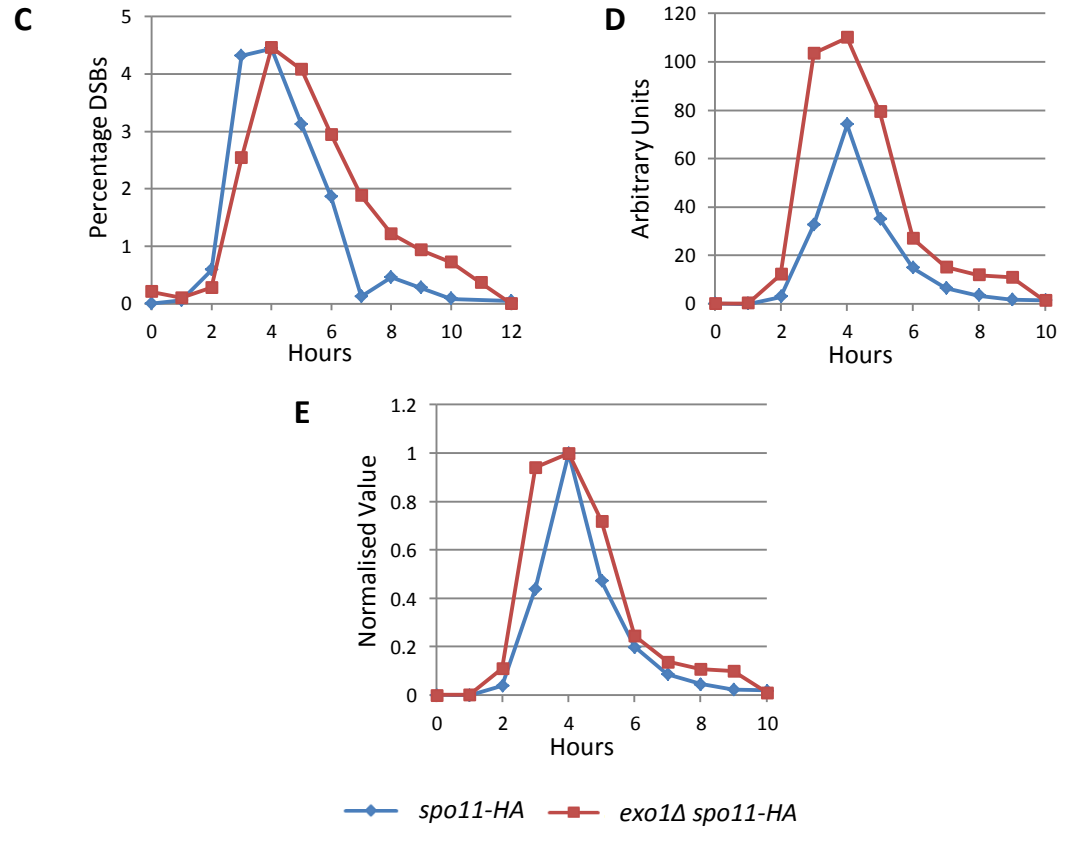
C
Percentage DSBs
Hours
D
Arbitrary Units
Hours
E
Normalised Value
Hours
spo11-HA
exo1Δ spo11-HA

Figure 3.2.2: DSB and Spo11-oligonucleotide levels are affected in *exo1Δ spo11-HA* compared to *spo11-HA*. A) Southern blot of DSBs at the *HIS4::LEU2* hotspot. Meiotic time courses were performed for the *spo11-HA* and the *exo1Δ spo11-HA* strains and samples were taken at the marked times. Genomic DNA was extracted, digested and run on a 0.7% TAE agarose gel for 20 hours at 60 volts. The gel was transferred to nylon membrane under denaturing conditions and hybridised with a radioactive probe for the *HIS4::LEU2* locus. The membrane was exposed to a phosphor screen and image taken using a Fuji phosphor scanner. DSBs marked with arrowhead (➢) mark DSBs. **B)** TCA Extracts from the same meiotic cultures were immunoprecipitated (IP) and end labeled according to the Spo11-oliognucleotide assay (see 2.7). Samples were run on a 7.5% SDS PAGE for 1 hour 30 minutes at 150 volts, transferred to PVDF at 0.65 amps for 1 hour and exposed to phosphor screens. Open triangles (▷) mark upper and lower Spo11-oligo species. Asterisk (*) marks non-specific terminal transferase (TdT) band. **C)** Quantification of DSB levels over time. Image Gauge was used to analyse DSB signal as a percentage of total DNA and signal is plotted and displayed. **D)** Quantification of total Spo11-oligonucleotide signal from both species using Image Gauge is displayed. **E)** Quantified signal from the Spo11-oligonucleotide blot (B), with values normalized to the maximum signal.

background (and consistent with the *exo1Δ* phenotype (Zakharyevich, Ma et al. 2010)) persist for longer, instead of forming more DSBs. This observation indicates that the increased Spo11-oligonucleotide signal detected in the *exo1Δ spo11-HA* is not a consequence of more DSBs and therefore is due to increased Spo11-oligonucleotide persistence.

To confirm that the differences in DSB and Spo11-oligonucleotide signal between *spo11-HA* and *exo1Δ spo11-HA* were not due to a difference in culture synchronicity, samples were processed by fluorescent activated cell sorting (FACS). FACS measures the efficiency and progression of DNA replication, and is a way of assessing meiotic cell cycle progression. In the *spo11-HA* culture over half the cells had undergone pre-meiotic S phase by 2 hours and almost two thirds by 3 hours (figure 3.2.3). The *exo1Δ spo11-HA* strain has a slight increase (between 2.8% and 5.3%) in the number of cells which have undergone S phase at 2, 3 and 4 hours (figure 3.2.3). The small difference between *exo1Δ spo11-HA* and *spo11-HA* is unlikely to account for the large increase in Spo11-oligonucleotide signal. The FACS data suggests that the differences seen in the abundance of Spo11-oligonucleotides in *spo11-HA* and *exo1Δ spo11-HA* is not due to asynchronous cultures.

To investigate if *exo1Δ* mutation affected early meiotic protein expression, samples were processed for Western blotting to measure their relative abundance. In the *spo11-HA* strain, Spo11-HA is present between 2 and 7 hours, peaking at 4 hours (figure 3.2.4). By contrast, in the *exo1Δ spo11-HA* strain Spo11-HA was detected between 2 hours and 10 hours with maximal intensity observed at 3 and 4 hours (figure 3.2.4A). Therefore *exo1Δ spo11-HA* has an increased persistence of Spo11-HA protein.

The abundance of the synaptonemal complex proteins Zip1 and Hop1 was also assessed. In both *spo11-HA* and *exo1Δ spo11*-HA, Zip1 was present between 2 and 5 hours with the

spo11-HA

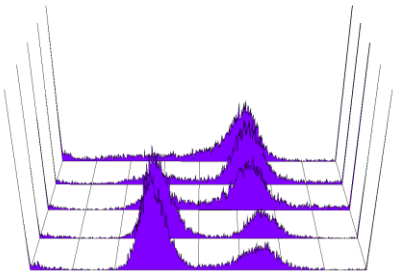

Time (Hours)	Percentage Cells with 2n
0	26.9
1	26.0
2	55.0
3	65.7
4	68.7

exo1Δ spo11-HA

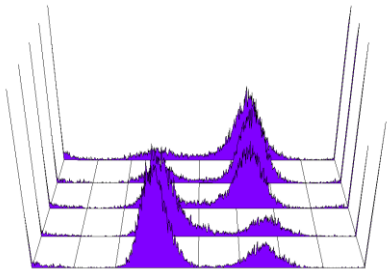

Time (Hours)	Percentage Cells with 2n
0	21.4
1	22.3
2	58.9
3	71.0
4	71.5

Figure 3.2.3: FACS analysis of *spo11-HA* and *exo1Δ spo11-HA* strains indicate similar S-phase kinetics. Samples from meiotic time courses used to analyse DSB levels and Spo11-oligonucleotide levels were fixed in 70% ethanol and stored at -20°C. Samples were then treated to remove protein and RNA, sonicated and DNA stained. FACS data collection was carried out on the Becton Dickinson FACS Canto with 10,000 events being scored and plotted for each time point. Analysis of the collected data was carried out by BD FACS Diva and WinMDI.

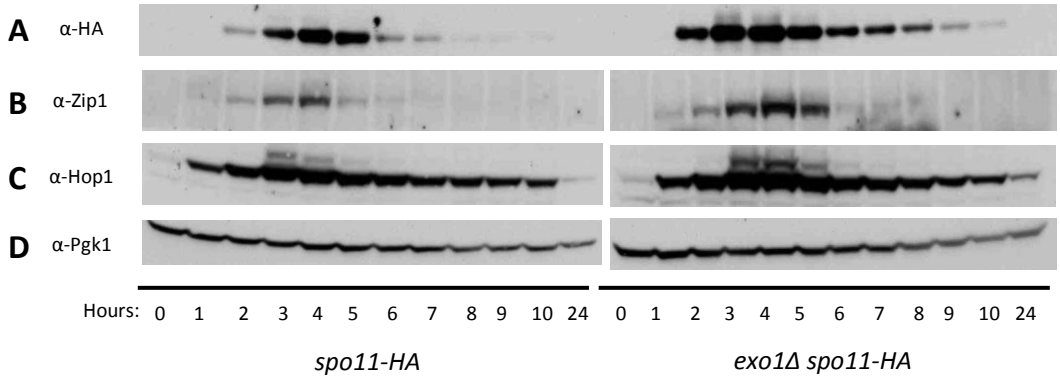

Figure 3.2.4: *exo1Δ spo11-HA* has prolonged protein expression or modification compared with *spo11-HA*. A) Western blot of the Spo11-oligonucleotide blot. 1:10,000 Santa Cruz antibody with HRP conjugate was used against the HA epitope attached to Spo11 and exposed to film. **B)** Western blot against Zip1. Anti-Zip1 (courtesy of Eva Hoffman) was used at 1 in 2,000 concentration followed by a secondary anti-rabbit antibody used at 1 in 3,000 concentration. **C)** Western blot against Hop1 (courtesy of Franz Klein) used at 1 in 4,000 concentration followed by a secondary anti-rabbit antibody used at 1 in 3,000 concentration. **D)** Western blot against the Pgk1 loading control (Invitrogen) used at 1 in 50,000 concentration followed by a secondary anti-mouse antibody used at 1 in 4,000 concentration.

maximal signal at 4 hours (figure 3.2.4B). *exo1Δ spo11-HA* had a stronger signal than *spo11-HA* suggesting a greater abundance and longer persistence of Zip1 (figure 3.2.4B). Hop1 protein was detected from 1 hour into the time-course (figure 3.2.4C). Phosphorylated Hop1 (a marker of unrepaired DSBs (Carballo, Johnson et al. 2008)) was detected at 3 and 4 hours in the *spo11-HA* background, but persisted for one hour longer in the *exo1Δ spo11-HA* background (figure 3.2.4C). Both Zip1 and phosphorylated Hop1 levels suggests that *exo1Δ spo11-HA* causes an increased persistence in early meiotic proteins. To confirm that the difference was not due to uneven loading between samples, blots were re-probed for Pgk1. Pgk1 is expressed at consistent levels throughout meiosis (Chambers, Tsang et al. 1989) allowing it to be used to distinguish differences in loading between samples. The Pgk1 loading control suggests even loading in each lane and between strains (figure 3.2.4D). Therefore the *exo1Δ* mutation causes longer persistence of DSBs, Spo11-oligonucleotides and early meiotic proteins.

3.2.3: Spo11-oligonucleotide kinetics were altered in *dmc1Δ spo11-HA* compared with *spo11-HA*

Removal of *DMC1* function prevents repair causing an accumulation of DSBs (Bishop, Park et al. 1992). Therefore an alternative way to test if Spo11-oligonucleotide degradation and DSB repair is mechanistically linked is by using the *dmc1Δ* mutation. The *dmc1Δ* mutation was introduced into the spo11-HA background to test the effect on Spo11-oligonucleotide degradation. In *spo11-HA* DSBs first appeared at 2 hours and peaked at 4 hours (figure 3.2.5A and C). By contrast, in *dmc1Δ spo11-HA* DSB levels continued to increase until 6 hours where DSB signal plateaued at approximately 17% and remained high for the 7 and 8 hour time points (figure 3.2.5A and C). The accumulated DSB signal in the *dmc1Δ spo11-HA* is consistent with published observations (Bishop, Park et al. 1992).

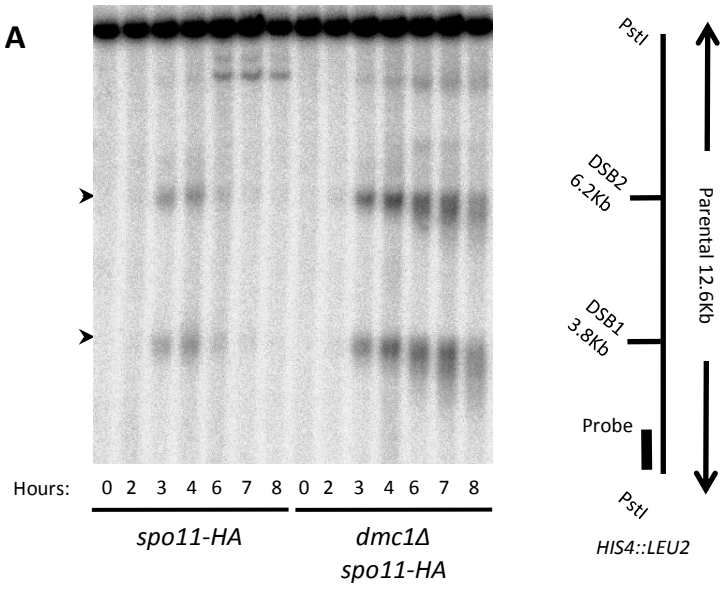
A
PstI
DSB2
6.2Kb
DSB1
3.8Kb
Probe
PstI
Parental 12.6Kb
HIS4::LEU2
Hours: 0 2 3 4 6 7 8 0 2 3 4 6 7 8
spo11-HA
dmc1Δ
spo11-HA

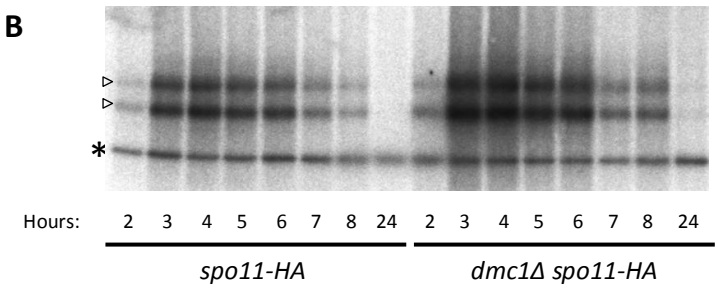
B
Hours: 2 3 4 5 6 7 8 24 2 3 4 5 6 7 8 24
spo11-HA
dmc1Δ spo11-HA

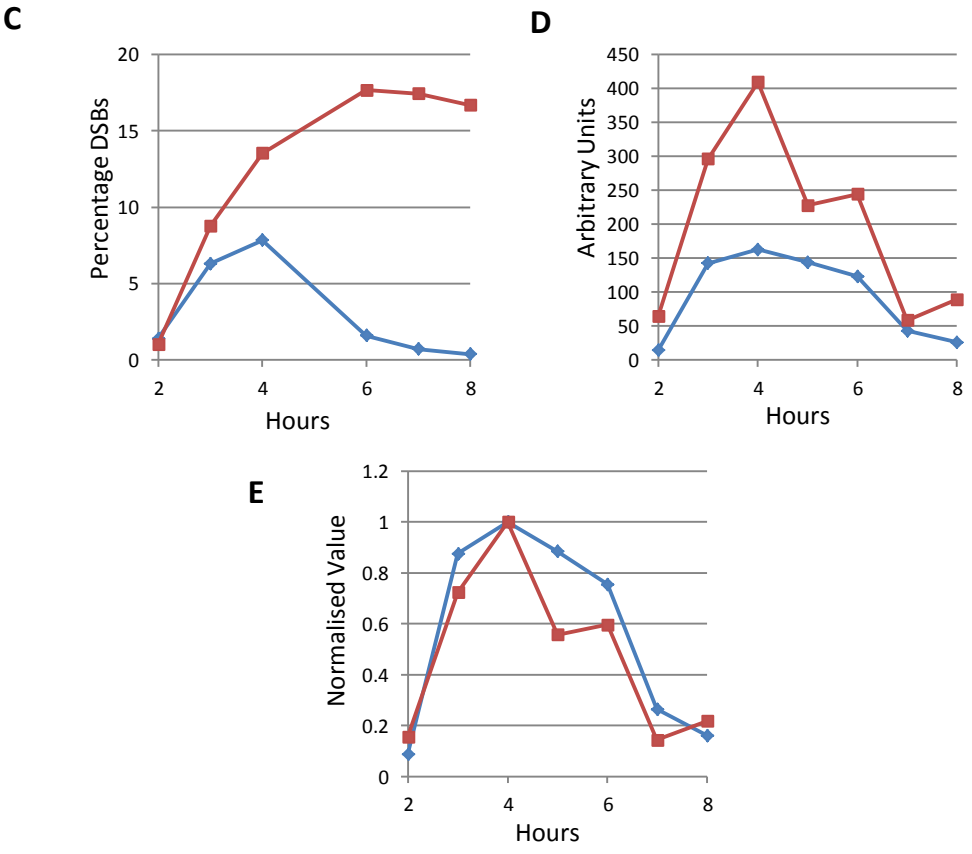
C
Percentage DSBs
Hours
D
Arbitrary Units
Hours
E
Normalised Value
Hours
spo11-HA
dmc1Δ spo11-HA

Figure 3.2.5: DSB and Spo11-oligonucleotide levels are affected in *dmc1Δ spo11-HA* compared to *spo11-HA*. A) Southern blot of DSBs at the *HIS4::LEU2* hotspot. Meiotic time courses were performed for the *spo11-HA* and the *dmc1Δ spo11-HA* strains and samples were taken at the marked times. Genomic DNA was extracted, digested and run on a 0.7% TAE agarose gel for 20 hours at 60 volts. The gel was transferred to nylon membrane under denaturing conditions and hybridised with a radioactive probe for the *HIS4::LEU2* locus. The membrane was exposed to a phosphor screen and image taken using a Fuji phosphor scanner. DSBs marked with arrowhead (➤) mark DSBs. **B)** TCA Extracts from the same meiotic cultures were immunoprecipitated (IP) and end labeled according to the Spo11-oliognucleotide assay (see 2.7). Samples were run on a 7.5% SDS PAGE for 1 hour 30 minutes at 150 volts, transferred to PVDF at 0.65 amps for 1 hour and exposed to phosphor screens. Open triangles (▷) mark upper and lower Spo11-oligo species. Asterisk (*) marks non-specific terminal transferase (TdT) band. **C)** Quantification of DSB levels over time. Image Gauge was used to analyse DSB signal as a percentage of total DNA and signal is plotted and displayed. **D)** Quantification of total Spo11-oligonucleotide signal from both species using Image Gauge is displayed. **E)** Quantified signal from the Spo11-oligonucleotide blot (B), with values normalized to the maximum signal.

Spo11-oligonucleotide levels were measured using protein samples from the same meiotic time course used for genomic DNA preparation and *HIS4::LEU2* analysis. In s*po11-HA*, the signal of Spo11-oligonucleotides first appeared at 2 hours and peaked at 4 hours with signal remaining high for 5 and 6 hour samples then decreasing (figure 3.2.5B and D). By contrast, in *dmc1Δ spo11-HA* the abundance of Spo11-oligonucleotides were greater than *spo11-HA* throughout the time course, peaking over 2.5 times higher at 4 hours (figure 3.2.5B and D). The increased Spo11-oligonucleotide signal suggests that either the Spo11-oligonucleotides persist for longer or more Spo11-oligonucleotides exist. The *dmc1Δ* mutation causes an accumulation of DSBs (Bishop, Park et al. 1992) as opposed to an increase in the DSBs that form. This observation suggests that the increased Spo11-oligonucleotide signal is a due to increased Spo11-oligonucleotide persistence caused by the *dmc1Δ* mutation. This observation is consistent with a DSB repair defect affecting Spo11-oligonucleotide degradation.

To confirm that these differences were not due to a difference in culture synchronicity, samples were processed for FACS analysis. In the *spo11-HA* culture almost half the cells had undergone pre-meiotic S phase by 2 hours and almost 80% by 4 hours (figure 3.2.6). The *dmc1Δ spo11-HA* strain has a slight increase (between 1.1% and 2.6%) in the number of cells which have undergone S phase at 2, 3 and 4 hours (figure 3.2.6). The small difference between *dmc1Δ spo11-HA* and *spo11-HA* is unlikely to account for the large increase in Spo11-oligonucleotide signal. The FACS data suggests that the differences seen in the abundance of Spo11-oligonucleotides in *spo11-HA* and *dmc1Δ spo11-HA* is not due to cultures that are asynchronous.

dmc1Δ spo11-HA protein samples were used to measure the abundance of early meiotic proteins. In the *spo11-HA* strain, Spo11-HA protein is present from 3 hours to 7 hours peaking at 4 hours (figure 3.2.7A). By contrast, in the *dmc1Δ spo11-HA* strain Spo11-HA is present from

spo11-HA

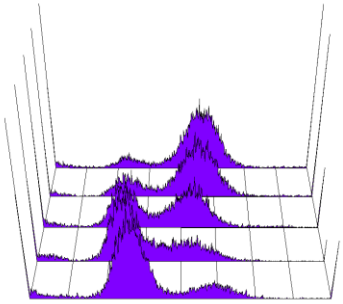

Time (Hours)	Percentage Cells with 2n
0	23.4
1	31.4
2	49.6
3	71.2
4	78.5

dmc1Δ spo11-HA

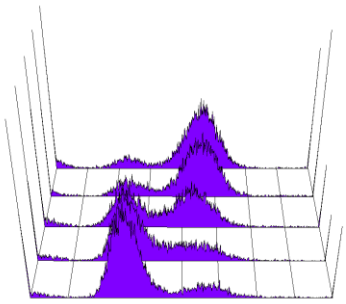

Time (Hours)	Percentage Cells with 2n
0	19.6
1	30.9
2	51.4
3	73.8
4	79.6

Figure 3.2.6: FACS analysis of *spo11-HA* and *dmc11Δ spo11-HA* strains indicate similar S-phase kinetics. Samples from meiotic time courses used to analyse DSB levels and Spo11-oligonucleotide levels were fixed in 70% ethanol and stored at -20°C. Samples were then treated to remove protein and RNA, sonicated and DNA stained. FACS data collection was carried out on the Becton Dickinson FACS Canto with 10,000 events being scored and plotted for each time point. Analysis of the collected data was carried out by BD FACS Diva and WinMDI.

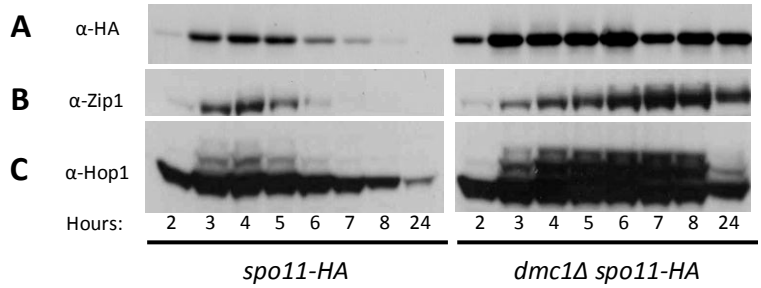

Figure 3.2.7: Prolonged protein expression or modification is observed in the *dmc1Δ spo11-HA* strain compared with *spo11-HA*. A) Western blot of the Spo11-oligonucleotide blot. 1:10,000 Santa Cruz antibody with HRP conjugate was used against the HA epitope attached to Spo11 and exposed to film. **B)** Western blot against Zip1. Anti-Zip1 (courtesy of Eva Hoffman) was used at 1 in 2,000 concentration followed by a secondary anti-rabbit antibody used at 1 in 3,000 concentration. **C)** Western blot against Hop1 (courtesy of Franz Klein) used at 1 in 4,000 concentration followed by a secondary anti-rabbit antibody used at 1 in 3,000 concentration.

2 hours onwards with high levels observed even at 24 hours (figure 3.2.7A). The *dmc1Δ spo11-HA* mutation therefore causes persistent Spo11-HA. Lack of *DMC1* function caused accumulation of immature synaptonemal complex structures (Bishop, Park et al. 1992). It would therefore be expected to observe persistent Zip1 protein. In the *spo11-HA* background Zip1 protein appeared between 3 and 6 hours, peaking at 4 hours (figure 3.2.7B). By contrast, in the *dmc1Δ spo11-HA* strain Zip1 was present from 3 hours to the end of the time course, with Zip1 protein increasing in abundance as the time course progresses (figure 3.2.7B). *dmc1Δ spo11-HA* therefore causes accumulation and persistence of Zip1 protein, consistent with expectations of prior work.

Persistent phosphorylated Hop1 protein has previously been observed in the *dmc1Δ* background (Carballo, Johnson et al. 2008). In the *spo11-HA* strain, Hop1 was detected from 2 hours to 24 hours (figure 3.2.7C). Phosphorylated Hop1 (the marker of unrepaired DSBs) was present between 3 and 6 hours (figure 3.2.7C). By contrast, in *dmc1Δ spo11-HA,* Hop1 was present throughout and phosphorylated Hop1 was observed from 3 hours (figure 3.2.7C). *dmc1Δ spo11-HA* therefore causes persistent phosphorylated Hop1, consistent with previously published observations regarding *dmc1Δ* (Carballo, Johnson et al. 2008). To conclude, *dmc1Δ spo11-HA* causes persistent DSBs, longer persisting Spo11-oligonucleotides and the persistence of early meiotic proteins.

3.2.4: Spo11-oligonucleotide levels were decreased in a checkpoint defective background

Removal of Exo1 causes a delay in meiotic progression and removal of Dmc1 causes meiotic progression to halt (Bishop, Park et al. 1992; Zakharyevich, Ma et al. 2010). The halt to progression is a result of the meiotic recombination checkpoint which prevents cell cycle progression until DSBs have been repaired (Lydall, Nikolsky et al. 1996). Thus the persistence in

Spo11-oligonucleotide signal observed in *exo1Δ spo11-HA* and *dmc1Δ spo11-HA* might be due to increased checkpoint activity. Rad24 is required for the meiotic recombination checkpoint (Lydall, Nikolsky et al. 1996). Along with RFC proteins, Rad24 acts as a clamp loader, loading Rad17-Mec3-Ddc1 onto the single stranded DNA (Majka and Burgers 2003) . Mec1 (human ATR), a DNA damage sensor that initiates a signal transduction pathway preventing cell cycle progression, also functions in the meiotic recombination checkpoint (Lydall, Nikolsky et al. 1996). Mutation of Rad24, Rad17 or Mec1 causes a bypass of the checkpoint (Lydall, Nikolsky et al. 1996).

To test whether the increased Spo11-oligonucleotide persistence observed in the *dmc1Δ spo11-HA* strain is due to longer checkpoint activity, the *rad24Δ* mutation was introduced. DSB levels measured in a *rad24Δ dmc1Δ* strains are at least as high as a *dmc1Δ* mutant (Lydall, Nikolsky et al. 1996). However, in the *rad24Δ dmc1Δ spo11-HA* strain DSBs were detected from 2 hours and plateaued at only around 4% of total DNA until the end of the time course (figure 3.2.8A and C). The DSB levels detected are below those observed in the *spo11-HA* strain and around 4 fold lower than *dmc1Δ spo11-HA*. The reduced DSB levels are unexpected considering the published levels for the *rad24Δ dmc1Δ* strain (Lydall, Nikolsky et al. 1996) and the predicted persistence of DSBs at a high level.

Spo11-oligonucleotides are produced proportionally to the DSBs that form. Therefore a decrease in DSBs will impact upon the Spo11-oligonucleotide signal. The Spo11-oligonucleotide signal was present from the start of the time course at 2 hours and peaked at 4 hours (figure 3.2.8B and D). In the *rad24Δ dmc1Δ spo11-HA* the detected signal was lower than those observed in *spo11-HA* and *dmc1Δ spo11-HA*. The decrease in Spo11-oligonucleotide signal is consistent with the decrease in DSB level.

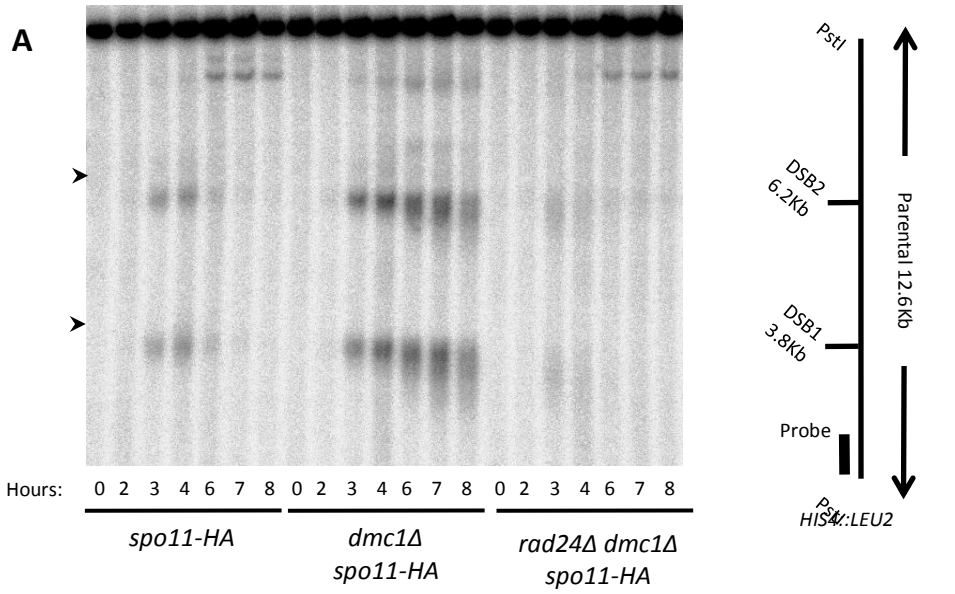
A
Hours: 0 2 3 4 6 7 8 0 2 3 4 6 7 8 0 2 3 4 6 7 8
spo11-HA
dmc1Δ spo11-HA
rad24Δ dmc1Δ spo11-HA
PstI
DSB2 6.2Kb
DSB1 3.8Kb
Probe
Parental 12.6Kb
HIS4:LEU2

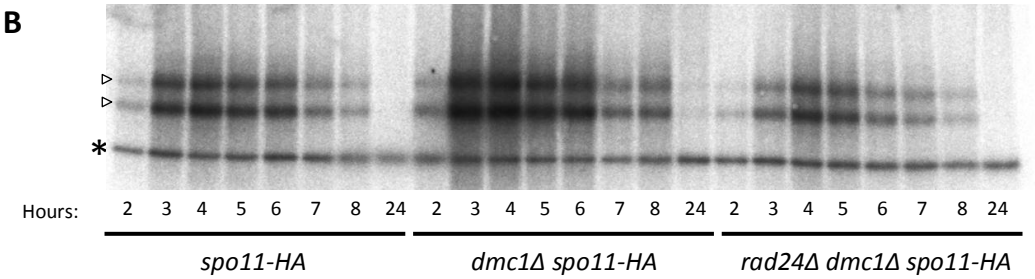
B
Hours: 2 3 4 5 6 7 8 24 2 3 4 5 6 7 8 24 2 3 4 5 6 7 8 24
spo11-HA
dmc1Δ spo11-HA
rad24Δ dmc1Δ spo11-HA

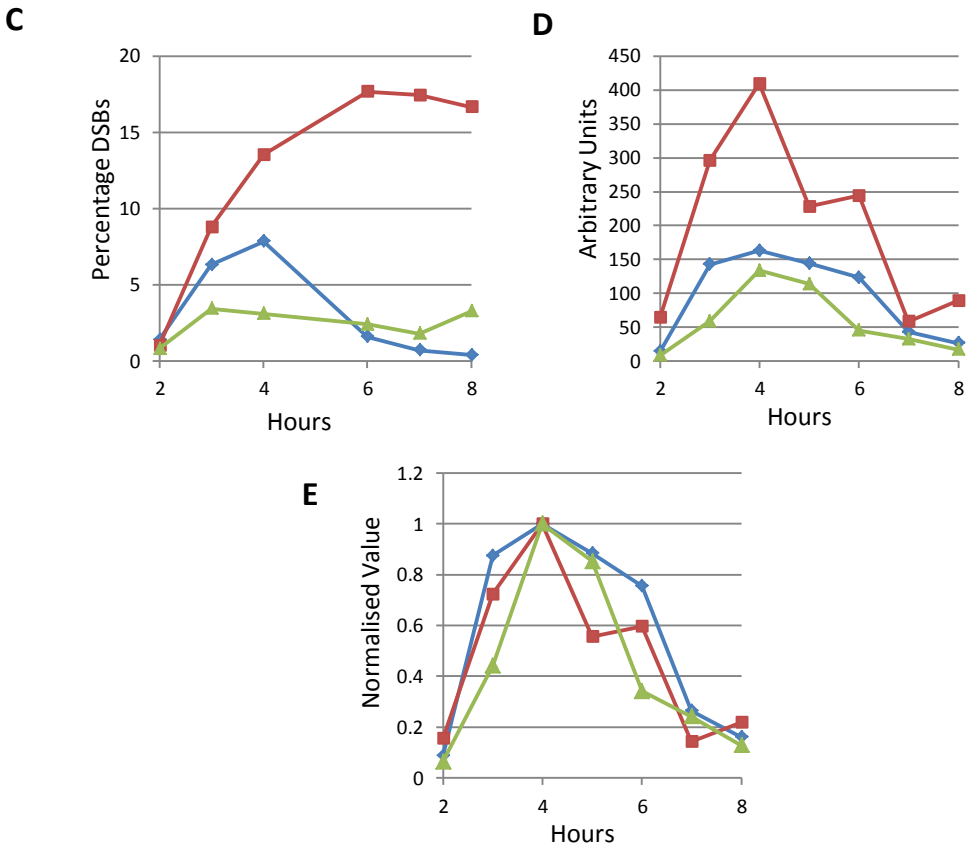
C
Percentage DSBs
Hours
D
Arbitrary Units
Hours
E
Normalised Value
Hours
spo11-HA
dmc1Δ spo11-HA
rad24Δ dmc1Δ spo11-HA

Figure 3.2.8: DSB signal and Spo11-oligonucleotide levels are reduced in *rad24Δ dmc1Δ spo11-HA*. A) Southern blot of DSBs at the *HIS4::LEU2* hotspot. Meiotic time courses were performed for the *spo11-HA, dmc1Δ spo11-HA* and *rad24Δ dmc1Δ spo11-HA* strains and samples were taken at the marked times. Genomic DNA was extracted, digested and run on a 0.7% TAE agarose gel for 20 hours at 60 volts. The gel was transferred to nylon membrane under denaturing conditions and hybridised with a radioactive probe for the *HIS4::LEU2* locus. The membrane was exposed to a phosphor screen and image taken using a Fuji phosphor scanner. DSBs marked with arrowhead (➤) mark DSBs. **B)** TCA Extracts from the same meiotic cultures were immunoprecipitated (IP) and end labeled according to the Spo11-oliognucleotide assay (see 2.7). Samples were run on a 7.5% SDS PAGE for 1 hour 30 minutes at 150 volts, transferred to PVDF at 0.65 amps for 1 hour and exposed to phosphor screens. Open triangles (▷) mark upper and lower Spo11-oligo species. Asterisk (*) marks non-specific terminal transferase (TdT) band. **C)** Quantification of DSB levels over time. Image Gauge was used to analyse DSB signal as a percentage of total DNA and signal is plotted and displayed. **D)** Quantification of total Spo11-oligonucleotide signal from both species using Image Gauge is displayed. **E)** Quantified signal from the Spo11-oligonucleotide blot (B), with values normalized to the maximum signal.

To confirm that the decrease in both DSB signal and Spo11-oligonucleotide signal is not due to synchronicity of the culture, FACS analysis was performed. The *rad24Δ dmc1Δ spo11-HA* had fewer cells that had undertaken pre-meiotic S phase at 2, 3 and 4 hours compared with both the *spo11-HA* and *dmc1Δ spo11-HA* strains (between 3.3% and 14.8%) (figure 3.2.9). However, the decrease in cell number between cultures is not enough to account for the large decrease in DSB and Spo11-oligonucleotide levels. The FACS data suggests that the decreased DSB and Spo11-oligonucleotides levels in *rad24Δ dmc1Δ spo11-HA* is not due to cultures that are asynchronous.

rad24Δ dmc1Δ spo11-HA protein samples were used to measure the abundance of early meiotic proteins. In the *rad24Δ dmc1Δ spo11-HA* strain Spo11-HA was present from 2 hours to 7 hours (figure 3.2.20A). Zip1 protein is present at 3, 4 and 5 hours and peaks at 4 hours (figure 3.2.20B). Hop1 protein is abundant throughout the time course but the phosphorylated form (a signal for the presence of DSBs) is present at 4 and 5 hours (figure 3.2.20C). The lack of persistence of Spo11-HA, Zip1 and Hop1 protein in the *rad24Δ dmc1Δ spo11-HA* compared to the *dmc1Δ spo11-HA* suggests that the checkpoint function is compromised. In addition the decrease in presence of phosphorylated Hop1 is consistent with the fewer DSBs observed, however this is also consistent with a *rad24Δ* mutation (Carballo, Johnson et al. 2008).

spo11-HA

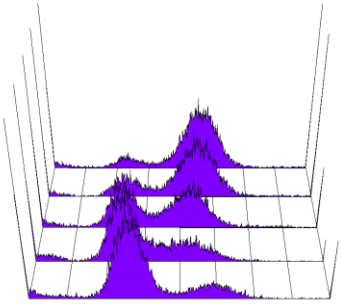

Time (Hours)	Percentage Cells with 2n
0	23.4
1	31.4
2	49.6
3	71.2
4	78.5

dmc1Δ spo11-HA

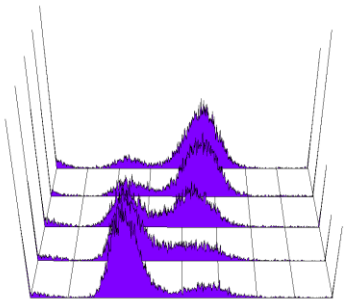

Time (Hours)	Percentage Cells with 2n
0	19.6
1	30.9
2	51.4
3	73.8
4	79.6

rad24Δ dmc1Δ spo11-HA

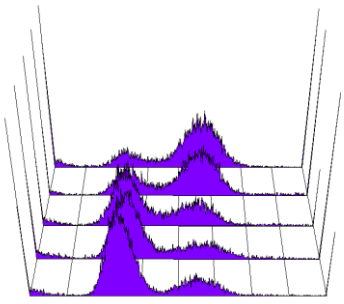

Time (Hours)	Percentage Cells with 2n
0	23.6
1	28.1
2	36.6
3	63.0
4	70.9

Figure 3.2.9: FACS analysis of *spo11-HA*, *dmc1Δ spo11-HA* and *rad24Δ dmc1Δ spo11-HA* strains indicate similar S-phase kinetics. Samples from meiotic time courses used to analyse DSB levels and Spo11-oligonucleotide levels were fixed in 70% ethanol and stored at -20°C. Samples were then treated to remove protein and RNA, sonicated and DNA stained. FACS data collection was carried out on the Becton Dickinson FACS Canto with 10,000 events being scored and plotted for each time point. Analysis of the collected data was carried out by BD FACS Diva and WinMDI.

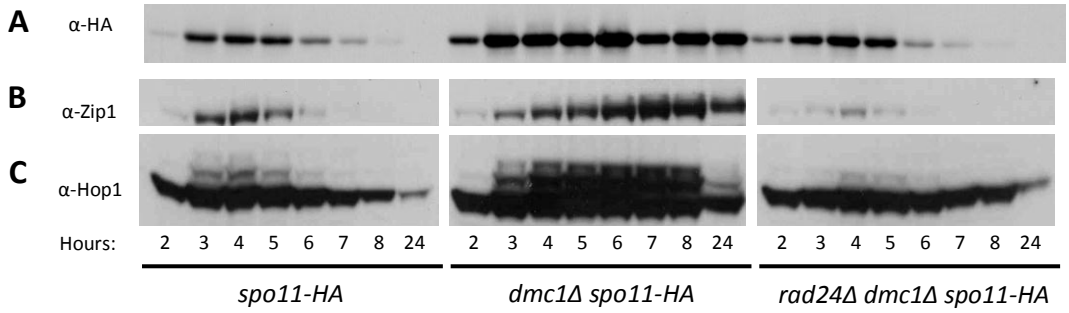

Figure 3.2.10: Decreased meiotic protein expression or modification occurred in *rad24Δ dmc1Δ spo11-HA* compared with *spo11-HA* and *dmc1Δ spo11-HA* strains. A) Western blot of the Spo11-oligonucleotide blot. 1:10,000 Santa Cruz antibody with HRP conjugate was used against the HA epitope attached to Spo11 and exposed to film. **B)** Western blot against Zip1. Anti-Zip1 (courtesy of Eva Hoffman) was used at 1 in 2,000 concentration followed by a secondary anti-rabbit antibody used at 1 in 3,000 concentration. **C)** Western blot against Hop1 (courtesy of Franz Klein) used at 1 in 4,000 concentration followed by a secondary anti-rabbit antibody used at 1 in 3,000 concentration.

3.2.5: Discussion

The similar kinetics of Spo11-oligonucleotide degradation and DSB repair led to a hypothesis that the two may be mechanistically linked (Neale, Pan et al. 2005). DSB repair was compromised by mutating Exo1 or Dmc1 and testing the effect on Spo11-oligonucleotide degradation. In the *exo1Δ spo11-HA* mutant, DSBs repair was delayed, early meiotic proteins were present for longer and the Spo11-oligonucleotide signal was higher for longer. In the *dmc1Δ spo11-HA* mutant, unrepaired DSBs and early meiotic proteins accumulated and Spo11-oligonucleotides persisted for longer. However, when normalising the Spo11-oligonucleotide signal and comparing strains based upon degradation pattern (figure 3.2.2E, 3.2.5E and 3.2.8E), it is observed that rate of degradation is not altered. The *exo1Δ spo11-HA* and *dmc1Δ spo11-HA* mutations therefore increase the number of Spo11-oligonucleotides but do not affect the degradation.

If DSB repair and Spo11-oligonucleotide persistence were tightly coupled mechanistically, it may be expected that in a *dmc1Δ* background, Spo11-oligonucleotides would behave like the DSBs and persist without being degraded. Two recombinases function in meiosis, Dmc1 and Rad51 (Bishop, Park et al. 1992; Shinohara, Ogawa et al. 1992). Dmc1 is meiosis specific but both are required for meiotic DSB repair (Bishop, Park et al. 1992; Shinohara, Ogawa et al. 1992). One possibility for the lack of continued persistence of Spo11-oligonucleotides in the *dmc1Δ spo11-HA* background could be due to action of Rad51. If for example Spo11-oligonucleotide lifespan is linked to removal from the DSB ends by both Rad51 and Dmc1, removing either could delay (but not prevent) Spo11-oligonucleotide degradation. It has been observed that in the absence of *dmc1Δ,* Rad51 still forms foci, supporting the hypothesis that Rad51 could function in the absence of Dmc1 (Dresser, Ewing et al. 1997). Testing the *rad51Δ*

dmc1Δ spo11-HA mutant would test this hypothesis and may cause continued persistence of the Spo11-oligonucleotides.

Increased checkpoint activity in the *exo1Δ spo11-HA* and *dmc1Δ spo11-HA* was another possibility to explain the increased persistence of the Spo11-oligonucleotides. Removal of the checkpoint protein Rad24 was designed to test the role of the checkpoint on the stability of Spo11-oligonucleotides but instead caused an unexpected dramatic decrease in DSB signal (figure 3.2.8). It was therefore not surprising to observe a decrease in Spo11-oligonucleotide signal. As the DSB signal was not high, the observations are unable to clarify whether the persistence of Spo11-oligonucleotides is due to prolonged checkpoint activity.

The checkpoint proteins play a role in establishing inter-homolog repair bias (Carballo, Johnson et al. 2008). Therefore one explanation for the reduction in DSB signal observed in the *rad24Δ dmc1Δ spo11-HA* strain could be due repair by the *RAD51* recombinase. Addition of the *rad51Δ* mutation would help to test this hypothesis.

Previous observations have indicated that the *spo11-HA* mutation causes a slight reduction in DSB levels (Diaz, Alcid et al. 2002; Martini, Diaz et al. 2006). The *dmc1Δ* mutation causes a halt to DSB repair and DSB formation is competent in its absence (Bishop, Park et al. 1992) (figure 3.2.5). Similarly, the *rad24Δ* mutation is competent at DSB formation (Lydall, Nikolsky et al. 1996; Grushcow, Holzen et al. 1999). Neither *RAD24* nor *DMC1* has been implicated in meiotic DSB formation or their absence causing a reduction in meiotic DSB levels. It is therefore surprising that the combination of *rad24Δ dmc1Δ* mutations with the *spo11-HA* causes a reduction in observed DSB levels.

Recent observations have indicated that mutating the checkpoint protein ATM in mice causes an increase in Spo11-oligonucleotides, implying increased DSB levels (Lange, Pan et al. 2011). Increased foci identifying DSBs have been observed in ATM mutants in *Drosophila melanogaster* (Joyce, Pedersen et al. 2011). Mutants defective in the *Saccharomyces cerevisiae* ATM homolog Tel1 also have increased DSBs (Zhang, Kim et al. 2011)(Jesus Carballo, Rita Cha personal communication). These observations imply a role to inhibit DSB levels by checkpoint proteins, contrary to what has been observed in the *rad24Δ dmc1Δ spo11-HA* mutant (figure 3.2.8).

Experiments to understand the reduction in the DSB levels observed in *rad24Δ dmc1Δ spo11-HA* will be presented in chapter 4.

3.3: Investigating the Spo11 processing event

3.3.1: Introduction

In the process of creating a DSB during meiosis, Spo11 becomes covalently attached to the end of the DSB (Bergerat, de Massy et al. 1997; Keeney, Giroux et al. 1997; Neale, Pan et al. 2005). In order for repair to take place, Spo11 must be removed. Endonucleolytic cleavage liberates Spo11 from the end of the DSB with a short DNA attachment: a Spo11-oligonucleotide (Neale, Pan et al. 2005). In *sae2Δ* (Keeney and Kleckner 1995; Prinz, Amon et al. 1997)*, rad50S* (Alani, Padmore et al. 1990) and *mre11* nuclease mutants (Moreau, Ferguson et al. 1999), Spo11 remains attached at the end of the DSB. These observations indicate a requirement for the nuclease function of Mre11 in addition to functional Rad50 and Sae2. After Spo11 processing, DSBs are resected to create 3' single stranded DNA tails (Sun, Treco et al. 1989).

Sae2 is phosphorylated by Mec1 and Tel1 during meiosis (Cartagena-Lirola, Guerini et al. 2006). In mutants where the phosphorylation site is modified to prevent addition of a phosphate (phosphomutants), DSBs remain unresected (Cartagena-Lirola, Guerini et al. 2006). These observations suggest that Sae2 phosphorylation is required for Spo11 processing. In order to test whether Sae2 phosphorylation by Mec1 and Tel1 is required for Spo11 processing, mutants in Mec1, Tel1 or both can be used to measure levels of Spo11-oligonucleotides. If phosphorylation is required for Spo11 processing, then in the double mutant Spo11-oligonucleotides will not be detected. However, if Sae2 phosphorylation is not required, then Spo11-oligonucleotides will be detected. In addition, observations of the levels of Spo11-oligonucleotides in the Mec1 or Tel1 single mutants may provide insight into their requirement for Spo11 processing.

3.3.2: Spo11-oligonucleotides are detectable in *mec1-mn spo11-HA* and *tel1Δ spo11-HA* and a low level detected in *mec1-mn tel1Δ spo11-HA*

Mutants defective in either *MEC1* or *TEL1* were crossed into the *spo11-HA* background and tested to determine if Spo11-oligonucleotides were present. Because Mec1 functions in vegetative cells to ensure genomic stability (Kato and Ogawa 1994), the meiotic null mutant (*mec1-mn*) was used to remove its expression in meiosis. *RAD24*, a protein involved in the same meiotic checkpoint as *MEC1* (Lydall, Nikolsky et al. 1996) was also tested in the *tel1Δ spo11-HA* background. All samples were prepared on the same day and repeated in duplicate to account for radiolabelling variation. In addition, all samples were run on the same gel and compared on the same blot. In *spo11-HA* the Spo11-oligonucleotide signal was slightly over 1500 arbitrary units (au)(figure 3.3.1). By contrast, in the *mec1-mn spo11-HA* strain Spo11-oligonucleotide signal was lower at just over 1000 au (figure 3.3.1). This observation indicates that the removal of *MEC1* causes a reduction in Spo11-oligonucleotide levels.

In the *tel1Δ spo11-HA* strain the Spo11-oligonucleotide levels detected were approximately 1670 au (figure 3.3.1), a slight increase compared with *spo11-HA* and a large increase compared with the *mec1-mn spo11-HA* strain. This observation suggests that removal of *TEL1* causes a slight increase in the levels of Spo11-oligonucleotides. By contrast, in the *mec1-mn tel1Δ spo11-HA* strain, the detected Spo11-oligonucleotide is approximately 154 au, a large decrease compared with all strains (figure 3.3.1). In the *rad24Δ tel1Δ spo11-HA* strain, detected spo11 levels were over double the *mec1-mn tel1Δ spo11-HA* at approximately 369 au, but still lower than the levels observed in the *mec1-mn spo11-HA* or *tel1Δ spo11-HA* mutants (figure 3.3.1). These observations suggest that both *MEC1* and *TEL1* are required for Spo11-oligonucleotide formation, but because Spo11-oligonucleotides were detected in the *mec1-mn tel1Δ spo11-HA* background, it suggests that other mechanisms function to initiate Spo11

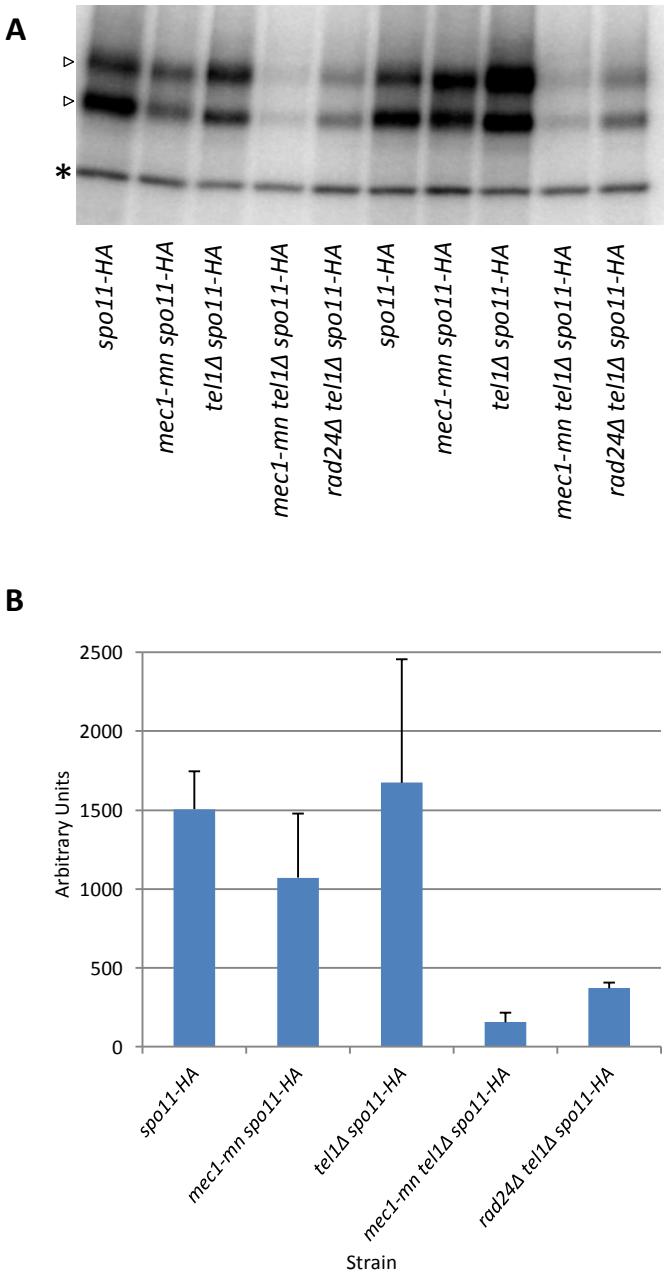

Figure 3.3.1: Spo11-oligonucleotide levels decrease in the absence of Mec1 and Tel1 or Rad24 and Tel1 in the *spo11-HA* background. A) Meiotic time courses were carried out in for the mentioned strains. 10ml samples were taken at 0, 2, 3, 4, 5, 6, 7 and 8 hours, TCA extracts prepared, eluted into 600µl SDS loading buffer and 30µl from each time point was taken and pooled together. Another 30µl from each time point also pooled together to allow the strains to be carried out in duplicate. The samples were then used to carry out the Spo11-oligonucleotide assay with the blot displayed. Samples were run on a 7.5% SDS PAGE for 1 hour 30 minutes at 150 volts, transferred to PVDF at 0.65 amps for 1 hour and exposed to phosphor screens. Open triangles (▹) mark long and short Spo11-oligonucleotide species. Asterisk (*) marks non-specific terminal transferase (TdT) band. **B)** Quantification of Spo11-oligonucleotide levels using Image Gauge. Both short and long oligonucleotide species were measured and added together to give readings. Average readings were calculated and plot along with standard deviation for each sample.

processing. In the previous chapter, it was observed that *rad24Δ dmc1Δ spo11-HA* (figure 3.2.8) had decreased DSB levels compared with *spo11-HA.* Therefore the reduction in Spo11-oligonucleotide levels may be a consequence of decreased DSB levels.

3.3.3: DSB levels are reduced in mec1-mn spo11-HA, mec1-mn tel1Δ spo11-HA and rad24Δ tel1Δ spo11-HA

An alternative explanation for the reduction and increase in Spo11-oligonucleotides in the tested mutants, other than the efficiency of Spo11 processing, is that a differing number of DSBs form in these backgrounds. Therefore if more DSBs were to form it would expected that more Spo11-oligonucleotides would form. Equally, if there were fewer DSBs, then it would be expected that there would be fewer Spo11-oligonucleotides. To test if DSB levels account for the change in Spo11-oligonucleotide levels, as opposed to a change in the ability to process Spo11, DSB levels were measured at the *HIS4::LEU2* locus. Two frequently used DSB sites exist within the *HIS4::LEU2* recombination site, separated by 2.4Kb*,* enabling DSB levels to be measured.

In *spo11-HA*, DSBs peaked at 5 hours around 4% of total DNA signal (figure 3.3.2). The published phenotype for the *MEC1* mutant is that it produces approximately similar DSB levels to wildtype (Lydall, Nikolsky et al. 1996). In contrast to the *spo11-HA* strain, *mec1-mn spo11-HA* peaked at less than 2% of total DNA at 4 hours (figure 3.3.2). This observation suggests that in a *mec1-mn spo11-HA* background DSB levels are decreased, contrary to published observations for the *mec1* mutant. This is however, consistent with the *rad24Δ dmc1Δ spo11-HA* strain, where DSB levels were reduced, supporting the idea that reduction in DSB signal is related to loss of the checkpoint.

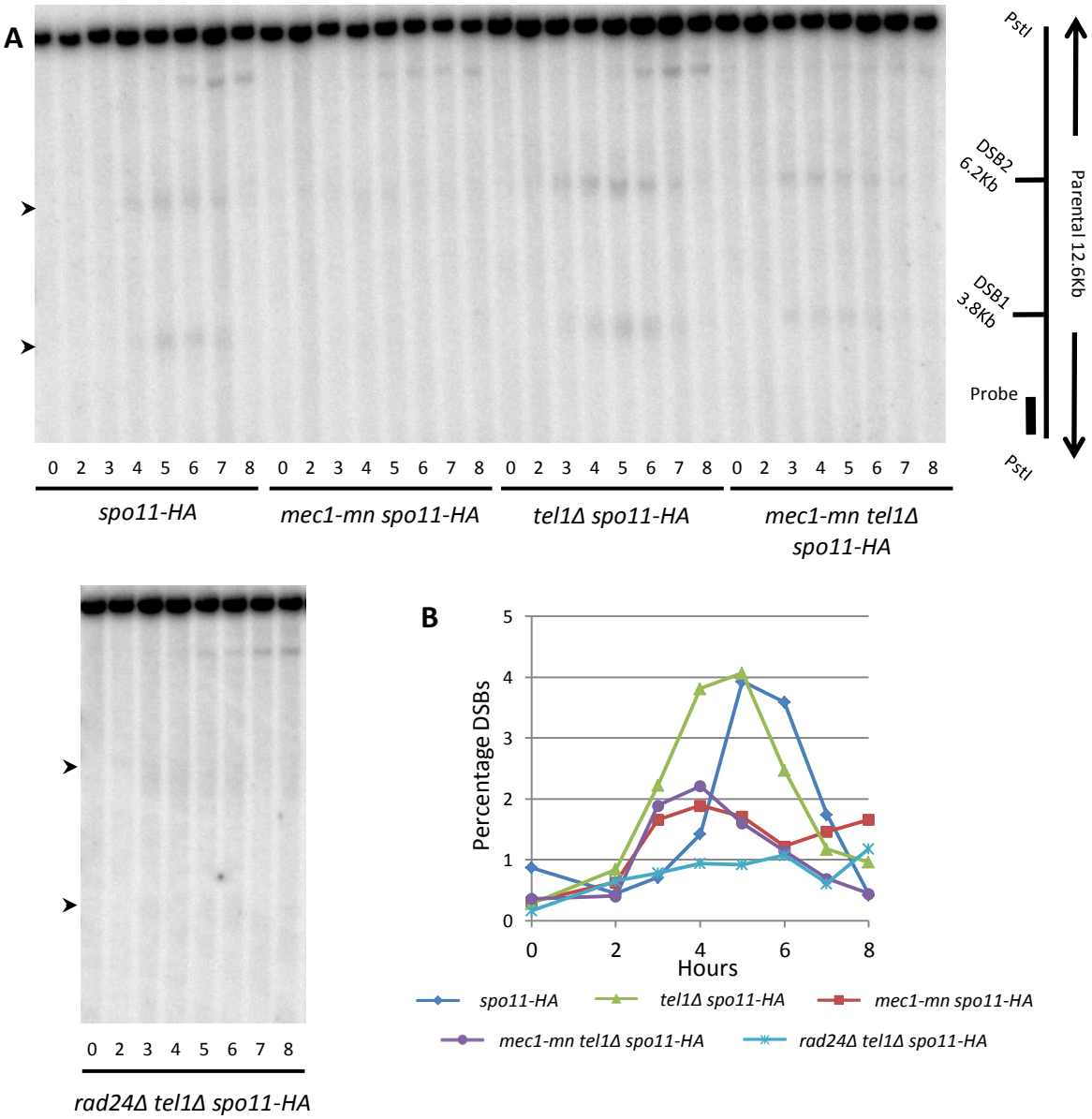

Figure 3.3.2: DSB levels are decreased in *mec1-mn spo11-HA, mec1-mn tel1Δ spo11-HA* and *rad24Δ tel1Δ spo11-HA*. A) Southern blot of DSBs at the *HIS4::LEU2* hotspot. Meiotic time courses were performed for the strains and samples were taken at the marked times. Genomic DNA was extracted, digested and run on a 0.7% TAE agarose gel for 20 hours at 60 volts. The gel was transferred to nylon membrane under denaturing conditions and hybridised with a radioactive probe for the *HIS4::LEU2* locus. The membrane was exposed to a phosphor screen and image taken using a Fuji phosphor scanner. DSBs marked with arrowhead (➤) mark DSBs. **B)** Quantification of DSB levels over time. Image Gauge was used to analyse DSB signal as a percentage of total DNA and signal is plotted and displayed.

In the *tel1Δ spo11-HA* mutant, DSBs peak at around 4% of total DNA at 5 hours and, in contrast to the *spo11-HA* strain, persists at a higher level, being over 2% for 4 hours (figure 3.3.2). This suggests that either more DSBs form in the *tel1Δ spo11-HA* background or DSBs persist for longer. In contrast to *tel1Δ spo11-HA*, the *mec1-mn tel1Δ spo11-HA* strain peaks at over 2% of total DNA at 4 hours (figure 3.3.2). In addition, the *rad24Δ tel1Δ spo11-HA* mutant achieves around 1% of total DNA throughout the time course (figure 3.3.2). These observations suggest that DSB formation is compromised in *mec1-mn tel1Δ spo11-HA* and *rad24Δ tel1Δ spo11-HA* backgrounds.

3.3.4: Discussion

Sae2 phosphorylation by Mec1 and Tel1 in meiosis causes the change in DSB from an unresected to resected state (Cartagena-Lirola, Guerini et al. 2006). This observation suggests that Mec1 and Tel1 function to stimulate Spo11 processing by phosphorylation of Sae2. By removing Mec1 and Tel1, it was expected that Spo11-oligonucleotides (a by-product of processing) would not be produced. In the *mec1-mn tel1Δ spo11-HA* background, low levels of Spo11-oligonucleotides were observed. This low level suggested that Spo11 processing could be initiated by a less efficient mechanism. However, the reduction in DSB levels observed in this strain means that it is more difficult to determine whether the reduction in DSB levels causes the decrease in Spo11-oligonucleotides or whether a reduction in Spo11 processing causes the decrease. Because the reduction in DSB signal is approximately 50% compared with *spo11-HA,* and the Spo11-oligonucleotide signal produced is approximately 25% of *spo11-HA,* it would suggest that Mec1 and Tel1 activity are required for at least 50% of the Spo11-oligonucleotides formed.

The observations from this section suggest that Spo11-oligonucleotides are formed proportionally to the amount of DSBs. In the *tel1Δ spo11-HA,* DSB signal was maintained for longer and a slight increase in Spo11-oligonucleotide levels was observed, suggesting more DSBs were formed. The reduction in signal observed in the *mec1-mn spo11-HA* is also consistent with the decreased DSB signal. Interestingly, *mec1-mn spo11-HA* and *mec1-mn tel1Δ spo11-HA* have a similar decrease in DSB signal yet there is a larger decrease in the Spo11-oligonucleotide signal detected in the *mec1-mn tel1Δ spo11-HA*. In addition a reduction in DSB signal and Spo11-oligonucleotide signal is also observed in the *rad24Δ tel1Δ spo11-HA* compared with *spo11-HA*. These observations suggest that the processing of Spo11 to form Spo11-oligonucleotides is largely Mec1/Rad24 and Tel1 dependent.

The reduction in DSB signal within the *mec1-mn spo11-HA, mec1-mn tel1Δ spo11-HA* and *rad24Δ tel1Δ spo11-HA* are unexpected and may also fit with the observed decrease in DSB levels in the *rad24Δ dmc1Δ spo11-HA.* Investigations into the reduction in DSBs levels compared to what is expected are the focus of chapter 4.

CHAPTER 4:

Investigating the decrease in DSB signal observed in the *rad24Δ dmc1Δ spo11-HA* mutant

Chapter 4: Investigating the decrease in DSB signal observed in the rad24Δ dmc1Δ spo11-HA mutant.

4.1: Introduction.

Mutants defective in the Mec1 meiotic recombination checkpoint (e.g. *mec1Δ, rad17Δ* and *rad24Δ*) and the strand exchange step of DSB repair (e.g. *dmc1Δ*) have a DSB signal of between approximately 20 and 30% of total DNA at the *his4::LEU2* locus (Lydall, Nikolsky et al. 1996). By contrast, in chapter 3.2 I observed that in the *rad24Δ dmc1Δ spo11-HA* strain, DSB signal peaked at approximately 3.5% of total DNA at the *HIS4::LEU2* locus (figure 3.2.8). This suggests that in the situation of the *rad24Δ dmc1Δ spo11-HA* strain, detected DSB levels are lower than expected. The *spo11-HA* tag is reported to cause a reduction of between 11 to 31% in DSB signal compared to wildtype (Martini, Diaz et al. 2006). As the *spo11-HA* tag alone is unable to account for the decrease observed in the *rad24Δ dmc1Δ spo11-HA* it therefore suggests that other factors contribute to the reduction in DSB levels. The topic of this chapter is an investigation into the mechanism that causes the reduction in DSB signal.

4.2: rad24Δ spo11-HA and rad24Δ dmc1Δ spo11-HA have decreased DSB signal.

Wildtype, *dmc1Δ*, *rad24Δ* and *rad24 dmc1Δ* strains in the presence of either *SPO11* or *spo11-HA* were tested to ascertain which mutant backgrounds caused a decrease in DSB levels. All samples were taken from synchronous meiotic time courses. DSB levels were analysed at the *HIS4::LEU2* locus, a meiotic recombination hotspot with two DSB sites separated by 2.4Kb. DSB signal was the addition of signal from both DSB sites as a proportion of total DNA. In wildtype DSBs peaked at 3 hours at just below 6% of total DNA (figure 4.1B, D and E). *Spo11-HA* DSBs peaked an hour later, at slightly higher levels reaching just below 8% (figure 4.1A, C and E). The small difference observed between the wildtype and *spo11-HA* DSB signal is likely due to variations between southern blots. This therefore suggests that wildtype and *spo11-HA* form similar levels of DSBs at the *HIS4::LEU2* locus.

The DSBs in *dmc1Δ* plateaued at over 16% by 4 hours (figure 4.1B, D and E). The *dmc1Δ spo11-HA* DSBs reached a similar level by 6 hours (figure 4.1A, C and E). This suggests that there is no difference in DSB levels between these strains, but a slight delay in forming the DSBs in *dmc1Δ spo11-HA*. In the *rad24Δ* strain, DSBs reached the maximum peak by 4 hours at around 9% of total DNA (figure 4.1B, D and E). Similarly, in the *rad24Δ spo11-HA* strain DSBs also reached the maximum peak at 4 hours but the DSBs only reached around 5% of total DNA (figure 4.1A, C and E). This indicates that when the *rad24Δ* mutation is combined with the *spo11-HA* tag there is a reduction in DSB levels.

In the *rad24Δ dmc1Δ* strain, DSBs reached the maximum level at 6 hours at around 24% of total DNA (figure 4.1B, D and E). By contrast, in the *rad24Δ dmc1Δ spo11-HA* DSBs reached fewer than 5% of total DNA (figure 4.1A, C and E). This indicates, as previously observed in the comparison between *rad24Δ* and *rad24Δ spo11-HA*, that the combination of *rad24Δ* and

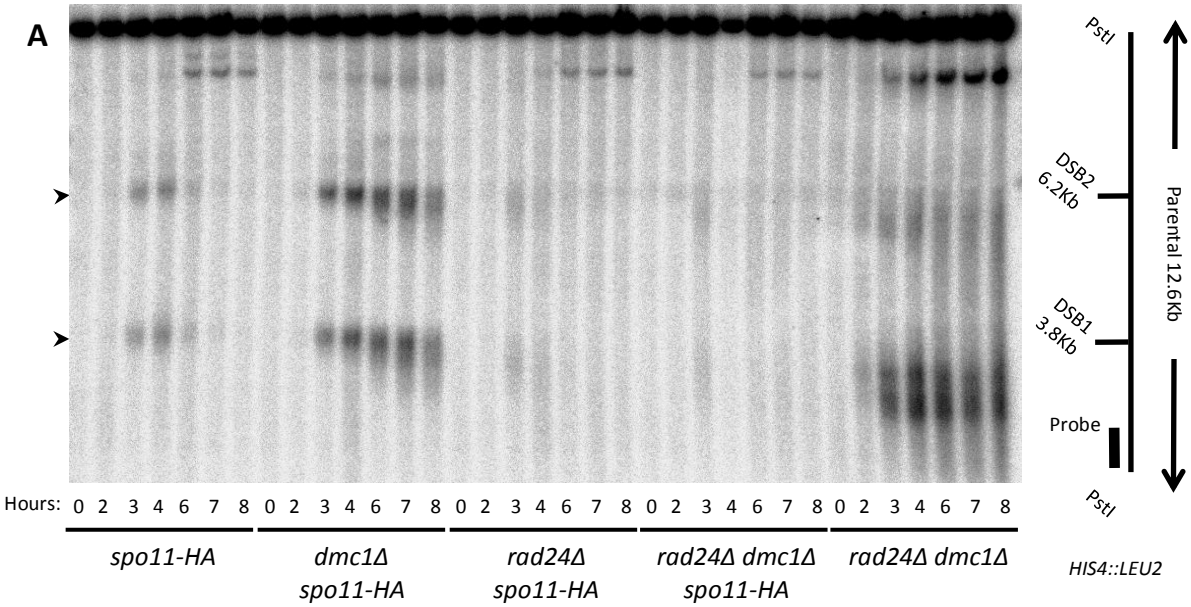
A
PstI
DSB2
6.2Kb
DSB1
3.8Kb
Probe
PstI
Parental 12.6Kb
Hours: 0 2 3 4 6 7 8 0 2 3 4 6 7 8 0 2 3 4 6 7 8 0 2 3 4 6 7 8 0 2 3 4 6 7 8
spo11-HA
dmc1Δ spo11-HA
rad24Δ spo11-HA
rad24Δ dmc1Δ spo11-HA
rad24Δ dmc1Δ
HIS4::LEU2

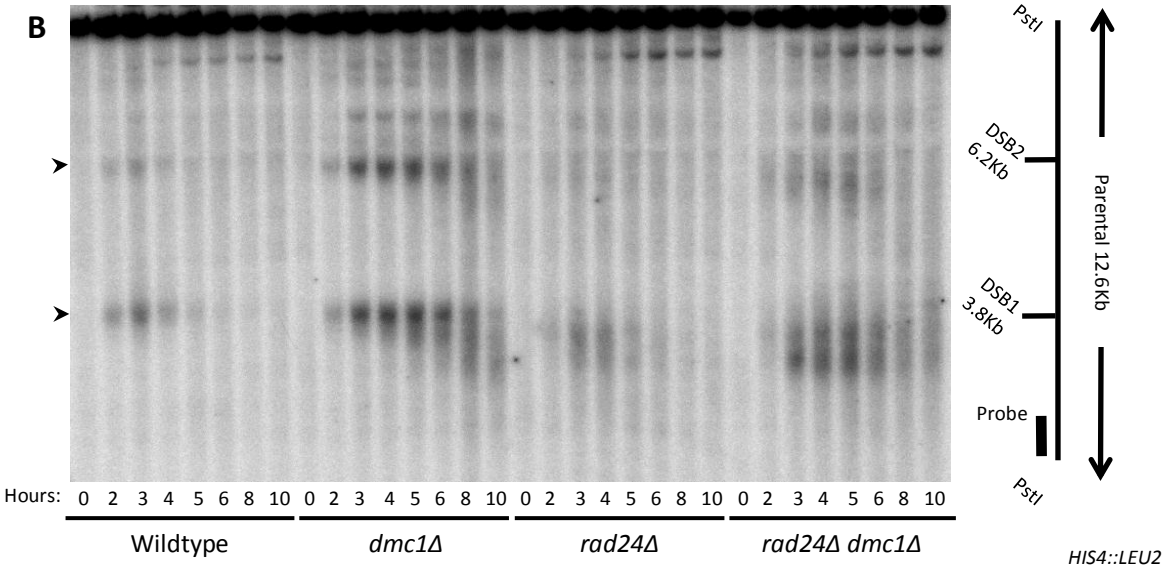
B
PstI
DSB2
6.2Kb
DSB1
3.8Kb
Probe
PstI
Parental 12.6Kb
Hours: 0 2 3 4 5 6 8 10 0 2 3 4 5 6 8 10 0 2 3 4 5 6 8 10 0 2 3 4 5 6 8 10
Wildtype
dmc1Δ
rad24Δ
rad24Δ dmc1Δ
HIS4::LEU2

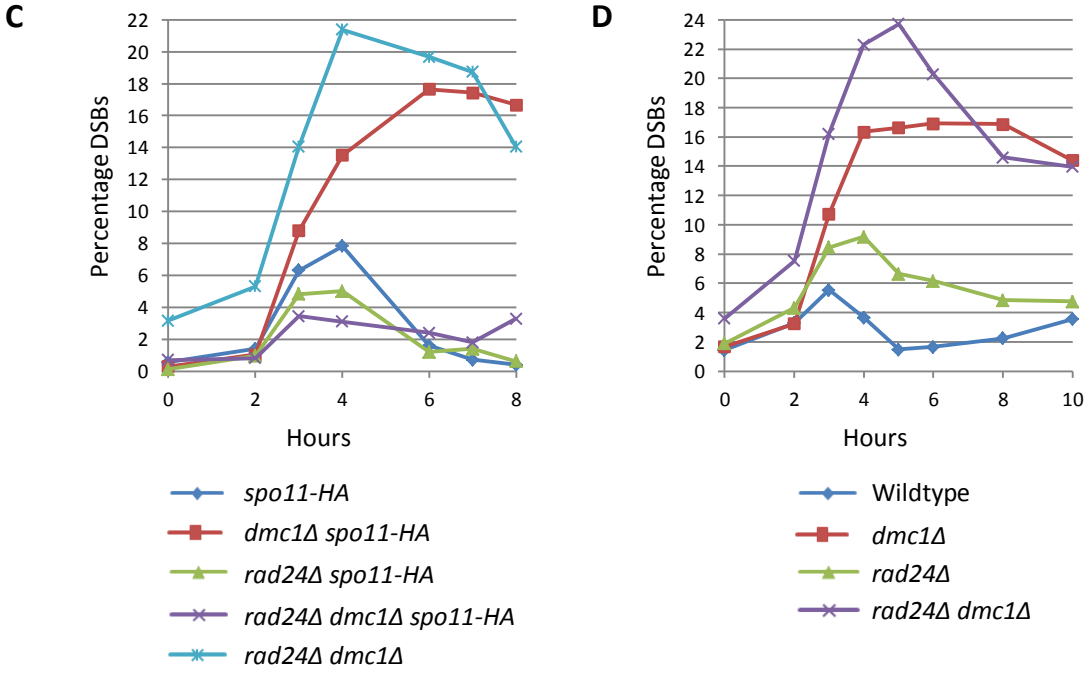
C
Percentage DSBs
Hours
spo11-HA
dmc1Δ spo11-HA
rad24Δ spo11-HA
rad24Δ dmc1Δ spo11-HA
rad24Δ dmc1Δ
D
Percentage DSBs
Hours
Wildtype
dmc1Δ
rad24Δ
rad24Δ dmc1Δ

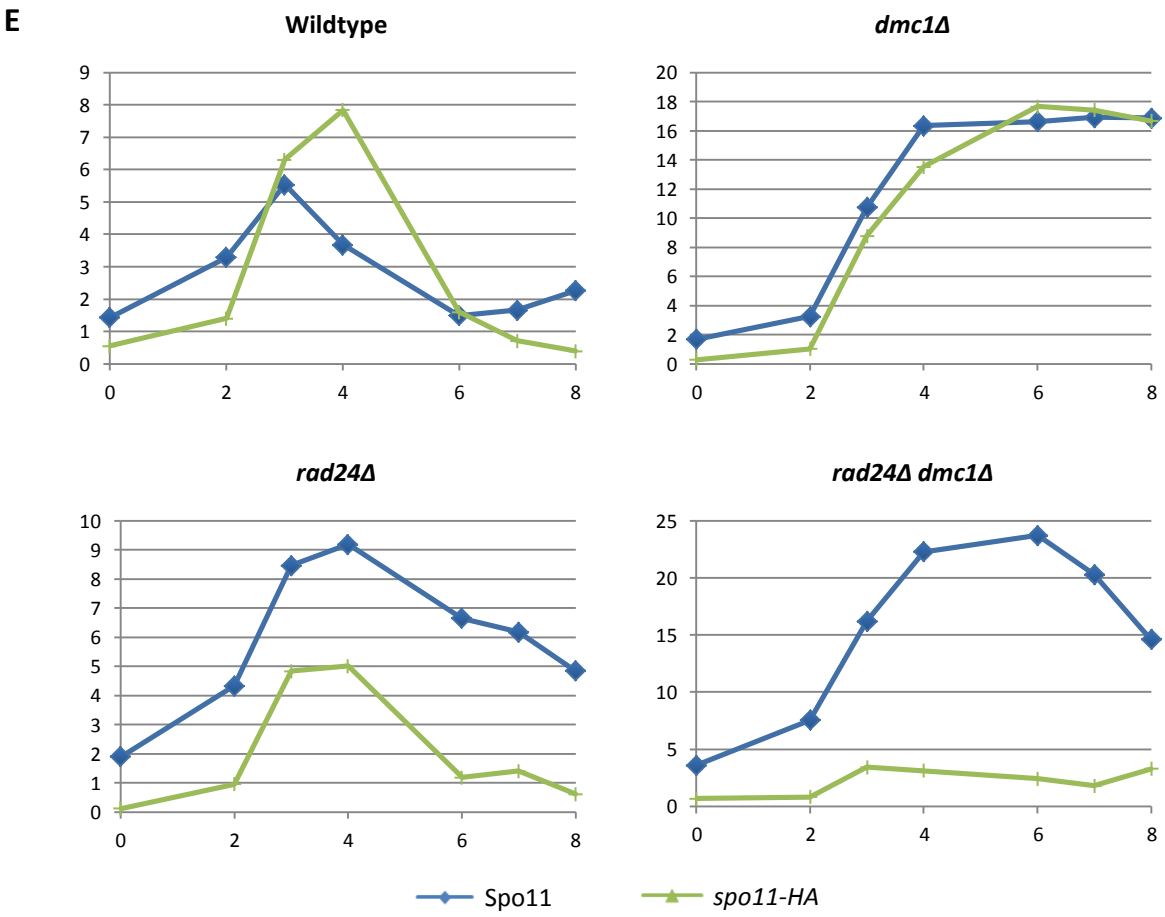

Figure 4.1: DSB levels decrease in the *rad24Δ* mutant in the presence of *spo11-HA.* A and **B)** Genomic DNA from meiotic time courses were digested and run on a 0.7% 1xTAE agarose gel for 20 hours at 60 volts. The gel was transferred to nylon membrane under denaturing conditions and hybridised with a radioactive probe for the *HIS4::LEU2* locus. The membrane was exposed to a phosphor screen and image taken using a Fuji phosphor scanner. DSBs marked with arrowhead (➢). **C** and **D)** Quantification of DSB levels over time. Image Gauge was used to analyse DSB signal as a percentage of total DNA and signal is plotted and displayed. **E)** Comparisons between mutants in the *SPO11* and *spo11-HA* backgrounds.

spo11-HA causes a reduction in DSB signal. This observation contrasts the *dmc1Δ* results, which had no reduction in DSB signal when both *dmc1Δ* and *spo11-HA* were combine. This therefore indicates that the reduction is not due to the *dmc1Δ* mutation.

4.3: Decrease in DSB signal is observed in two newly derived *rad24Δ dmc1Δ spo11-HA* isolates.

One explanation for the reduction in DSBs observed in the *rad24Δ spo11-HA* strains is that in creating the *spo11-HA* strains, a random mutation leading to a severe defect in *SPO11* was selected for. To rule out this possibility, two new isolates of the *rad24Δ dmc1Δ spo11-HA* were generated. The *dmc1Δ* mutant was utilised as this causes an accumulation of DSBs, preventing any issues with culture synchronicity affecting measured DSB levels. To construct the new strains, opposite mating types of haploid strains of *spo11-HA* and *rad24Δ dmc1Δ* were mated and dissected. The strains used were the haploids that made the experimental diploids tested in figure 4.1. The *rad24Δ dmc1Δ spo11-HA* mutations were selected for, new haploids chosen and mated leading to the formation of new experimental diploid isolates.

In both of the new *rad24Δ dmc1Δ spo11-HA* isolates, DSB levels did not reach higher than 6% of total DNA (figure 4.2). This suggests that the phenotype previously observed in the *rad24Δ dmc1Δ spo11-HA* strain is consistent with these mutations and not due to a severe mutation of Spo11.

4.4: DSB levels are also decreased at the *ARE1* locus in *rad24Δ spo11-HA* mutants.

The *HIS4::LEU2* locus is an artificially constructed recombination hotspot. To test whether the decreased measured DSB level observed in the *rad24Δ spo11-HA* backgrounds also occurs at

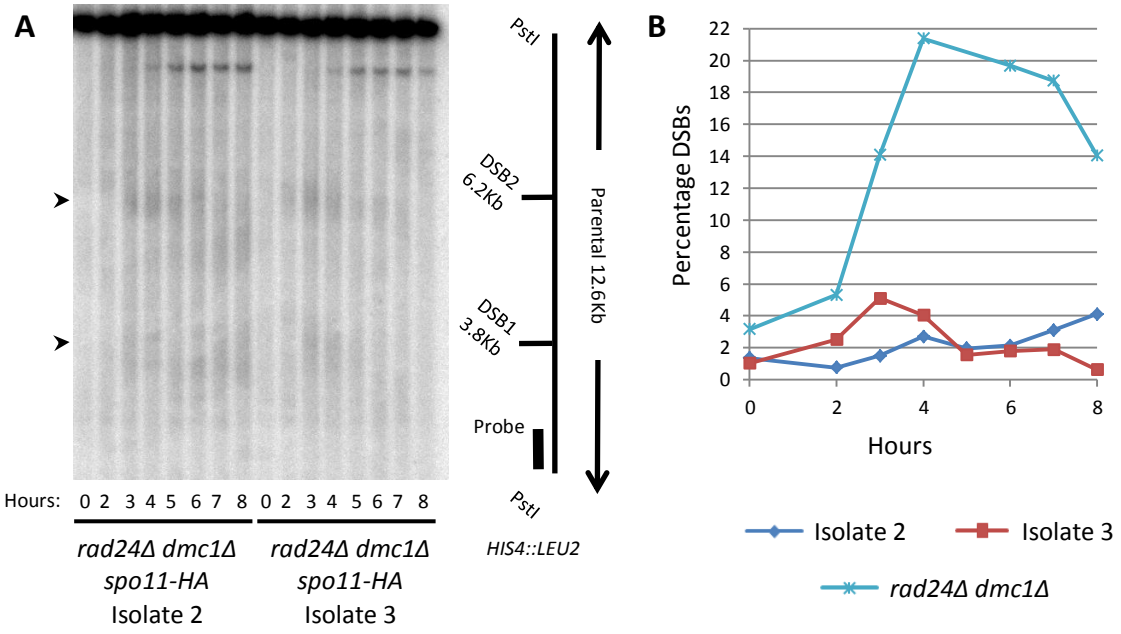

Figure 4.2: Low DSB levels are observed in two new isolates of *rad24Δ dmc1Δ spo11-HA*. A) Genomic DNA from meiotic time courses were digested and run on a 0.7% 1xTAE agarose gel for 20 hours at 60 volts. The gel was transferred to nylon membrane under denaturing conditions and hybridised with a radioactive probe for the *HIS4::LEU2* locus. The membrane was exposed to a phosphor screen and image taken using a Fuji phosphor scanner. DSBs marked with arrowhead (➤). **B)** Quantification of DSB levels over time. Image Gauge was used to analyse DSB signal as a percentage of total DNA and signal is plotted and displayed compared with *rad24Δ dmc1Δ* (from figure 4.1)

other loci throughout the genome, the naturally occurring *ARE1* recombination hotspot was probed.

Consistent with the kinetics of DSB formation observed at the *HIS4::LEU2,* wildtype peaked at 3 hours (at just over 2% of total DNA) and *spo11-HA* peaked at 4 hours (at around 5% of total DNA) (figure 4.3). The reduction is DSB signal at the *ARE1* hotspot suggests that the *spo11-HA* mutant causes an increase in DSBs at the *ARE1* locus. In the *dmc1Δ* strain, DSB signal peaked at 4 hours but was around 8% of total DNA (figure 4.3B, D and E). By contrast, *dmc1Δ spo11-HA* peaked at 7 hours just under 14% of total DNA from 6 hours onwards (figure 4.3A, C and E). This suggests that *dmc1Δ spo11-HA* has an increase in DSBs at *ARE1*.

In the *rad24Δ* strain DSBs peak at 3 hours reaching around 1% of total DNA (figure 4.3B, D and E). In the *rad24Δ spo11-HA* strain, detected DSB levels peak at below 2% of total DNA signal at 4 hours (figure 4.3A, C and E). Because of the low levels of DSBs formed in both of these strains, it is difficult to directly compare the strains, other than to conclude that these strains have a low level of DSBs.

In the *rad24Δ dmc1Δ* strain, DSBs peak at 6 hours forming around 11% DSB signal of the total DNA (figure 4.3B, D and E). By contrast, the *rad24Δ dmc1Δ spo11-HA* strain peaks at around 3% of total DNA at 3 hours (figure 4.3A, C and E). This suggests that the *rad24Δ dmc1Δ spo11-HA* has a decrease in DSB levels compared with *rad24Δ dmc1Δ.*

Visual observations of the southern blot containing the *SPO11* strains suggest that there is a transfer or hybridisation issue with this southern blot, leading to an overall reduction in signal. This therefore suggests that the observed DSB increase in *spo11-HA* compared with wildtype and *dmc1Δ spo11-HA* compared with *dmc1Δ* is artificial. Taking the overall reduction of DSBs in

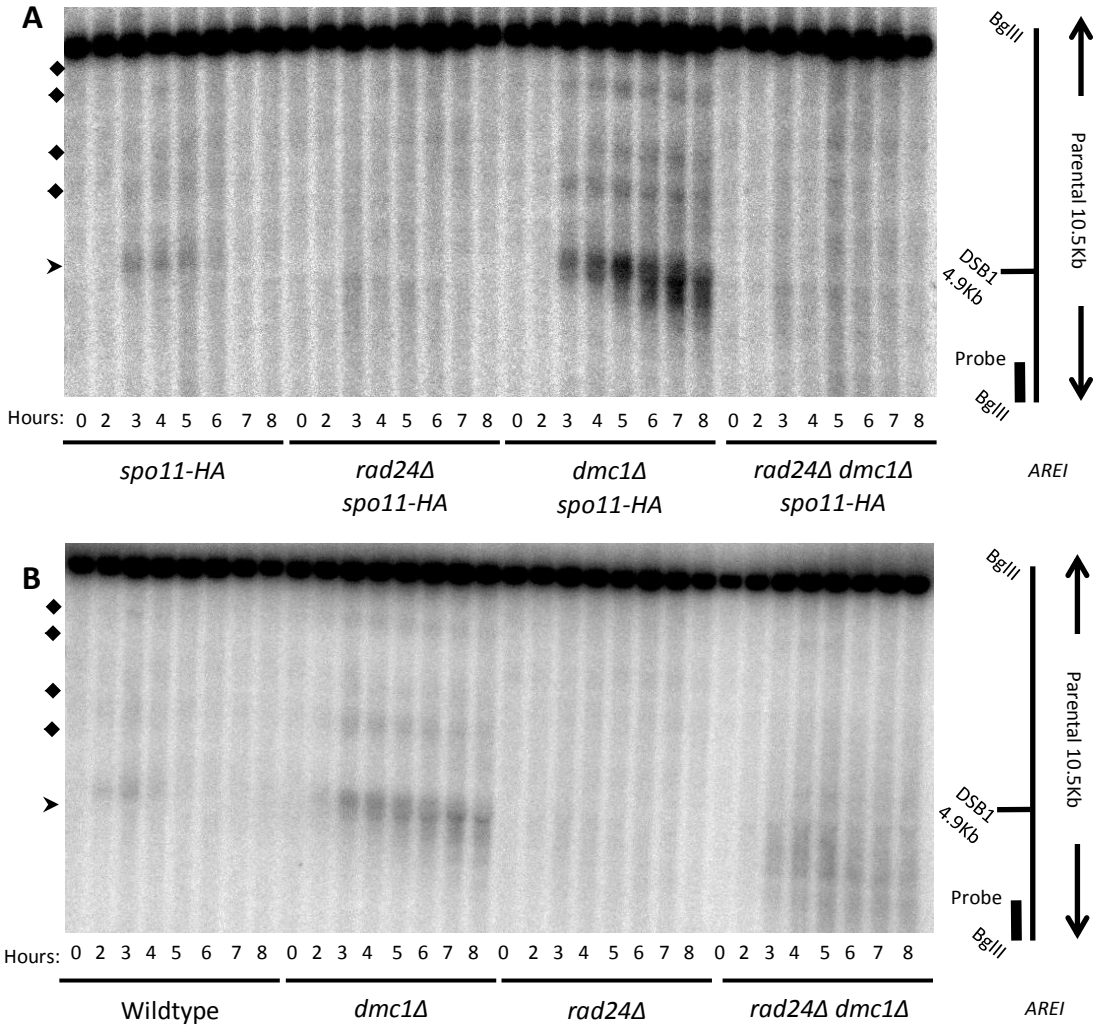
A
BglII
Parental 10.5Kb
DSB1 4.9Kb
Probe
BglII
Hours: 0 2 3 4 5 6 7 8 0 2 3 4 5 6 7 8 0 2 3 4 5 6 7 8 0 2 3 4 5 6 7 8
spo11-HA
rad24Δ spo11-HA
dmc1Δ spo11-HA
rad24Δ dmc1Δ spo11-HA
AREI
B
BglII
Parental 10.5Kb
DSB1 4.9Kb
Probe
BglII
Hours: 0 2 3 4 5 6 7 8 0 2 3 4 5 6 7 8 0 2 3 4 5 6 7 8 0 2 3 4 5 6 7 8
Wildtype
dmc1Δ
rad24Δ
rad24Δ dmc1Δ
AREI

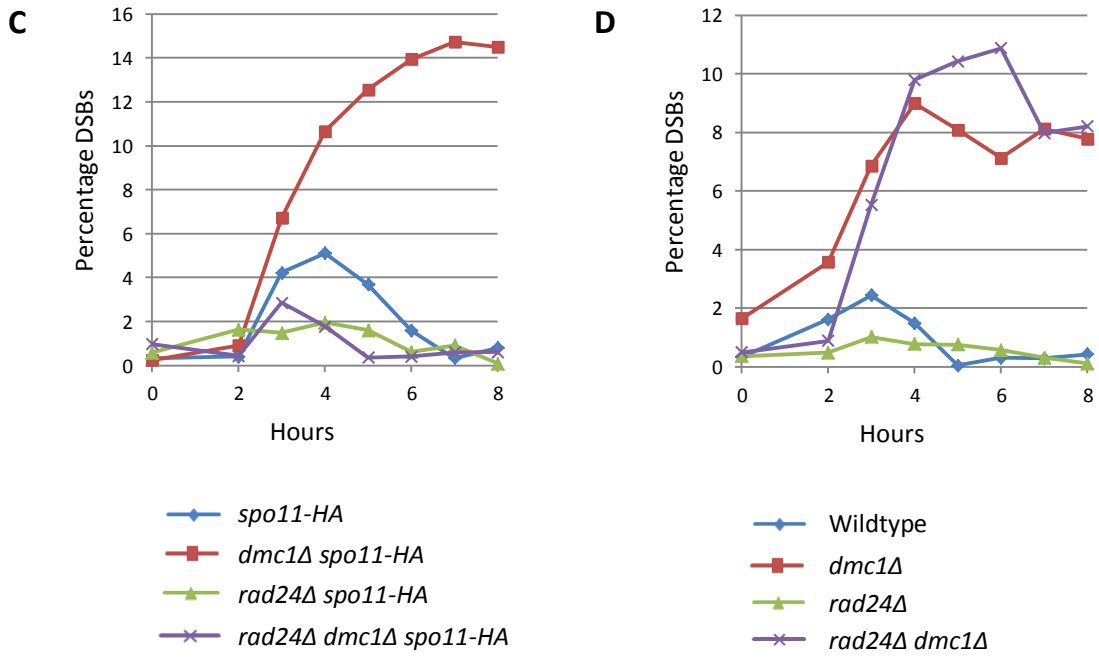
C
Percentage DSBs
Hours
spo11-HA
dmc1Δ spo11-HA
rad24Δ spo11-HA
rad24Δ dmc1Δ spo11-HA
D
Percentage DSBs
Hours
Wildtype
dmc1Δ
rad24Δ
rad24Δ dmc1Δ

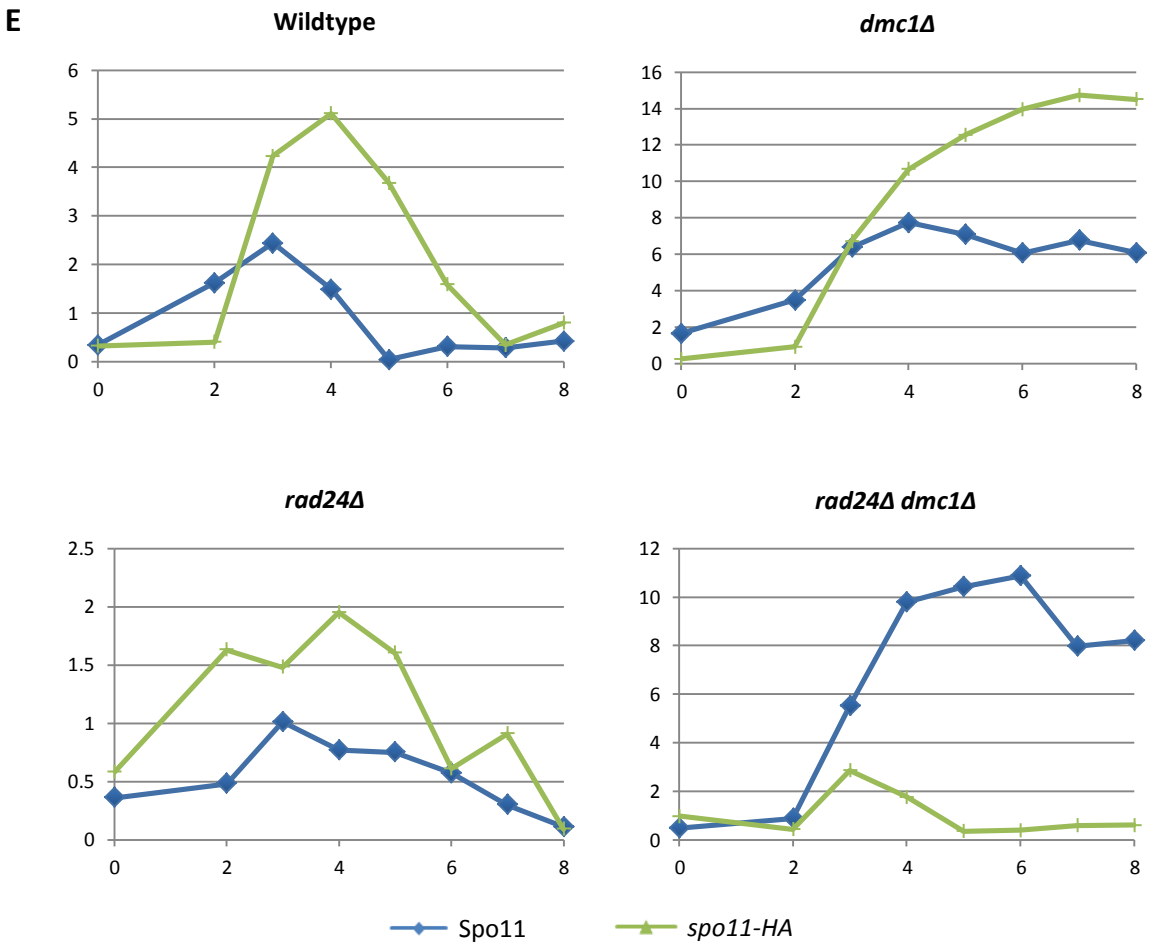

Figure 4.3: DSB levels decrease in *rad24Δ dmc1Δ spo11-HA* at the *ARE1* locus. A and **B)** Genomic DNA from meiotic time courses were digested and run on a 0.7% 1xTAE agarose gel for 20 hours at 60 volts. The gel was transferred to nylon membrane under denaturing conditions and hybridised with a radioactive probe for the *ARE1* (YCR048W) locus. The membrane was exposed to a phosphor screen and image taken using a Fuji phosphor scanner. Quantified DSB marked with arrowhead (➢) and additional DSBs marked with a diamond (◆). **C** and **D)** Quantification of DSB levels over time. Image Gauge was used to analyse DSB signal as a percentage of total DNA and signal is plotted and displayed. **E)** Comparisons between mutants in the *SPO11* and *spo11-HA* backgrounds.

SPO11 strains into account, the increase in DSB signal in the *rad24Δ dmc1Δ* compared with *rad24Δ dmc1Δ spo11-HA* is greater than observed. The observations from the *ARE1* locus are consistent with the observations at the *HIS4::LEU2* locus: the combination of *rad24Δ* and *spo11-HA* background causes a decrease in measured DSB signal.

4.5: *rad17Δ* and *mec1-mn* display the same phenotype as *rad24Δ* when combined with the *spo11-HA* tag.

The Mec1 meiotic recombination checkpoint requires not only Rad24 but also Rad17 and Mec1 (Lydall, Nikolsky et al. 1996). Rad24, the clamp loader (Majka and Burgers 2004), (Rad17 in *Schizosaccharomyces pombe* and Humans) loads the Rad17 clamp (Majka and Burgers 2003) (equivalent to the 9-1-1 complex) onto the DSB. Mec1 (Human ATR) is the downstream kinase which acts to inhibit cell cycle progression. To test whether the decreased DSB signal was a consequence of Rad24, or a function of the Mec1 checkpoint, mutants in Rad17 and Mec1 function were tested. Mec1 has multiple signalling roles in the vegetative and mitotic cells, and to prevent interference with these processes, the expression of Mec1 was placed under the *CLB2* promoter, thereby creating a meiotic null (mn) ((Grandin and Reed 1993)).

In the *rad17Δ* strain, DSBs peaked at 3 hours reaching almost 14% of total DNA (figure 4.4A, C and E). By contrast, in the *rad17Δ spo11-HA* strain the DSBs peaked at 3 hours but DSB levels reached 10% (figure 4.4A, C and E). In the *rad17Δ dmc1Δ* strain, DSBs reached approximately 20% of total DNA levels by 4 hours (figure 4.4A, C and E). By contrast, the *rad17Δ dmc1Δ spo11-HA* strain peaked at approximately 8% at 5 hours (figure 4.4A, C and E). These observations indicate that *rad17Δ* mutation when combined with the *spo11-HA* tag causes a decrease in DSB signal, consistent with the observations in the *rad24Δ* mutants.

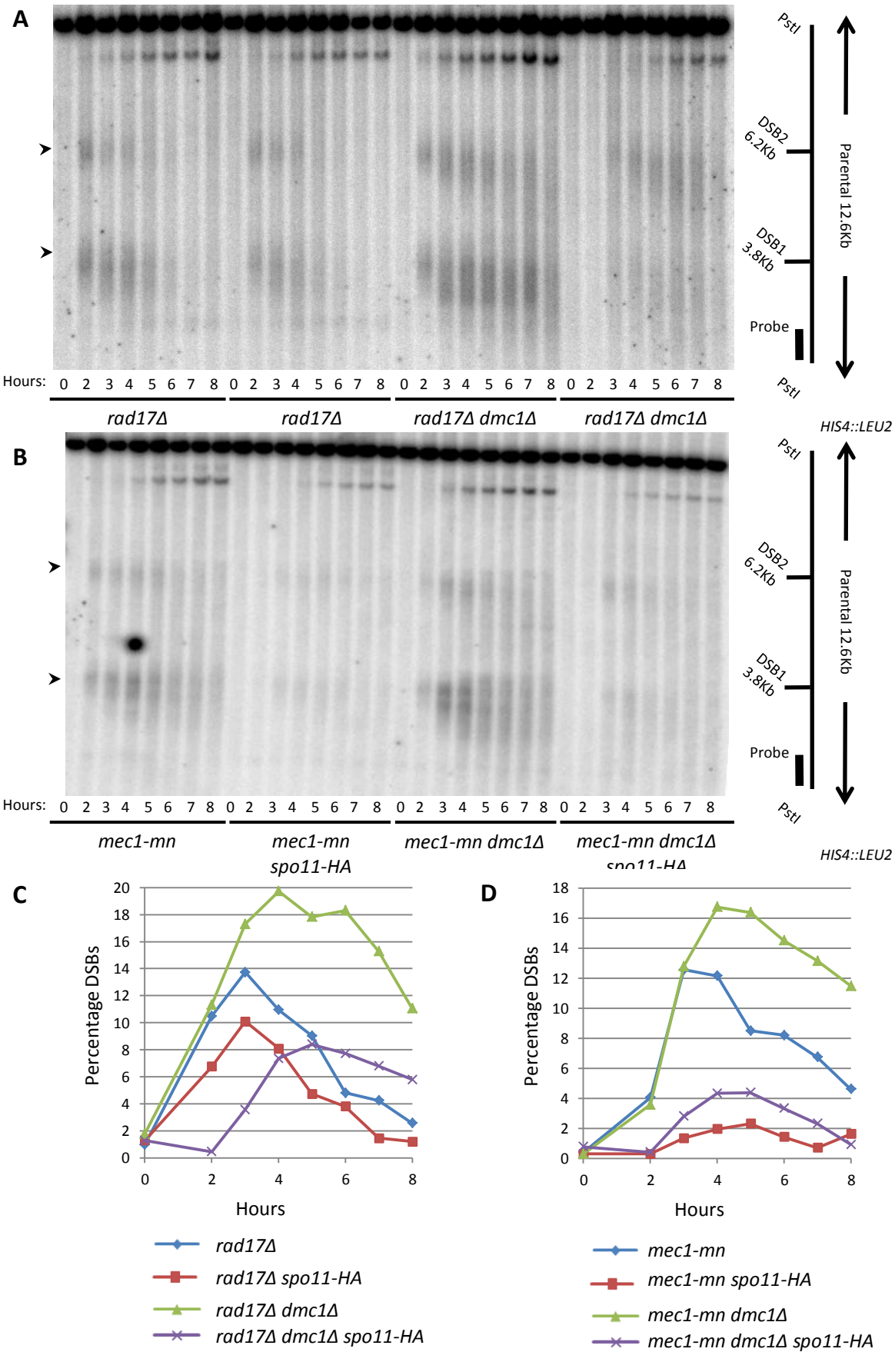
A
PstI
DSB2
6.2Kb
DSB1
3.8Kb
Probe
Parental 12.6Kb
PstI
HIS4::LEU2
Hours: 0 2 3 4 5 6 7 8 0 2 3 4 5 6 7 8 0 2 3 4 5 6 7 8 0 2 3 4 5 6 7 8
rad17Δ
rad17Δ
rad17Δ dmc1Δ
rad17Δ dmc1Δ
B
PstI
DSB2
6.2Kb
DSB1
3.8Kb
Probe
Parental 12.6Kb
PstI
HIS4::LEU2
Hours: 0 2 3 4 5 6 7 8 0 2 3 4 5 6 7 8 0 2 3 4 5 6 7 8 0 2 3 4 5 6 7 8
mec1-mn
mec1-mn spo11-HA
mec1-mn dmc1Δ
mec1-mn dmc1Δ spo11-HA
C
Percentage DSBs
Hours
rad17Δ
rad17Δ spo11-HA
rad17Δ dmc1Δ
rad17Δ dmc1Δ spo11-HA
D
Percentage DSBs
Hours
mec1-mn
mec1-mn spo11-HA
mec1-mn dmc1Δ
mec1-mn dmc1Δ spo11-HA

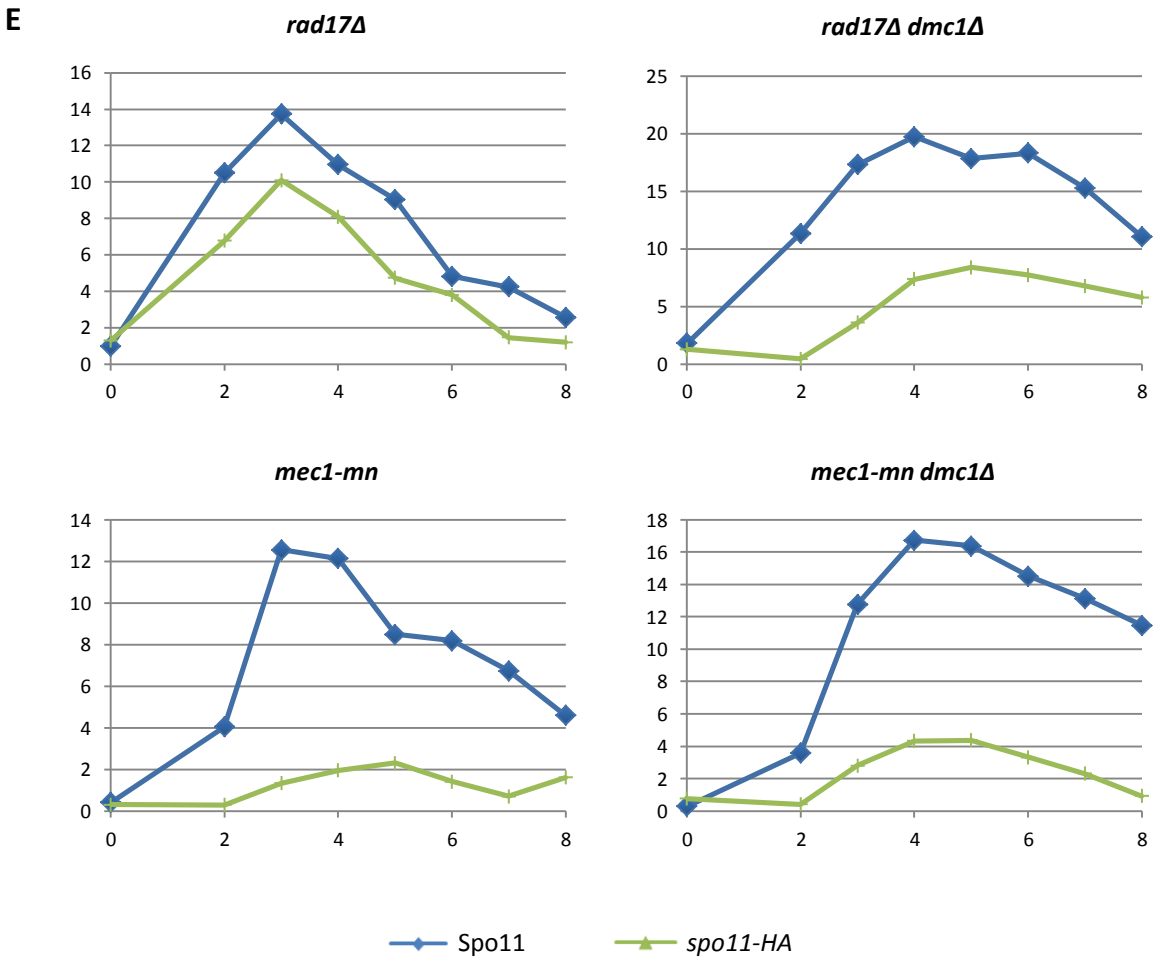

Figure 4.4: DSB levels decreased in *rad17Δ spo11-HA* and *mec1-mn spo11-HA* mutants. A and **B)** Genomic DNA from meiotic time courses were digested and run on a 0.7% 1xTAE agarose gel for 20 hours at 60 volts. The gel was transferred to nylon membrane under denaturing conditions and hybridised with a radioactive probe for the *HIS4::LEU2* locus. The membrane was exposed to a phosphor screen and image taken using a Fuji phosphor scanner. DSBs marked with arrowhead (➤). **C** and **D)** Quantification of DSB levels over time. Image Gauge was used to analyse DSB signal as a percentage of total DNA and signal is plotted and displayed. **E)** Comparisons between mutants in the *SPO11* and *spo11-HA* backgrounds.

In the *mec1-mn* strain, DSBs peaked at 3 hours reaching just over 12% of total DNA (figure 4.4B, D and E). By contrast, the *mec1-mn spo11-HA* strain peaked at 5 hours reaching just over 2% of total DNA (figure 4.4B, D and E). In the *mec1-mn dmc1Δ* strain, DSBs peaked at 4 hours plateauing between 12 and 16% of total DNA (figure 4.4B, D and E). By contrast, the *mec1-mn dmc1Δ spo11-HA* peaked around 4 hours reaching just over 4% of total DNA (figure 4.4B, D and E). This indicates that the *mec1-mn* in combination with the *spo11-HA* tag causes a decrease in the DSB signal. The observations from the *mec1-mn* strains are consistent with the *rad17Δ* and *rad24Δ* strains. As similar observations were seen in all Mec1 checkpoint mutants it suggests that the decrease in DSB signal is due to the absence of the Mec1 meiotic recombination checkpoint and the presence of the *spo11-HA* tag.

4.6: *rad51Δ* does not significantly increase DSB levels in a *rad24Δ dmc1Δ spo11-HA* mutant.

The Mec1 meiotic recombination checkpoint proteins Mec1/Rad24 and Tel1 phosphorylate Hop1 in the presence of Spo11 DSBs (Carballo, Johnson et al. 2008). The Hop1 phosphorylation is required for establishment of an inter-homolog repair bias as opposed to inter-sister repair (Carballo, Johnson et al. 2008). One hypothesis to explain the decrease in DSBs observed in the Mec1 checkpoint mutants when combined with the *spo11-HA* tag is that some of the DSBs formed are repairing in an inter-sister manner.

The *spo11-HA* tag is reported to cause a reduction in DSB levels (Martini, Diaz et al. 2006). This reduction could cause a decrease in the Hop1 dependent phosphorylation. *mec1Δ* mutants had decreased phosphorylation of Hop1 which was further reduced in the absence of Tel1 (Carballo, Johnson et al. 2008). The combinations of a decrease in DSB signal from the *spo11-HA* and the lack of phosphorylation in a *mec1Δ* mutant may prevent the Tel1 phosphorylation from being sufficient to establish the inter-homolog bias.

Rad51, like Dmc1, is a recombinase (Shinohara, Ogawa et al. 1992; Sheridan, Yu et al. 2008). Unlike Dmc1, Rad51 is expressed throughout the cell cycle and repairs DSBs using the sister chromatid as a template (Shinohara, Ogawa et al. 1992). Removal of Rad51 and Dmc1 prevents all repair by homologous recombination during meiosis (Bishop, Park et al. 1992; Shinohara, Ogawa et al. 1992; Sheridan, Yu et al. 2008). To test if inter-sister repair is taking place and accounting for the decrease in DSB levels, the *rad51Δ* mutation was introduced.

In the *rad24Δ rad51Δ dmc1Δ* strain, DSBs reach approximately 16% of total DNA by 6 hours and remained above 16% until the end of the time course (figure 4.5). By contrast, the *rad24Δ rad51Δ dmc1Δ spo11-HA* DSBs reaches around 6% of total DNA by 7 hours and remains around this level (figure 4.5). When compared with the *rad24Δ dmc1Δ spo11-HA* strain there is a slight increase in DSB levels caused by the *rad51Δ* mutation. These observations indicate that although DSB levels increase slightly in *rad24Δ rad51Δ dmc1Δ spo11-HA* compared with *rad24Δ dmc1Δ spo11-HA*, a decrease in DSB levels still exists when compared with *rad24Δ rad51Δ dmc1Δ.* These observations therefore indicate that the decrease in DSBs observed in the *rad24Δ dmc1Δ spo11-HA* is not a consequence of inter-sister repair.

4.7: *spo11-HA* causes a reduction in DSB levels in a *sae2Δ* mutant.

An alternative hypothesis to explain the decreased DSB levels is that fewer DSBs form in the Mec1 meiotic recombination checkpoint mutants when combined with the *spo11-HA* tag. Some evidence from *Saccharomyces cerevisiae* (Zhang, Kim et al. 2011)*, Drosophila melanogaster (Joyce, Pedersen et al. 2011)* and mouse (Lange, Pan et al. 2011) have implicated checkpoint proteins in inhibiting meiotic DSBs. However, there is currently no published data to support the idea that the Mec1 checkpoint may function to form meiotic DSBs.

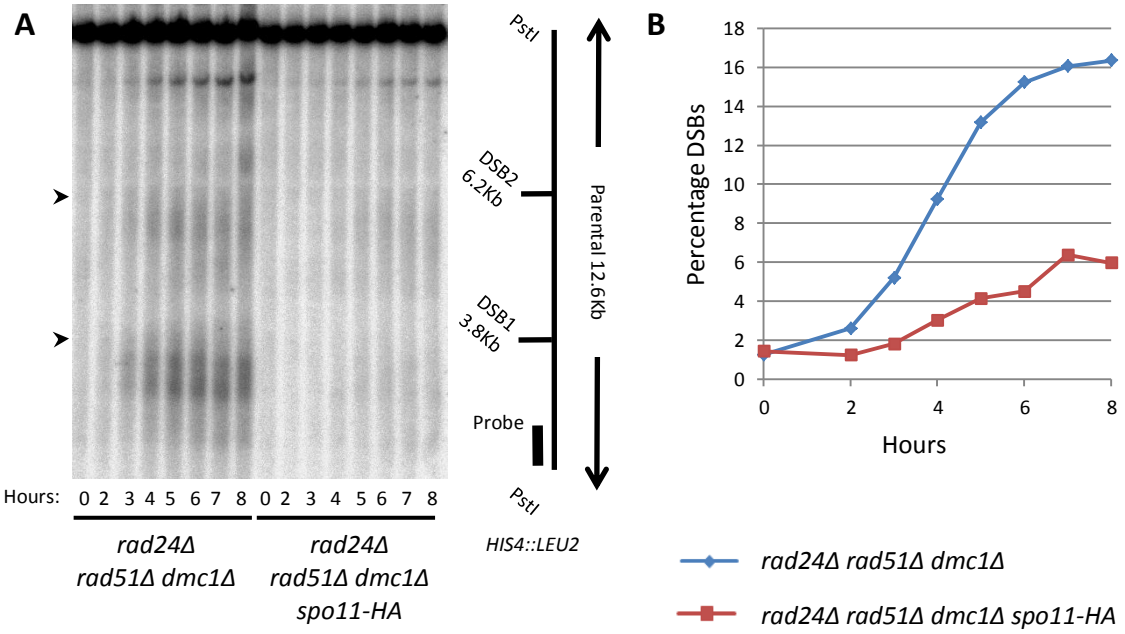

Figure 4.5: DSB levels do not return to expected levels when removing Rad51. A) Genomic DNA from meiotic time courses were digested and run on a 0.7% 1xTAE agarose gel for 20 hours at 60 volts. The gel was transferred to nylon membrane under denaturing conditions and hybridised with a radioactive probe for the *HIS4::LEU2* locus. The membrane was exposed to a phosphor screen and image taken using a Fuji phosphor scanner. DSBs marked with arrowhead (➤). **B)** Quantification of DSB levels over time. Image Gauge was used to analyse DSB signal as a percentage of total DNA and signal is plotted and displayed.

Sae2 is required to endonucleolytically remove Spo11 from the ends of the DSB (Neale, Pan et al. 2005). In the absence of *SAE2,* DSBs are prevented from repairing due to the covalent Spo11 attachment (McKee and Kleckner 1997; Neale, Pan et al. 2005). To determine the levels of DSBs formed in mutants the *sae2Δ* mutation was utilised.

In the *sae2Δ* strain, DSBs peaked around 14% of total DNA at 6 hours and fluctuated slightly but remained around this level (figure 4.6). By contrast, the *sae2Δ spo11-HA* DSBs reached between 6 and 8% of total DNA (figure 4.6). In the *sae2Δ rad24Δ* strain, DSBs reached 16% of total DSBs by the end of the time course, slightly higher than the DSBs observed in the *sae2Δ* (figure 4.6). By contrast, the DSBs in the *sae2Δ rad24Δ spo11-HA* strain reached less than 6% of total DNA (figure 4.6). These observations indicate that *spo11-HA* causes around a 2-fold reduction in DSB levels in the *sae2Δ* background and *rad24Δ* has little or no effect. More importantly, there is no large additive reduction observed when both the *rad24Δ* and *spo11-HA* tag is combined. These results contrast with measurements made in *dmc1Δ*, where the *spo11-HA* tag had no effect on DSB levels on its own, or in a *dmc1Δ* background, but caused a decrease DSB levels when combined with *rad24Δ*.

The observations made from the *dmc1Δ* block and the *sae2Δ* block therefore suggest that the meiotic checkpoint proteins Rad24, Rad17 and Mec1 function to stimulate DSB formation in the *dmc1Δ* block when combine with the *spo11-HA* tag (figures 4.1, 4.3 and 4.4). However, the observations also suggest that the checkpoint proteins do not function to stimulate DSB formation in the *sae2Δ* block when combine with the *spo11-HA* tag (figure 4.6).

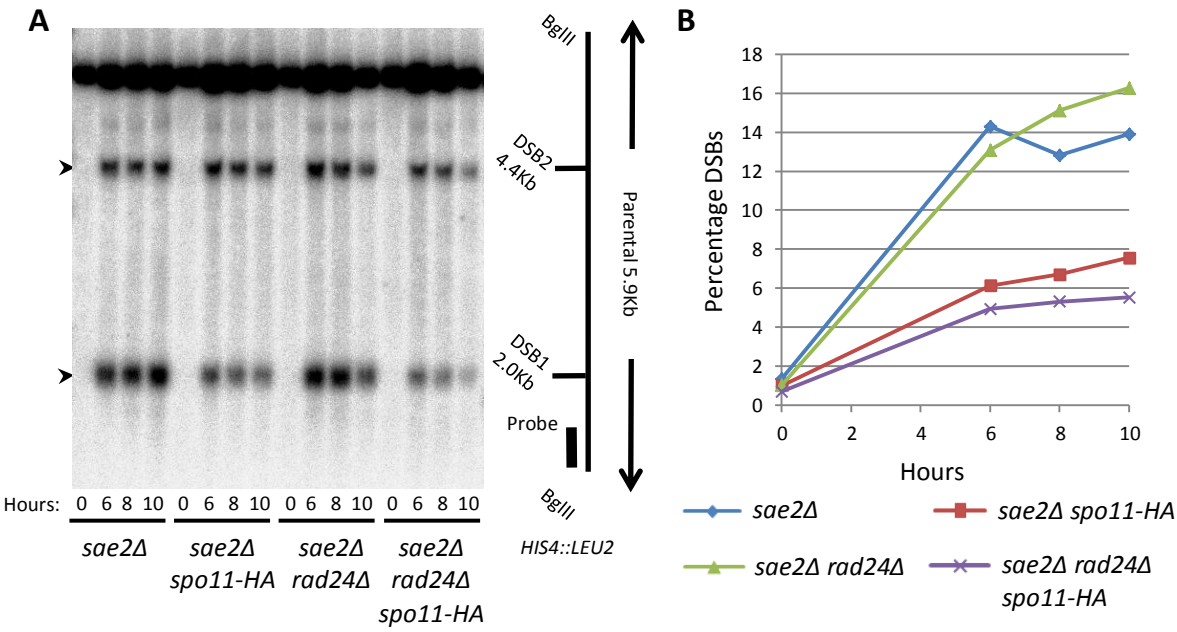

Figure 4.6: The *spo11-HA* tag causes a reduction in DSB levels in the *sae2Δ* background. A) Genomic DNA from meiotic time courses were digested and run on a 0.7% 1xTAE agarose gel for 18 hours at 60 volts. The gel was transferred to nylon membrane under denaturing conditions and hybridised with a radioactive probe for the *HIS4::LEU2* locus. The membrane was exposed to a phosphor screen and image taken using a Fuji phosphor scanner. DSBs marked with arrowhead (➤). **B)** Quantification of DSB levels over time. Image Gauge was used to analyse DSB signal as a percentage of total DNA and signal is plotted and displayed.

4.8: *mek1Δ* when combined with the *spo11-HA* tag causes a reduction in DSB levels.

To test whether the decreased DSB levels observed in the *rad24Δ spo11-HA, rad17Δ spo11-HA, or mec1-mn spo11-HA* is a direct consequence of the absence of the Mec1 meiotic recombination checkpoint proteins, a mutation was made in a downstream target of the checkpoint. Mek1 is the meiotic Rad53/Chk2 homolog and is a downstream target, phosphorylated by Hop1 due to Mec1 checkpoint activation (Bailis, Smith et al. 2000; Niu, Li et al. 2007; Carballo, Johnson et al. 2008). Mek1 is required for Mec1 checkpoint activation and inter-homolog bias (Bailis, Smith et al. 2000; Niu, Li et al. 2007; Carballo, Johnson et al. 2008).

If the ability to stimulate DSB formation is a direct consequence of Mec1 meiotic checkpoint proteins (but possibly independent of their roles in the checkpoint), then mutation of the downstream *MEK1* will have no effect on DSB levels. However, if the ability to stimulate DSB formation is a consequence of the Mec1 checkpoint activation, then the *mek1Δ* mutation will mirror that of a *rad24Δ, rad17Δ* or *mec1-mn* mutation and cause a reduction in DSBs.

Although it has been determined that DSB levels measured in a *rad24Δ dmc1Δ spo11-HA* are not low because of repair via Rad51 (figure 4.5), Mek1 is required for inter-homolog bias and therefore DSB levels will be measured in a *rad51Δ dmc1Δ* background.

In the *rad51Δ dmc1Δ spo11-HA* strain, DSBs peaked at around 14% of total DSB levels at 7 hours (figure 4.7). By contrast, the DSBs measured in the *mek1Δ rad51Δ dmc1Δ spo11-HA* mutant failed to reach 2% of total DNA (figure 4.7). This observation suggests that *mek1Δ* in addition to *spo11-HA* causes a reduction in DSBs. This is consistent with the DSB reduction being a general consequence of defective Mec1 checkpoint activity, as opposed to a direct effect of the Rad24, Rad17 and Mec1 proteins.

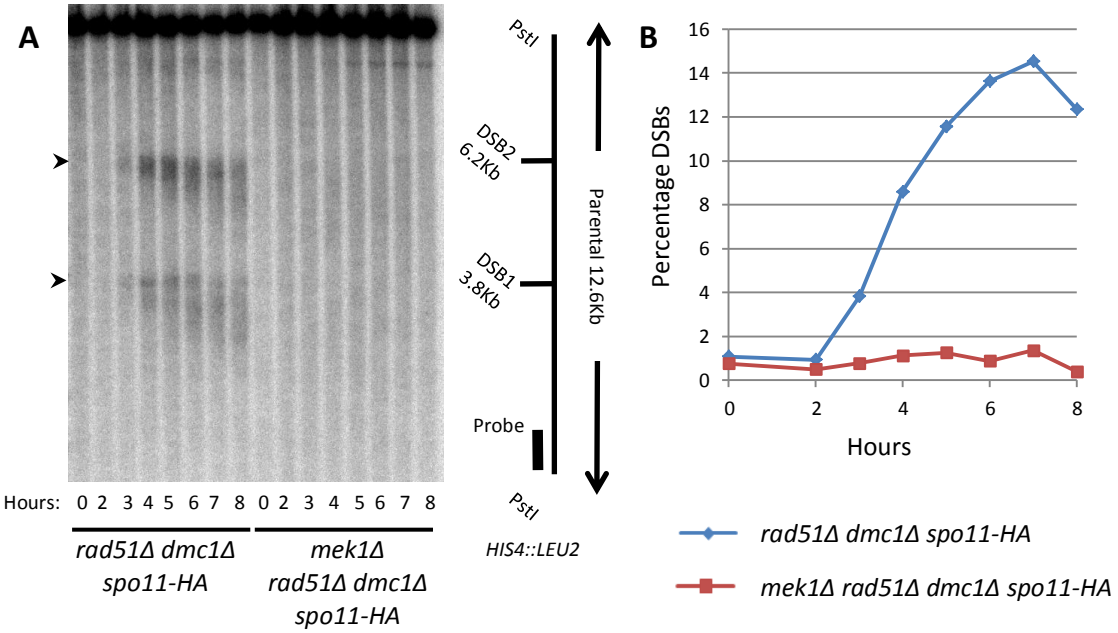

Figure 4.7: DSB levels are low in the *mek1Δ spo11-HA* background. A) Genomic DNA from meiotic time courses were digested and run on a 0.7% 1xTAE agarose gel for 18 hours at 60 volts. The gel was transferred to nylon membrane under denaturing conditions and hybridised with a radioactive probe for the *HIS4::LEU2* locus. The membrane was exposed to a phosphor screen and image taken using a Fuji phosphor scanner. DSBs marked with arrowhead (➤). **B)** Quantification of DSB levels over time. Image Gauge was used to analyse DSB signal as a percentage of total DNA and signal is plotted and displayed.

4.9: Mek1 has decreased phosphorylation in *rad24Δ spo11-HA* background.

Mek1 is phosphorylated in response to checkpoint activity (Niu, Li et al. 2007; Carballo, Johnson et al. 2008). Hop1 phosphorylation is decreased in the absence of Mec1 and Tel1 and this in turn causes a reduction in Mek1 phosphorylation (Carballo, Johnson et al. 2008). To test whether the Mek1 phosphorylation was reduced in response to either the *rad24Δ* mutation, *spo11-HA* tag or by a combination of the two, western blotting against the Mek1 protein was performed in the mutant strains. To increase the resolution between the phosphorylated and non-phosphorylated species, phostag was added to the SDS-PAGE gels.

In all strains *DMC1* strains, Mek1 was present from 3 to 8 hours (figure 4.8). In the wildtype strain phosphorylation of Mek1 was present between 3 and 6 hours. In the *spo11-HA* strain, Mek1 phosphorylation was present from 3 to 6 hours, although signal was lower. In the *rad24Δ* strain Mek1 phosphorylation was present from 4 to 6 hours with less abundance compared with wildtype. By contrast, in the *rad24Δ spo11-HA* strain, all Mek1 phosphorylation was absent. These observations suggest that *spo11-HA* and *rad24Δ* cause a reduction in Mek1 phosphorylation and when combined, the phosphorylation is completely absent. However, these observations also suggest that lack of Mek1 phosphorylation cause a reduction in DSB levels.

In the *dmc1Δ* strains, Mek1 was present from 3 to 8 hours except for the *rad24Δ dmc1Δ spo11-HA* strain where Mek1 was present from 3 to 6 hours (figure 4.8). In the *dmc1Δ* strain, phosphorylated Mek1 was present at 3 to 8 hours with the phosphorylated forms most abundant at 8 hours. In the *dmc1Δ spo11-HA* strain phosphorylated Mek1 was observed from 4 hours onwards, becoming most abundant at 8 hours. By contrast, in the *rad24Δ dmc1Δ* strain the phosphorylated Mek1 was in low abundance at 4 and 8 hours and peaking at 6 hours. In

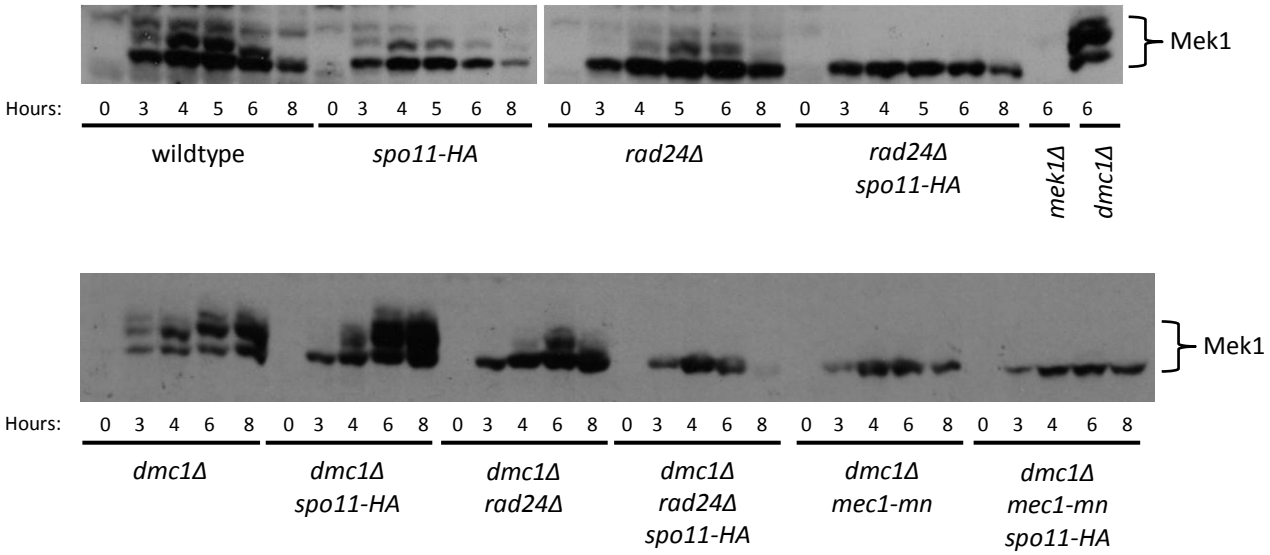

Figure 4.8: Mek1 phosphorylation is decreased in checkpoint defective *spo11-HA* mutants (Data from Matt Neale). Synchronous meiotic time courses were performed and TCA extraction took place. Samples were run on a phostag SDS PAGE and transferred to a PVDF membrane for western blotting. Primary anti-Mek1 (courtesy of Pedro A. San-Segundo) was used at a concentration of 1 in 3,000 followed by secondary anti-Rabbit.

The *rad24Δ dmc1Δ spo11-HA* strain no phosphorylated Mek1 was observed at any of the time points. This suggests that the combination of the checkpoint mutants with the *spo11-HA* tag causes a reduction in Mek1 phosphorylation.

In contrast to Mec1 checkpoint defective *spo11*-HA strains, in the *mec1-mn dmc1Δ* no Mek1 phosphorylation observed at any time point. A lack of Mek1 phosphorylation was also observed in the *mec1-mn dmc1Δ spo11-HA* strains. The Mek1 phosphorylation observed in the *rad24Δ dmc1Δ* and the lack of phosphorylation in the *mec1-mn dmc1Δ* suggests that the *rad24Δ* allows residual phosphorylation which is not observed or that does not occur in the *mec1-mn* background. These observations suggest that *spo11-HA* and mutation of the Mec1 checkpoint cause a reduction in Mek1 phosphorylation which either causes a decrease in DSBs or is a consequence of a lack of DSBs.

4.10: *rad24Δ spo11-HA* progresses through meiosis faster than *rad24Δ.*

Mutants defective in the Mec1 meiotic recombination checkpoint progress through meiosis slower than wildtype (Shinohara, Sakai et al. 2003). To measure meiotic progression, samples throughout meiosis were taken and stained with DAPI. Cells were then scored according to whether the cell had one, two or four nuclei indicating the stage through the meiotic divisions. Meiotic nuclei were tested to determine whether the delay is observed when combined with the *spo11-HA* background. In the wildtype strain, just over 40% of cells had undergone at least meiosis I and this reached over 80% by 6 hours (figure 4.9). The *dmc1Δ* strain failed to progress through meiosis I due to an inability to repair DSBs leading to activation of the Mec1 meiotic recombination checkpoint (Bishop, Park et al. 1992; Lydall, Nikolsky et al. 1996). This observation is consistent with the published phenotype for the *dmc1Δ* strain (Bishop, Park et al. 1992). The *rad24Δ* strain was delayed by 1 hour in comparison to wildtype, reaching over

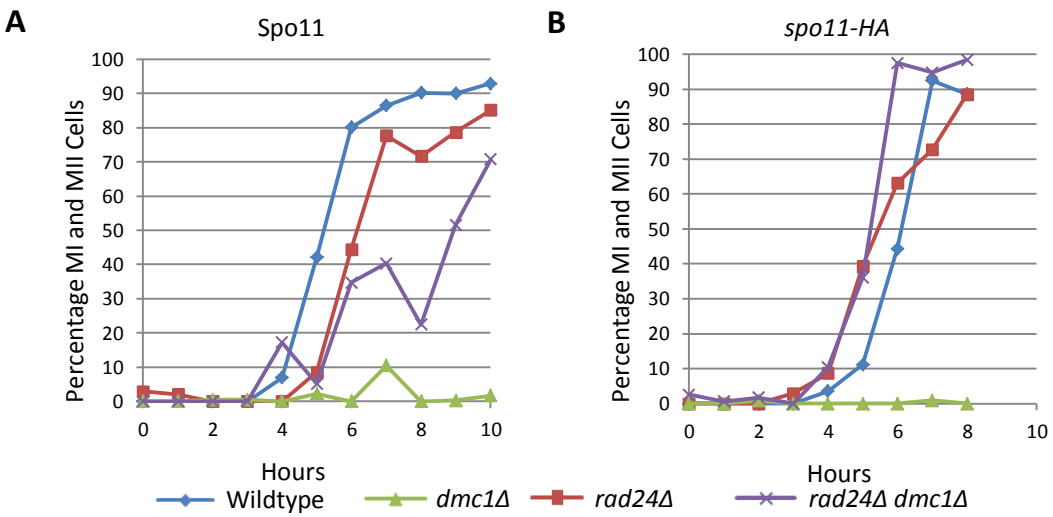

Figure 4.9: Meiotic progression increases when *rad24Δ* strains are tagged with *spo11-HA.* Fixed samples were stained with DAPI and a minimum of 200 cells were scored for one, two (MI) or four nuclei (MII). Percentage cells that had two or four nuclei were calculated and plotted. **A)** Meiotic progression of Spo11 strains **B)** Meiotic progression of *spo11-HA* strains

40% of cells undergone at least meiosis I at 6 hours and almost 80% at 7 hours. In the *rad24Δ dmc1Δ* strain, just over 30% of cells had undergone at least meiosis I by 6 hours and over 50% by 9 hours. This indicates that the Mec1 checkpoint block established by the *dmc1Δ* mutation is bypassed by removal of *RAD24* and also shows the delay compared with wildtype. This is consistent with the published phenotype (Shinohara, Sakai et al. 2003).

In the *spo11-HA* strain, just over 40% of cells had undergone at least meiosis I by 6 hours, reaching 90% by 7 hours (figure 4.9). This indicates that the *spo11-HA* is slightly delayed compared with wildtype. In the *dmc1Δ spo11-HA* strain, the cells did not progress through meiosis I due to persistent unrepaired DSBs and activation of the Mec1 meiotic recombination checkpoint (Bishop, Park et al. 1992; Lydall, Nikolsky et al. 1996). In the *rad24Δ spo11-HA* strain approximately 40% of cells went through at least meiosis I by 5 hours.
The rate of progression through meiosis decreased in the *rad24Δ spo11*-HA compared with *spo11-HA*, with just over 70% of cells having undergone at least meiosis I compared with over 90% at 7 hours. However, by 8 hours both strains had a similar percentage of cells having undergone at least meiosis I. In the *rad24Δ dmc1Δ spo11-HA* strain just under 40% of cells underwent at least meiosis I by 5 hours and under just 100% by 6 hours. This suggests that the *rad24Δ spo11-HA* and *rad24Δ dmc1Δ spo11-HA* cells progressed through meiosis at a similar rate as wildtype. Therefore the delay observed in the *rad24Δ* mutants is no longer observed when combined with the *spo11-HA* tag.

4.11: Spore viability decreases in *rad24Δ spo11-HA* background.

To test whether the decrease in DSB signal observed in the *rad24Δ spo11-HA* strain had an effect on spore viability, tetrads were dissected and scored according to total percentage growth and number of viable spores per tetrad. The wildtype strain had a viability of 96.3%

with the majority of tetrads producing 4 viable spores, with a small number of 3 and 2 viable spores and 2 tetrads forming 0 viable spores (figure 4.10). In the *spo11-HA* strain there was a slight decrease in spore viability compared with wildtype (95.2%) with a decrease in the number of 4 spore viable tetrads, a similar number of 3 spore viable tetrads and an increase in the number of 2 viable spores from tetrads (figure 4.10).

In the *rad24Δ* strain the total spore viability was almost 28% (figure 4.10) (higher than the published 15.3% (Lydall, Nikolsky et al. 1996)). Over 40% of the tetrads formed 0 viable spores, 30% of tetrads forming 1 viable spore, less than 14% of tetrads forming 2 viable spores and less than 10% of tetrads forming 3 and 4 viable spores. By contrast, the *rad24Δ spo11-HA* had a low total spore viability of less than 5 %, with the majority of tetrads forming 0 viable spores and a low proportion forming either 1 or 2 viable spores per tetrad. These observations suggest that the combination of *rad24Δ* and *spo11-HA* tag causes a reduction in spore viability. DSBs are required for pairing homologous chromosomes and ensuring at least one obligate crossover per homolog pair. Reducing the number of DSBs causes a reduction in spore viability (for example *hop1Δ* (Mao-Draayer, Galbraith et al. 1996) and *spo11Δ* (Klapholz, Waddell et al. 1985)), likely due to the reduction in crossovers and homolog pairing events. It is therefore likely that the reduction in spore viability in the *rad24Δ spo11-HA* strain is a consequence of reduced DSBs.

4.12: *ndt80Δ* does not cause DSBs to return to expected levels in a *rad24Δ rad51Δ dmc1Δ spo11-HA* strain.

DSB levels are reduced in situations where *rad24Δ* and the *spo11-HA* tag are combined. A reduction is also observed in a *spo11-HA sae2Δ* strain. However, *spo11*-HA does not have a reduction in an otherwise wildtype strain or when combine with just the *dmc1Δ* mutation.

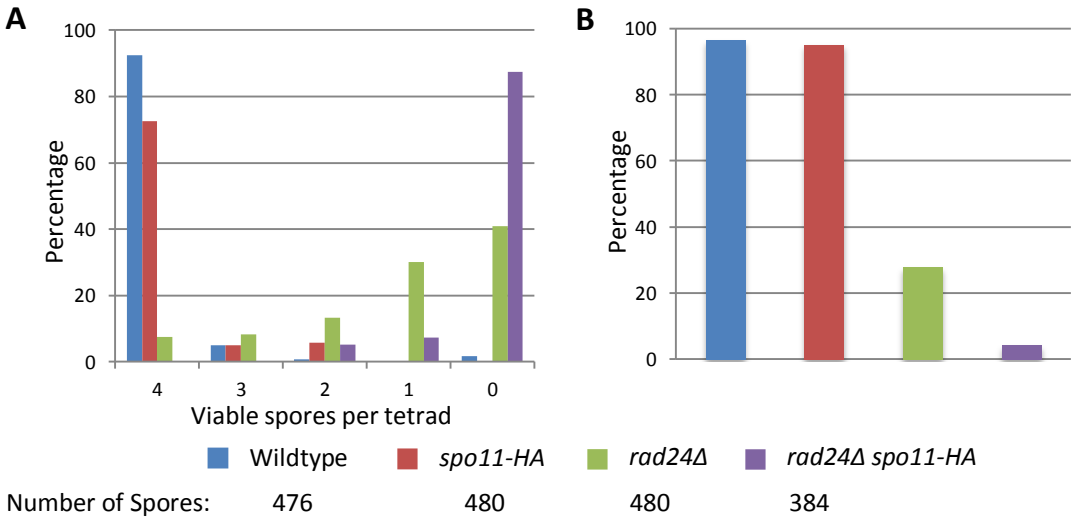

Figure 4.10: Spore viability decreases when *rad24Δ* strains are also *spo11-HA* tagged. Samples from time courses were sporulated for a minimum of 48 hours then dissected as documented in material and methods. **A)** Number of viable spores per tetrad. **B)** Total number of viable spores in each class.

These observations highlighted that in the *spo11-HA* strain the reduction in DSB levels were compensated for in an otherwise wildtype situation or in the *dmc1Δ* block, but not in the *sae2Δ* block. The removal of *rad24Δ* caused a reduction in DSB levels in *spo11-HA* strains, highlighting a role for Rad24 to compensate for the reduction.

Observations from *rad17Δ, mec1-mn* and *mek1Δ* strains indicated that the compensation mechanism is a function of the Mec1 checkpoint, as opposed to an independent function of the proteins. The reduction in spore viability in *rad24Δ spo11-HA* compared with *rad24Δ* and *spo11-HA* support a decrease in DSBs. In addition, the observed slower meiotic progression in the *rad24Δ* is no longer present in the *rad24Δ spo11-HA*, possibly due to less physical barriers to progression and division due to decreased DSBs.

An alternative explanation for the reduction in DSBs levels observed in the *rad24Δ spo11-HA* strain relates to the meiotic progression observation. DSB formation occurs after DNA synthesis and before the first meiotic division. If this window where the cell is competent to form DSBs is shorter, then it may cause a reduction in DSB levels. The *rad24Δ spo11-HA* strain has a faster meiotic progression compared with the *rad24Δ* strain and therefore the reduction might be due to a shorter DSB formation proficient window, in contrast to the Mec1 checkpoint functioning as a DSB compensation mechanism.

Ndt80 is a meiotic transcription factor that is expressed when the Mec1 meiotic recombination checkpoint is alleviated causing progression to the first meiotic division (Xu, Ajimura et al. 1995). In the absence of *NDT80*, cells are blocked after DSB formation and before joint molecule resolution. *ndt80Δ* mutants however continue to be competent at forming Spo11-dependent DSBs (Allers and Lichten 2001). To test whether the decrease in DSB levels observed in the *rad24Δ spo11-HA* strain is a consequence of a shorter DSB formation window,

the *ndt80Δ* mutation was introduced into the *rad24Δ spo11-HA* background to increase the DSB formation window. In order to account for all DSBs that are formed, the *rad51Δ* and *dmc1Δ* mutations were also introduced, prevent repair and causing accumulation of DSB signal.

In the *rad24Δ rad51Δ dmc1Δ* strain, DSBs reached above 12% of total DNA signal from 6 hours onwards (figure 4.11). By contrast, the *rad24Δ rad51Δ dmc1Δ spo11-HA* plateaued at approximately 4% of total DNA by 5 hours (slightly lower than previously observed in figure 4.5). The *ndt80Δ rad24Δ rad51Δ dmc1Δ spo11-HA* strain peaked at approximately 5% at 6 hours (figure 4.11). The lack of increase in the *ndt80Δ* background suggests that the reduction in DSBs in not due to a shortening of a DSB proficient window. However, although the *ndt80Δ* block prevents progression to the meiotic division, the alleviation of the Mec1 checkpoint may be the end of the DSB formation window. If this is the case, then the absence of the Mec1 checkpoint would cause a reduction in DSBs and the *ndt80Δ* block would not be able to cause an increase in DSB levels.

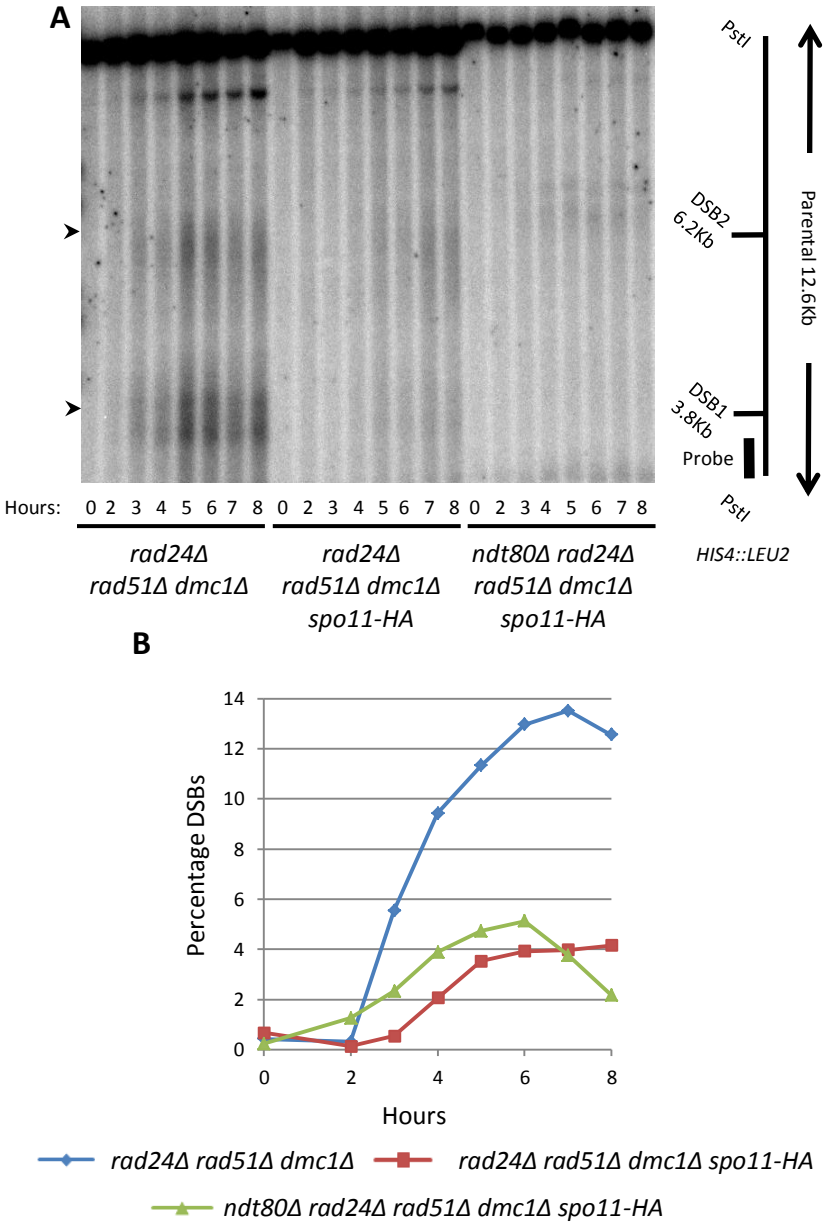

Figure 4.11: DSB signal does not return when mutating Ndt80. A) Genomic DNA from meiotic time courses were digested and run on a 0.7% 1xTAE agarose gel for 20 hours at 60 volts. The gel was transferred to nylon membrane under denaturing conditions and hybridised with a radioactive probe for the *HIS4::LEU2* locus. The membrane was exposed to a phosphor screen and image taken using a Fuji phosphor scanner. DSBs marked with arrowhead (➤). **B)** Quantification of DSB levels over time. Image Gauge was used to analyse DSB signal as a percentage of total DNA and signal is plotted and displayed.

4.13: Discussion.

In chapter 3.2 it was observed that *rad24Δ dmc1Δ spo11-HA* produced lower than expected DSBs at the *HIS4::LEU2* locus (figure 3.2.8) based on published data (Lydall, Nikolsky et al. 1996) and observations from *dmc1Δ spo11-HA* (figure 3.2.5). Although *spo11-HA* is reported to cause an 11-31% reduction in DSB levels (Martini, Diaz et al. 2006), the observed reduction was greater than this. Interestingly in contrast to the published observations, the *spo11-HA* and *dmc1Δ spo11-HA* strains did not show a reduction in DSB levels (figures 3.2.2 and 4.1). Initial observations from this chapter clarified that the DSB reduction was a consequence of the combination of *rad24Δ* with the *spo11-HA* tag. These observations were confirmed at the natural *ARE1* hotspot (figure 4.3). The decreased DSB levels were also observed in two new isolates of *rad24Δ dmc1Δ spo11-HA*, ruling out any possibility of a random mutation causing the observed phenotype.

To test whether the decrease in DSBs was due to an absence of Rad24 or a general effect of not having a functional Mec1 checkpoint, DSB levels were measured in mutants in Rad17, Mec1 or Mek1 in combination with the *spo11-HA* tag. Low levels of DSBs were observed in these strains indicating that the reduction was a consequence of a lack of Mec1 checkpoint function in the *spo11-HA* strains. Checkpoint proteins are required to establish the inter-homolog repair bias during meiosis (Carballo, Johnson et al. 2008; Niu, Wan et al. 2009). It was hypothesised that the reduction in DSBs observed was an additive effect of a reduction in DSBs from the presence of the *spo11-HA* tag and inter-sister repair by Rad51 taking place in the Mec1 checkpoint defective strains. In order to remove residual repair that might be occurring, DSB levels were measured in the *rad24Δ rad51Δ dmc1Δ spo11-HA* background. The DSB levels measured were slightly higher in the absence of Rad51, but still low compared to the *rad24Δ*

rad51Δ dmc1Δ strain. These observations rule out Rad51 dependent repair being the cause for the reduction in DSB levels.

Another hypothesis to explain the reduction in DSBs observed in the Mec1 checkpoint defective *spo11-HA* strains are that fewer DSBs are formed in these backgrounds. DSB levels were measured in the *rad24Δ, spo11-HA* and *rad24Δ spo11-HA* backgrounds using the *sae2Δ* block. The *sae2Δ* block accumulates DSBs in an unprocessed, unresected state. The *sae2Δ* block revealed a reduction in DSB levels in the *spo11-HA* strains, with the *rad24Δ* mutation having no effect. The *sae2Δ* experiments add to the observations made in the otherwise wildtype background and the *dmc1Δ* background, which are as follows:

1. In an otherwise wildtype background, *spo11-HA* does not have a reduction in DSB levels compared with wildtype
2. The *dmc1Δ spo11-HA* mutant does not have a reduction in DSB levels compared with *dmc1Δ*
3. The *rad24Δ spo11-HA* and *rad24Δ dmc1Δ spo11-HA* had a reduction in DSB levels when compared to their *SPO11* equivalents
4. The *spo11-HA* when combines with the *sae2Δ* mutation has a reduction in DSB levels compared with *sae2Δ*
5. The *rad24Δ* mutation does not cause a reduction in DSB levels in the *sae2Δ* background.

With the reduction in DSB levels observed in the *sae2Δ spo11-HA* strain, one question that is raised is why does the *spo11-HA* and *dmc1Δ spo11-HA* strains not show a reduction in DSB levels? One possible explanation for the lack of *spo11-HA* effect relates to the *rad24Δ* observations. When combined with the *spo11-HA* tag, the *rad24Δ* mutation has a reduction in DSB levels. This is also observed in the *dmc1Δ* background. The differences between the *RAD24* and *rad24Δ* strains imply that *RAD24* functions to promote DSB formation by a

feedback mechanism in the *spo11-HA* background. This is extremely surprising as the Mec1 checkpoint has not previously been described as a mechanism for promoting DSBs. In addition, recent publications have described an inhibitory role for Tel1 checkpoint machinery in meiotic DSB formation (Joyce, Pedersen et al. 2011; Lange, Pan et al. 2011; Zhang, Kim et al. 2011), in contrast to the suggestion made here.

With the suggestion that the Mec1 checkpoint functions as a feedback mechanism to promote DSB formation in the *spo11-HA* background, it is important to address why the absence or presence of the Mec1 checkpoint does not cause a change in DSB levels in the *sae2Δ* block, but does in the *dmc1Δ* block. One explanation for this relates to the type of DNA molecule that is accumulated at the two blocks. In the *sae2Δ* block, DSBs accumulate in an unprocessed, unresected state in contrast to the *dmc1Δ* block where DSBs accumulate in a processed, resected state. Components of the Mec1 meiotic recombination checkpoint are activated in the presence of single-stranded DNA (Zou and Elledge 2003). Therefore, in the *sae2Δ* background, the DSBs formed do not produce a strong Mec1 checkpoint activating signal, and do not promote DSB formation. However, in the *dmc1Δ* block, the DSBs formed become resected producing extensive stretches of ssDNA causing stimulation of the Mec1 meiotic checkpoint and allowing DSB formation compensation to occur. Figure 4.12 depicts a model demonstrating Mec1 checkpoint activation and DSB compensation in the different stages of DSB repair.

The observations described within this chapter, and more specifically the DSB levels in the *sae2Δ* and *dmc1Δ* mutations, indicate the differences between the two blocks to repair. In the *dmc1Δ* mutation, DSB levels are sensitive to the presence of the checkpoint, whereas the *sae2Δ* mutation is not. Differences in the distribution of meiotic DSBs have been observed

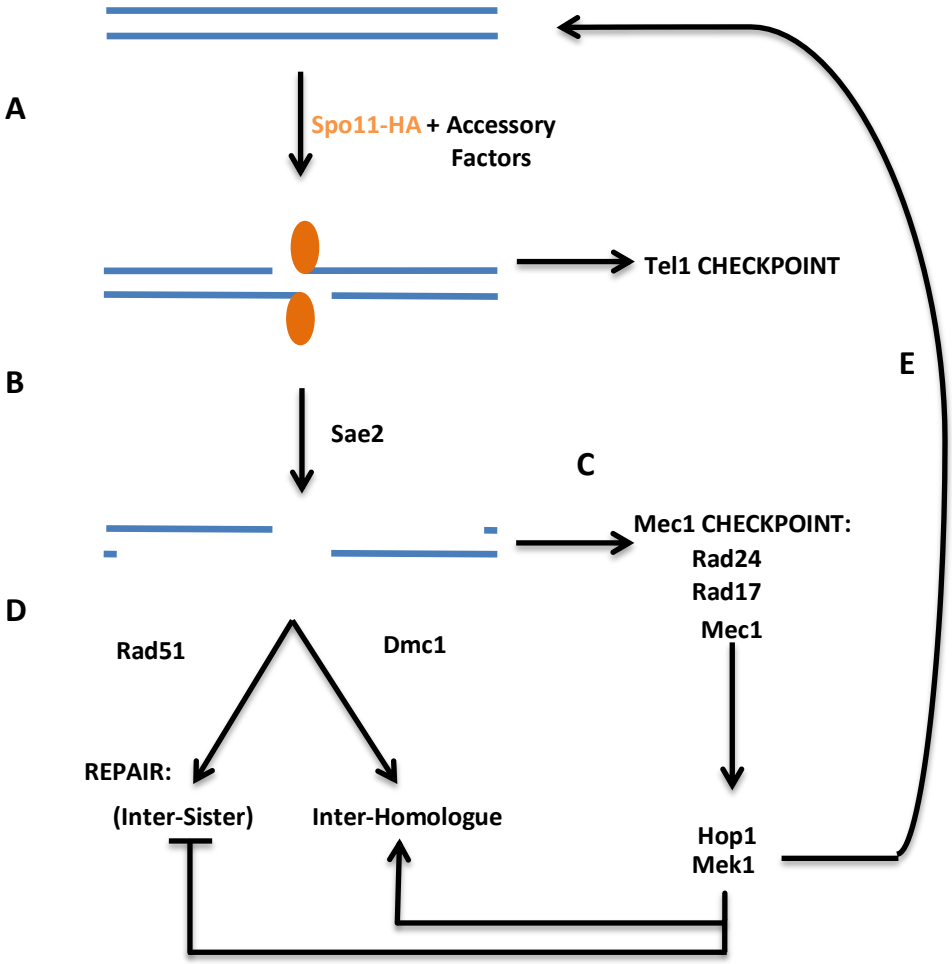

Figure 4.12: Model for DSB feedback mechanism. A) DSBs form by s*po11-HA* and its accessory factors and *spo11-HA* becomes attached to both sides of the DSB. **B)** Sae2, in addition to the MRX complex, is required to process the DSB causing resection to occur. **C)** The meiotic recombination checkpoint is activated by single stranded DNA and activates downstream kinases causing enforcement of the inter-homolog bias for repair. **D)** Dmc1 and Rad51 enable strand invasion and subsequent stages of DSB repair to occur. Activation of the inter-homolog bias machinery, specifically Mek1, causes phosphorylation of Mek1 and activation of the DSB feedback mechanism **(E)** promoting DSBs formation.

within the field when comparing *sae2Δ* and *dmc1Δ* datasets (Gerton, DeRisi et al. 2000; Buhler, Borde et al. 2007). With the observations made within this chapter, it is possible that the differences are as a result of the Mec1 checkpoint. To test this hypothesis, removal of the Mec1 checkpoint in the *dmc1Δ* background may provide similar results to the *sae2Δ* dataset.

In addition to the observations made regarding total DSB levels, interestingly the *spo11-HA* effect changes the distribution of DSB signal within the *HIS4::LEU2* locus. The *HIS4::LEU2* locus consists of two DSB sites, separated by 2.4Kb. In a wildtype situation, DSB1 is the strongest site. However, in the *spo11-HA* background, when DSB signal is present, the DSB sites either become more similar or have an increase at DSB2. This observation suggests that the action of *spo11-HA* causes a site specific reduction or increase in DSB levels, therefore changing the DSB distribution.

The idea that the Mec1 checkpoint functions to promote DSB formation by a feedback mechanism in the *spo11-HA* background, and therefore compensate for the decrease in DSB levels, has implications in the observations regarding crossover homeostasis. In experiments that uncovered crossover homeostasis, Spo11 mutants that were increasing hypomorphic in DSB formation were used (Martini, Diaz et al. 2006). Combining the hypomorphic Spo11 mutant with the *rad50S* mutation provided allowed DSBs to accumulate and levels measured from pulsed field gels. The *rad50S* mutation is equivalent to the *sae2Δ* mutation, where DSBs form but remain unprocessed and unrepaired. The importance of the DSB levels in investigating crossover homeostasis was that it was an accurate measure of the DSBs forming in these mutants. The observations from this chapter however, highlight the possibility that the *rad50S* block does not take into account the DSB compensation that might occur through activation of the Mec1 checkpoint.

This chapter presents the concept of Mec1 checkpoint dependent mechanism which functions in the *spo11-HA* background. The focus of chapter 5 will be to further uncover this mechanism.

CHAPTER 5:

Investigating the DSB feedback mechanism

Chapter 5: Investigating the DSB feedback mechanism

5.1: Introduction

It was observed in chapter 3.2 that the *rad24Δ dmc1Δ spo11-HA* strain had an unexpected reduction in DSB levels (figure 3.2.8). Observations from experiments performed in chapter 4 further isolated the DSB reduction to strains defective in the Mec1-dependent meiotic recombination checkpoint in combination with the *spo11-HA* tag (figures 4.1, 4.4 and 4.7). The comparison between strains also carrying either the *dmc1Δ* or *sae2Δ* mutations suggested the presence of a DSB feedback mechanism that functions through the Mec1-dependent meiotic recombination checkpoint. If the DSB feedback mechanism exists, it seems reasonable to imagine that it can compensate for a reduction in DSB levels in situations other than just the *spo11-HA* background. To test this idea, mutants in Spo11 that have a greater reduction in DSBs compared with *spo11-HA* will be combined with either the *sae2Δ* or *dmc1Δ* mutations. According to the DSB feedback model (figure 4.12), in the *sae2Δ* block the DSB feedback mechanism will not be functional whereas the *dmc1Δ* mutation will activate the DSB feedback mechanism. Therefore, if the DSB feedback mechanism idea is correct, comparing the *sae2Δ* and *dmc1Δ* mutants will show an increase in DSB levels in the *dmc1Δ* mutant. Removal of *RAD24* in the *dmc1Δ* background, and therefore removal of the DSB feedback mechanism, should lead to a reduction in DSB levels compared to the *dmc1Δ* mutant.

The DSB feedback mechanism is thought to function by activation of the Mec1-dependent checkpoint in response to ssDNA (figure 4.12). To test this idea, the *sae2Δ spo11-HA* mutations can be utilised as the DSB feedback mechanism is not believed to function in this background, but DSB levels can be higher (potentially up to *sae2Δ* DSB levels). Using the *sae2Δ spo11-HA* mutation, a DNA damaging agent can be added, creating events that will cause stimulation of

the Mec1-dependent checkpoint and therefore stimulation of the DSB feedback mechanism. As the experiment will be performed using the *sae2Δ* background, any additional Spo11 dependent DSBs will accumulate in an unprocessed manner, allowing for any increases in DSB levels to be detected.

5.2: DSB levels do not increase in *spo11-Y135F-HA/spo11-HA* or *spo11-D290A-HA* in situations where the DSB feedback mechanism may function.

Sequence comparison between Spo11 and Spo11 homologs in other organisms identified a crucial residue required for DSB formation: tyrosine 135 (Keeney, Giroux et al. 1997). A *spo11-Y135F* mutant fails to form DSBs but when a *spo11-Y135F-HA/spo11*-HA heterozygote diploid is constructed, DSB levels are reduced to approximately 29% of wildtype (Martini, Diaz et al. 2006). Additional sequence and structural analysis of Spo11 identified sites that, when mutagenized, caused a reduction in meiotic DSB levels when combined with the HA tag (Diaz, Alcid et al. 2002). One mutation identified was *spo11-D290A-HA* which caused a reduction of DSB levels to approximately 8% of wildtype signal at the *his4::LEU2* locus (when measured in the *rad50S* background) (Diaz, Alcid et al. 2002) and approximately 17% of wildtype signal when multiple chromosomes are compared (Martini, Diaz et al. 2006). Therefore the *spo11-Y135F-HA/spo11-HA* and the *spo11-D290A-HA* backgrounds provide situations where DSB formation is compromised to a greater extent than the *spo11-HA* background. In order to test the ability for the DSB feedback mechanism to compensate for decrease in Spo11 DSB formation ability, the *spo11-Y135F-HA/spo11-HA* and the *spo11-D290A-HA* backgrounds were combined with either the *sae2Δ, dmc1Δ* or *rad24Δ dmc1Δ* mutations. If the DSB feedback mechanism is correct then *sae2Δ* mutation will give a DSB level without the action of the feedback, a *dmc1Δ* mutation will give a higher DSB level due to the feedback functioning and the *rad24Δ dmc1Δ* will give a DSB level where the feedback mechanism is absent.

In the *sae2Δ spo11-Y135F-HA/spo11-HA* strain DSBs were between approximately 1.5 and 2.5% of total DNA signal (figure 5.1A and C). In the *dmc1Δ spo11-Y135F-HA/spo11-HA* strain, DSBs reached around 2.7% of total DNA signal between 5 and 7 hours (figure 5.1A and C). By contrast, in the *rad24Δ dmc1Δ spo11-Y135F-HA/spo11-HA* strain DSBs were only above 1% of

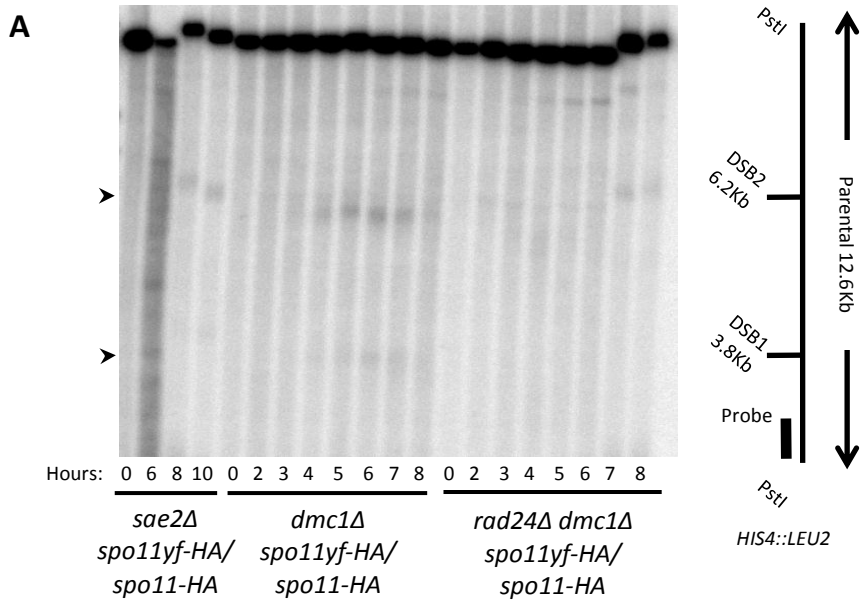
A
PstI
DSB2
6.2Kb
Parental 12.6Kb
DSB1
3.8Kb
Probe
PstI
HIS4::LEU2
Hours: 0 6 8 10 0 2 3 4 5 6 7 8 0 2 3 4 5 6 7 8
sae2Δ spo11yf-HA/ spo11-HA
dmc1Δ spo11yf-HA/ spo11-HA
rad24Δ dmc1Δ spo11yf-HA/ spo11-HA

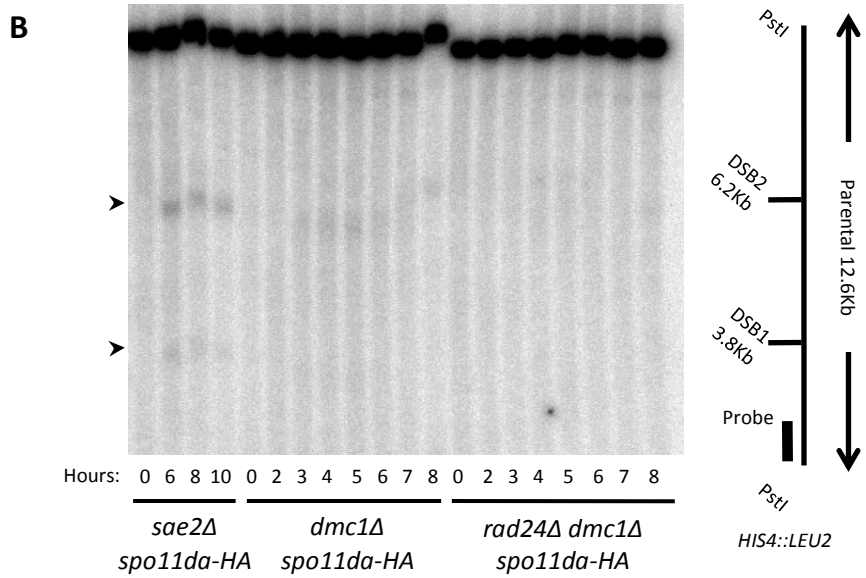
B
PstI
DSB2
6.2Kb
Parental 12.6Kb
DSB1
3.8Kb
Probe
PstI
HIS4::LEU2
Hours: 0 6 8 10 0 2 3 4 5 6 7 8 0 2 3 4 5 6 7 8
sae2Δ spo11da-HA
dmc1Δ spo11da-HA
rad24Δ dmc1Δ spo11da-HA

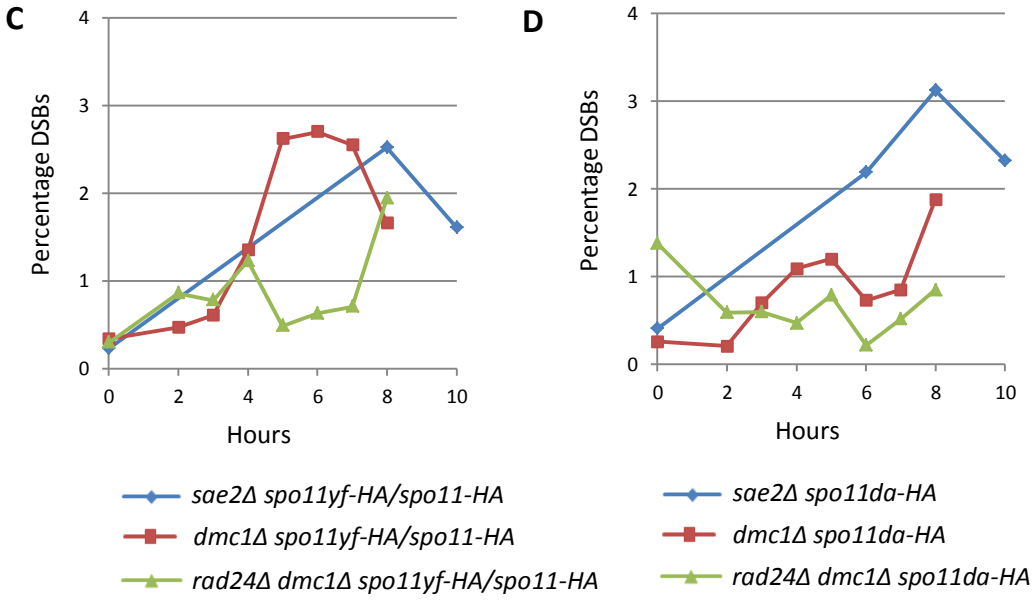
C
Percentage DSBs
Hours
D
Percentage DSBs
Hours
sae2Δ spo11yf-HA/spo11-HA
dmc1Δ spo11yf-HA/spo11-HA
rad24Δ dmc1Δ spo11yf-HA/spo11-HA
sae2Δ spo11da-HA
dmc1Δ spo11da-HA
rad24Δ dmc1Δ spo11da-HA

Figure 5.1: DSB levels do not increase in *dmc1Δ* compared with *sae2Δ* strains in the *spo11-Y135F-HA/spo11-HA* and *spo11-D290A-HA* backgrounds. A and **B)** Genomic DNA from meiotic time courses were digested and run on a 0.7% 1xTAE agarose gel for 20 hours at 60 volts. The gel was transferred to nylon membrane under denaturing conditions and hybridised with a radioactive probe for the *HIS4::LEU2* locus. The membrane was exposed to a phosphor screen and image taken using a Fuji phosphor scanner. DSBs marked with arrowhead (➢). **C** and **D)** Quantification of DSB levels over time. Image Gauge was used to analyse DSB signal as a percentage of total DNA and signal is plotted and displayed.

total DNA at two time points (figure 5.1A and C). Because the *dmc1Δ spo11-Y135F-HA/spo11-HA* reaches similar levels of DSB signal compared with the *sae2Δ spo11-Y135F-HA/spo11-HA* this suggests that the DSB feedback is unable to compensate for the decrease DSB formation observed in the *spo11-Y135F-HA/spo11-HA* background.

In the *sae2Δ spo11-D290A-HA* strain DSB signal was between approximately 2 and 3% of total DNA signal at 6, 8 and 10 hours (figure 5.1B and D). By contrast, in the *dmc1Δ spo11-D290A-HA* strain DSBs levels were approximately 1% of total DNA from 4 to 7 hours and almost 2% at 8 hours (figure 5.1B and D). In the *rad24Δ dmc1Δ spo11-D290A-HA* strain DSBs were less than 1% of total DNA from 2 hours to the end of the time course (figure 5.1B and D). Because the DSB levels in *dmc1Δ spo11-D290A-HA* is lower than the DSB levels measure in *sae2Δ spo11-D290A-HA* this suggests that the DSB feedback is unable to compensate for the decreased in DSBs formed in by the *spo11-D290A-HA* mutation.

5.4: Artificial stimulation of the DSB feedback mechanism by DNA damaging agents causes a reduction in detected DSB levels

The increase in DSB levels observed in the *dmc1Δ spo11-HA* strain compared with the *sae2Δ spo11-HA* strain is thought to be due to the action of the DSB feedback mechanism. In *dmc1Δ spo11-HA* the DSBs are processed and resected leading to the activation of the Mec1-dependent checkpoint and DSB feedback mechanism. This leads to an increase in the DSB levels. In the *sae2Δ spo11-HA*, DSBs are unprocessed and unresected leading to minimal activation of the Mec1-dependent meiotic recombination checkpoint and no activation of the DSB feedback mechanism.

If the way in which the DSB feedback functions is correct, then the *sae2Δ spo11-HA* mutations provide a background where the DSB feedback mechanism is functional but not activated and where DSB levels are potentially able to be increased (up to *sae2Δ* DSB levels). The DNA damaging agent phleomycin is proficient in activating the Mec1-dependent meiotic checkpoint in the absence of DSBs (Cartagena-Lirola, Guerini et al. 2008). Therefore, to test whether the DSB feedback mechanism can be activated and increase DSB levels in a *sae2Δ spo11-HA* background, phleomycin was added.

A synchronous meiotic culture of *sae2Δ spo11-HA* was split into three cultures at three and a half hours, with one culture remaining as an un-treated control and the other two cultures having phleomycin added at 2.5µg/ml and 5µg/ml. The phleomycin treated cultures were exposed for 30 minutes and then washed and resuspended into fresh sporulation media. In the *sae2Δ spo11-HA* untreated control, DSB signal was around 8 % of total DNA at 6, 8 and 10 hours (figure 5.2). By contrast, in both of the *sae2Δ spo11-HA* cultures treated with phleomycin, the DSB signal was between 5 and 7% of total DNA (figure 5.2). This indicates that, in contrast to the expected increase due to DSB feedback activation, the addition of phleomycin causes a reduction in DSB signal.

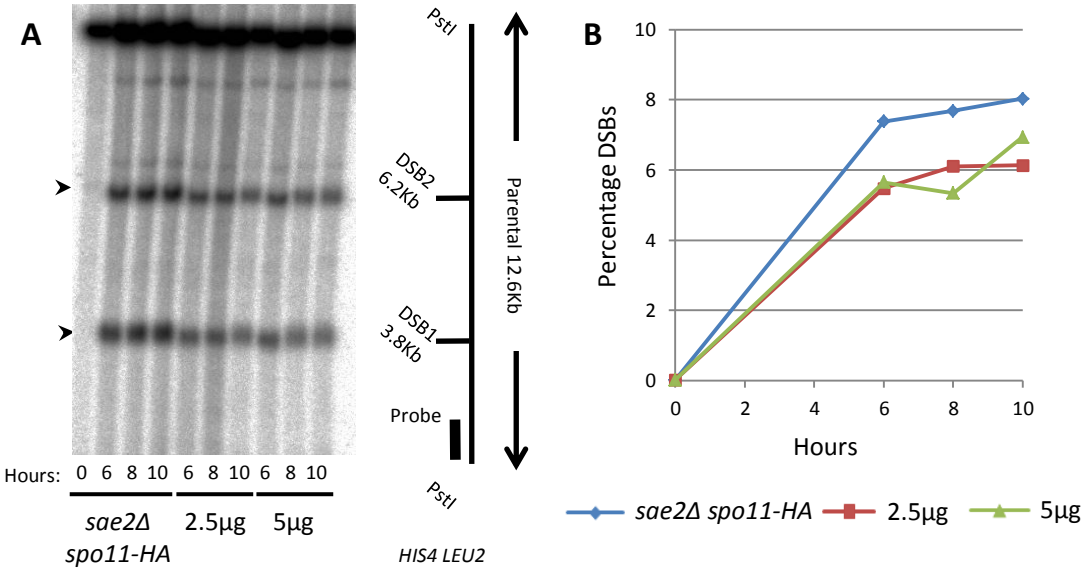

Figure 5.2: Phelomycin treatment causes a reduction in DSB levels in the *sae2Δ spo11-HA* background. **A)** Genomic DNA from meiotic time courses of treated and untreated cultures were digested and run on a 0.7% 1xTAE agarose gel for 20 hours at 60 volts. The gel was transferred to nylon membrane under denaturing conditions and hybridised with a radioactive probe for the *HIS4::LEU2* locus. The membrane was exposed to a phosphor screen and image taken using a Fuji phosphor scanner. DSBs marked with arrowhead (➤). **B)** Quantification of DSB levels over time. Image Gauge was used to analyse DSB signal as a percentage of total DNA and signal is plotted and displayed.

5.6: Discussion

The observations from *spo11-HA* strains in the presence of either the *sae2Δ, dmc1Δ or rad24Δ dmc1Δ* mutations lead to the hypothesis that a DSB feedback mechanisms functions through the Mec1-dependent meiotic checkpoint to increase DSBs in the *dmc1Δ* background. To test whether the DSB feedback mechanism could function to compensate for a greater reduction in DSB levels, previously reported Spo11 mutants (Diaz, Alcid et al. 2002; Martini, Diaz et al. 2006) were combined with *sae2Δ, dmc1Δ* or *dmc1Δ rad24Δ*. In both of the Spo11 hypomorph backgrounds, measured DSB levels in the *dmc1Δ* mutants either do not reach or are around the same level as the *sae2Δ* mutation. The DSB feedback model would suggest that in the *sae2Δ* mutant the DSB feedback mechanism would not be functional and in the *dmc1Δ* mutant to the mechanism would be functioning to increase DSB levels. Therefore the lack of increase in DSB levels detected between the strains would suggest that the DSB feedback mechanism is not functioning. However, the removal of *RAD24*, and therefore the feedback mechanism does cause a reduction in the DSB levels compared with the *dmc1Δ* mutants. This would suggest that the feedback mechanism is functioning in the *dmc1Δ* background, but not to the same extent as previously observed in the *spo11-HA* background.

There are observations from the Spo11 hypomorph mutants that both support and refute the DSB feedback mechanism but these experiments are difficult to fully interpret because of the detection of DSB signal above noise. Measuring DSB signal relies upon the detection of a signal above the background noise generated from the membranes. When dealing with mutants that produce between 17 and 29% of wildtype signal, and introducing additional mutations that will cause a further reduction in signal, the detection becomes below what is possible from this assay. However, alternative experimental procedures, such as preparing genomic DNA in agarose plugs prevents DNA shearing and can decrease background signal.

Another issue in the detection of DSB signal from the Spo11 hypomorph mutants relates to the additional mutations made to the strains and the change that this has on the DNA molecule. The DSB feedback mechanism idea suggests that the type of DNA molecule allows activation of the feedback mechanism. Therefore the idea is that the *sae2Δ* mutation which has unprocessed and unresected DNA molecules will not stimulate the feedback whereas the *dmc1Δ* mutation that has processed and resected molecules will stimulate the feedback. On southern blots, the *sae2Δ* mutation will create a discrete band where all DSB signal for that DSB site will accumulate. However in the *dmc1Δ* background, the DSBs are resected causing signal to be spread over a larger distance, making the signal harder to detect above background noise. In addition, the *rad24Δ dmc1Δ* mutation causes the DSBs to become hyper-resected causing the DSB signal to be spread over an even larger distance than the *dmc1Δ* DSBs. These differences in DNA molecule and subsequent detection make it difficult to determine the real DSB levels in these mutants. Other experimental methods, such as pulse field gel electrophoresis, would separate whole chromosomes, allowing separation of a DSB over a much smaller distance thereby removing differences in resection between strains.

The idea of the DSB feedback mechanism is that it functions through the Mec1-dependent checkpoint, via currently unknown factors leading to the stimulation of more DSBs. The final component of the pathway (and essentially the first part) is the action of Spo11. The Spo11 hypomorphs provide a background to test the function of the DSB feedback mechanism in more severe DSB formation situations. However, the difficulty with this system is that, if the DSB feedback mechanism exists, the target that is eventually stimulated is Spo11, which is defective in its ability to form DSBs. Therefore these Spo11 hypomorph backgrounds may be unable to test the action of the DSB feedback mechanism.

The different DSB levels detected in the *sae2Δ spo11-HA* compared with the *dmc1Δ spo11-HA* is thought to be the function of the DSB feedback mechanism. It was therefore thought that artificial stimulation of the DSB feedback mechanism by addition of phleomycin (a DNA damaging agent) in the *sae2Δ spo11-HA* would lead to a higher level of DSBs to form. Contrary to the expected increase in DSB levels, addition of phleomycin caused a reduction in DSB levels. One possibility for the reduction of DSB signal is that components of the DSB formation machinery, such as the MRX complex, are titrated out in response to the damage created by the presence of the phleomycin. In this situation, MRX would go to the damaged regions (Lisby, Barlow et al. 2004), consistent with its processing function. However, as it is required to form Spo11-dependent DSBs (Ajimura, Leem et al. 1993), the remaining abundance may not be enough to enable further increases in Spo11-dependent DSBs. This explanation is only valid if the increase in DSBs created by the phleomycin, and the abundance of MRX is too low, to promote new Spo11-dependent DSBs.

Another explanation for the reduction in DSBs observed in the phleomycin treated samples is if an inhibitor functions to prevent Spo11-dependent DSBs. ATM, the homologue of Tel1, has been implicated as an inhibitor of DSBs, with the *Atm*$^{-/-}$ mutants having increased levels of Spo11-oligonucleotides, suggesting increased levels of DSBs (Lange, Pan et al. 2011). Mutants in the *Drosophila melanogaster* ATM also demonstrate increased DSB levels (Joyce, Pedersen et al. 2011) and work in *Saccharomyces cerevisiae* suggest that Tel1 functions to inhibit DSB formation (Zhang, Kim et al. 2011). These observations support the idea that Tel1 functions to inhibit DSB formation when the *sae2Δ spo11-HA* strain is treated with phleomycin. To test the role of Tel1 as a DSB formation inhibitor, phleomycin treatment of a *tel1Δ sae2Δ spo11*-HA strain and measuring DSB levels compared to an untreated sample would expect to see a DSB increase.

With observations from different organisms (Joyce, Pedersen et al. 2011; Lange, Pan et al. 2011) and assays (Zhang, Kim et al. 2011) providing evidence to suggest that Tel1 functions as an inhibitor, the focus of chapter 6 will be testing the effect of Tel1 on DSB formation in the *sae2Δ* and *dmc1Δ* backgrounds, in addition to the *spo11-HA* tag.

CHAPTER 6:

Investigating DSB feedback inhibition

Chapter 6: Investigating DSB feedback inhibition

6.1: Introduction

The focus of chapter 4 was to investigate the cause of the unexpected decrease in DSB signal observed in the *rad24Δ dmc1Δ spo11-HA* (figure 3.2.8 and figure 4.1). The conclusions from that work were that Mec1-dependent meiotic recombination checkpoint functions as a DSB feedback mechanism to compensate for the decreased DSB level caused by the *spo11-HA* tag. The DSB feedback mechanism is not thought to be active in situations where DSBs are unprocessed and unresected (e.g. *sae2Δ*) but is active in situations where DSBs are processed and resected (e.g. *dmc1Δ*) (figure 4.12). The action of the DSB feedback mechanism can be observed when comparing the DSB levels in *sae2Δ spo11-HA* (where the DSB feedback mechanism is not functioning), *dmc1Δ spo11-HA* (where the DSB feedback mechanism is functioning) and *rad24Δ dmc1Δ spo11-HA* (where the DSB feedback mechanism is absent).

With the observations from chapter 4 suggesting a means of increasing DSB levels, the mechanism was tested in chapter 5. Using the *sae2Δ spo11-HA* mutant, which is thought to have lower DSB levels compared to *dmc1Δ spo11-HA* due to inactive DSB feedback, DNA damaging agent was used to artificially stimulate the feedback mechanism. The expected outcome was to have an increase in DSB levels. However, the cultures treated with the DNA damaging agent had lower DSB levels compared with the untreated (figure 5.2). One explanation for this is that DSB formation was inhibited. Observations from mouse (Lange, Pan et al. 2011), fruitfly (Joyce, Pedersen et al. 2011) and from budding yeast (Zhang, Kim et al. 2011) suggest that Tel1 inhibits DSB formation. To test the function of Tel1 as an inhibitor for DSB formation, *tel1Δ* mutants were combined with either the *sae2Δ* or *dmc1Δ* mutations in addition to the *spo11-HA* tag and DSB levels were measured. If Tel1 acts as an inhibitor of DSB

formation, removal of Tel1 should cause an increase in DSB levels. The observations from chapter 5 would suggest that Tel1 functions to inhibit DSB formation in the *sae2Δ spo11-HA* background (figure 5.2). If Tel1 functions as a DSB inhibitor in *dmc1Δ*, removal would also expect to see an increase in DSB levels.

6.2: *tel1Δ* has a higher DSB level in *sae2Δ* background

To test whether Tel1 functions to inhibit DSB formation at the *sae2Δ* background, the *tel1Δ* mutation was introduced into the *sae2Δ* and *sae2Δ spo11-HA* strains. DSB levels were obtained from combining measurements of two DSBs at the *HIS4::LEU2* hotspot. In the *sae2Δ* mutant (figure 4.6 and figure 6.1C) DSB levels reached just under 15% of total DNA. By contrast, *tel1Δ sae2Δ* DSBs reached a level of around 25% of total DNA by 8 hours (figure 6.1). In *sae2Δ spo11-HA,* DSBs reached less than 8% of total DNA. In contrast to this, in *tel1Δ sae2Δ spo11-HA*, DSBs reached over 20% of total DNA. These observations suggest, because of the increase in DSB signal when Tel1 is removed, that Tel1 functions as a DSB inhibitor in the *sae2Δ* background. This inhibition functions regardless of whether Spo11 is wildtype or *spo11-HA* tag.

6.3: *tel1Δ* causes a reduction in DSB levels in the *spo11-HA* and the *dmc1Δ spo11-HA* background

The action of the DSB feedback mechanism was not observed in the *sae2Δ* background. One interpretation so far is that the DNA molecule in a *sae2Δ* block does not allow for activation of the DSB feedback mechanism. With the observations that Tel1 functions to inhibit DSB formation at the *sae2Δ* block, another interpretation is that Tel1 inhibition prevents the DSB feedback mechanism from functioning. As the DSB feedback mechanism has been observed in the *spo11-HA* and *dmc1Δ spo11-HA* backgrounds, this alternative hypothesis would mean that Tel1 is no longer inhibiting DSB formation or the feedback mechanism in the *spo11-HA* or *dmc1Δ spo11-HA* backgrounds. If this is correct, removal of Tel1 should have no effect on DSB levels in the *spo11-HA* or *dmc1Δ spo11-HA* backgrounds. To test if this is the case the *tel1Δ* mutation was introduced into the *spo11-HA* and *dmc1Δ spo11-HA* backgrounds in addition to the otherwise wildtype and *dmc1Δ* backgrounds.

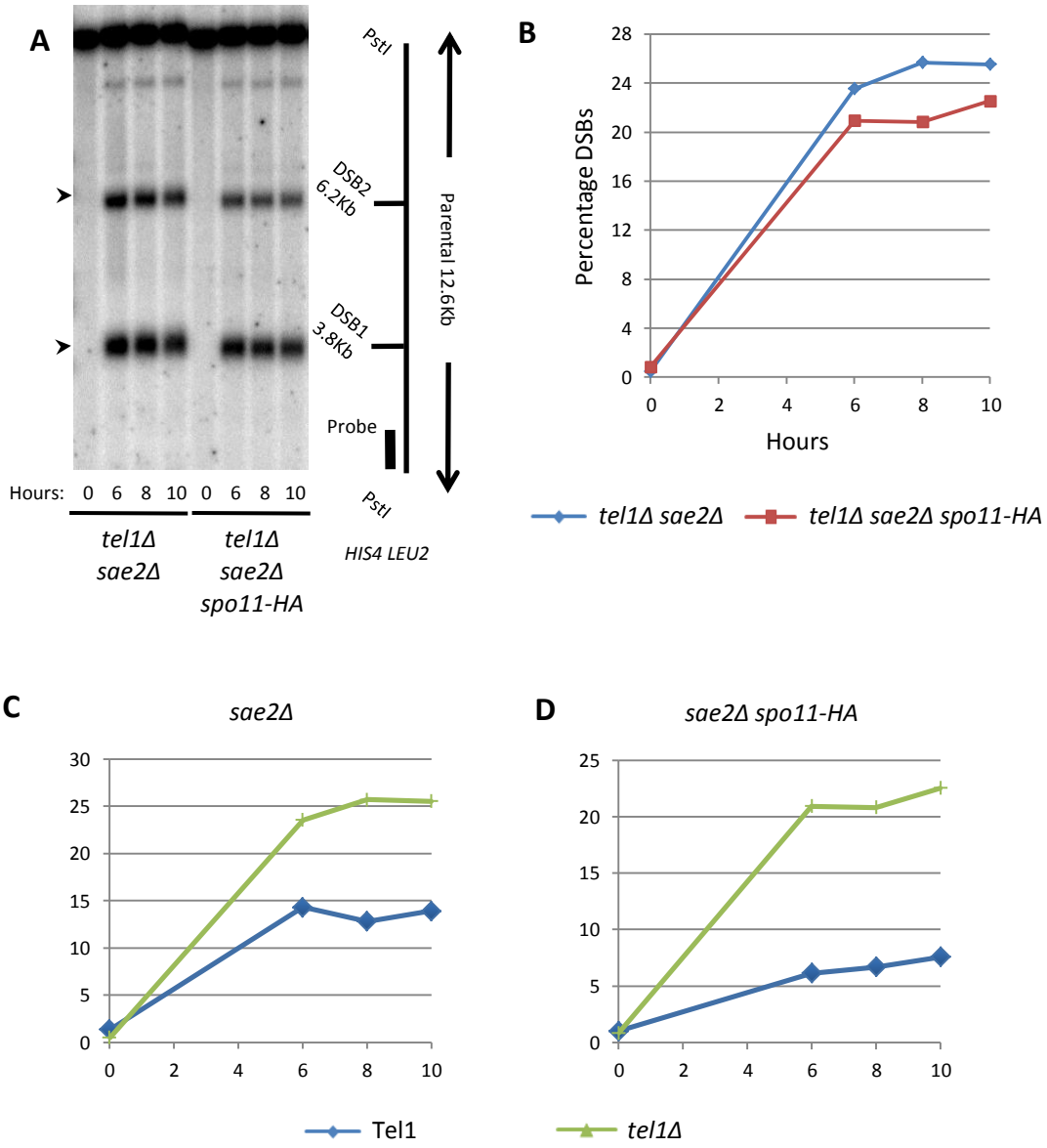

Figure 6.1: Removal of Tel1 causes an increase in DSB levels in the *sae2Δ* background. A) Genomic DNA from meiotic time courses were digested and run on a 0.7% 1xTAE agarose gel for 20 hours at 60 volts. The gel was transferred to nylon membrane under denaturing conditions and hybridised with a radioactive probe for the *HIS4::LEU2* locus. The membrane was exposed to a phosphor screen and image taken using a Fuji phosphor scanner. DSBs marked with arrowhead (➤). **B)** Quantification of DSB levels over time. Image Gauge was used to analyse DSB signal as a percentage of total DNA and signal is plotted and displayed. **C)** Comparison between DSB signal detected from equivalent Tel1 (data from figure 4.6) and *tel1Δ* mutants. **D)** Comparison between DSB signal detected from equivalent Tel1 *spo11-HA* (data from figure 4.6) and *tel1Δ spo11-HA* mutants.

In the wildtype strain (figure 4.1B, D and E and figure 6.2C) DSBs peaked at 3 hours just under 6% of total DNA. In the *tel1Δ* strain, DSBs peaked at above 6% of total DSBs at 4 hours (figure 6.2). These observations suggest that there is no change between DSB levels in wildtype and *tel1Δ*. In the *spo11-HA* strain (figure 4.1A, C and E and figure 6.2C) DSBs peaked at almost 8% of total DNA at 4 hours. By contrast, in the *tel1Δ spo11-HA* strain, DSBs peaked at 3 hours at less than 3 % of total DNA (figure 6.2). These observations indicate that, contrary to what was expected, *tel1Δ* causes a reduction in DSBs in the *spo11-HA* background. This suggests that Tel1 functions, not to inhibit DSB formation but to promote DSB formation in the *spo11-HA* background. This result is similar to the observations made in chapter 4 when Mec1-dependent checkpoint mutants are combined with the *spo11-HA* tag.

In the *dmc1Δ* strain (figure 4.1B, D and E and figure 6.2C) DSBs peaked around 17% of total DNA by 4 hours. In the *tel1Δ dmc1Δ* strain, DSBs plateaued around 20% of total DNA by 4 hours. These observations indicate that *tel1Δ* produces approximately the same level of DSBs at the *dmc1Δ* block. In the *dmc1Δ spo11-HA* strain (figure 4.1A, C and E and figure 6.2C) DSBs plateau above 16% of total DNA from 6 hours onwards. By contrast in the *tel1Δ dmc1Δ spo11-HA* strain, DSBs plateaued around 10% of total DNA at 5 hours and decreased slightly at 7 and 8 hours (figure 6.2). These observations indicate that *tel1Δ* causes a reduction in DSB levels at the *dmc1Δ* block when combined with the *spo11-HA* tag. This suggests that, consistent with the observations in the *tel1Δ spo11-HA* and in contrast to what was expected, Tel1 functions to promote DSB formation in the *spo11-HA* background.

The observations from the otherwise *spo11-HA* and *dmc1Δ spo11-HA* backgrounds suggest that Tel1 functions as a positive mechanism for DSB formation in situations where DSB formation is reduced such as the *spo11-HA* background.

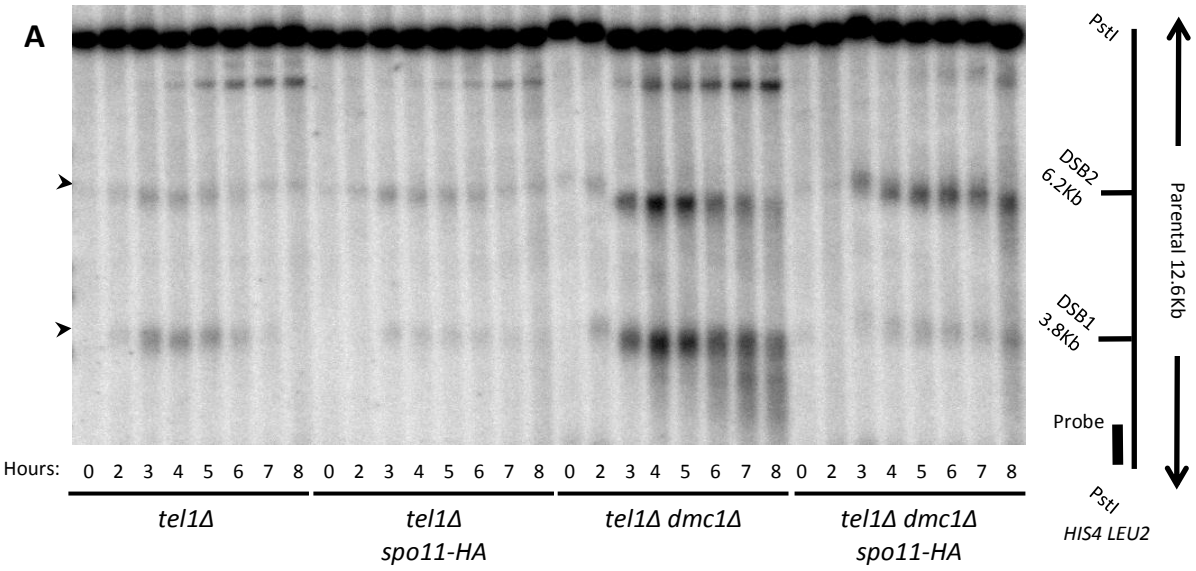
A
PstI
DSB2
6.2Kb
DSB1
3.8Kb
Parental 12.6Kb
Probe
PstI
HIS4 LEU2
Hours: 0 2 3 4 5 6 7 8 0 2 3 4 5 6 7 8 0 2 3 4 5 6 7 8 0 2 3 4 5 6 7 8
tel1Δ
tel1Δ spo11-HA
tel1Δ dmc1Δ
tel1Δ dmc1Δ spo11-HA

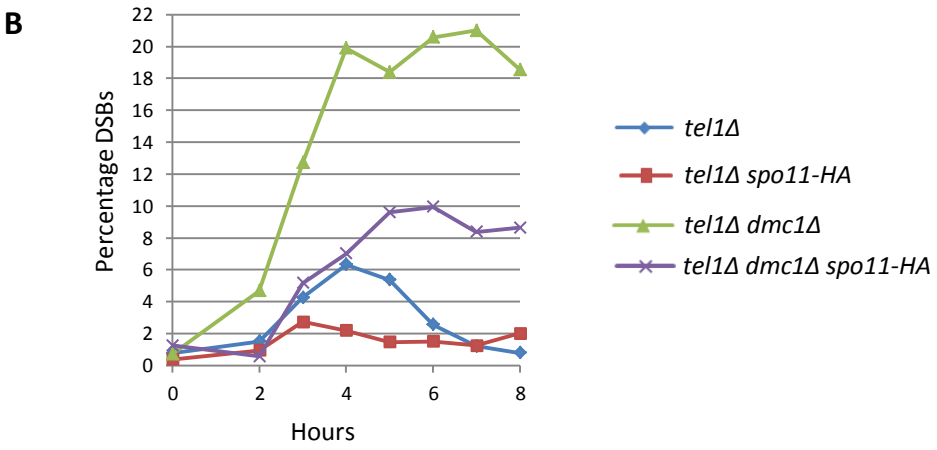
B
Percentage DSBs
Hours
tel1Δ
tel1Δ spo11-HA
tel1Δ dmc1Δ
tel1Δ dmc1Δ spo11-HA

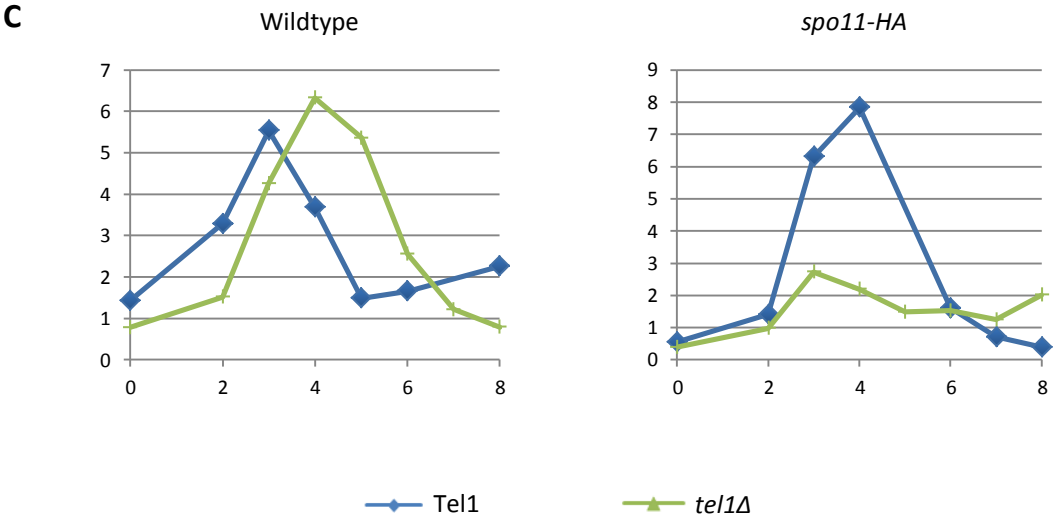
C
Wildtype
spo11-HA
Tel1
tel1Δ

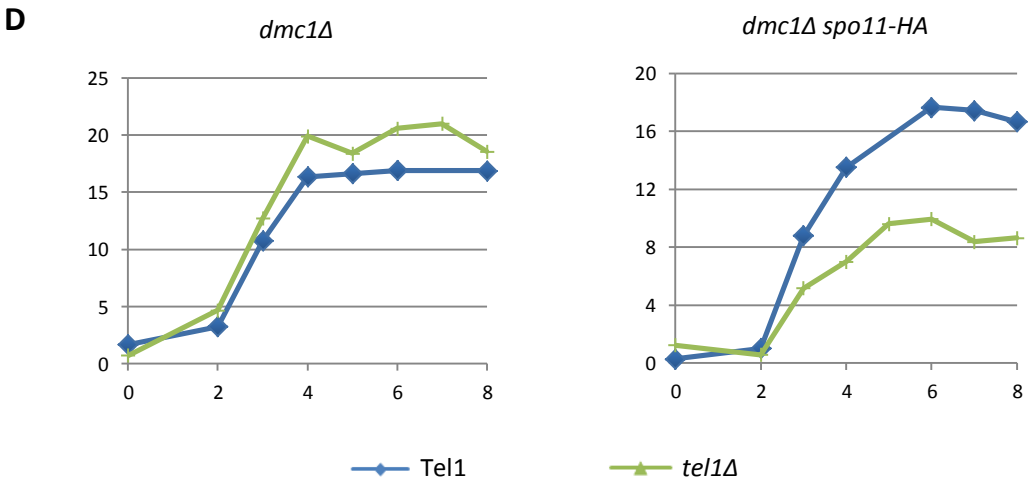

Figure 6.2: Removal of Tel1 has no effect on DSB levels except in the presence of the *spo11-HA* tag. A) Genomic DNA from meiotic time courses were digested and run on a 0.7% 1xTAE agarose gel for 20 hours at 60 volts. The gel was transferred to nylon membrane under denaturing conditions and hybridised with a radioactive probe for the *HIS4::LEU2* locus. The membrane was exposed to a phosphor screen and image taken using a Fuji phosphor scanner. DSBs marked with arrowhead (➤). **B)** Quantification of DSB levels over time. Image Gauge was used to analyse DSB signal as a percentage of total DNA and signal is plotted and displayed. **C)** Comparison between DSB signal detected from equivalent Tel1 (data from figure 4.1) and *tel1Δ* mutants. **D)** Comparison between DSB signal detected from equivalent Tel1 *dmc1Δ* (data from figure 4.1) and *tel1Δ dmc1Δ* mutants

6.4: *rad24Δ tel1Δ* mutations causes an increase in DSBs in the Spo11 background and an almost total loss of DSB signal in the *spo11-HA* background.

Observations from chapter 4 indicate that a DSB feedback mechanism functions in the *spo11-HA* background by means of the Mec1-dependent meiotic recombination checkpoint that is not functional in the *sae2Δ* background. This chapter has identified that Tel1 functions to inhibit DBS formation in the *sae2Δ* and *sae2Δ spo11-HA* backgrounds. In addition Tel1 also functions to promote DSB formation in the *spo11-HA* background in otherwise wildtype or *dmc1Δ* backgrounds. With factors that both promote and inhibit DSB formation, one question highlighted is what level of DSBs form when removing both mechanisms, e.g. in a *rad24Δ tel1Δ* mutant.

In the otherwise wildtype and *dmc1Δ* backgrounds the *rad24Δ* mutation did not have an effect on DSB levels. In addition, the *tel1Δ* mutation did not have an effect on DSB levels. Therefore it would be expected that the *rad24Δ tel1Δ* and *rad24Δ tel1Δ dmc1Δ* mutants would produce DSB levels similar to otherwise wildtype and *dmc1Δ* respectively. As the mechanism of inter-homologue repair bias relies upon activation by either Mec1/Rad24 or Tel1, when creating the *rad24Δ tel1Δ* mutant in the *dmc1Δ* background, the *rad51Δ* mutation will also have to be added. This will therefore ensure that no Rad51-dependent repair is taking place. In the *sae2Δ* background, previous observations are that *rad24Δ* does not cause an effect, but *tel1Δ* causes an increase in DSB levels. Therefore it would be expected that the *rad24Δ tel1Δ sae2Δ* would produce DSB levels similar to *tel1Δ sae2Δ*.

In the *spo11-HA* and the *dmc1Δ spo11-HA* backgrounds the removal of *rad24Δ* caused a reduction in DSB levels. Similarly, the *tel1Δ* mutation in the *spo11-HA* and *dmc1Δ spo11-HA* backgrounds caused a reduction in DSB levels. Therefore it would be expected that in the

rad24Δ tel1Δ spo11-HA and *rad24Δ tel1Δ dmc1Δ spo11-HA* strains, the DSB levels would be low. As mentioned in the preceding paragraph, because of the role of these proteins in inter-homologue bias, the *rad51Δ* mutation will also be added to remove Rad51-dependent inter-sister repair. In the *sae2Δ spo11-HA* strain the *rad24Δ* mutation caused no effect on DSB levels. By contrast in the *tel1Δ sae2Δ spo11-HA* strain, DSB levels were increased. This therefore suggests that DSB levels in *rad24Δ tel1Δ sae2Δ spo11-HA* will be as high as the *tel1Δ sae2Δ spo11-HA*.

In the *rad24Δ* strain (figure 4.1B, D and E) DSB signal peaked at above 9% of total DNA at 4 hours. In the *tel1Δ* strain (figure 6.2) DSB signal peaked at above 6% of total DNA at 4 hours. By contrast to both *rad24Δ* and *tel1Δ*, in the *rad24Δ tel1Δ* DSBs had reached approximately 32% of total DNA by 5 hours and remained above this level until the end of the time course (figure 6.3A and B). This level of DSBs was unexpected considering the DSB levels observed in *rad24Δ* and *tel1Δ* and suggests that the removal of both Tel1 and Rad24 causes an increase in DSB levels. The DSB molecules do not change in migration as the time course progresses and appear to be unprocessed. The lack of processing is consistent with previous observations of *mec1Δ tel1Δ* mutants (Cartagena-Lirola, Guerini et al. 2006). Although the *rad24Δ tel1Δ dmc1Δ rad51Δ* was viable, the strain failed to grow substantially to be able to perform meiotic time courses. Because of the unprocessed nature of the DSBs in the *rad24Δ tel1Δ* strain, the inability to create the *rad24Δ tel1Δ rad51Δ dmc1Δ* strain was not an issue as the DSBs would not progress to requiring recombinases. Therefore the *rad24Δ tel1Δ* strain is expected to produce DSB levels that would be observed if the *rad24Δ tel1Δ rad51Δ dmc1Δ* were viable.

In the *sae2Δ* strain (figure 4.6 and figure 6.1C) DSB levels peaked just below 15% of total DNA. Similarly In the *rad24Δ sae2Δ* strain (figure 4.6) DSB levels peaked around 15% of total DNA. By

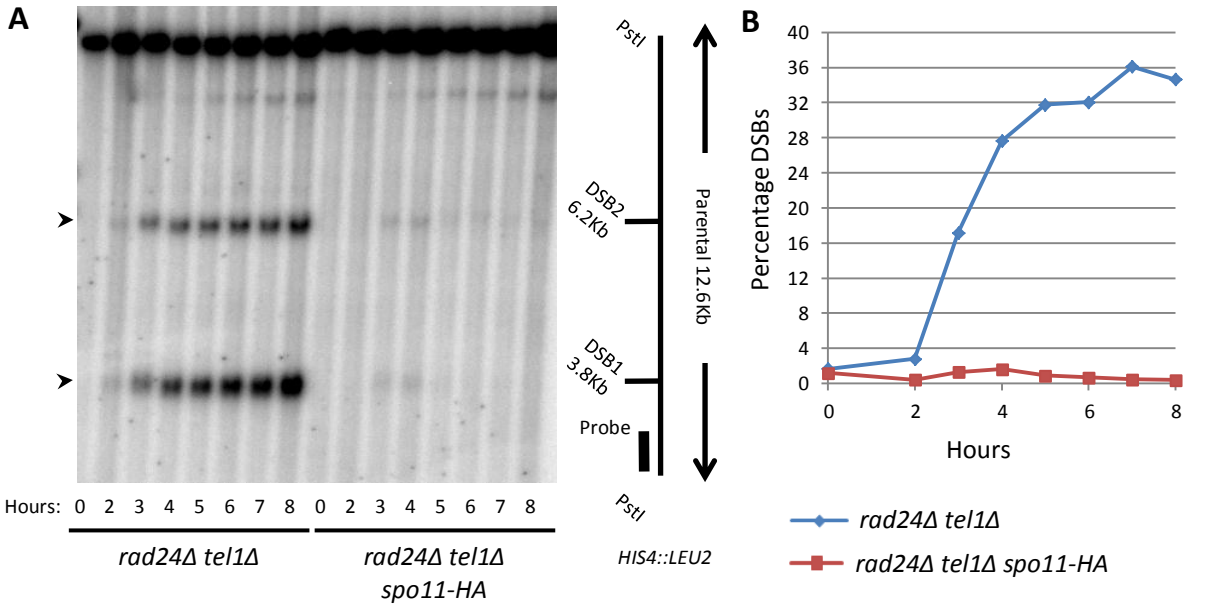
A
PstI
DSB2
6.2Kb
Parental 12.6Kb
DSB1
3.8Kb
Probe
PstI
Hours: 0 2 3 4 5 6 7 8 0 2 3 4 5 6 7 8
rad24Δ tel1Δ
rad24Δ tel1Δ spo11-HA
HIS4::LEU2
B
Percentage DSBs
Hours
rad24Δ tel1Δ
rad24Δ tel1Δ spo11-HA

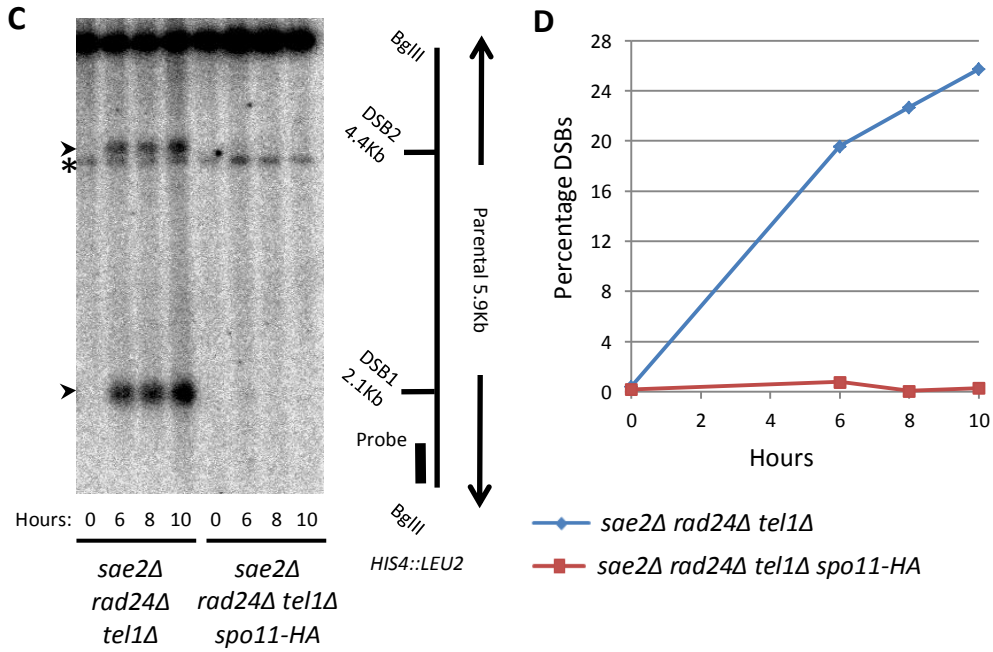
C
BglII
DSB2
4.4Kb
Parental 5.9Kb
DSB1
2.1Kb
Probe
BglII
Hours: 0 6 8 10 0 6 8 10
sae2Δ rad24Δ tel1Δ
sae2Δ rad24Δ tel1Δ spo11-HA
HIS4::LEU2
D
Percentage DSBs
Hours
sae2Δ rad24Δ tel1Δ
sae2Δ rad24Δ tel1Δ spo11-HA

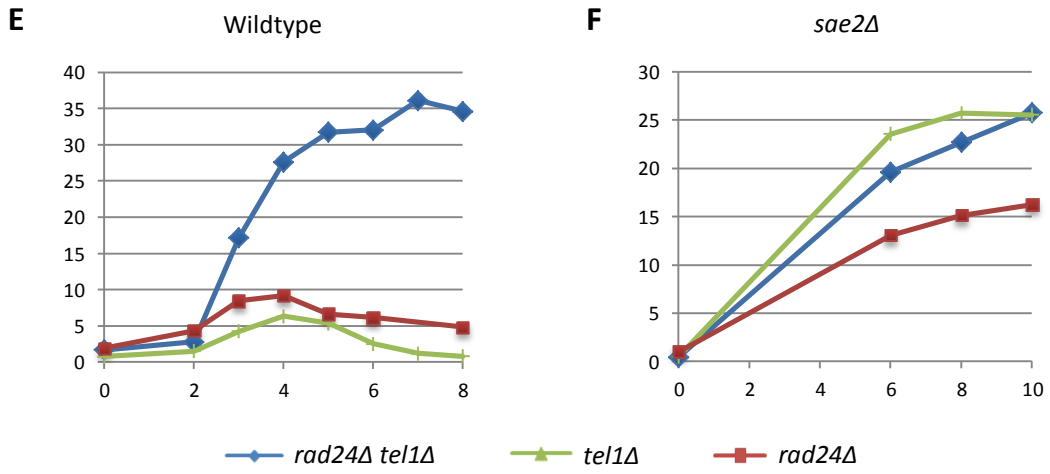
E
Wildtype
F
sae2Δ
rad24Δ tel1Δ
tel1Δ
rad24Δ

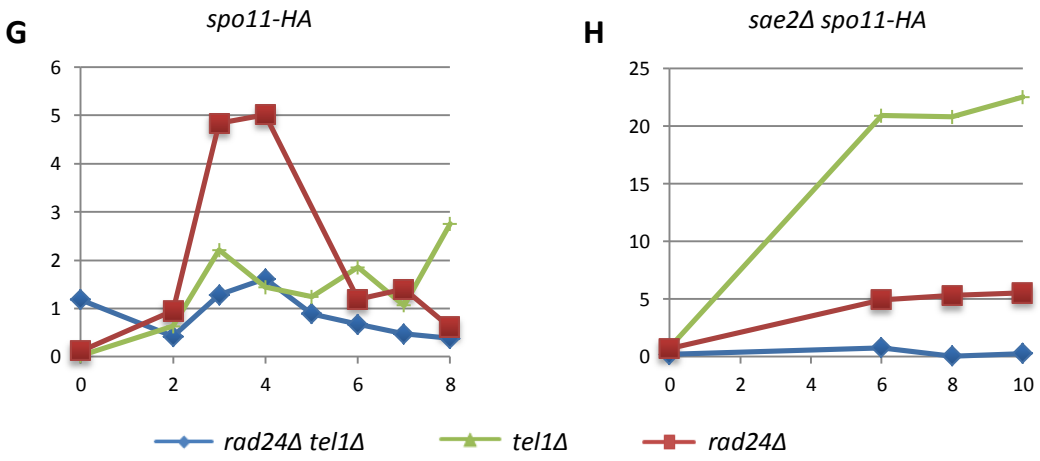

Figure 6.3: *rad24Δ tel1Δ* has high levels of DSBs but very low DSB levels in the presence of the *spo11-HA* tag. A and **C)** Genomic DNA from meiotic time courses were digested and run on a 0.7% 1xTAE agarose gel for 20 hours at 60 volts (gel **A**) and 18 hours at 60 volts (gel **C**). The gel was transferred to nylon membrane under denaturing conditions and hybridised with a radioactive probe for the *HIS4::LEU2* locus. The membrane was exposed to a phosphor screen and image taken using a Fuji phosphor scanner. DSBs marked with arrowhead (➤). Asterisk (∗) marks non-specific band. **B** and **D)** Quantification of DSB levels over time. Image Gauge was used to analyse DSB signal as a percentage of total DNA and signal is plotted and displayed. **E)** Comparison between DSB signal detected from equivalent Tel1 or Rad24 backgrounds (data from figures 4.1 and 6.2). **F)** Comparison between DSB signal detected from equivalent Tel1 or Rad24 backgrounds in the *sae2Δ* background (data from figures 4.6 and 6.1) **G)** Comparison between DSB signal detected from equivalent Tel1 or Rad24 backgrounds in the presence of the *spo11-HA* tag (data from figures 4.1 and 6.2). **H)** Comparison between DSB signal detected from equivalent Tel1 or Rad24 backgrounds in the *spo11-HA sae2Δ* background (data from figures 4.6 and 6.1)

contrast in the *tel1Δ sae2Δ* strain (figure 6.1) DSB levels peaked at around 25% of total DNA. Similar to the *tel1Δ sae2Δ* strain, in the *rad24Δ tel1Δ sae2Δ* strain (figure 6.3C and D) DSB levels also peaked at around 25% of total DNA. This observation is similar to what was expected and suggests that, in the *sae2Δ* block, Rad24 does not function to increase DSB levels, but Tel1 functions to inhibit DSB formation.

In the *spo11-HA* background (figure 4.1A, C and E), DSB signal peaked at just below 6% of total DNA at 3 hours. In the *rad24Δ spo11-HA* strain, DSB signal peaked at just below 5% of total DNA at 4 hours. By contrast, in the *tel1Δ spo11-HA* strain DSBs peaked at below 3% at 3 hours. In the *rad24Δ tel1Δ spo11-HA* strain DSB levels peaked at just over 1.5% of total DNA signal. This result is lower than expected but maybe due to a combination of both the reductions in DSB signal from the *rad24Δ* and *tel1Δ* mutations. This is consistent with the observation previously made in chapter 3.3 in the *rad24Δ tel1Δ spo11-HA* and *mec1-mn tel1Δ spo11-HA* which had a decrease in DSB levels compared with *spo11-HA* (figure 3.3.2). This suggests that because of the reduction in DSB level compared to both *rad24Δ spo11-HA* and *tel1Δ spo11-HA* that *RAD24* and *TEL1* function to promote DSB formation in the *spo11-HA* background.

In the *sae2Δ spo11-HA* strain (figure 4.6) DSB signal peaked around 7% of total DNA. In the *rad24Δ sae2Δ spo11-HA* strain DSB levels peaked around the same level, at 5.5% of total DNA. By contrast in the *tel1Δ sae2Δ spo11-HA* strain (figure 6.2) DSBs peaked at over 20% of total DNA. In contrast to all of the other *sae2Δ spo11-HA* backgrounds, in the *rad24Δ tel1Δ sae2Δ spo11-HA* strain DSBs did not even reach 1% of total DNA. This reduction in DSBs compared with the *tel1Δ sae2Δ spo11-HA* (the expected level of DSBs) suggests a requirement for Tel1 or Rad24 in the *sae2Δ spo11-HA* background. This observation is consistent with the *rad24 tel1Δ spo11-HA* although the decreased level of DSBs compared with the expected level suggests a currently described role for Rad24 and/or Tel1.

6.5: Tel1 DSB inhibition does not function through Mek1

In chapter 4 it was observed that the proposed DSB feedback mechanism functioned through the Mec1-dependent meiotic recombination checkpoint and acted through Mek1 (figure 4.7). Mek1 is a phosphorylation target of Hop1 which itself is phosphorylated by Mec1/Rad24 and Tel1 (Carballo, Johnson et al. 2008). The phosphorylation action of Hop1 functions to establish inter-homologue bias in repair (Niu, Li et al. 2007; Carballo, Johnson et al. 2008). Mek1 has been observed to be required for the DSB feedback mechanisms with mutants forming low levels of DSBs in the *spo11-HA* background.

Tel1 functions to inhibit DSB formation at the *sae2Δ* with removal of Tel1 causing an increase in DSB levels (as seen in figure 6.1). As the mechanism of DSB feedback functions through Mek1, and Mek1 is phosphorylated by both Mec1/Rad24 and Tel1, it was proposed that DSB inhibition functioned through Mek1. If this is the case, then removal of *MEK1* in the *sae2Δ* background will cause DSB levels to increase, similar to *tel1Δ sae2Δ*. As Tel1 also functions to inhibit DSB formation in the *sae2Δ spo11-HA* background, if Tel1 functions through Mek1 then an increase in DSB levels similar to *tel1Δ sae2Δ spo11-HA* should also be observed in the *mek1Δ sae2Δ spo11-HA*. In addition, removal of *MEK1* in either the *tel1Δ sae2Δ* or *tel1Δ sae2Δ spo11-HA* backgrounds should not cause any additional effect on DSB formation.

In the *sae2Δ* strain, DSBs reached approximately 14% of total DNA (figure 6.4A and B). By contrast, in *tel1Δ sae2Δ* DSBs reached around 25% of total DNA (figure 6.1 and figure 6.4B). In *mek1Δ sae2Δ* strain DSBs peaked at less than 12% of total DNA (figure 6.4A and B). In addition, the DSBs in the *sae2Δ mek1Δ tel1Δ* strain reached just over 20% of total DNA (figure 6.4A and B).Therefore the DSBs in the *mek1Δ sae2Δ* strain are below the expected DSB levels observed in *tel1Δ sae2Δ* and also slightly below DSB signal observed in *sae2Δ*. The DSB signal observed in

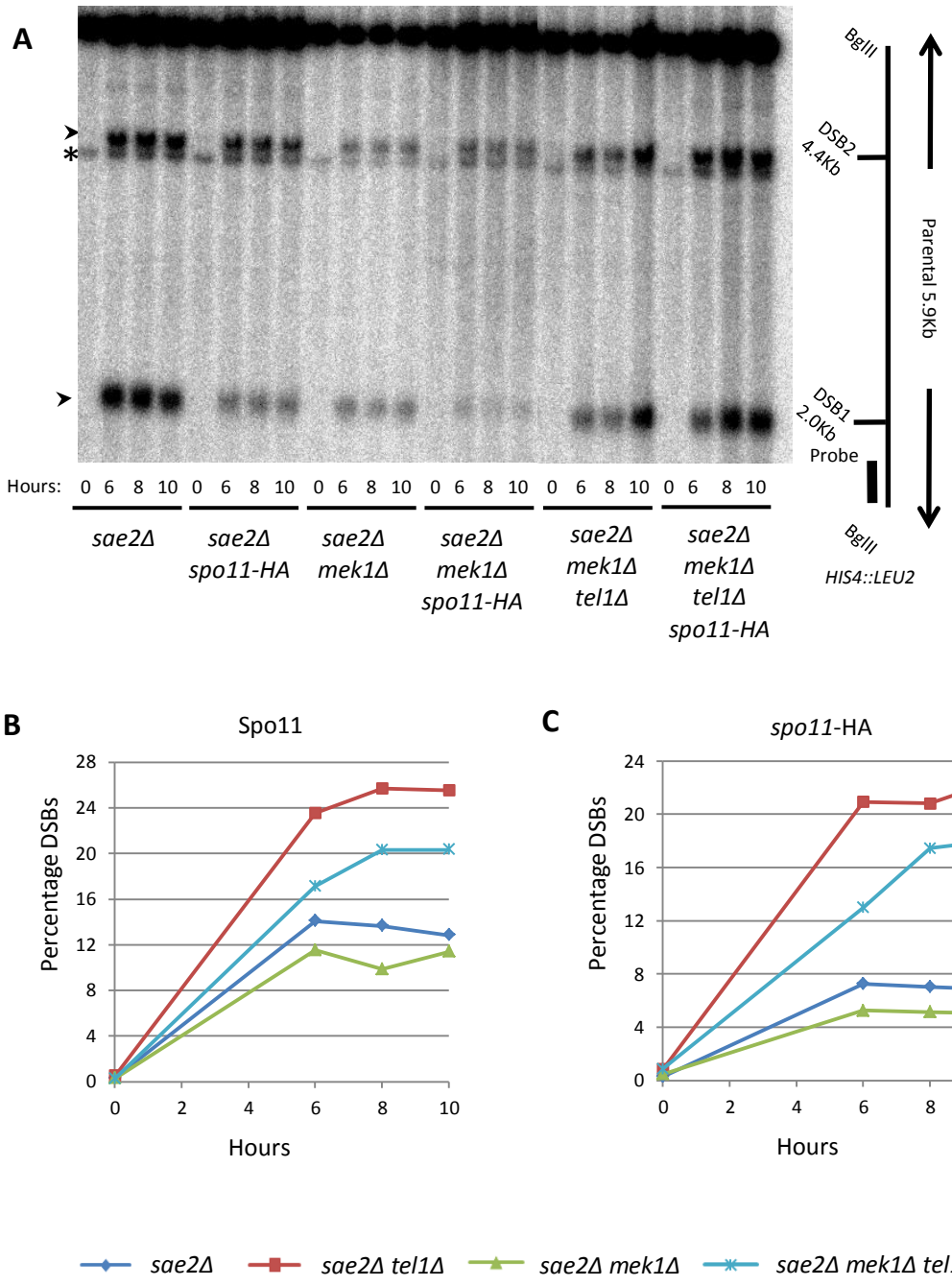

Figure 6.4: DSB levels decrease in the presence of the *mek1Δ* mutation. A) Genomic DNA from meiotic time courses were digested and run on a 0.7% 1xTAE agarose gel for 20 hours at 60 volts. The gel was transferred to nylon membrane under denaturing conditions and hybridised with a radioactive probe for the *HIS4::LEU2* locus. The membrane was exposed to a phosphor screen and image taken using a Fuji phosphor scanner. DSBs marked with arrowhead (➤). Asterisk (⁎) marks non-specific band. **B** and **C)** Quantification of DSB levels over time. Image Gauge was used to analyse DSB signal as a percentage of total DNA and signal is plotted and displayed.

the *mek1Δ tel1Δ sae2Δ* was below the signal observed in *tel1Δ sae2Δ.* This reduction in the *mek1Δ* compared to the *tel1Δ sae2Δ* suggests that Tel1 inhibition does not function through Mek1. In addition, the reduction in DSB signal observed in the *mek1Δ tel1Δ sae2Δ* compared with *tel1Δ sae2Δ*, and *mek1Δ sae2Δ* compared with *sae2Δ,* suggests that Mek1 functions to promote DSB formation.

In the *sae2Δ spo11-HA* strain, DSBs peak at less than 8% of total DNA from 6 hours onwards (figure 6.4A and C). By contrast in the *tel1Δ spo11-HA* strain, DSBs peaked at over 20% (figure 6.1 and figure 6.4C). In the *sae2Δ mek1Δ spo11-HA* strain, DSBs peaked at around 5% from 6 hours onwards (figure 6.4A and C). In addition, the DSBs in the *sae2Δ mek1Δ tel1Δ spo11-HA* DSBs peaked around 18% of total DNA (figure 6.4A and C). The reduction in DSB signal observed in the *mek1Δ sae2Δ spo11-HA* compared to the *tel1Δ sae2Δ spo11-HA* suggests that Tel1 inhibition does not function through Mek1. This is consistent with observations from the *SPO11 sae2Δ* background. In addition, the reduction in DSB signal in the *mek1Δ tel1Δ sae2Δ spo11-HA* compared to the *tel1Δ sae2Δ spo11-HA*, and in the *mek1Δ sae2Δ spo11-HA* compared with the *sae2Δ spo11-HA*, suggests that Mek1 functions to promote DSB formation. This observation is consistent with the observations made in the *SPO11* background.

6.6: Discussion

Observations from chapter 4 suggested the presence of a DSB feedback mechanism that functions in the *spo11-HA* background through the Mec1-dependent meiotic recombination checkpoint. In the process of testing the DSB feedback mechanism in chapter 5, the observed DSB levels were lower than expected and lower than in a strain where the feedback mechanism is not thought to function. This decrease in DSB levels lead to the suggestion that a mechanism functions to inhibit DSB formation. Observations from budding yeast (Zhang, Kim et al. 2011) and other organisms (Joyce, Pedersen et al. 2011; Lange, Pan et al. 2011) suggest that Tel1 functions as an inhibitor of DSB formation.

The *sae2Δ* and *dmc1Δ* backgrounds were utilised to investigate the role of Tel1 as an inhibitor of DSB formation. These backgrounds were also combined with the *spo11-HA* tag which revealed the role of the Mec1-dependent checkpoint in promoting DSB formation. In the *sae2Δ* background, removal of Tel1 leads to an increase in DSB levels, both in *SPO11* and *spo11-HA.* This suggests that Tel1 acts as an inhibitor of DSB formation. In the otherwise wildtype and *dmc1Δ* backgrounds, DSBs were approximately the same as when Tel1 is present. In *spo11-HA* and *dmc1Δ spo11-HA* however, removal of Tel1 lead to a reduction in DSB levels. These observations suggest that Tel1 functions to promote DSB formation in the *spo11-HA* background.

These observations suggest that Tel1 functions to inhibit DSB formation in the *sae2Δ* background and both promote and inhibit DSB formation in the *spo11-HA* background. As observations from chapter 4 suggest that Rad24 functions to promote DSB formation in the *spo11-HA* background, it was interesting to determine what effect removal of both Rad24 and Tel1 had on the different backgrounds. It was expected that in the *sae2Δ* background, because

of the lack of any effect in the *rad24Δ* mutant and an increase in the DSB signal in the *tel1Δ* background, that the *rad24Δ tel1Δ sae2Δ* would have a DSB signal comparable to *tel1Δ sae2Δ.* The observed DSB levels were as expected supporting the idea that Tel1 functions to inhibit DSB formation at the *sae2Δ* block and Rad24 does not function. In the *rad24Δ tel1Δ* background it was expected that due to no effect of removing either Rad24 or Tel1 that DSBs would be similar to wildtype. However, unexpectedly the DSBs in *rad24Δ tel1Δ* were higher than both the *rad24Δ* or *tel1Δ* mutants. In addition, the DSB levels went above 25% indicating that more than one chromatid was broken at the *HIS4::LEU2* locus per pair of homologous chromosomes. This suggests that in the absence of Tel1, Rad24 functions to inhibit DSB formation in the *sae2Δ* background.

In the *spo11-HA* background different observations were made for the Rad24 and Tel1 mutants compared with the *SPO11* background. In the *sae2Δ spo11-HA* background the removal of Tel1 caused an increase in DSB levels (because of removal of inhibition to DSB formation) and removal of Rad24 caused no effect on DSB levels (because the Mec1-dependent checkpoint is not active). The expected observation was that the *rad24Δ tel1Δ sae2Δ spo11-HA* mutant would have DSB levels comparable to *tel1Δ sae2Δ.* However, the *rad24Δ tel1Δ sae2Δ spo11-HA* mutant produced an extremely low level of DSBs. This suggests that in the *sae2Δ spo11-HA* background, DSB formation requires the presence of either Rad24 or Tel1.

In the *spo11-HA* background, removal of either Rad24 or Tel1 caused a decrease in DSB levels, suggesting that both Rad24 and Tel1 act as a promoter of DSB formation. Similar observations were also made in the *dmc1Δ spo11-HA* background. The expected observation was that removal of both Rad24 and Tel1 would cause a reduction in DSB signal in the *spo11-HA* background. In the *rad24Δ tel1Δ spo11-HA* mutant DSB levels were lower than in the *rad24Δ*

spo11-HA and *tel1Δ spo11-HA.* This observation supports the idea that in the *spo11-HA* background, DSB formation requires Rad24 or Tel1, consistent with the observations made in the *sae2Δ spo11-HA* background.

Taken together, these observations suggest that, in an otherwise wildtype situation, DSBs form by Spo11 (figure 6.5A). Before processing by Sae2, Tel1 functions to inhibit DSB formation (figure 6.5B and C). In the absence of Tel1, Mec1/Rad24/Rad17 can function to inhibit DSB formation (figure 6.5C). Once processed by Sae2, DSBs levels are no longer affected by the removal of Rad24 or Tel1 in a *SPO11* background. In the *spo11-HA* background, DSBs form and before processing by Sae2, DSBs formation is inhibited by Tel1. Once processed (figure 6.5D) the DNA molecule can stimulate the Mec1-dependent checkpoint (figure 6.5E) allowing for activation of the DSB feedback mechanism causing promotion of the DSB formation (figure 6.5G). Tel1 activation can also cause stimulation of a DSB formation mechanism (figure 6.5H). The differences listed highlight the mechanisms to create the DSB levels observed in the different backgrounds.

With Tel1 functioning to inhibit DSB formation in the *sae2Δ* background, and the DSB feedback mechanism functioning through Mek1, one idea was that the Tel1 inhibition of DSB formation also functioned through Mek1. Removal of Mek1 in the *sae2Δ* background failed to mimic a *tel1Δ* mutant and instead had a reduction in DSB levels. This was also observed in the *sae2Δ spo11-HA* background. This suggests that inhibition of DSB formation by Tel1 does not function through Mek1. In addition it highlighted that Mek1 promotes DSB formation.

The different DSB levels observed in the varying strain backgrounds highlight the complicated system that functions to either promote or inhibit DSB formation. Tel1 has been observed to be an inhibitor of DSB formation however the lack of DSB signal in the *rad24Δ tel1Δ spo11-HA*

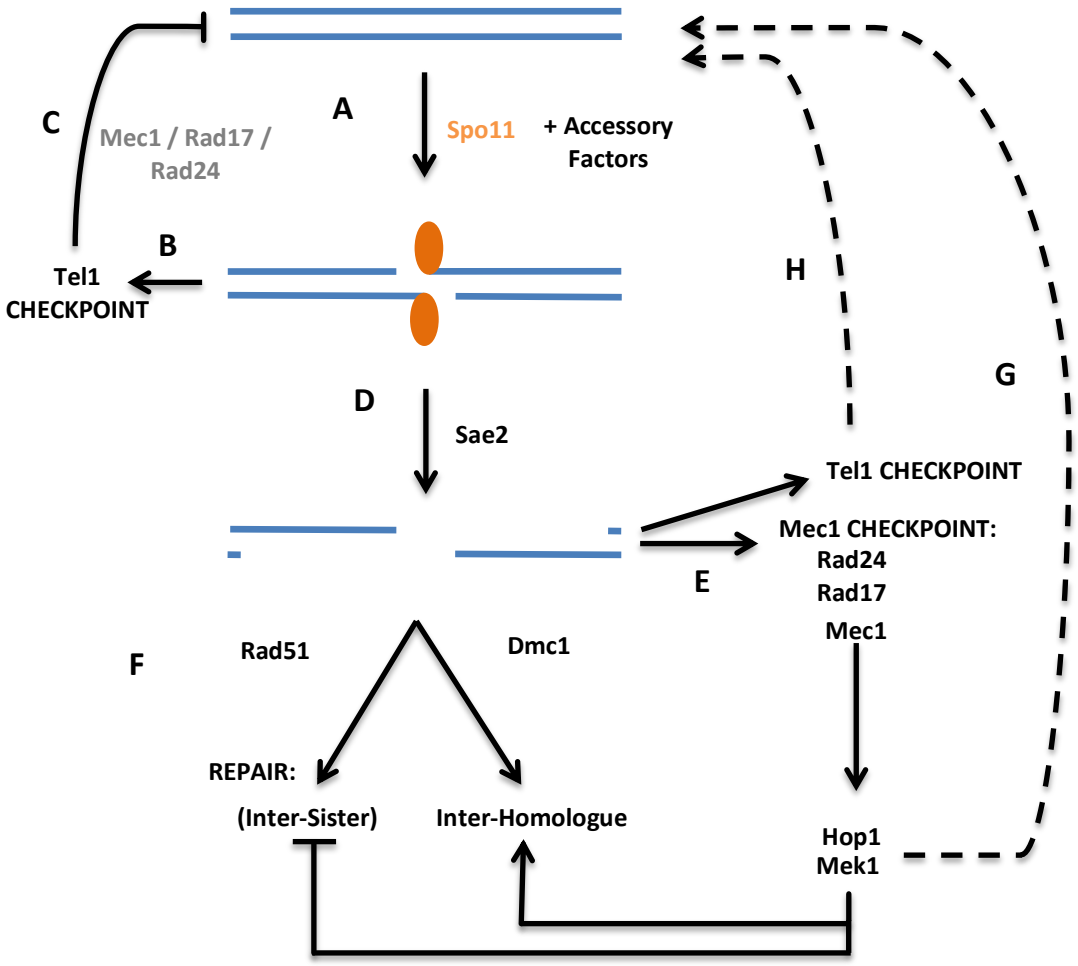

Figure 6.5: Model for DSB promotion and inhibition mechanism. A) DSBs form by Spo11 and its accessory factors and Spo11 becomes attached to both sides of the DSB. **B)** In the absence of Sae2 or before Sae2 processing, Tel1 is activated by DSB molecules and **(C)** inhibits further DSB formation. In the presence of wildtype Spo11, DSB inhibition also functions through Mec1/Rad24/Rad17 (in grey). **D)** Sae2, in addition to the MRX complex, is required to process the DSB causing resection to occur. **E)** The Mec1-dependent meiotic recombination checkpoint is activated by single stranded DNA and, in addition to Tel1, activates downstream kinases causing enforcement of the inter-homolog bias for repair. **F)** Dmc1 and Rad51 enable strand invasion and subsequent stages of DSB repair to occur. In the presence of *spo11-HA*, activation of the Mec1-dependent checkpoint, specifically Mek1, causes phosphorylation of Mek1 and activation of the DSB feedback mechanism **(G)** allowing for more DSBs to form. **H)** Mek1 independent promotion of DSB feedback may function from Tel1 activation but may also function through **(G).**

backgrounds and *tel1Δ spo11-HA* backgrounds highlight its role as an DSB promoter. The difference in DSB levels between the *rad24Δ tel1Δ* mutants in the *SPO11* and *spo11-HA* backgrounds indicate the very different mechanisms that are functioning to produce an optimal level of DSBs.

One reason for these mechanisms to exist is to ensure the correct number of DSBs for accurate chromosome segregation. These "DSB homeostasis" mechanisms ensure that when DSB formation abilities are optimal, new DSBs are inhibited. When DSB formation is compromised however (such as in the *spo11-HA* background) DSB formation is either inhibited (at the *sae2Δ* block) or promoted (when otherwise wildtype or *dmc1Δ* block). The high levels of DSBs that form in the *tel1Δ sae2Δ* block, even in the presence of *spo11-HA* (when a DSB promotion mechanism is required at a later stage) may indicate that the *sae2Δ* block causes an increase in DSBs. These mechanisms ensure that the optimum number of DSBs form ensuring that enough crossovers exist to accurately pair and segregate homologs, but not too many to cause incorrect repair or to take too long for repair.

CHAPTER 7:

Control of resection at meiotic DSBs

Chapter 7: Control of resection at meiotic DSBs

7.1: Introduction

A double-stranded DNA molecule when separated on an agarose gel migrates at a position relative to its size. The presence of a DSB within a molecule causes a reduction in size and therefore migrates at a different position, relative to its new size. In a wildtype background, DSBs introduced during meiosis have ssDNA tails due to exonuclease processing (Sun, Treco et al. 1989). The DSB molecules are therefore reduced in size due to the resection and migrate at a position relative to its new size. In backgrounds where DSBs form but are not processed and resection does not take place (such as in *rad50S* (Alani, Padmore et al. 1990) and *sae2Δ* (Keeney and Kleckner 1995; Prinz, Amon et al. 1997)) molecules with DSBs introduced migrate at the position of a larger molecule compared with wildtype. In contrast, in situations where additional resection takes place (such as *dmc1Δ* (Bishop, Park et al. 1992)), molecules with DSBs introduced migrate at the position of a smaller and smaller molecule compared to wildtype as more and more resection occurs.

In the wildtype background, the first appearance of a DSB is that of a resected molecule (Sun, Treco et al. 1989), suggesting the rapid processing of the DSB by exonucleases. In addition, the DSB molecules migrate at a relative size position and do not migrate at a position of a smaller size as meiosis progresses. This suggests that the amount of resection that takes place in a wildtype background is limited.

In Mec1 meiotic recombination checkpoint mutants DSBs are hyper-resected (Grushcow, Holzen et al. 1999; Shinohara, Sakai et al. 2003). This hyper-resection causes the DSB signal to migrate at a smaller position compared to wildtype (Grushcow, Holzen et al. 1999; Shinohara,

Sakai et al. 2003). In addition, the resection is less uniform and therefore the DSB signal is distributed over a larger distance (Grushcow, Holzen et al. 1999; Shinohara, Sakai et al. 2003). The hyper-resection suggests a deficiency in resection control.

In mitosis, DSBs are resected by Mre11/Sae2, Exo1 and Sgs1/Dna2 (Mimitou and Symington 2008). In meiosis, the main nuclease that resects DSBs is Exo1 (Zakharyevich, Ma et al. 2010). Mre11/Sae2 has been implicated in producing 3' ssDNA tails by endonucleolytic processing of Spo11 (Neale, Pan et al. 2005). In contrast to mitosis, Sgs1/Dna2 does not play a role in resecting meiotic DSBs (Zakharyevich, Ma et al. 2010). Previous observations at telomeres (in a mutant background where the telomere is "uncapped" and able to be resected) have identified that phosphorylation of Exo1 inhibits its activity (Morin, Ngo et al. 2008). This phosphorylation requires components of the checkpoint machinery (Morin, Ngo et al. 2008). It is therefore possible that the control of Exo1 resection at meiotic DSBs is by checkpoint dependent phosphorylation. This may explain why meiotic DSBs are hyper-resected in Mec1 checkpoint defective strains. As DSB molecules migrate at a particular location proportional to its size, migration of DSB molecules on a southern blot can be used as a measure of the amount of resection that has taken place. I will utilise this assay to test resection and Mec1 checkpoint defective mutants to measure resection and to determine whether the hyper-resected DSBs in a Mec1 checkpoint defective strain are a consequence of Exo1 resection.

7.2: *exo1Δ* causes a reduction in resection and *sgs1-mn* causes a reduction in resection in the absence of Exo1 at DSB2

In order to compare the amount of resection occurring in wildtype, *exo1Δ, sgs1-mn* and *exo1Δ sgs1-mn* mutants samples were taken from synchronous meiotic cultures and genomic DNA prepared. Samples were digest and separated according to size on an agarose gel. Southern blotting allowed identification of the probed locus of interest (*HIS4::LEU2*) and observed migration of the DSB molecules. The *HIS4::LEU2* locus is a meiotic recombination hotspot with two DSBs separated by approximately 2.4Kb. The DSB migration distance was measured from the mode of the parental uncut band to the mode of each DSB band. Agarose gels can be optimised according to the size of the molecule that is being resolved. Using a restriction site close to the DSB allows smaller molecules to be resolved and small migration differences to be more easily detected. DSB signal is transient due to formation and repair. Therefore signals were analysed at 3, 4, 5 and 6 hours when DSB signal is at its peak (Neale, Pan et al. 2005). All strains, except for the *sgs1-mn* strain, peaked at 4 hours for DSB signal, with *sgs1-mn* peaking at 3 hours (figure 7.1A and B). Wildtype DSB signal dropped within 2hours. By contrast the *exo1Δ, sgs1-mn* and *exo1Δ sgs1-mn* had a shallower arc of signal following the peak (figure 7.1A and B).

In wildtype, DSB1 migrated between 86.5 and 89mm from parental band and DSB2 migrated between 27.4 and 28mm (figure 7.1A, C and D). s*gs1-mn* migrates around the same position as wildtype at DSB1(between 87.4 and 88.4mm) and DSB2 (between 27.4 and 28.8mm)(figure 7.1A and C). By contrast, *exo1Δ* migrates closer to the parental band at DSB1 (between 83 and 84.1mm) and DSB2 (between 24.9 and 26.9mm)(figure 7.1A and C). *exo1Δ sgs1-mn* migrated at a similar position as *exo1Δ* at DSB1(between 82.9 and 84mm) but migrated even closer to parental than *exo1Δ* at DSB2(between 25.6 and 22.8mm)(figure 7.1A and C). These

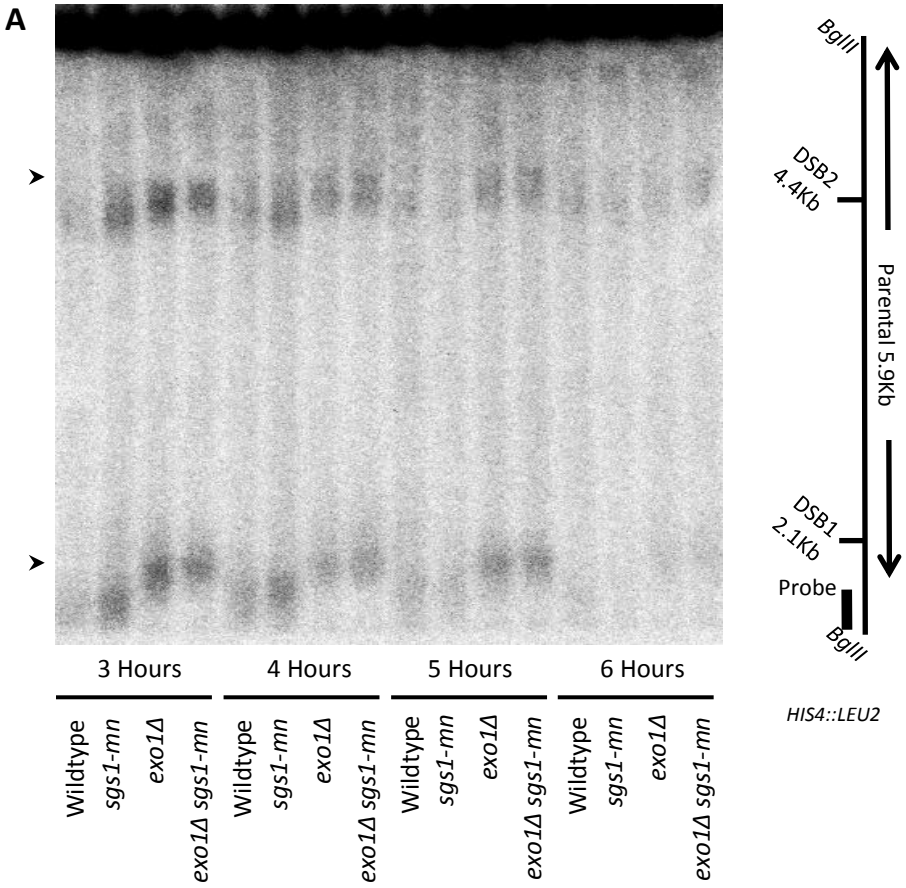
A
BglII
DSB2
4.4Kb
Parental 5.9Kb
DSB1
2.1Kb
Probe
BglII
HIS4::LEU2
3 Hours
4 Hours
5 Hours
6 Hours
Wildtype
sgs1-mn
exo1Δ
exo1Δ sgs1-mn

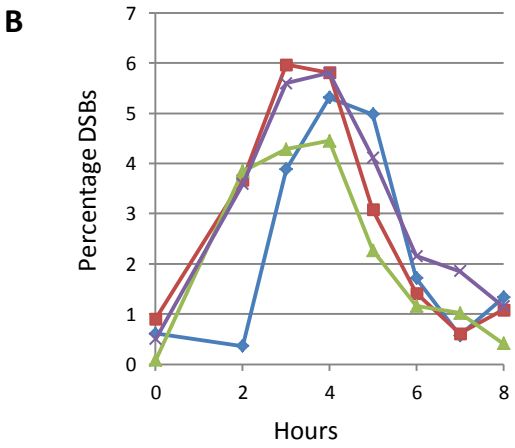
B
Percentage DSBs
Hours

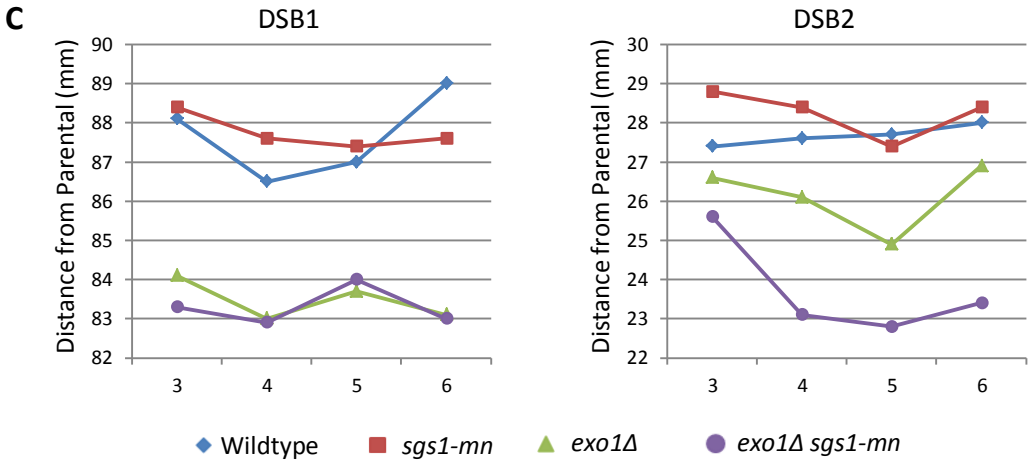
C
DSB1
DSB2
Distance from Parental (mm)
Wildtype
sgs1-mn
exo1Δ
exo1Δ sgs1-mn

Figure 7.1: DSB migration is decreased in *exo1Δ* and *exo1Δ sgs1-mn* mutants.
A) Genomic DNA from meiotic time courses were digested and run on a 0.7% 1xTAE agarose gel for 20 hours at 60 volts. The gel was transferred to nylon membrane under denaturing conditions and hybridised with a radioactive probe for the *HIS4::LEU2* locus. The membrane was exposed to a phosphor screen and image taken using a Fuji phosphor scanner. DSBs marked with arrowhead (➢). **B)** Quantification of DSB levels over time. **C)** Image Gauge was used to analyse each lane and record the distance between the mode of the parental signal and the mode of each DSB with the difference being plotted and displayed.

observations suggest that removal of Exo1 causes a reduction in DSB migration, consistent with less resection taking place. In addition, removal of Sgs1 does not cause a reduction in migration compared to wildtype, suggesting that Sgs1 does not play a role in resecting meiotic DSBs. However, in the *exo1Δ sgs1-mn* mutant, migration of DSB2 was further reduced compared with *exo1Δ* suggesting that Sgs1 functions to resect DSB2 in the absence of Exo1. Interestingly, the reduction in migration compared to *exo1Δ* was not observed at DSB1 suggesting that Sgs1 dependent resection is DSB specific.

7.3: *rad24Δ* causes hyper-resection at meiotic DSBs and a proportion of the hyper-resection is Exo1 dependent

Strains absent of *RAD24* function have hyper-resected DSBs (Shinohara, Sakai et al. 2003; Morin, Ngo et al. 2008). Exo1 has been identified as the main nuclease in meiosis (Zakharyevich, Ma et al. 2010) and (figure 7.1). To test if the hyper-resection observed in the *rad24Δ* background is due to Exo1, DSB migration of *rad24Δ* and *rad24Δ exo1Δ* mutants were compared. Experiments for earlier chapters were also focusing on the Mec1 meiotic checkpoint but in the presence of the *spo11-HA* tag. As the strains created to test whether the hyper-resection in Mec1 checkpoint defective strains is Exo1-dependent may also have been used in investigating questions in earlier chapters, they were created in the *spo11-HA* background. Because the DSBs in a Mec1 checkpoint defective strain are hyper-resected, there was concern that the previous digest used (*BglII*) was too close to the DSB1 site. If this is the case, the signal from DSB1 would to migrate past the restriction site and not be measured. To ensure this did not happen, a restriction site further from the DSB was used.

In all strains DSB formation followed similar kinetics, with DSB signal peaking between 3 and 5 hours and reaching around 2.5% of total DNA (figure 7.2A and B). These are quite low DSB

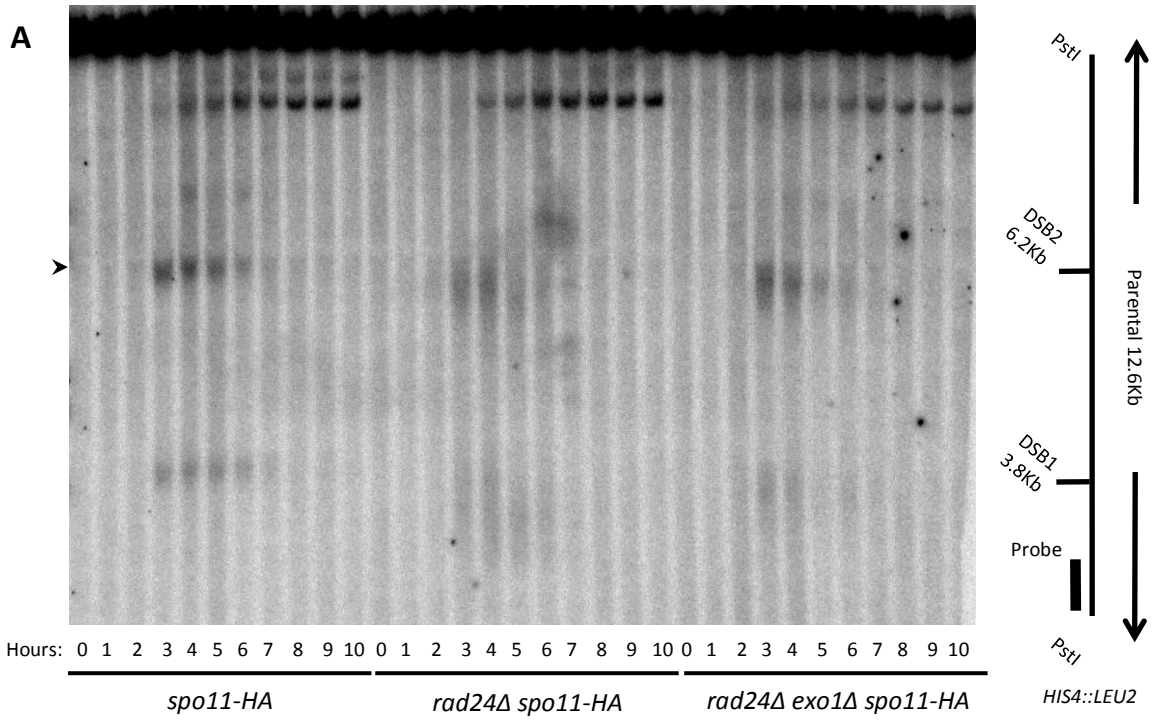
A
PstI
DSB2
6.2Kb
Parental 12.6Kb
DSB1
3.8Kb
Probe
PstI
HIS4::LEU2
Hours: 0 1 2 3 4 5 6 7 8 9 10 0 1 2 3 4 5 6 7 8 9 10 0 1 2 3 4 5 6 7 8 9 10
spo11-HA
rad24Δ spo11-HA
rad24Δ exo1Δ spo11-HA

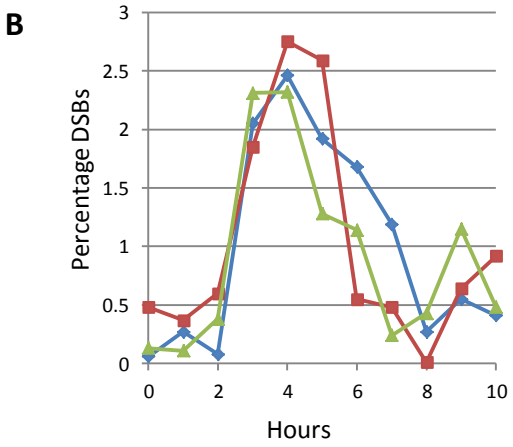
B
Percentage DSBs
3
2.5
2
1.5
1
0.5
0
0 2 4 6 8 10
Hours

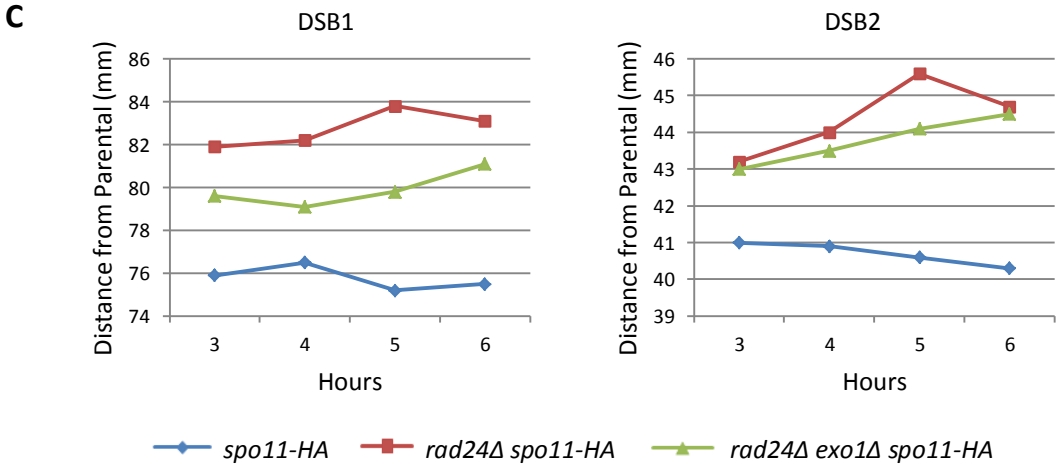
C
DSB1
DSB2
Distance from Parental (mm)
86
84
82
80
78
76
74
3 4 5 6
Hours
46
45
44
43
42
41
40
39
3 4 5 6
Hours
spo11-HA
rad24Δ spo11-HA
rad24Δ exo1Δ spo11-HA

Figure 7.2: DSB migration is decreased in the *rad24Δ exo1Δ spo11-HA* compared with *rad24Δ spo11-HA* but only at DSB1. A) Genomic DNA from meiotic time courses were digested and run on a 0.7% 1xTAE agarose gel for 18 hours at 60 volts. The gel was transferred to nylon membrane under denaturing conditions and hybridised with a radioactive probe for the *HIS4::LEU2* locus. The membrane was exposed to a phosphor screen and image taken using a Fuji phosphor scanner. DSBs marked with arrowhead (➤). **B)** Quantification of DSB levels over time. **C)** Image Gauge was used to analyse each lane and record the distance between the mode of the parental signal and the mode of each DSB with the difference being plotted and displayed.

percentages and lower than expected for the *spo11-HA* strain. Observations of the southern blot indicate a large amount of lane background, especially at 4 and 5 hours of the *spo11-HA* strain. This may be due to degraded DNA within the sample or partially digested DNA molecules. The increased lane background reduces the ability to detect signal. Although the signal is lower than expected, the migration of the DSB compared to the parental can be measured therefore enabling this southern blot to be used. The migration of DSB molecules were measured at 3, 4, 5 and 6 hours because of the peak of DSB signal. In the *spo11-HA* strain, DSBs migrated the shortest distance from parental signal with DSB1 migrating around 76mm and DSB2migrating between 40 and 41mm (figure 7.2A and C). By contrast, in the *rad24Δ spo11-HA* strain DSBs migrated a greater distance from parental, with DSB1 migrating between 82 and 84mm and DSB2 migrating between 43 and 46mm (figure 7.2A and C). This observation is consistent with the *rad24Δ* mutant phenotype having hyper-resected DSBs (Shinohara, Sakai et al. 2003; Morin, Ngo et al. 2008). In the *rad24Δ exo1Δ spo11-HA* strain DSB1 migrates between the *spo11-HA* and *rad24Δ spo11-HA* strains, between 79 and 81mm (figure 7.2A and C). At DSB2 however, *rad24Δ exo1Δ spo11-HA* signal migrates close to *rad24Δ spo11-HA* (between 43 and 44mm) (figure 7.2A and C).

These results suggest that because of the reduction in resection in the *rad24Δ exo1Δ spo11-HA* compared to *rad24Δ spo11-HA* at DSB1, Exo1 contributes to some of the resection that takes place in the *rad24Δ* background. However, at DSB2 *rad24Δ exo1Δ spo11-HA* migrates at a similar position to *rad24Δ spo11-HA* suggesting that Exo1 does not contribute to the hyper-resection at DSB2. The lack of effect at DSB2 in the *rad24Δ exo1Δ spo11-HA* background indicates that another nuclease mechanism functions to resect the DSB. Interestingly, *exo1Δ* previously caused resection to decrease compared to wildtype (figure 7.1) but in the *rad24Δ exo1Δ spo11-HA* background, resection was reduced but still greater than *spo11-HA*. This

suggests that in the *rad24Δ exo1Δ spo11-HA* background at DSB1, nucleases other than just Exo1 are functioning to resect DSB1.

7.4: Exo1, Sgs1 and another unknown nuclease functions in a *rad24Δ* background

The *rad24Δ spo11-HA* background identified that removing Exo1 did not cause a decrease in the migration of DSB2 and although migration decreased at DSB1, it did not decrease as much as DSB1 in *spo11-HA* (figure 7.2). These observations suggest that another nuclease functions to resect DSBs in the *rad24Δ spo11-HA* background. Additional observations identified that at DSB2, removal of Sgs1 in the *exo1Δ* background caused a reduction in DSB migration compared with *exo1Δ* (figure 7.1). This observation suggests that Sgs1 functions to resect DSBs in the absence of Exo1. Together, these observations lead to the hypothesis that the additional nuclease functioning to resect DSBs in the *rad24Δ* background is Sgs1.

To test whether Sgs1 is functioning to resect DSBs in the *rad24Δ* background, the *sgs1-mn* mutation was introduced into the *rad24Δ* and *rad24Δ exo1Δ* backgrounds. Because of the decrease in DSB signal in the *spo11-HA* background, the strains did not have the *spo11-HA* tag. In all of the strains, DSB signal peaked at 3 hours or 4 hours (figure 7.3A and B). The *rad24Δ sgs1-mn* strain DSBs peaked almost 2-fold higher than the DSB signal in other strains. In the *rad24Δ exo1Δ sgs1-mn* strain DSB signal remained the longest and decreased slower than it formed.

In the *rad24Δ* strain DSBs migrated furthest from the parental band (79.1 to 80.65mm for DSB1 and 42.35 to 44.8mm for DSB2) (figure 7.3A and C). Consistent with previous observations at DSB1, *rad24Δ exo1Δ* migrates closer to parental band compared with *rad24Δ* (migrating between 76.5 and 73.75mm) (figure 7.3A and C). However, in contrast to previous

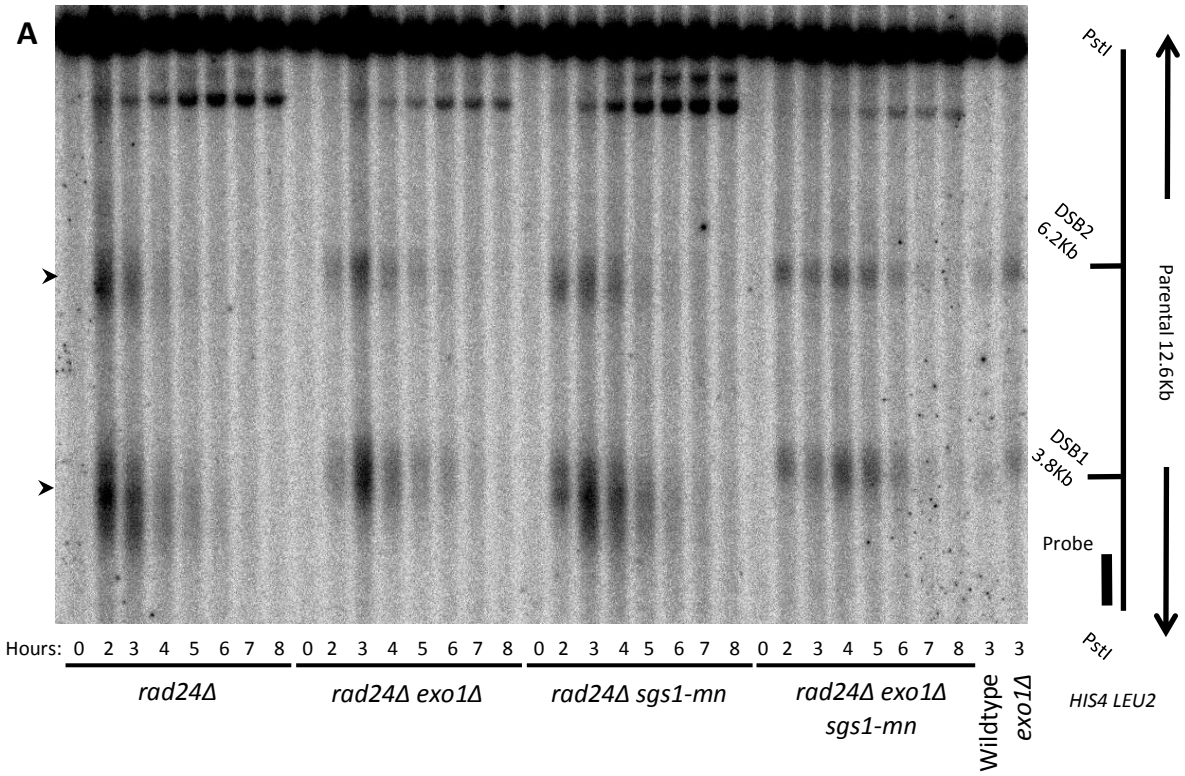
A
PstI
DSB2
6.2Kb
Parental 12.6Kb
DSB1
3.8Kb
Probe
PstI
Hours: 0 2 3 4 5 6 7 8 0 2 3 4 5 6 7 8 0 2 3 4 5 6 7 8 0 2 3 4 5 6 7 8 3 3
rad24Δ
rad24Δ exo1Δ
rad24Δ sgs1-mn
rad24Δ exo1Δ sgs1-mn
Wildtype
exo1Δ
HIS4 LEU2

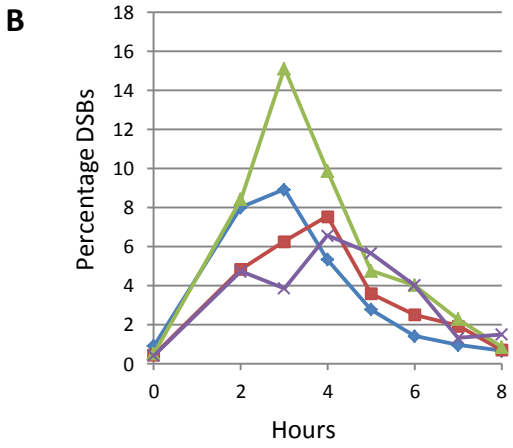
B
Percentage DSBs
Hours

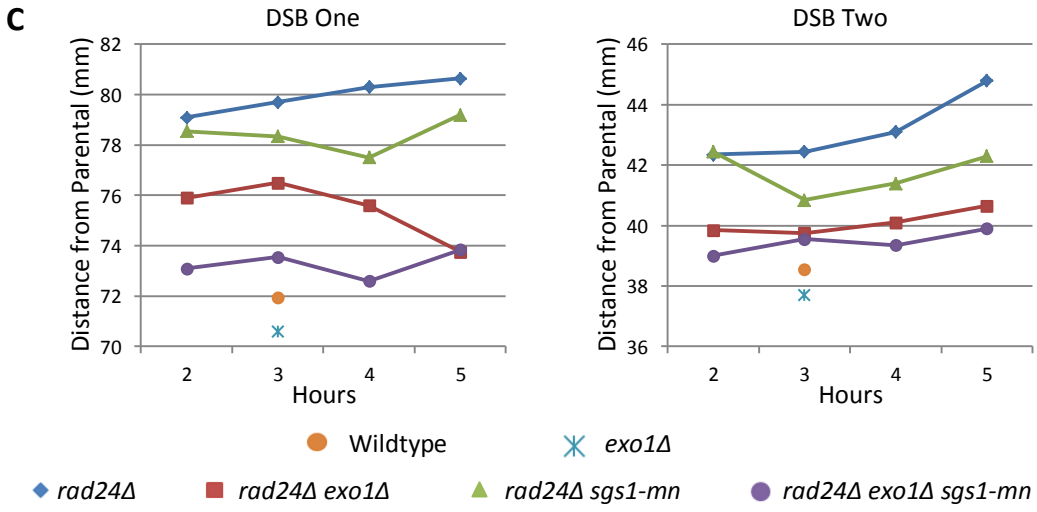
C
DSB One
DSB Two
Distance from Parental (mm)
Hours
Wildtype
exo1Δ
rad24Δ
rad24Δ exo1Δ
rad24Δ sgs1-mn
rad24Δ exo1Δ sgs1-mn

Figure 7.3: DSB migration is decreased in the *rad24Δ* background by removal Sgs1, Exo1 or both. A) Genomic DNA from meiotic time courses were digested and run on a 0.7% 1xTAE agarose gel for 18 hours at 60 volts. The gel was transferred to nylon membrane under denaturing conditions and hybridised with a radioactive probe for the *HIS4::LEU2* locus. The membrane was exposed to a phosphor screen and image taken using a Fuji phosphor scanner. DSBs marked with arrowhead (➢). **B)** Quantification of DSB levels over time. **C)** Image Gauge was used to analyse each lane and record the distance between the mode of the parental signal and the mode of each DSB with the difference being plotted and displayed.

observations at DSB2, *rad24Δ exo1Δ* also migrated closer to the parental band compared to *rad24Δ* (migrating between 39.75 and 40.65mm)(figure 7.3A and C). These observations indicate that removal of Exo1 in a *rad24Δ* background reduces the amount of resection observed at both DSBs in the *rad24Δ* strain. One explanation for the change in migration observed at DSB2 between the *rad24Δ exo1Δ spo11-HA* and the *rad24Δ exo1Δ* strains could be related to the *spo11-HA* tag. As the *spo11-HA* tag causes a reduction in DSB levels it is possible that the resection machinery functioning at DSB2 is able to carry out more extensive resection because of the decrease in DSBs. This idea is consistent with DSBs levels regulating the amount of resection (Neale, Ramachandran et al. 2002).

The *rad24Δ sgs1-mn* migrates in between *rad24Δ exo1Δ* and *rad24Δ* at both DSBs (between 77.5 and 79.2mm at DSB1 and 40.85 and 42.45mm at DSB2) (figure 7.3A and C). Because of the reduction in migration in the *sgs1-mn* compared with *rad24Δ* this suggests that Sgs1 functions to resect DSBs in a *rad24Δ* background.

In the *rad24Δ exo1Δ sgs1-mn* strain, both DSBs migrates closer to the parental band that the *rad24Δ, rad24Δ sgs1-mn* and *rad24Δ exo1Δ* strains (between 72.6 and 73.85mm for DSB1 and between 39 and 39.9mm for DSB2) (figure 7.3A and C). This reduction in resection suggests that in the *rad24Δ* background, the hyper-resection is due to both Exo1 and Sgs1. However, one sample of wildtype and *exo1Δ* at 3 hours was measured for migration on the same blot (figure 7.3A and C). Both the wildtype and *exo1Δ* migrated closer to parental band than all *rad24Δ* mutants. As the DSBs in wildtype and *exo1Δ* migrates closer to parental than all *rad24Δ* mutants this indicates that, in addition to Exo1 and Sgs1, another nuclease is functioning to resect DSBs in the *rad24Δ* background.

All nuclease defective mutants were directly compared on the same Southern blot, using the *BglII* digest, which cuts the DNA molecule close to the DSB. This digest enables the molecules to be resolved for longer and differences between DSB migrations to be more easily detected. In Mec1 checkpoint proficient strains, it is observed that *exo1Δ sgs1*-mn has the greatest reduction in resection due to the decreased migration (figure 7.4). This observation matches what was previously observed in earlier figures (figure 7.1). The *rad24Δ* strains have increased migration compared with wildtype, with the removal of both Exo1 and Sgs1 causing the largest reduction in migration, suggesting the biggest decrease in resection (figure 7.4). These observations also support what was previously observed.

However, subtle differences previously observed between *exo1Δ sgs1-mn* and *exo1Δ* at DSB2, and *rad24Δ* and *rad24Δ sgs1-mn* are no longer apparent. One explanation for this is that, contrary to what was expected, this Southern blot was not sufficiently optimised to allow for small differences to be detected. This is likely as the resolution of the otherwise wildtype strains, for example, was previously separated by 6mm (figure 7.1) and is now separated by 3mm (figure 7.4).

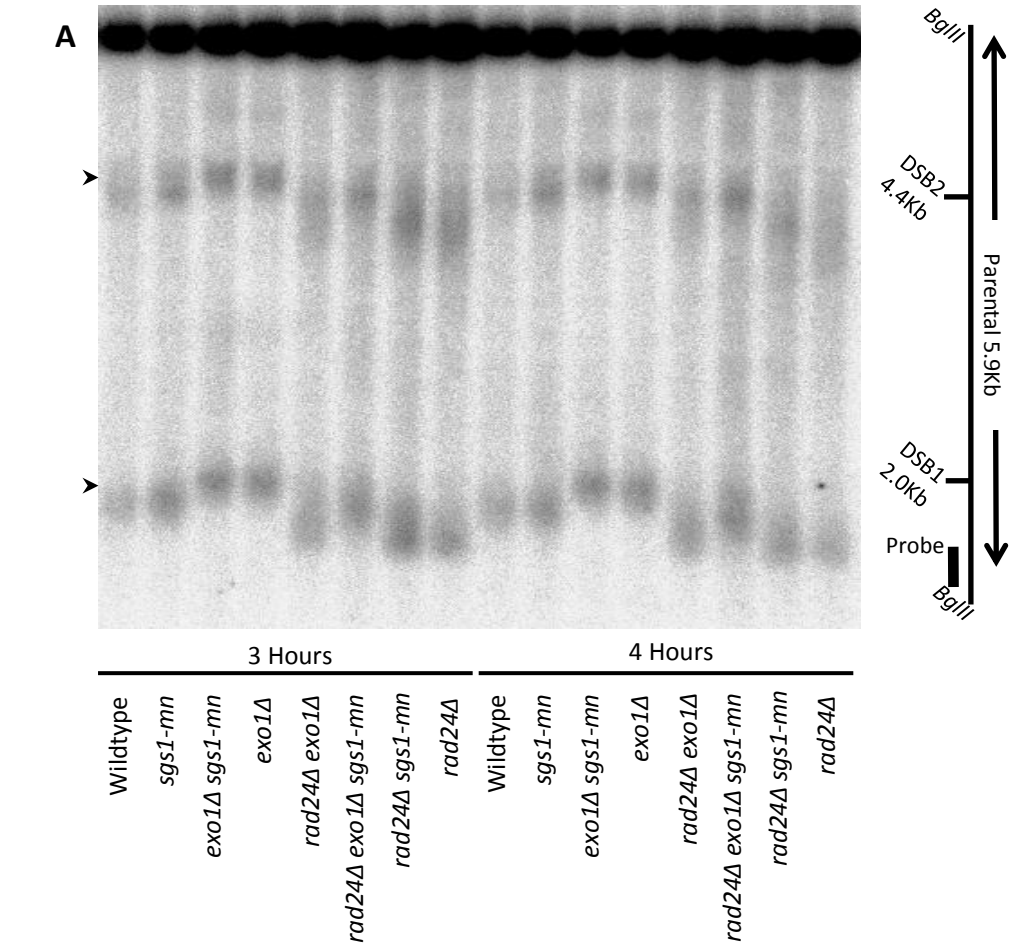
A
BglII
DSB2
4.4Kb
Parental 5.9Kb
DSB1
2.0Kb
Probe
BglII
3 Hours
4 Hours
Wildtype
sgs1-mn
exo1Δ sgs1-mn
exo1Δ
rad24Δ exo1Δ
rad24Δ exo1Δ sgs1-mn
rad24Δ sgs1-mn
rad24Δ
Wildtype
sgs1-mn
exo1Δ sgs1-mn
exo1Δ
rad24Δ exo1Δ
rad24Δ exo1Δ sgs1-mn
rad24Δ sgs1-mn
rad24Δ

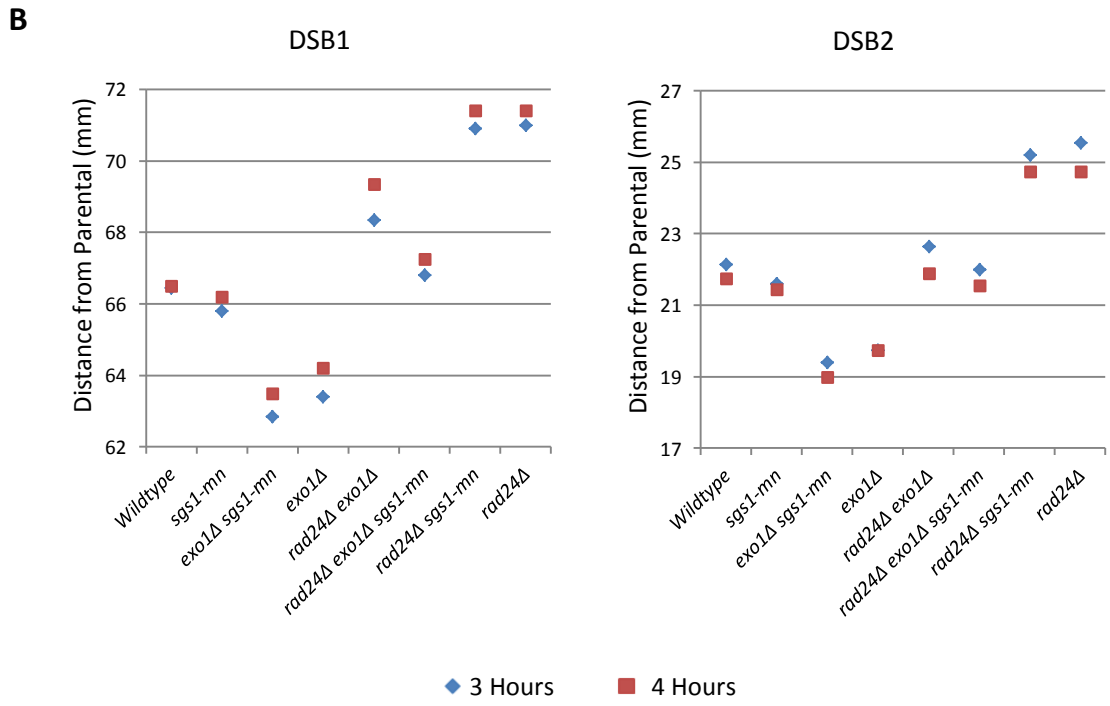
B
DSB1
DSB2
Distance from Parental (mm)
72
70
68
66
64
62
27
25
23
21
19
17
Wildtype
sgs1-mn
exo1Δ sgs1-mn
exo1Δ
rad24Δ exo1Δ
rad24Δ exo1Δ sgs1-mn
rad24Δ sgs1-mn
rad24Δ
3 Hours
4 Hours

Figure 7.4: Resection profile of wildtype, resection defective and checkpoint defective mutants. A) Genomic DNA from meiotic time courses were digested and run on a 0.7% 1xTAE agarose gel for 20 hours at 60 volts. The gel was transferred to nylon membrane under denaturing conditions and hybridised with a radioactive probe for the *HIS4::LEU2* locus. The membrane was exposed to a phosphor screen and image taken using a Fuji phosphor scanner. DSBs marked with arrowhead (➤). **B)** Image Gauge was used to analyse each lane and record the distance between the mode of the parental signal and the mode of each DSB with the difference being plotted and displayed.

7.5: Discussion

After the formation of meiotic DSBs and processing of Spo11, DSBs are resected to form 3' ssDNA tails (Sun, Treco et al. 1989). In investigating proteins responsible for resecting meiotic DSBs, different observations have been made compared to DSBs formed in mitosis. Current published observations suggest that Exo1 functions to resect meiotic DSBs and Sgs1 does not play a role (Zakharyevich, Ma et al. 2010). By contrast, mitotic observations suggest that Mre11/Sae, Exo1 and Sgs1 function to resect DSBs (Mimitou and Symington 2008). By separating DNA molecules according to size and then probing for the *HIS4::LEU2* locus, DSBs were observed in positions relative to the amount of resection that had taken place. Using this assay Exo1 and Sgs1 mutants were tested to determine the amount of resection compared with wildtype and each other.

Initial investigations focused on the role of Exo1 and Sgs1 on meiotic DSB resection. Observations indicated that removal of Exo1 causes a reduction in distance migrated and therefore a reduction in resection, This is consistent with published observations (Zakharyevich, Ma et al. 2010) that Exo1 is responsible for a large amount of resection. However, in the absence of Exo1, removal of Sgs1 causes a further reduction in DSB migration at DSB2. This suggests that Sgs1 functions to resect specific DSBs in the absence of Exo1. Published interpretations of Sgs1 function in the *exo1Δ* background are based on analysis at DSB1 (Zakharyevich, Ma et al. 2010). This may be why Sgs1 has not previously been identified as resecting DSBs in the absence of Exo1, as observed in these experiments. These observations highlight the possibility that the machinery used to resect each DSB is not the same. This could be due to factors such as localisation of different accessory proteins, inhibition of resection mechanisms at certain regions or local chromatin structure for example.

Exo1 phosphorylation by checkpoint components leading to its inhibition was identified in work on telomeres (Morin, Ngo et al. 2008). As Mec1 checkpoint defective strains have hyper-resected meiotic DSBs, I hypothesised that the same mechanism of Exo1 control existed at meiotic DSBs. To test if the hyper-resection is Exo1 dependent, DSB migration in *rad24Δ exo1Δ spo11-HA* was compared with *rad24Δ spo11-HA* to determining the amount of resection.

A reduction in the migration of DSB1 was observed in the *rad24Δ exo1Δ spo11-HA* compared with *rad24Δ spo11-HA* indicating a reduction in resection. As the *exo1Δ* mutation caused both DSBs to migrate closer than wildtype, it would therefore be expected that the *rad24Δ exo1Δ spo11-HA* would migrate closer than *spo11-HA*. However, DSB1 in *rad24Δ exo1Δ spo11-HA* still migrated further than *spo11-HA* and *rad24Δ spo11-HA*. In addition DSB2 in *rad24Δ exo1Δ spo11-HA* did not have a reduced migration compared with *rad24Δ spo11-HA*. These observations suggest that additional nucleases other than Exo1 function to resect DSBs in the absence of Rad24.

Previous observations had implicated Sgs1 in resecting DSBs in the absence of Exo1 (and specifically at DSB2) leading to the hypothesis that Sgs1 is the other nuclease functioning in the *rad24Δ* background. The similar DSB migration observed in the *rad24Δ exo1Δ spo11-HA* compared with *rad24Δ spo11-HA* at DSB2 was no longer observed in the *rad24Δ exo1Δ* compared with *rad24Δ* (figure 7.2 and figure 7.3). This difference may be due to the decrease in DSB levels observed in the *spo11-HA* background leading to increased abundance or action of the nuclease. In the *rad24Δ* background DSB migration decreased by removing Sgs1, further decreased by removal of Exo1 and decreased the most by removal of both (figure 7.3). This suggested that Exo1 and Sgs1 both function to resect meiotic DSBs in the absence of *rad24Δ*. However because the DSBs in *rad24Δ exo1Δ sgs1-mn* still migrate further than wildtype and

exo1Δ this suggests that another, currently unknown nuclease functions to resect meiotic DSBs in the absence of Rad24.

All of these observations feed into a model of recombination control (figure 7.5). In wildtype conditions, DSBs are resected by Exo1. Once resection has reached a certain stage, Rad24 inhibits Exo1. Sgs1 is inhibited by Exo1 but because of the decrease in resection observed in the *rad24Δ sgs1-mn*, it suggests that Sgs1 inhibition is also by Rad24. As Sgs1 functions in the absence of Exo1 it suggests that the inhibition requires both Exo1 and Rad24. Sgs1 action in the absence of Exo1 is only observed at DSB2, therefore suggesting that local DSB environmental factors inhibit resection by Sgs1.

The amount of resection in the *rad24Δ exo1Δ sgs1-mn* suggested another nuclease functions to resect DSBs in the *rad24Δ* background. Mre11 is one candidate for the remaining resection. Mre11 is required for break formation (Ajimura, Leem et al. 1993), removal of Spo11 (Neale, Pan et al. 2005) and has 3'-5' exonuclease function (Paull and Gellert 1998; Garcia, Phelps et al. 2011). Because of Mre11's role in DSB formation, deletion mutations are unable to create DSBs therefore preventing investigating its role in DSB resection. In addition, nuclease mutants are not able to be used as, although DSBs would form, processing would not occur and therefore DSBs would not be resected. One option is using the VDE system. The VDE system, when both the nuclease and the cut site are present, creates a meiotic DSB from forming independent of Spo11 (Bremer, Gimble et al. 1992; Gimble and Thorner 1992). This system allows mutants that would normally prevent DSBs from forming (such as the *mre11Δ*) or being processed (such as the *mre11-H125N* or *sae2Δ*) to be measured for the amount of resection that has taken place.

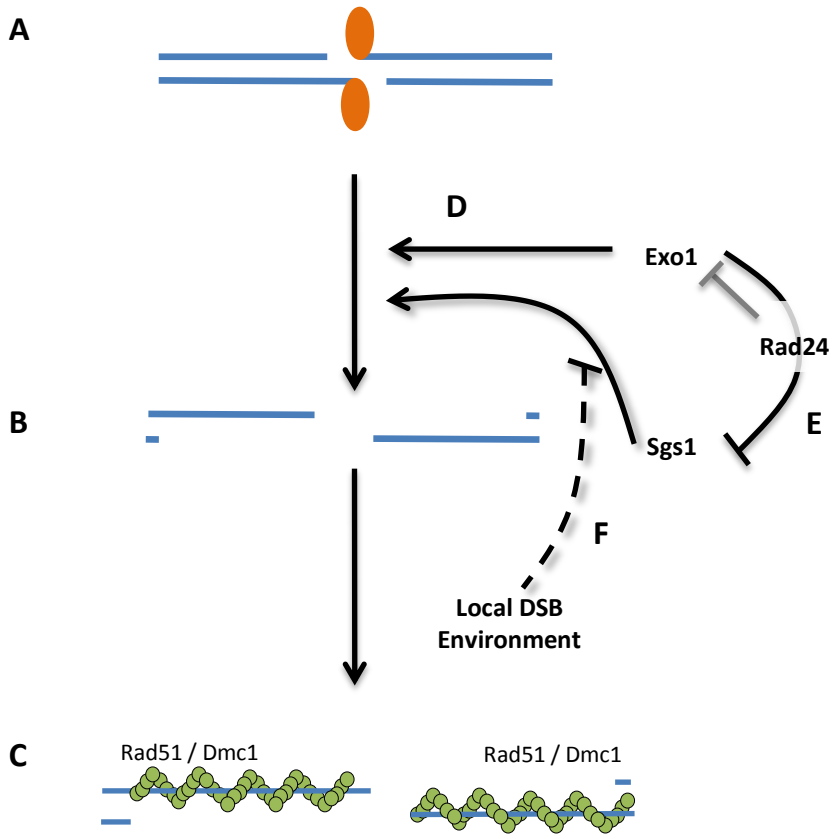

Figure 7.5: Model for resection control at meiotic DSBs. (A) DSBs formed by Spo11 and its accessory proteins. Following Spo11 processing by endonucleolytic cleavage, DSB ends undergo resection to form single stranded DNA tails **(B)** which are coated with recombinase proteins Rad51 and Dmc1 **(C). D)** Exo1 resects meiotic DSBs to a certain extent and is then inhibited by Rad24 (grey line). Sgs1 is inhibited by the presence of Exo1 by the checkpoint (Rad24). When either Exo1 or Rad24 are absent, Sgs1 can function **(E)**. However, local DSB environment inhibits Sgs1 resection at some DSB sites (dashed line) **(F)**.

Here I have shown that control of resection at meiotic DSBs is altered in situations where the Mec1 checkpoint is not functional. Unpublished work from the Aragon lab has suggested that the checkpoint functions to stabilise cohesin which forms a barrier to resection. Specifically it has been proposed that in the absence of the checkpoint, cohesin is not stabilised and resection can occur further from the DSB. Redistribution of cohesin requires cleavage of the Rec8 subunit. Therefore, one way to test if redistribution of cohesin allows hyper-resection would be to make a non-cleavable form of Rec8. This would cause Rec8 to be stabilised and, if the hypothesis is true, prevent DSBs in the *rad24Δ* background from being hyper-resected, thereby removing the need for checkpoint stabilisation. If a return to wildtype levels of resection was observed it would indicate that control of resection is by means of the cohesin barrier and not a directly regulated function of resection machinery.

CHAPTER 8:

Discussion

Chapter 8: Discussion

8.1: Using Spo11-oligonucleotides provides insight into DSB formation and Spo11 processing.

In the process of creating meiotic DSBs, Spo11 becomes covalently attached to the end (Keeney and Kleckner 1995; Bergerat, de Massy et al. 1997; Keeney, Giroux et al. 1997). In order to resect the DSB and perform strand exchange events which can lead to crossovers, Spo11 must first be processed. The endonucleolytic cleavage that liberates Spo11, releases the protein with a short oligonucleotide attachment, thereby creating Spo11-oligonucleotides (Neale, Pan et al. 2005). For every Spo11 meiotic DSB that is created, two Spo11-oligonucleotides are formed. The detection of the Spo11-oligonucleotides therefore produces a signal proportional to the amount of DSBs that are formed.

Previous identification of a protein involved in meiotic DSB formation was through use of the *spo13* and *spo13 rad52* mutants which, if meiotic DSB formation did not occur, would cause increased spore viability (Game, Zamb et al. 1980; Malone and Esposito 1981; Menees and Roeder 1989; Malone, Bullard et al. 1991; Ivanov, Korolev et al. 1992; Ajimura, Leem et al. 1993). Mutants were also identified by a reduction in recombination between genetic markers or by a lack of DSB signal detected at recombination hotspots (Ivanov, Korolev et al. 1992). The detection of Spo11-oligonucleotides is a novel, highly sensitive assay allowing DSB formation and initial processing to be measured. Here I have provided evidence that the *rec102Δ*, *rec104Δ*, *rec114Δ* and *mei4Δ* mutants did not produce 0.5% of wild type Spo11-oligonucleotide signal or above (figure 3.1.1).

The processing event of Spo11 requires Sae2 activity (Neale, Pan et al. 2005). Sae2 activity is dependent on phosphorylation of CDK, Mec1 and Tel1, with phosphomutants of the CDK site

or Mec1 and Tel1 mutants producing unprocessed DSBs (Cartagena-Lirola, Guerini et al. 2006; Terasawa, Ogawa et al. 2008; Manfrini, Guerini et al. 2010). It was therefore hypothesised that the formation of Spo11-oligonucleotides was dependent upon the activity of Mec1 and Tel1. Removing Mec1 in the *spo11-HA* background (allowing Spo11-oligonucleotide levels to be measured) caused a reduction in DSB and Spo11-oligonucleotide signal (figure 3.3.1 and 3.3.2). In contrast, Tel1 removal caused an increase in both DSB and Spo11-oligonucleotide signal (figure 3.3.1 and 3.3.2). In the double mutant, DSB signal was reduced but a bigger reduction in Spo11-oligonucleotide signal was observed (figure 3.3.1 and 3.3.2). Here I have provided evidence that, due to the reduction in Spo11-oligonucleotide signal, the majority of Spo11 processing is initiated by Mec1 and Tel1. However, the unexpected reduction in DSB signal in the *mec1-mn spo11-HA, rad24Δ tel1Δ spo11-HA* and *mec1-mn tel1Δ spo11-HA* backgrounds highlighted that there were problems with DSB signal detection or formation.

In investigating the Spo11-oligonucleotide signal, it was observed that the formation and degradation of the protein-DNA complex had similar kinetics to the formation and repair of DSBs (Neale, Pan et al. 2005). As Spo11-oligonucleotides are formed as a process of DSB processing, and the initial detection of a DSB molecule is in a resected (and therefore processed) state (Sun, Treco et al. 1989) it is expected that the formation of both DSB and Spo11-oligonucleotide would be matched. However, the similar degradation of both DSB and Spo11-oligonucleotide signal suggested that there may be a mechanistic link between these two processes. To test this hypothesis mutants in *exo1Δ* and *dmc1Δ*, which causes a delay in DSB repair, were used to determine if there was also an effect on Spo11-oligonucleotides levels. In delaying repair, Spo11-oligonucleotide signal was increased, suggesting an increase in the lifespan in the complex (due to no more additional DSBs thought to be formed) and supporting the idea of a mechanistic link (figures 3.2.2 and 3.2.5). However, the DSB repair mutants also caused a prolonged activity of the Mec1 meiotic recombination checkpoint, and

therefore removal of the Mec1 checkpoint may see a return of Spo11-oligonucleotide signal. Removing *Rad24* in the *dmc1Δ spo11-HA* background had a decrease in Spo11-oligonucleotide signal but also an unexpected affect; a significant reduction in DSB levels (figure 3.2.8).

8.2: Investigating reduction in DSB levels uncovered a DSB feedback mechanism.

Experiments to determine why there was a reduction in DSBs in the *rad24Δ dmc1Δ spo11-HA* first focussed on investigating which backgrounds the DSB reduction was observed in (figure 4.1, 4.2, 4.4 and 4.7). In mutants defective in components of the Mec1 meiotic recombination checkpoint in addition to the *spo11-HA* had low levels of DSB signal. The low levels of DSB signal was also observed at the *ARE1* hotspot as well as the *HIS4::LEU2* locus (figure 4.3). Because of the function that the meiotic recombination checkpoint has in enforcing inter-homologue repair, it was hypothesised that the reduction in DSB signal could be due to Rad51 dependent inter-sister repair. Removal of Rad51 failed to cause a return to expected DSB levels, ruling out this hypothesis (figure 4.5). Using the *sae2Δ* mutation, DSB levels were measured in combinations of the Mec1 checkpoint mutants, the *spo11-HA* tagged strains and in both (figure 4.6). DSB levels were decreased in the *spo11-HA* strain, with no effect observed in the absence of the Mec1 checkpoint. The difference observed between otherwise wildtype or *dmc1Δ* and the *sae2Δ* backgrounds identified that the *spo11-HA* mutation has a decrease in DSB levels in the *sae2Δ* background that is no longer present in wildtype or *dmc1Δ*. Removal of the Mec1 checkpoint caused a decrease in DSB signal in the *spo11-HA* background in either otherwise wildtype or *dmc1Δ* conditions, suggesting that the Mec1 checkpoint normally functions as a DSB feedback mechanism to compensate for a decrease in DSBs (figure 4.12). In addition to the reduction in DSB signal observed in the Mec1 checkpoint defective *spo11-HA* mutant, spore viability was also decreased. The slow progression through meiosis observed in the *rad24Δ* mutant was also absent in the *rad24Δ spo11-HA* background.

The use of Spo11 mutant backgrounds that cause a reduction in DSB levels aimed to test the DSB feedback mechanism under different conditions. However, the assay used to detect DSB levels was not sensitive enough to support the DSB feedback mechanism (figure 5.1). The DSB feedback mechanism was hypothesised to not be functioning in the *sae2Δ spo11-HA* background, therefore leading to a reduction in DSB levels (figure 4.12). It was proposed that stimulation of the Mec1 checkpoint by addition of a DNA damaging agent in this background would therefore cause an increase in DSB levels. In contrast to what was expected however, the addition of DNA damaging agent caused a reduction in DSB levels (figure 5.2). One hypothesis to explain this reduction was that an inhibitor of DSB formation was functioning.

Recent observations in mouse (Lange, Pan et al. 2011), fruit fly (Joyce, Pedersen et al. 2011) and budding yeast (Zhang, Kim et al. 2011) suggested that one mechanism of meiotic DSB inhibition is Tel1. As Tel1 is stimulated by unprocessed DSBs (Fukunaga, Kwon et al. 2011), which are abundant in the *sae2Δ* background, it was hypothesised that Tel1 is the inhibition mechanism. Observations from the *sae2Δ* background supported its role as an inhibitor, with removal causing an increase in DSB levels (figure 6.1). However, in the *spo11-HA* and *dmc1Δ spo11-HA* backgrounds, DSB levels were lower in the absence of Tel1 (figure 6.2). This therefore suggests that Tel1 functions as an inhibitor of DSB formation at the *sae2Δ* block, but as a promoter of DSB formation in the *spo11-HA* background.

Observations from the *rad24Δ tel1Δ* mutants provided further insight into the requirement of both to process DSBs, but also to limit DSB levels in backgrounds where Spo11 is wildtype (figure 6.3). However, an almost complete loss of DSB signal in backgrounds where both Rad24 and Tel1 are removed and the *spo11-HA* tag is present highlighted the requirement of Rad24 and Tel1 to stimulate DSB formation in backgrounds where Spo11 is not fully functional.

8.3: Resection of meiotic DSBs is performed by Exo1, Sgs1 and another unidentified nuclease.

The first appearance of a meiotic DSB has 3' ssDNA tails due to the action of resection (Sun, Treco et al. 1989). As the migration of the DSB does not change, it suggests that the amount of resection that occurs is controlled. Observations from telomeres suggest that the Exo1 nuclease is controlled by phosphorylation of checkpoint proteins (Morin, Ngo et al. 2008). As Exo1 has been identified as the main nuclease that functions through meiosis (Zakharyevich, Ma et al. 2010), and hyper-resected DSBs observed in Mec1 checkpoint defective strains (Grushcow, Holzen et al. 1999; Shinohara, Sakai et al. 2003), it was hypothesised that a similar controlling mechanism existed at meiotic DSBs. Here I observed two DSB sites (as opposed to one previously observed (Zakharyevich, Ma et al. 2010)) and suggested that another nuclease mechanism, Sgs1, functions at particular sites in the absence of Exo1 (figure 7.1).

In Mec1 checkpoint defective strains it was observed that removal of Exo1 caused a reduction in migration, therefore a reduction in resection, but DSBs were still resected further than expected (figure 7.2). Removal of Exo1 and Sgs1 caused a further decrease in migration but still further than an *exo1Δ* mutant (figure 7.3). This observation suggests that another nuclease functions in the absence of both Exo1 and Sgs1 (figure 7.4). As Mre11 has both exonuclease and endonuclease action (Paull and Gellert 1998; Garcia, Phelps et al. 2011), in addition to its requirement in both DSB formation and processing (Neale, Pan et al. 2005), it is a likely candidate.

8.4: Future outlook

Here I have provided evidence that detection of Spo11-oligonuclotides allows for investigation of proteins required for DSB formation. This novel, sensitive assay has reinforced findings for DSB formation mutants, but also allows analysis of mutants that have a decreased DSB formation ability, such as Hop1 and Red1, to more accurately determine DSB levels. The investigation into Spo11-oligonucleotide and DSB signal kinetics identified a situation where decreased DSB levels are lower than expected. Investigating the decreased DSB signal uncovered complex mechanisms that function through checkpoint proteins to both promote and inhibit DSB formation. These "DSB homeostasis" mechanisms functions to ensure that an optimal number of DSBs form to accurately pair and segregate homologous chromosomes.

Within this thesis, observations from *spo11-HA* mutants have enabled a DSB feedback mechanism to be uncovered. This novel hypothesis fits within a model of DSB homeostasis which functions to ensure the optimal level of DSBs. Observations from this thesis have also investigated resection, identifying exonucleases which had previously been ruled out, as having a role at meiotic DSBs, rectifying differences between resection in mitosis and meiosis. The observations made within this thesis provide insight, and complexity, to meiotic recombination.

Appendix: References

Adams, I. R. and J. V. Kilmartin (2000). "Spindle pole body duplication: a model for centrosome duplication?" Trends Cell Biol **10**(8): 329-335.

Ajimura, M., S. H. Leem, et al. (1993). "Identification of new genes required for meiotic recombination in Saccharomyces cerevisiae." Genetics **133**(1): 51-66.

Alani, E., R. Padmore, et al. (1990). "Analysis of wild-type and rad50 mutants of yeast suggests an intimate relationship between meiotic chromosome synapsis and recombination." Cell **61**(3): 419-436.

Allers, T. and M. Lichten (2001). "Differential timing and control of noncrossover and crossover recombination during meiosis." Cell **106**(1): 47-57.

Allshire, R. (2004). "Cell division: guardian spirit blesses meiosis." Nature **427**(6974): 495-497.

Amon, A. (1999). "The spindle checkpoint." Curr Opin Genet Dev **9**(1): 69-75.

Arora, C., K. Kee, et al. (2004). "Antiviral protein Ski8 is a direct partner of Spo11 in meiotic DNA break formation, independent of its cytoplasmic role in RNA metabolism." Mol Cell **13**(4): 549-559.

Ashton, T. M., H. W. Mankouri, et al. (2011). "Pathways for Holliday junction processing during homologous recombination in Saccharomyces cerevisiae." Mol Cell Biol **31**(9): 1921-1933.

Bailis, J. M., A. V. Smith, et al. (2000). "Bypass of a meiotic checkpoint by overproduction of meiotic chromosomal proteins." Mol Cell Biol **20**(13): 4838-4848.

Baroni, E., V. Viscardi, et al. (2004). "The functions of budding yeast Sae2 in the DNA damage response require Mec1- and Tel1-dependent phosphorylation." Mol Cell Biol **24**(10): 4151-4165.

Baudat, F., K. Manova, et al. (2000). "Chromosome synapsis defects and sexually dimorphic meiotic progression in mice lacking Spo11." Mol Cell **6**(5): 989-998.

Baudat, F. and A. Nicolas (1997). "Clustering of meiotic double-strand breaks on yeast chromosome III." Proc Natl Acad Sci U S A **94**(10): 5213-5218.

Bergerat, A., B. de Massy, et al. (1997). "An atypical topoisomerase II from Archaea with implications for meiotic recombination." Nature **386**(6623): 414-417.

Bishop, D. K., D. Park, et al. (1992). "DMC1: a meiosis-specific yeast homolog of E. coli recA required for recombination, synaptonemal complex formation, and cell cycle progression." Cell **69**(3): 439-456.

Bishop, D. K. and D. Zickler (2004). "Early decision; meiotic crossover interference prior to stable strand exchange and synapsis." Cell **117**(1): 9-15.

Blat, Y., R. U. Protacio, et al. (2002). "Physical and functional interactions among basic chromosome organizational features govern early steps of meiotic chiasma formation." Cell **111**(6): 791-802.

Blitzblau, H. G., G. W. Bell, et al. (2007). "Mapping of meiotic single-stranded DNA reveals double-stranded-break hotspots near centromeres and telomeres." Curr Biol **17**(23): 2003-2012.

Borde, V., A. S. Goldman, et al. (2000). "Direct coupling between meiotic DNA replication and recombination initiation." Science **290**(5492): 806-809.

Borner, G. V., N. Kleckner, et al. (2004). "Crossover/noncrossover differentiation, synaptonemal complex formation, and regulatory surveillance at the leptotene/zygotene transition of meiosis." Cell **117**(1): 29-45.

Borts, R. H., M. Lichten, et al. (1986). "Analysis of meiosis-defective mutations in yeast by physical monitoring of recombination." Genetics **113**(3): 551-567.

Bremer, M. C., F. S. Gimble, et al. (1992). "VDE endonuclease cleaves Saccharomyces cerevisiae genomic DNA at a single site: physical mapping of the VMA1 gene." Nucleic Acids Res **20**(20): 5484.

Brunet, S. and M. H. Verlhac (2011). "Positioning to get out of meiosis: the asymmetry of division." Hum Reprod Update **17**(1): 68-75.

Buhler, C., V. Borde, et al. (2007). "Mapping meiotic single-strand DNA reveals a new landscape of DNA double-strand breaks in Saccharomyces cerevisiae." PLoS Biol **5**(12): e324.

Buonomo, S. B., R. K. Clyne, et al. (2000). "Disjunction of homologous chromosomes in meiosis I depends on proteolytic cleavage of the meiotic cohesin Rec8 by separin." Cell **103**(3): 387-398.

Cao, L., E. Alani, et al. (1990). "A pathway for generation and processing of double-strand breaks during meiotic recombination in S. cerevisiae." Cell **61**(6): 1089-1101.

Carballo, J. A., A. L. Johnson, et al. (2008). "Phosphorylation of the axial element protein Hop1 by Mec1/Tel1 ensures meiotic interhomolog recombination." Cell **132**(5): 758-770.

Carpenter, A. T. (1994). "Chiasma function." Cell **77**(7): 957-962.

Cartagena-Lirola, H., I. Guerini, et al. (2008). "Role of the Saccharomyces cerevisiae Rad53 checkpoint kinase in signaling double-strand breaks during the meiotic cell cycle." Mol Cell Biol **28**(14): 4480-4493.

Cartagena-Lirola, H., I. Guerini, et al. (2006). "Budding Yeast Sae2 is an In Vivo Target of the Mec1 and Tel1 Checkpoint Kinases During Meiosis." Cell Cycle **5**(14): 1549-1559.

Cejka, P., J. L. Plank, et al. (2010). "Rmi1 stimulates decatenation of double Holliday junctions during dissolution by Sgs1-Top3." Nat Struct Mol Biol **17**(11): 1377-1382.

Chambers, A., J. S. Tsang, et al. (1989). "Transcriptional control of the Saccharomyces cerevisiae PGK gene by RAP1." Mol Cell Biol **9**(12): 5516-5524.

Chen, Y. K., C. H. Leng, et al. (2004). "Heterodimeric complexes of Hop2 and Mnd1 function with Dmc1 to promote meiotic homolog juxtaposition and strand assimilation." Proc Natl Acad Sci U S A **101**(29): 10572-10577.

Chu, S. and I. Herskowitz (1998). "Gametogenesis in yeast is regulated by a transcriptional cascade dependent on Ndt80." Mol Cell **1**(5): 685-696.

Cimprich, K. A., T. B. Shin, et al. (1996). "cDNA cloning and gene mapping of a candidate human cell cycle checkpoint protein." Proc Natl Acad Sci U S A **93**(7): 2850-2855.

Ciosk, R., W. Zachariae, et al. (1998). "An ESP1/PDS1 complex regulates loss of sister chromatid cohesion at the metaphase to anaphase transition in yeast." Cell **93**(6): 1067-1076.

Clerici, M., D. Mantiero, et al. (2005). "The Saccharomyces cerevisiae Sae2 protein promotes resection and bridging of double strand break ends." J Biol Chem **280**(46): 38631-38638.

Clerici, M., D. Mantiero, et al. (2006). "The Saccharomyces cerevisiae Sae2 protein negatively regulates DNA damage checkpoint signalling." EMBO Rep **7**(2): 212-218.

Clever, B., H. Interthal, et al. (1997). "Recombinational repair in yeast: functional interactions between Rad51 and Rad54 proteins." EMBO J **16**(9): 2535-2544.

Clift, D., F. Bizzari, et al. (2009). "Shugoshin prevents cohesin cleavage by PP2A(Cdc55)-dependent inhibition of separase." Genes Dev **23**(6): 766-780.

Costa, Y., R. Speed, et al. (2005). "Two novel proteins recruited by synaptonemal complex protein 1 (SYCP1) are at the centre of meiosis." J Cell Sci **118**(Pt 12): 2755-2762.

Creighton, H. B. and B. McClintock (1931). "A Correlation of Cytological and Genetical Crossing-Over in Zea Mays." Proc Natl Acad Sci U S A **17**(8): 492-497.

De Muyt, A., D. Vezon, et al. (2007). "AtPRD1 is required for meiotic double strand break formation in Arabidopsis thaliana." EMBO J **26**(18): 4126-4137.

DeCesare, J. M. and D. T. Stuart (2012). "Among B-type cyclins only CLB5 and CLB6 promote premeiotic S phase in Saccharomyces cerevisiae." Genetics **190**(3): 1001-1016.

Dernburg, A. F., K. McDonald, et al. (1998). "Meiotic recombination in C. elegans initiates by a conserved mechanism and is dispensable for homologous chromosome synapsis." Cell **94**(3): 387-398.

Diaz, R. L., A. D. Alcid, et al. (2002). "Identification of residues in yeast Spo11p critical for meiotic DNA double-strand break formation." Mol Cell Biol **22**(4): 1106-1115.

Dirick, L., L. Goetsch, et al. (1998). "Regulation of meiotic S phase by Ime2 and a Clb5,6-associated kinase in Saccharomyces cerevisiae." Science **281**(5384): 1854-1857.

Dresser, M. E., D. J. Ewing, et al. (1997). "DMC1 functions in a Saccharomyces cerevisiae meiotic pathway that is largely independent of the RAD51 pathway." Genetics **147**(2): 533-544.

Engebrecht, J. and G. S. Roeder (1989). "Yeast mer1 mutants display reduced levels of meiotic recombination." Genetics **121**(2): 237-247.

Engebrecht, J. and G. S. Roeder (1990). "MER1, a yeast gene required for chromosome pairing and genetic recombination, is induced in meiosis." Mol Cell Biol **10**(5): 2379-2389.

Engebrecht, J. A., K. Voelkel-Meiman, et al. (1991). "Meiosis-specific RNA splicing in yeast." Cell **66**(6): 1257-1268.

Esposito, M. S. and R. E. Esposito (1969). "The genetic control of sporulation in Saccharomyces. I. The isolation of temperature-sensitive sporulation-deficient mutants." Genetics **61**(1): 79-89.

Ferrari, S. R., J. Grubb, et al. (2009). "The Mei5-Sae3 protein complex mediates Dmc1 activity in Saccharomyces cerevisiae." J Biol Chem **284**(18): 11766-11770.

Fiorentini, P., K. N. Huang, et al. (1997). "Exonuclease I of Saccharomyces cerevisiae functions in mitotic recombination in vivo and in vitro." Mol Cell Biol **17**(5): 2764-2773.

Fogel, S. and R. K. Mortimer (1970). "Fidelity of meiotic gene conversion in yeast." Mol Gen Genet **109**(2): 177-185.

Freese, E. B., M. I. Chu, et al. (1982). "Initiation of yeast sporulation of partial carbon, nitrogen, or phosphate deprivation." J Bacteriol **149**(3): 840-851.

Fukunaga, K., Y. Kwon, et al. (2011). "Activation of protein kinase Tel1 through recognition of protein-bound DNA ends." Mol Cell Biol **31**(10): 1959-1971.

Game, J. C. and R. K. Mortimer (1974). "A genetic study of x-ray sensitive mutants in yeast." Mutat Res **24**(3): 281-292.

Game, J. C., T. J. Zamb, et al. (1980). "The Role of Radiation (rad) Genes in Meiotic Recombination in Yeast." Genetics **94**(1): 51-68.

Garcia, V., S. E. Phelps, et al. (2011). "Bidirectional resection of DNA double-strand breaks by Mre11 and Exo1." Nature **479**(7372): 241-244.

Gerton, J. L., J. DeRisi, et al. (2000). "Global mapping of meiotic recombination hotspots and coldspots in the yeast Saccharomyces cerevisiae." Proc Natl Acad Sci U S A **97**(21): 11383-11390.

Gerton, J. L. and J. L. DeRisi (2002). "Mnd1p: an evolutionarily conserved protein required for meiotic recombination." Proc Natl Acad Sci U S A **99**(10): 6895-6900.

Gimble, F. S. and J. Thorner (1992). "Homing of a DNA endonuclease gene by meiotic gene conversion in Saccharomyces cerevisiae." Nature **357**(6376): 301-306.

Goldman, A. S. and M. Lichten (1996). "The efficiency of meiotic recombination between dispersed sequences in Saccharomyces cerevisiae depends upon their chromosomal location." Genetics **144**(1): 43-55.

Grandin, N. and S. I. Reed (1993). "Differential function and expression of Saccharomyces cerevisiae B-type cyclins in mitosis and meiosis." Mol Cell Biol **13**(4): 2113-2125.

Greenwell, P. W., S. L. Kronmal, et al. (1995). "TEL1, a gene involved in controlling telomere length in S. cerevisiae, is homologous to the human ataxia telangiectasia gene." Cell **82**(5): 823-829.

Gruber, S., C. H. Haering, et al. (2003). "Chromosomal cohesin forms a ring." Cell **112**(6): 765-777.

Grushcow, J. M., T. M. Holzen, et al. (1999). "Saccharomyces cerevisiae checkpoint genes MEC1, RAD17 and RAD24 are required for normal meiotic recombination partner choice." Genetics **153**(2): 607-620.

Guttmann-Raviv, N., S. Martin, et al. (2002). "Ime2, a meiosis-specific kinase in yeast, is required for destabilization of its transcriptional activator, Ime1." Mol Cell Biol **22**(7): 2047-2056.

Hamer, G., K. Gell, et al. (2006). "Characterization of a novel meiosis-specific protein within the central element of the synaptonemal complex." J Cell Sci **119**(Pt 19): 4025-4032.

Harrington, J. J. and M. R. Lieber (1994). "Functional domains within FEN-1 and RAD2 define a family of structure-specific endonucleases: implications for nucleotide excision repair." Genes Dev **8**(11): 1344-1355.

Hassold, T., H. Hall, et al. (2007). "The origin of human aneuploidy: where we have been, where we are going." Hum Mol Genet **16 Spec No. 2**: R203-208.

Hassold, T. and P. Hunt (2001). "To err (meiotically) is human: the genesis of human aneuploidy." Nat Rev Genet **2**(4): 280-291.

Hassold, T. and S. Sherman (2000). "Down syndrome: genetic recombination and the origin of the extra chromosome 21." Clin Genet **57**(2): 95-100.

Hawley, R. S. (2002). "Meiosis: how male flies do meiosis." Curr Biol **12**(19): R660-662.

Hayase, A., M. Takagi, et al. (2004). "A protein complex containing Mei5 and Sae3 promotes the assembly of the meiosis-specific RecA homolog Dmc1." Cell **119**(7): 927-940.

Henderson, K. A., K. Kee, et al. (2006). "Cyclin-dependent kinase directly regulates initiation of meiotic recombination." Cell **125**(7): 1321-1332.

Henderson, K. A. and S. Keeney (2005). "Synaptonemal complex formation: where does it start?" Bioessays **27**(10): 995-998.

Hepworth, S. R., H. Friesen, et al. (1998). "NDT80 and the meiotic recombination checkpoint regulate expression of middle sporulation-specific genes in Saccharomyces cerevisiae." Mol Cell Biol **18**(10): 5750-5761.

Heyer, W. D., K. T. Ehmsen, et al. (2010). "Regulation of homologous recombination in eukaryotes." Annu Rev Genet **44**: 113-139.

Holliday, R. (1964). "A mechanism for gene conversion in fungi." Genetical Research **5**: 282-304.

Hollingsworth, N. M. and B. Byers (1989). "HOP1: a yeast meiotic pairing gene." Genetics **121**(3): 445-462.

Hollingsworth, N. M., L. Goetsch, et al. (1990). "The HOP1 gene encodes a meiosis-specific component of yeast chromosomes." Cell **61**(1): 73-84.

Huertas, P., F. Cortes-Ledesma, et al. (2008). "CDK targets Sae2 to control DNA-end resection and homologous recombination." Nature **455**(7213): 689-692.

Hunt Morgan, T. (1916). A Critique of the Theory of Evolution

Hunter, N. and N. Kleckner (2001). "The single-end invasion: an asymmetric intermediate at the double-strand break to double-holliday junction transition of meiotic recombination." Cell **106**(1): 59-70.

Ip, S. C., U. Rass, et al. (2008). "Identification of Holliday junction resolvases from humans and yeast." Nature **456**(7220): 357-361.

Ishiguro, K. and Y. Watanabe (2007). "Chromosome cohesion in mitosis and meiosis." J Cell Sci **120**(Pt 3): 367-369.

Ivanov, E. L., V. G. Korolev, et al. (1992). "XRS2, a DNA repair gene of Saccharomyces cerevisiae, is needed for meiotic recombination." Genetics **132**(3): 651-664.

Jessop, L., B. Rockmill, et al. (2006). "Meiotic chromosome synapsis-promoting proteins antagonize the anti-crossover activity of sgs1." PLoS Genet **2**(9): e155.

Jiao, K., L. Salem, et al. (2003). "Support for a meiotic recombination initiation complex: interactions among Rec102p, Rec104p, and Spo11p." Mol Cell Biol **23**(16): 5928-5938.

Jolivet, S., D. Vezon, et al. (2006). "Non conservation of the meiotic function of the Ski8/Rec103 homolog in Arabidopsis." Genes Cells **11**(6): 615-622.

Jones, G. H. (1984). "The control of chiasma distribution." Symp Soc Exp Biol **38**: 293-320.

Joyce, E. F., M. Pedersen, et al. (2011). "Drosophila ATM and ATR have distinct activities in the regulation of meiotic DNA damage and repair." J Cell Biol **195**(3): 359-367.

Kato, R. and H. Ogawa (1994). "An essential gene, ESR1, is required for mitotic cell growth, DNA repair and meiotic recombination in Saccharomyces cerevisiae." Nucleic Acids Res **22**(15): 3104-3112.

Kee, K. and S. Keeney (2002). "Functional interactions between SPO11 and REC102 during initiation of meiotic recombination in Saccharomyces cerevisiae." Genetics **160**(1): 111-122.

Keeney, S. (2001). "Mechanism and control of meiotic recombination initiation." Curr Top Dev Biol **52**: 1-53.

Keeney, S., C. N. Giroux, et al. (1997). "Meiosis-specific DNA double-strand breaks are catalyzed by Spo11, a member of a widely conserved protein family." Cell **88**(3): 375-384.

Keeney, S. and N. Kleckner (1995). "Covalent protein-DNA complexes at the 5' strand termini of meiosis-specific double-strand breaks in yeast." Proc Natl Acad Sci U S A **92**(24): 11274-11278.

Keeney, S. and M. J. Neale (2006). "Initiation of meiotic recombination by formation of DNA double-strand breaks: mechanism and regulation." Biochem Soc Trans **34**(Pt 4): 523-525.

King, R. W., R. J. Deshaies, et al. (1996). "How proteolysis drives the cell cycle." Science **274**(5293): 1652-1659.

Klapholz, S. and R. E. Esposito (1980). "Isolation of SPO12-1 and SPO13-1 from a natural variant of yeast that undergoes a single meiotic division." Genetics **96**(3): 567-588.

Klapholz, S. and R. E. Esposito (1980). "Recombination and chromosome segregation during the single division meiosis in SPO12-1 and SPO13-1 diploids." Genetics **96**(3): 589-611.

Klapholz, S., C. S. Waddell, et al. (1985). "The role of the SPO11 gene in meiotic recombination in yeast." Genetics **110**(2): 187-216.

Kleckner, N., D. Zickler, et al. (2004). "A mechanical basis for chromosome function." Proc Natl Acad Sci U S A **101**(34): 12592-12597.

Klein, F., P. Mahr, et al. (1999). "A central role for cohesins in sister chromatid cohesion, formation of axial elements, and recombination during yeast meiosis." Cell **98**(1): 91-103.

Klein, H. L. (1997). "RDH54, a RAD54 homologue in Saccharomyces cerevisiae, is required for mitotic diploid-specific recombination and repair and for meiosis." Genetics **147**(4): 1533-1543.

Kline-Smith, S. L., S. Sandall, et al. (2005). "Kinetochore-spindle microtubule interactions during mitosis." Curr Opin Cell Biol **17**(1): 35-46.

Kondo, T., T. Wakayama, et al. (2001). "Recruitment of Mec1 and Ddc1 checkpoint proteins to double-strand breaks through distinct mechanisms." Science **294**(5543): 867-870.

Krogh, B. O. and L. S. Symington (2004). "Recombination proteins in yeast." Annu Rev Genet **38**: 233-271.

Kumar, R., H. M. Bourbon, et al. (2010). "Functional conservation of Mei4 for meiotic DNA double-strand break formation from yeasts to mice." Genes Dev **24**(12): 1266-1280.

Lange, J., J. Pan, et al. (2011). "ATM controls meiotic double-strand-break formation." Nature **479**(7372): 237-240.

Leach, D. R., R. G. Lloyd, et al. (1992). "The SbcCD protein of Escherichia coli is related to two putative nucleases in the UvrA superfamily of nucleotide-binding proteins." Genetica **87**(2): 95-100.

Lengsfeld, B. M., A. J. Rattray, et al. (2007). "Sae2 is an endonuclease that processes hairpin DNA cooperatively with the Mre11/Rad50/Xrs2 complex." Mol Cell **28**(4): 638-651.

Leu, J. Y., P. R. Chua, et al. (1998). "The meiosis-specific Hop2 protein of S. cerevisiae ensures synapsis between homologous chromosomes." Cell **94**(3): 375-386.

Leu, J. Y. and G. S. Roeder (1999). "The pachytene checkpoint in S. cerevisiae depends on Swe1-mediated phosphorylation of the cyclin-dependent kinase Cdc28." Mol Cell **4**(5): 805-814.

Li, J., G. W. Hooker, et al. (2006). "Saccharomyces cerevisiae Mer2, Mei4 and Rec114 form a complex required for meiotic double-strand break formation." Genetics **173**(4): 1969-1981.

Libby, B. J., L. G. Reinholdt, et al. (2003). "Positional cloning and characterization of Mei1, a vertebrate-specific gene required for normal meiotic chromosome synapsis in mice." Proc Natl Acad Sci U S A **100**(26): 15706-15711.

Lin, Y. and G. R. Smith (1994). "Transient, meiosis-induced expression of the rec6 and rec12 genes of Schizosaccharomyces pombe." Genetics **136**(3): 769-779.

Lindgren, A., D. Bungard, et al. (2000). "The pachytene checkpoint in Saccharomyces cerevisiae requires the Sum1 transcriptional repressor." EMBO J **19**(23): 6489-6497.

Lisby, M., J. H. Barlow, et al. (2004). "Choreography of the DNA damage response: spatiotemporal relationships among checkpoint and repair proteins." Cell **118**(6): 699-713.

Liu, H., J. K. Jang, et al. (2002). "mei-P22 encodes a chromosome-associated protein required for the initiation of meiotic recombination in Drosophila melanogaster." Genetics **162**(1): 245-258.

Liu, J., T. C. Wu, et al. (1995). "The location and structure of double-strand DNA breaks induced during yeast meiosis: evidence for a covalently linked DNA-protein intermediate." EMBO J **14**(18): 4599-4608.

Lo, H. C., R. C. Kunz, et al. (2012). "Cdc7-Dbf4 is a gene-specific regulator of meiotic transcription in yeast." Mol Cell Biol **32**(2): 541-557.

Lydall, D., Y. Nikolsky, et al. (1996). "A meiotic recombination checkpoint controlled by mitotic checkpoint genes." Nature **383**(6603): 840-843.

Majka, J. and P. M. Burgers (2003). "Yeast Rad17/Mec3/Ddc1: a sliding clamp for the DNA damage checkpoint." Proc Natl Acad Sci U S A **100**(5): 2249-2254.

Majka, J. and P. M. Burgers (2004). "The PCNA-RFC families of DNA clamps and clamp loaders." Prog Nucleic Acid Res Mol Biol **78**: 227-260.

Maleki, S., M. J. Neale, et al. (2007). "Interactions between Mei4, Rec114, and other proteins required for meiotic DNA double-strand break formation in Saccharomyces cerevisiae." Chromosoma **116**(5): 471-486.

Malone, R. E., S. Bullard, et al. (1991). "Isolation of mutants defective in early steps of meiotic recombination in the yeast Saccharomyces cerevisiae." Genetics **128**(1): 79-88.

Malone, R. E. and R. E. Esposito (1981). "Recombinationless meiosis in Saccharomyces cerevisiae." Mol Cell Biol **1**(10): 891-901.

Manfrini, N., I. Guerini, et al. (2010). "Processing of meiotic DNA double strand breaks requires cyclin-dependent kinase and multiple nucleases." J Biol Chem **285**(15): 11628-11637.

Mao-Draayer, Y., A. M. Galbraith, et al. (1996). "Analysis of meiotic recombination pathways in the yeast Saccharomyces cerevisiae." Genetics **144**(1): 71-86.

Martini, E., V. Borde, et al. (2011). "Genome-wide analysis of heteroduplex DNA in mismatch repair-deficient yeast cells reveals novel properties of meiotic recombination pathways." PLoS Genet **7**(9): e1002305.

Martini, E., R. L. Diaz, et al. (2006). "Crossover homeostasis in yeast meiosis." Cell **126**(2): 285-295.

May, K. M. and K. G. Hardwick (2006). "The spindle checkpoint." J Cell Sci **119**(Pt 20): 4139-4142.

McKee, A. H. and N. Kleckner (1997). "A general method for identifying recessive diploid-specific mutations in Saccharomyces cerevisiae, its application to the isolation of mutants blocked at intermediate stages of meiotic prophase and characterization of a new gene SAE2." Genetics **146**(3): 797-816.

McKim, K. S. and A. Hayashi-Hagihara (1998). "mei-W68 in Drosophila melanogaster encodes a Spo11 homolog: evidence that the mechanism for initiating meiotic recombination is conserved." Genes Dev **12**(18): 2932-2942.

McMahill, M. S., C. W. Sham, et al. (2007). "Synthesis-dependent strand annealing in meiosis." PLoS Biol **5**(11): e299.

Melo, J. A., J. Cohen, et al. (2001). "Two checkpoint complexes are independently recruited to sites of DNA damage in vivo." Genes Dev **15**(21): 2809-2821.

Menees, T. M. and G. S. Roeder (1989). "MEI4, a yeast gene required for meiotic recombination." Genetics **123**(4): 675-682.

Meselson, M. S. and C. M. Radding (1975). "A general model for genetic recombination." Proc Natl Acad Sci U S A **72**(1): 358-361.

Meuwissen, R. L., H. H. Offenberg, et al. (1992). "A coiled-coil related protein specific for synapsed regions of meiotic prophase chromosomes." EMBO J **11**(13): 5091-5100.

Milman, N., E. Higuchi, et al. (2009). "Meiotic DNA double-strand break repair requires two nucleases, MRN and Ctp1, to produce a single size class of Rec12 (Spo11)-oligonucleotide complexes." Mol Cell Biol **29**(22): 5998-6005.

Mimitou, E. P. and L. S. Symington (2008). "Sae2, Exo1 and Sgs1 collaborate in DNA double-strand break processing." Nature **455**(7214): 770-774.

Mimitou, E. P. and L. S. Symington (2009). "DNA end resection: many nucleases make light work." DNA Repair (Amst) **8**(9): 983-995.

Mitchell, A. P. (1994). "Control of meiotic gene expression in Saccharomyces cerevisiae." Microbiol Rev **58**(1): 56-70.

Moens, P. B., N. K. Kolas, et al. (2002). "The time course and chromosomal localization of recombination-related proteins at meiosis in the mouse are compatible with models that can resolve the early DNA-DNA interactions without reciprocal recombination." J Cell Sci **115**(Pt 8): 1611-1622.

Molnar, M., S. Parisi, et al. (2001). "Characterization of rec7, an early meiotic recombination gene in Schizosaccharomyces pombe." Genetics **157**(2): 519-532.

Moreau, S., J. R. Ferguson, et al. (1999). "The nuclease activity of Mre11 is required for meiosis but not for mating type switching, end joining, or telomere maintenance." Mol Cell Biol **19**(1): 556-566.

Morin, I., H. P. Ngo, et al. (2008). "Checkpoint-dependent phosphorylation of Exo1 modulates the DNA damage response." EMBO J **27**(18): 2400-2410.

Murakami, H. and S. Keeney (2008). "Regulating the formation of DNA double-strand breaks in meiosis." Genes Dev **22**(3): 286-292.

Nagaoka, S. I., T. J. Hassold, et al. (2012). "Human aneuploidy: mechanisms and new insights into an age-old problem." Nat Rev Genet **13**(7): 493-504.

Nakada, D., K. Matsumoto, et al. (2003). "ATM-related Tel1 associates with double-strand breaks through an Xrs2-dependent mechanism." Genes Dev **17**(16): 1957-1962.

Nakagawa, T. and H. Ogawa (1997). "Involvement of the MRE2 gene of yeast in formation of meiosis-specific double-strand breaks and crossover recombination through RNA splicing." Genes Cells **2**(1): 65-79.

Nasmyth, K. (1996). "At the heart of the budding yeast cell cycle." Trends Genet **12**(10): 405-412.

Nasmyth, K. (2011). "Cohesin: a catenase with separate entry and exit gates?" Nat Cell Biol **13**(10): 1170-1177.

Neale, M. J. and S. Keeney (2006). "Clarifying the mechanics of DNA strand exchange in meiotic recombination." Nature **442**(7099): 153-158.

Neale, M. J. and S. Keeney (2009). "End-labeling and analysis of Spo11-oligonucleotide complexes in Saccharomyces cerevisiae." Methods Mol Biol **557**: 183-195.

Neale, M. J., J. Pan, et al. (2005). "Endonucleolytic processing of covalent protein-linked DNA double-strand breaks." Nature **436**(7053): 1053-1057.

Neale, M. J., M. Ramachandran, et al. (2002). "Wild-type levels of Spo11-induced DSBs are required for normal single-strand resection during meiosis." Mol Cell **9**(4): 835-846.

Nicolas, A., D. Treco, et al. (1989). "An initiation site for meiotic gene conversion in the yeast Saccharomyces cerevisiae." Nature **338**(6210): 35-39.

Niu, H., X. Li, et al. (2007). "Mek1 kinase is regulated to suppress double-strand break repair between sister chromatids during budding yeast meiosis." Mol Cell Biol **27**(15): 5456-5467.

Niu, H., L. Wan, et al. (2005). "Partner choice during meiosis is regulated by Hop1-promoted dimerization of Mek1." Mol Biol Cell **16**(12): 5804-5818.

Niu, H., L. Wan, et al. (2009). "Regulation of meiotic recombination via Mek1-mediated Rad54 phosphorylation." Mol Cell **36**(3): 393-404.

Nugent, C. I., T. R. Hughes, et al. (1996). "Cdc13p: a single-strand telomeric DNA-binding protein with a dual role in yeast telomere maintenance." Science **274**(5285): 249-252.

Offenberg, H. H., J. A. Schalk, et al. (1998). "SCP2: a major protein component of the axial elements of synaptonemal complexes of the rat." Nucleic Acids Res **26**(11): 2572-2579.

Ogawa, H., K. Johzuka, et al. (1995). "Functions of the yeast meiotic recombination genes, MRE11 and MRE2." Adv Biophys **31**: 67-76.

Okada, T. and S. Keeney (2005). "Homologous recombination: needing to have my say." Curr Biol **15**(6): R200-202.

Page, S. L. and R. S. Hawley (2004). "The genetics and molecular biology of the synaptonemal complex." Annu Rev Cell Dev Biol **20**: 525-558.

Pak, J. and J. Segall (2002). "Role of Ndt80, Sum1, and Swe1 as targets of the meiotic recombination checkpoint that control exit from pachytene and spore formation in Saccharomyces cerevisiae." Mol Cell Biol **22**(18): 6430-6440.

Pan, J. and S. Keeney (2007). "Molecular cartography: mapping the landscape of meiotic recombination." PLoS Biol **5**(12): e333.

Pan, J., M. Sasaki, et al. (2011). "A hierarchical combination of factors shapes the genome-wide topography of yeast meiotic recombination initiation." Cell **144**(5): 719-731.

Paques, F. and J. E. Haber (1999). "Multiple pathways of recombination induced by double-strand breaks in Saccharomyces cerevisiae." Microbiol Mol Biol Rev **63**(2): 349-404.

Paull, T. T. and M. Gellert (1998). "The 3' to 5' exonuclease activity of Mre 11 facilitates repair of DNA double-strand breaks." Mol Cell **1**(7): 969-979.

Pereira, G. and E. Schiebel (1997). "Centrosome-microtubule nucleation." J Cell Sci **110 (Pt 3)**: 295-300.

Perez-Hidalgo, L., S. Moreno, et al. (2003). "Regulation of meiotic progression by the meiosis-specific checkpoint kinase Mek1 in fission yeast." J Cell Sci **116**(Pt 2): 259-271.

Petrini, J. H. (1999). "The mammalian Mre11-Rad50-nbs1 protein complex: integration of functions in the cellular DNA-damage response." Am J Hum Genet **64**(5): 1264-1269.

Petronczki, M., M. F. Siomos, et al. (2003). "Un menage a quatre: the molecular biology of chromosome segregation in meiosis." Cell **112**(4): 423-440.

Petukhova, G., S. Stratton, et al. (1998). "Catalysis of homologous DNA pairing by yeast Rad51 and Rad54 proteins." Nature **393**(6680): 91-94.

Pezza, R. J., R. D. Camerini-Otero, et al. (2010). "Hop2-Mnd1 condenses DNA to stimulate the synapsis phase of DNA strand exchange." Biophys J **99**(11): 3763-3772.

Pinsky, B. A. and S. Biggins (2005). "The spindle checkpoint: tension versus attachment." Trends Cell Biol **15**(9): 486-493.

Prinz, S., A. Amon, et al. (1997). "Isolation of COM1, a new gene required to complete meiotic double-strand break-induced recombination in Saccharomyces cerevisiae." Genetics **146**(3): 781-795.

Rockmill, B. and G. S. Roeder (1988). "RED1: a yeast gene required for the segregation of chromosomes during the reductional division of meiosis." Proc Natl Acad Sci U S A **85**(16): 6057-6061.

Roeder, G. S. (1997). "Meiotic chromosomes: it takes two to tango." Genes Dev **11**(20): 2600-2621.

Romanienko, P. J. and R. D. Camerini-Otero (1999). "Cloning, characterization, and localization of mouse and human SPO11." Genomics **61**(2): 156-169.

Romanienko, P. J. and R. D. Camerini-Otero (2000). "The mouse Spo11 gene is required for meiotic chromosome synapsis." Mol Cell **6**(5): 975-987.

Sartori, A. A., C. Lukas, et al. (2007). "Human CtIP promotes DNA end resection." Nature **450**(7169): 509-514.

Sasanuma, H., K. Hirota, et al. (2008). "Cdc7-dependent phosphorylation of Mer2 facilitates initiation of yeast meiotic recombination." Genes Dev **22**(3): 398-410.

Schramm, S., J. Fraune, et al. (2011). "A novel mouse synaptonemal complex protein is essential for loading of central element proteins, recombination, and fertility." PLoS Genet **7**(5): e1002088.

Schwacha, A. and N. Kleckner (1995). "Identification of double Holliday junctions as intermediates in meiotic recombination." Cell **83**(5): 783-791.

Shannon, M., L. Richardson, et al. (1999). "Differential gene expression of mammalian SPO11/TOP6A homologs during meiosis." FEBS Lett **462**(3): 329-334.

Sheridan, S. D., X. Yu, et al. (2008). "A comparative analysis of Dmc1 and Rad51 nucleoprotein filaments." Nucleic Acids Res **36**(12): 4057-4066.

Shingu, Y., T. Tokai, et al. (2012). "The double-stranded break-forming activity of plant SPO11s and a novel rice SPO11 revealed by a Drosophila bioassay." BMC Mol Biol **13**: 1.

Shinohara, A., H. Ogawa, et al. (1992). "Rad51 protein involved in repair and recombination in S. cerevisiae is a RecA-like protein." Cell **69**(3): 457-470.

Shinohara, M., K. Sakai, et al. (2003). "The mitotic DNA damage checkpoint proteins Rad17 and Rad24 are required for repair of double-strand breaks during meiosis in yeast." Genetics **164**(3): 855-865.

Shinohara, M., K. Sakai, et al. (2003). "Crossover interference in Saccharomyces cerevisiae requires a TID1/RDH54- and DMC1-dependent pathway." Genetics **163**(4): 1273-1286.

Shinohara, M., E. Shita-Yamaguchi, et al. (1997). "Characterization of the roles of the Saccharomyces cerevisiae RAD54 gene and a homologue of RAD54, RDH54/TID1, in mitosis and meiosis." Genetics **147**(4): 1545-1556.

Shonn, M. A., R. McCarroll, et al. (2000). "Requirement of the spindle checkpoint for proper chromosome segregation in budding yeast meiosis." Science **289**(5477): 300-303.

Shonn, M. A., R. McCarroll, et al. (2002). "Spo13 protects meiotic cohesin at centromeres in meiosis I." Genes Dev **16**(13): 1659-1671.

Shubassi, G., N. Luca, et al. (2003). "Activity of phosphoforms and truncated versions of Ndt80, a checkpoint-regulated sporulation-specific transcription factor of Saccharomyces cerevisiae." Mol Genet Genomics **270**(4): 324-336.

Simchen, G., D. Idar, et al. (1976). "Recombination and hydroxyurea inhibition of DNA synthesis in yeast meiosis." Mol Gen Genet **144**(1): 21-27.

Smith, K. N., A. Penkner, et al. (2001). "B-type cyclins CLB5 and CLB6 control the initiation of recombination and synaptonemal complex formation in yeast meiosis." Curr Biol **11**(2): 88-97.

Stahl, F. W. (1994). "The Holliday junction on its thirtieth anniversary." Genetics **138**(2): 241-246.

Stewart, G. S., R. S. Maser, et al. (1999). "The DNA double-strand break repair gene hMRE11 is mutated in individuals with an ataxia-telangiectasia-like disorder." Cell **99**(6): 577-587.

Stoop-Myer, C. and A. Amon (1999). "Meiosis: Rec8 is the reason for cohesion." Nat Cell Biol **1**(5): E125-127.

Stracker, T. H. and J. H. Petrini (2011). "The MRE11 complex: starting from the ends." Nat Rev Mol Cell Biol **12**(2): 90-103.

Stuart, D. and C. Wittenberg (1998). "CLB5 and CLB6 are required for premeiotic DNA replication and activation of the meiotic S/M checkpoint." Genes Dev **12**(17): 2698-2710.

Sun, H., D. Treco, et al. (1989). "Double-strand breaks at an initiation site for meiotic gene conversion." Nature **338**(6210): 87-90.

Sung, P. (1994). "Catalysis of ATP-dependent homologous DNA pairing and strand exchange by yeast RAD51 protein." Science **265**(5176): 1241-1243.

Sung, P., L. Krejci, et al. (2003). "Rad51 recombinase and recombination mediators." J Biol Chem **278**(44): 42729-42732.

Sym, M., J. A. Engebrecht, et al. (1993). "ZIP1 is a synaptonemal complex protein required for meiotic chromosome synapsis." Cell **72**(3): 365-378.

Symington, L. S. and W. K. Holloman (2008). "Resolving resolvases: the final act?" Mol Cell **32**(5): 603-604.

Szankasi, P. and G. R. Smith (1992). "A DNA exonuclease induced during meiosis of Schizosaccharomyces pombe." J Biol Chem **267**(5): 3014-3023.

Szostak, J. W., T. L. Orr-Weaver, et al. (1983). "The double-strand-break repair model for recombination." Cell **33**(1): 25-35.

Terasawa, M., T. Ogawa, et al. (2008). "Sae2p phosphorylation is crucial for cooperation with Mre11p for resection of DNA double-strand break ends during meiotic recombination in Saccharomyces cerevisiae." Genes Genet Syst **83**(3): 209-217.

Thomas, N. S. and T. J. Hassold (2003). "Aberrant recombination and the origin of Klinefelter syndrome." Hum Reprod Update **9**(4): 309-317.

Tishkoff, D. X., A. L. Boerger, et al. (1997). "Identification and characterization of Saccharomyces cerevisiae EXO1, a gene encoding an exonuclease that interacts with MSH2." Proc Natl Acad Sci U S A **94**(14): 7487-7492.

Traven, A. and J. Heierhorst (2005). "SQ/TQ cluster domains: concentrated ATM/ATR kinase phosphorylation site regions in DNA-damage-response proteins." Bioessays **27**(4): 397-407.

Tsai, J. H. and B. D. McKee (2011). "Homologous pairing and the role of pairing centers in meiosis." J Cell Sci **124**(Pt 12): 1955-1963.

Tsubouchi, H. and H. Ogawa (2000). "Exo1 roles for repair of DNA double-strand breaks and meiotic crossing over in Saccharomyces cerevisiae." Mol Biol Cell **11**(7): 2221-2233.

Tsubouchi, H. and G. S. Roeder (2006). "Budding yeast Hed1 down-regulates the mitotic recombination machinery when meiotic recombination is impaired." Genes Dev **20**(13): 1766-1775.

Tung, K. S., E. J. Hong, et al. (2000). "The pachytene checkpoint prevents accumulation and phosphorylation of the meiosis-specific transcription factor Ndt80." Proc Natl Acad Sci U S A **97**(22): 12187-12192.

Uetz, P., L. Giot, et al. (2000). "A comprehensive analysis of protein-protein interactions in Saccharomyces cerevisiae." Nature **403**(6770): 623-627.

Uhlmann, F., F. Lottspeich, et al. (1999). "Sister-chromatid separation at anaphase onset is promoted by cleavage of the cohesin subunit Scc1." Nature **400**(6739): 37-42.

Usui, T., H. Ogawa, et al. (2001). "A DNA damage response pathway controlled by Tel1 and the Mre11 complex." Mol Cell **7**(6): 1255-1266.

Wan, L., H. Niu, et al. (2008). "Cdc28-Clb5 (CDK-S) and Cdc7-Dbf4 (DDK) collaborate to initiate meiotic recombination in yeast." Genes Dev **22**(3): 386-397.

Wang, J. C. (1996). "DNA topoisomerases." Annu Rev Biochem **65**: 635-692.

Watanabe, Y. and P. Nurse (1999). "Cohesin Rec8 is required for reductional chromosome segregation at meiosis." Nature **400**(6743): 461-464.

Watt, P. M., E. J. Louis, et al. (1995). "Sgs1: a eukaryotic homolog of E. coli RecQ that interacts with topoisomerase II in vivo and is required for faithful chromosome segregation." Cell **81**(2): 253-260.

Williams, R. S., G. Moncalian, et al. (2008). "Mre11 dimers coordinate DNA end bridging and nuclease processing in double-strand-break repair." Cell **135**(1): 97-109.

Winter, E. (2012). "The Sum1/Ndt80 transcriptional switch and commitment to meiosis in Saccharomyces cerevisiae." Microbiol Mol Biol Rev **76**(1): 1-15.

Xu, L., M. Ajimura, et al. (1995). "NDT80, a meiosis-specific gene required for exit from pachytene in Saccharomyces cerevisiae." Mol Cell Biol **15**(12): 6572-6581.

Young, J. A., R. W. Hyppa, et al. (2004). "Conserved and nonconserved proteins for meiotic DNA breakage and repair in yeasts." Genetics **167**(2): 593-605.

Zakharyevich, K., Y. Ma, et al. (2010). "Temporally and biochemically distinct activities of Exo1 during meiosis: double-strand break resection and resolution of double Holliday junctions." Mol Cell **40**(6): 1001-1015.

Zakharyevich, K., S. Tang, et al. (2012). "Delineation of joint molecule resolution pathways in meiosis identifies a crossover-specific resolvase." Cell **149**(2): 334-347.

Zhang, L., K. P. Kim, et al. (2011). "Meiotic double-strand breaks occur once per pair of (sister) chromatids and, via Mec1/ATR and Tel1/ATM, once per quartet of chromatids." Proc Natl Acad Sci U S A **108**(50): 20036-20041.

Zhu, Z., W. H. Chung, et al. (2008). "Sgs1 helicase and two nucleases Dna2 and Exo1 resect DNA double-strand break ends." Cell **134**(6): 981-994.

Zou, L. and S. J. Elledge (2003). "Sensing DNA damage through ATRIP recognition of RPA-ssDNA complexes." Science **300**(5625): 1542-1548.

Publication

LETTER

doi:10.1038/nature10515

Bidirectional resection of DNA double-strand breaks by Mre11 and Exo1

Valerie Garcia[1], Sarah E. L. Phelps[1], Stephen Gray[1] & Matthew J. Neale[1]

Repair of DNA double-strand breaks (DSBs) by homologous recombination requires resection of 5′-termini to generate 3′-single-strand DNA tails[1]. Key components of this reaction are exonuclease 1 and the bifunctional endo/exonuclease, Mre11 (refs 2–4). Mre11 endonuclease activity is critical when DSB termini are blocked by bound protein—such as by the DNA end-joining complex[5], topoisomerases[6] or the meiotic transesterase Spo11 (refs 7–13)—but a specific function for the Mre11 3′–5′ exonuclease activity has remained elusive. Here we use *Saccharomyces cerevisiae* to reveal a role for the Mre11 exonuclease during the resection of Spo11-linked 5′-DNA termini *in vivo*. We show that the residual resection observed in Exo1-mutant cells is dependent on Mre11, and that both exonuclease activities are required for efficient DSB repair. Previous work has indicated that resection traverses unidirectionally[1]. Using a combination of physical assays for 5′-end processing, our results indicate an alternative mechanism involving bidirectional resection. First, Mre11 nicks the strand to be resected up to 300 nucleotides from the 5′-terminus of the DSB—much further away than previously assumed. Second, this nick enables resection in a bidirectional manner, using Exo1 in the 5′–3′ direction away from the DSB, and Mre11 in the 3′–5′ direction towards the DSB end. Mre11 exonuclease activity also confers resistance to DNA damage in cycling cells, suggesting that Mre11-catalysed resection may be a general feature of various DNA repair pathways.

We sought to clarify Mre11-dependent processing reactions at DSBs with blocked termini. Blocked DSB ends are created in meiosis by the topoisomerase-like transesterase Spo11 to initiate crossover recombination[14] (Supplementary Fig. 1a). Aside from the importance of meiotic recombination to sexual reproduction and genetic diversity, we reasoned that the molecular reactions pertaining to repair of covalently blocked Spo11–DSBs would be informative to the repair of DNA lesions with other types of end blockage, such as failed topoisomerase reactions and DSB ends competitively bound by the non-homologous end-joining (NHEJ) machinery.

Mre11-dependent endonucleolytic processing (nicking) of Spo11–DSBs generates two classes of Spo11–oligonucleotide fragments originating from the DSB end[15] (Supplementary Fig. 1). Spo11–oligonucleotide complexes do not form in *mre11* mutants completely abrogated for nuclease activity (*mre11-D56N* and *mre11-H125N*; Fig. 1a), corroborating earlier conclusions that Mre11 directly processes Spo11–DSBs[7–13]. Recently, a mutant of Mre11 that is exonuclease deficient, but mostly endonuclease proficient was described for the orthologous proteins in *Schizosaccharomyces pombe* and *Pyrococcus furiosus*[16]. We generated the equivalent mutation in *S. cerevisiae* Mre11 (His 59 to Ser; Supplementary Fig. 2a) and tested its function. During meiosis, Spo11–oligonucleotide complexes were readily detected in *mre11-H59S* cells (Fig. 1a), indicating that the allele is endonuclease proficient *in vivo*. Biochemical assays with recombinant Mre11-H59S showed reduced, but not abolished, 3′–5′ exonuclease activity on linear duplex DNA, and retention of much of the single-stranded (ss)DNA endonuclease activity (Supplementary Fig. 2)—observations consistent with *mre11-H59S* partially separating the two nuclease functions.

We assessed DSB repair kinetics at two meiotic recombination hotspots using Southern blotting and probes for the relevant genomic loci (*HIS4*::*LEU2* and *ARE1*; Fig. 1b and Supplementary Fig. 3). In the *mre11-H59S* strain, DSBs formed at normal levels and repaired as crossovers with normal timing (Fig. 1b, c). ssDNA resection, which can be qualitatively assessed by the relative migration of the DSB band on native agarose gels, also seemed unaffected by the *mre11-H59S* mutation (Fig. 1d, lanes 1 and 6, and Supplementary Fig. 4).

The lack of an obvious defect in ssDNA resection proficiency suggested that any potential contribution to ssDNA generation by Mre11 might be masked by the activity of another nuclease. During meiosis, the major resection pathway requires Exo1 (refs 17–21). We tested this idea by combining the *mre11-H59S* allele with an *EXO1* deletion (*exo1*Δ), which we found itself to have slightly delayed DSB repair kinetics, with fewer DSBs repairing as crossovers (Fig. 1b, c). Migration of the DSB band on agarose gels revealed that ssDNA resection was measurably reduced in *exo1*Δ—but not entirely abolished relative to a *mre11-H125N* control (where the failure to remove Spo11 prevents all resection; Fig. 1d, lanes 3, 4 and 5, and Supplementary Fig. 4). Our data agree with those of others investigating a meiotic role for Exo1 (refs 17–21).

The combination of *mre11-H59S* with *exo1*Δ caused DSBs to transiently accumulate for a longer period, with DSBs detectable for 2 h longer than in matched controls (Fig. 1b), and with formation of crossover recombinants reduced and delayed (Fig. 1c). These defects in DSB repair are correlated with a reduction in the mobility of DSB DNA on agarose gels (Fig. 1d and Supplementary Fig. 4). Specifically, in comparison to the *mre11-H59S* or *exo1*Δ single mutants, we observed DSB signals to migrate similarly to DSBs from the *mre11-H125N* control (Fig. 1d, lanes 2 and 3). This reduction in mobility is indicative of less ssDNA resection in *mre11-H59S*/*exo1*Δ than of either single mutant. We conclude that Exo1 and Mre11 collaborate to enable efficient ssDNA generation at meiotic DSBs.

Unrepaired DSBs activate Tel1 and Mec1 (yeast orthologues of the mammalian checkpoint kinases ATM and ATR respectively) to induce phosphorylation of histone H2Ax on Ser 129 and hyper-phosphorylation of Hop1 (a meiosis-specific adaptor of the DNA damage response[22]). Phosphorylated H2Ax and Hop1 were detected in all strains, indicating that significant resection is not essential for checkpoint activation (Fig. 1e). However, phospho-H2Ax accumulated and persisted until late time points only in *mre11-H59S*/*exo1*Δ, and Hop1 phosphorylation persisted for at least 2 h longer than in matched controls. These observations are consistent with a genome-wide defect in DSB repair in *mre11-H59S*/*exo1*Δ. The Tel1 branch of the signalling pathway is primarily activated by unresected DSBs[23]. We observed that Hop1 phosphorylation in the *mre11-H59S*/*exo1*Δ background is highly dependent on Tel1 (Supplementary Fig. 5), consistent with less resection occurring genome-wide.

To investigate if DSB processing defects were affecting meiotic chromosome segregation, we determined the efficiency of progression through anaphase I and II (Fig. 1f). Meiotic progression of wild type and *mre11-H59S* was essentially identical, whereas *exo1*Δ was delayed

[1]Genome Damage and Stability Centre, The University of Sussex, Brighton, BN1 9RQ, UK.

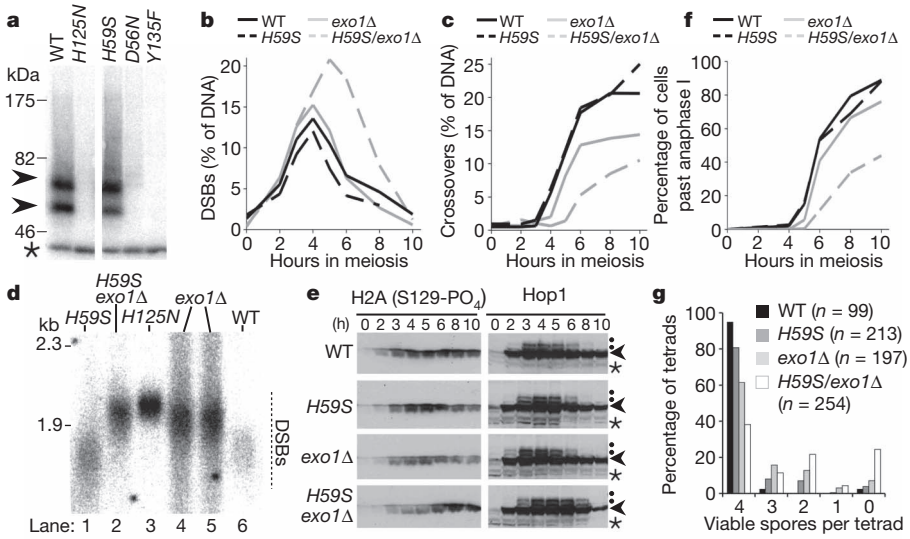

Figure 1 | Mre11- and Exo1-dependent resection and repair of meiotic DSBs. a, Autoradiograph of Spo11–oligonucleotide formation (arrowheads) in Mre11 nuclease-defective cells: *mre11-D56N*, *-H125N*, *-H59S*; and control *spo11-Y135F* cells in which Spo11–DSBs do not form. WT, wild type. Immunoprecipitated Spo11–oligonucleotide complexes are 3′-end-labelled using terminal transferase and separated on SDS–PAGE[15] (see Supplementary Fig. 1). Asterisk marks an unrelated labelling artefact. **b**–**f**, Time course of events during meiosis for the indicated genotypes. **b**, **c**, Quantitative analysis of DSB (**b**) and crossover (**c**) signals at *HIS4*::*LEU2*. DNA at each time point was digested with PstI (**b**) or XhoI (**c**), separated by agarose gel electrophoresis and blots hybridized with probes to *LSB5* (**b**) or *STE50* (**c**). DSB signals were quantified as a percentage of specific lane signal (see also Supplementary Fig. 3). **d**, Relative extent of DSB resection at *HIS4*::*LEU2* (at 4 h in meiosis). DNA was digested with BglII and blots hybridized with a *STE50* probe (see also Supplementary Fig. 4). **e**, Western blot analysis of phosphorylated H2Ax and Hop1 (arrowhead) detected from TCA-precipitated whole-cell lysates. Phosphorylated Hop1 is indicated by dot. Asterisk marks cross-reacting band. **f**, Progression through anaphase I and II assessed by microscopic examination of 4′,6-diamidino-2-phenylindole (DAPI)-stained cells. **g**, Distribution of spore viabilities per tetrad (*n*, number of 4-spore tetrads dissected). The difference in distribution between *mre11-H59S*/*exo1*Δ and *exo1*Δ is highly significant (χ^2 test for goodness-of-fit; $\chi = 63.084$, 4 degrees of freedom, $P < 0.0001$). Absolute spore viabilities are: wild type, 97%; *mre11-H59S*, 90%; *exo1*Δ, 76%, *mre11-H59S*/*exo1*Δ, 59%.

by about 1 h, with slightly reduced overall efficiency. In contrast, nuclear division in the *mre11-H59S*/*exo1*Δ double mutant was poor, with more than half of the cells having failed to complete even the first meiotic nuclear division after 10 h in meiosis. Analysis of sporulation efficiency after 24 h revealed increased incidence of aberrant tetrad maturation and/or nuclear packaging where orphaned chromosome fragments were observed outside the maturing spore wall (Supplementary Fig. 6). These defects in meiotic chromosome segregation manifested as reduced spore viability in the double mutant compared to controls (Fig. 1g).

To characterize in greater detail the molecular defect caused by *mre11-H59S*, we looked carefully at the distribution of Spo11–oligonucleotide products generated *in vivo* by the 5′-DSB processing reaction (Fig. 2a, b). In wild-type cells, two major classes of Spo11–oligonucleotide are observed, which differ by the length of attached DNA[15]. By contrast, in *mre11-H59S* we observed a shift in this distribution towards higher molecular weight Spo11–oligonucleotide species (Fig. 2a and Supplementary Fig. 7). Importantly, total Spo11–oligonucleotide formation was not itself delayed (Supplementary Fig. 7), indicating that the Spo11-removal reaction initiates with normal timing in *mre11-H59S* cells, but is defective in forming shorter molecules. To clarify the precise size distribution of the Spo11–oligonucleotide molecules, we fractionated de-proteinized oligonucleotides using denaturing polyacrylamide gel electrophoresis (PAGE; Fig. 2b). In wild-type cells, two peak areas of signal 10–17 nucleotides (nt) and 28–40 nt were apparent. These correspond to the shorter and longer Spo11–oligonucleotide classes detected on SDS–PAGE (Fig. 2a). We additionally detected signal (24% of total)

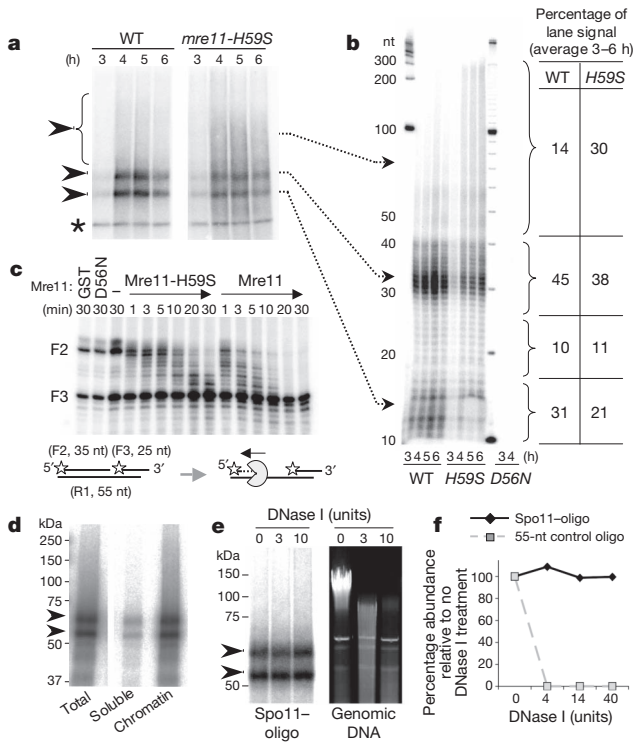

Figure 2 | Mre11-exonucleolytic processing of DSB ends. a, **b**, Spo11–oligonucleotide detection in wild type (WT) and *mre11-H59S* during meiosis. 3′-end-labelled Spo11 complexes are fractionated by SDS–PAGE (**a**) or by nucleotide resolution urea/PAGE after proteolytic removal of Spo11 peptide (**b**). **c**, Mre11-H59S shows reduced 3′–5′ exonuclease activity on a nicked duplex. Reactions were performed as for Supplementary Fig. 2c. Stars indicate 5′ label, F3 3′ end has 5-nt extension and is refractory to Mre11-mediated resection[25]. **d**, Chromatin association of Spo11–oligonucleotide complexes. Wild-type cell extracts were fractionated and the abundance of Spo11–oligonucleotide complexes assessed in soluble versus chromatin-enriched material. **e**, **f**, Nuclease resistance of Spo11–oligonucleotide (Spo11–oligo) complexes. Chromatin-enriched material from **d** was treated with DNase I, and abundance of Spo11–oligonucleotide complexes compared to the simultaneous degradation of genomic DNA (**e**), or of a control 55-nt oligonucleotide (**f**).

in molecules 18–27 and 41–300 nt long (Fig. 2b), indicating that the length distribution of processed molecules is significantly more heterogeneous than previously assumed, and that nicks are made at up to 300 nt from the DSB end.

In the *mre11-H59S* mutant, the distribution was shifted such that the long oligonucleotide molecules of 41–300 nt made up a third of the material detected (Fig. 2b). Although it is possible that the altered distribution of oligonucleotide molecules is caused by a reduction in the endonuclease activity of Mre11-H59S, our physical and genetic observations in both wild type and *mre11-H59S* can be readily explained if resection begins at relatively distant nicks (up to 300 nt from the DSB) and traverses bidirectionally both away from (using Exo1) and towards (using Mre11) the DSB end[21]. Such a model is consistent with the opposing polarities of the Mre11 and Exo1 exonuclease activities[24,25], and with the synergistic loss in resection we observe in *mre11-H59S*/*exo1*Δ. Moreover, the length distribution of Spo11–oligonucleotides is compatible with the extent of Exo1-independent resection reported recently by others[21] and, as predicted, Spo11–oligonucleotide length is unchanged by loss of *EXO1* (Supplementary Fig. 8). Lastly, only a low background of Spo11–oligonucleotide complexes are detected in endonuclease-defective *mre11-D56N*, ruling out the possibility that the long oligonucleotide molecules arise via an alternative nuclease nicking the 5′ strand (Fig. 2b). To test this mechanism *in vitro*, we incubated Mre11 protein with a nicked duplex substrate designed to mimic this proposed *in vivo* reaction, and found that Mre11-H59S resected from the nick with lower efficiency than wild-type Mre11 (Fig. 2c).

Together, these observations led us to consider that the steady-state length of Spo11–oligonucleotide complexes might arise via the relative processivity of the 3′–5′ Mre11 exonuclease and the relative sensitivity to nucleolytic degradation of DNA close to the DSB end. Spo11–DSB formation requires at least ten factors[14], suggesting that a large protein complex may reside at—and protect—the DSB end. If this model were correct, we expected Spo11–oligonucleotide complexes to be associated with chromatin and resistant to nucleolytic degradation. We tested this idea by incubating a chromatin-enriched nuclear pellet from meiotic yeast cells with DNase I, then assessed the quantity of Spo11–oligonucleotide complexes remaining, relative to both bulk DNA and to an exogenous protein-free oligonucleotide included in parallel reactions (Fig. 2d–f). Greater than 90% of Spo11–oligonucleotides are found in the chromatin fraction and, remarkably, no loss in signal was observed despite extensive nucleolytic degradation of both the chromosomal DNA and the control oligonucleotide. We conclude that Spo11–oligonucleotide complexes are occluded from degradation even by exogenous nucleases—a prediction of our model.

In cycling cells, Mre11 nuclease activity promotes the onset of resection—a requisite for repair of DSBs by homologous recombination[1]. To investigate a specific role for the Mre11 3′–5′ exonuclease during DNA repair in cycling cells, we challenged yeast cells with exposure to DNA damaging agents. Similar to complete abrogation of the endo/exonuclease activities (*mre11-H125N*), reduced Mre11 exonuclease activity (*mre11-H59S*) sensitized cells to the DNA alkylating agent methyl methanesulphonate (MMS) and to the topoisomerase poison camptothecin (CPT; Fig. 3). Compared to an *MRE11* deletion, however, *mre11-H59S* and *mre11-H125N* are themselves far less sensitive, consistent with physical interactions within the Mre11 complex being retained (Supplementary Fig. 9). In agreement with Mre11 endonuclease activity being unaffected in *mre11-H59S*, and allowing redundant processing pathways, combining *mre11-H59S* with a deletion of *EXO1* did not further sensitize cells to MMS (Supplementary Fig. 10). Together these observations indicate that the exonuclease activity of Mre11 is involved in the repair of various classes of DNA lesion.

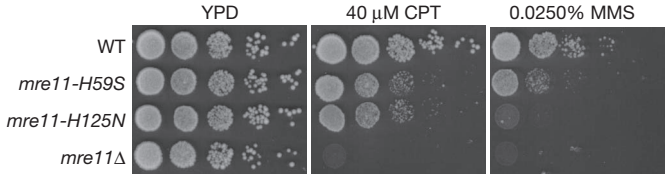

Figure 3 | DNA damage sensitivity of exonuclease-defective Mre11 cells. Tenfold serial dilutions of the indicated strains were spotted onto solid media containing the indicated compounds and incubated at 30 °C for 2 days (CPT) or 3 days (MMS).

Understanding the regulation of DSB repair is a complex issue involving multiple factors with overlapping roles. Here, we propose a biological function for the 3′–5′ exonuclease activity of the evolutionarily conserved Mre11 protein. Previous work has indicated DSB resection to traverse unidirectionally[1]. We propose a refined model that involves the coordination of two resection activities of opposing polarity: Exo1 away from the DSB and Mre11 towards the DSB end (Fig. 4). We favour the view that this exonuclease reaction begins at nicks created by the Mre11 endonuclease (in conjunction with Sae2) and which are positioned at variable distance from the DSB end, perhaps due to locus-specific chromatin architecture[26]. Although our assay detects only the site of incision closest to the DSB end, Mre11 and Sae2 may create multiple nicks on the resecting strand[17,21,27] (A. S. H. Goldman, personal communication) that, in combination with exonucleolytic processing, might further enhance resection efficiency. Lastly, the recent observation that the length and abundance of SPO11–oligonucleotide complexes is increased in $Atm^{-/-}$ mice[28] (S. Keeney and M. Jasin, personal communication), suggests that Mre11 exonuclease activity may be an evolutionarily conserved feature directly regulated by ATM.

During meiosis, bidirectional processing may help to reinforce subsequent steps of repair, which at least in some cases seem to occur differentially on either side of the DSB[26,29,30]. Our observation that liberated Spo11–oligonucleotide complexes remain chromatin bound and relatively protected provides a clue to potential mechanisms of end differentiation. For example, retention of proteins on one or both of the DSB ends could influence subsequent steps of repair[15] (Fig. 4b). Lastly, our observation that Mre11-dependent incision occurs at some

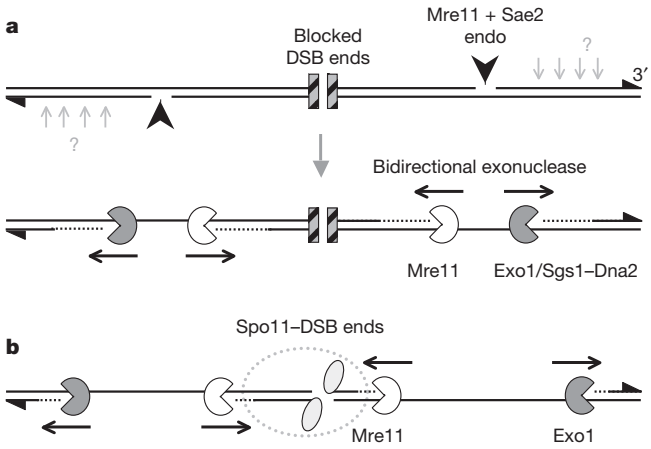

Figure 4 | Model for bidirectional processing of DSBs by Mre11 and Exo1. **a**, After DSB formation with blocked ends (hatched squares), Mre11/Sae2-dependent nicks flanking the DSB ends create initiation sites for bidirectional resection by Exo1 and/or Sgs1–Dna2 away from the DSB, and by Mre11 towards the DSB end. Such terminal blocks could arise after base damage, trapping of a topoisomerase, or by avid binding of the NHEJ complex. 3′ ends are marked with triangles. Mre11/Sae2 may make multiple nicks on the 5′ strand (light grey arrows), facilitating resection. **b**, In meiosis, the DSB ends are terminally blocked by covalently bound Spo11 protein (grey ellipses), and may be protected from Mre11-dependent exonuclease degradation by a large metastable multisubunit complex (dashed outline), thereby generating the observed size distribution of Spo11–oligonucleotide complexes.

distance from the DSB end indicates that DSB formation and processing reactions are coordinated over a considerable distance (300 bp of B-form DNA is ~100 nm). How these incision points are regulated—and restricted to only the 5′-ending strand—are fascinating questions for the future.

Although much of this work concerns specifics of meiotic DSB processing, we suggest that a similar pathway may occur whenever the DSB end is blocked by a lesion or protein complex that prevents direct loading of the 5′–3′ exonuclease machinery. Such DNA blockages may be crosslinked protein, damaged DNA ends, or simply the stable binding of high affinity proteins to the DSB. As such, the nucleolytic incision pathway may provide the key point of regulation that controls the balance between NHEJ and homologous recombination.

METHODS SUMMARY

Yeast strains and culture methods. Meiotic cultures were prepared as described[15]. Strains were derived from SK1 using standard techniques. Spo11 protein is tagged by the HA3His6 epitope[15]. Mre11 mutations were introduced by pop-in/out using plasmids derived from pRS414-MRE11 (ref. 10). *exo1*Δ, *tel1*Δ and *sae2*Δ are full replacements of the open reading frame (ORF) with kanMX4, hphNT2 and kanMX6, respectively. A full strain list is available on request. For chronic DNA damage sensitivity, exponentially growing cultures were spotted in tenfold dilutions onto freshly prepared media.

Molecular techniques. Spo11–oligonucleotide complexes were detected by two rounds of immunoprecipitation and end labelling as described[15]. DSBs and crossover recombinants were detected by Southern blotting genomic DNA after fractionation on agarose gels using standard techniques[29]. Radioactive signals were collected on phosphor screens, scanned with a Fuji FLA5100, and quantified using ImageGauge software. Phosphorylated H2Ax and Hop1 protein were detected using Ab17353 (Abcam) and anti-Hop1 antisera (F. Klein), respectively. Subcellular fractionation of cell contents was performed by purifying hypotonically lysed spheroplasts through a sucrose cushion. Chromatin digests were performed at 25 °C with DNase I (NEB). Reactions were split and processed for DNA extraction or Spo11–oligonucleotide purification. As a positive control, parallel reactions included a 5′-labelled 55-nt oligonucleotide. Recombinant GST-Mre11 proteins were purified and reacted with DNA substrates as described[10].

Full Methods and any associated references are available in the online version of the paper at www.nature.com/nature.

Received 25 February; accepted 30 August 2011.
Published online 16 October 2011.

1. Paques, F. & Haber, J. E. Multiple pathways of recombination induced by double-strand breaks in *Saccharomyces cerevisiae*. *Microbiol. Mol. Biol. Rev.* **63,** 349 (1999).
2. Mimitou, E. P. & Symington, L. S. Sae2, Exo1 and Sgs1 collaborate in DNA double-strand break processing. *Nature* **455,** 770–774 (2008).
3. Nicolette, M. L. *et al.* Mre11–Rad50–Xrs2 and Sae2 promote 5′ strand resection of DNA double-strand breaks. *Nature Struct. Mol. Biol.* **17,** 1478–1485 (2010).
4. Zhu, Z., Chung, W. H., Shim, E. Y., Lee, S. E. & Ira, G. Sgs1 helicase and two nucleases Dna2 and Exo1 resect DNA double-strand break ends. *Cell* **134,** 981–994 (2008).
5. Mimitou, E. P. & Symington, L. S. Ku prevents Exo1 and Sgs1-dependent resection of DNA ends in the absence of a functional MRX complex or Sae2. *EMBO J.* **29,** 3358–3369 (2010).
6. Hartsuiker, E., Neale, M. J. & Carr, A. M. Distinct requirements for the Rad32(Mre11) nuclease and Ctp1(CtIP) in the removal of covalently bound topoisomerase I and II from DNA. *Mol. Cell* **33,** 117–123 (2009).
7. Furuse, M. *et al.* Distinct roles of two separable *in vitro* activities of yeast Mre11 in mitotic and meiotic recombination. *EMBO J.* **17,** 6412–6425 (1998).
8. Hartsuiker, E. *et al.* $Ctp1^{CtIP}$ and $Rad32^{Mre11}$ nuclease activity are required for $Rec12^{Spo11}$ removal, but $Rec12^{Spo11}$ removal is dispensable for other MRN-dependent meiotic functions. *Mol. Cell. Biol.* **29,** 1671–1681 (2009).
9. Milman, N., Higuchi, E. & Smith, G. R. Meiotic DNA double-strand break repair requires two nucleases, MRN and Ctp1, to produce a single size class of Rec12 (Spo11)-oligonucleotide complexes. *Mol. Cell. Biol.* **29,** 5998–6005 (2009).
10. Moreau, S., Ferguson, J. R. & Symington, L. S. The nuclease activity of Mre11 is required for meiosis but not for mating type switching, end joining, or telomere maintenance. *Mol. Cell. Biol.* **19,** 556–566 (1999).
11. Nairz, K. & Klein, F. *mre11S*—a yeast mutation that blocks double-strand-break processing and permits nonhomologous synapsis in meiosis. *Genes Dev.* **11,** 2272–2290 (1997).
12. Rothenberg, M., Kohli, J. & Ludin, K. Ctp1 and the MRN-complex are required for endonucleolytic Rec12 removal with release of a single class of oligonucleotides in fission yeast. *PLoS Genet.* **5,** e1000722 (2009).
13. Tsubouchi, H. & Ogawa, H. A novel *mre11* mutation impairs processing of double-strand breaks of DNA during both mitosis and meiosis. *Mol. Cell. Biol.* **18,** 260–268 (1998).
14. Keeney, S. Mechanism and control of meiotic recombination initiation. *Curr. Top. Dev. Biol.* **52,** 1–53 (2001).
15. Neale, M. J., Pan, J. & Keeney, S. Endonucleolytic processing of covalent protein-linked DNA double-strand breaks. *Nature* **436,** 1053–1057 (2005).
16. Williams, R. S. *et al.* Mre11 dimers coordinate DNA end bridging and nuclease processing in double-strand-break repair. *Cell* **135,** 97–109 (2008).
17. Hodgson, A. *et al.* Mre11 and Exo1 contribute to the initiation and processivity of resection at meiotic double-strand breaks made independently of Spo11. *DNA Repair* **10,** 138–148 (2010).
18. Keelagher, R. E., Cotton, V. E., Goldman, A. S. & Borts, R. H. Separable roles for Exonuclease I in meiotic DNA double-strand break repair. *DNA Repair* **10,** 126–137 (2010).
19. Manfrini, N., Guerini, I., Citterio, A., Lucchini, G. & Longhese, M. P. Processing of meiotic DNA double-strand breaks requires cyclin-dependent kinase and multiple nucleases. *J. Biol. Chem.* **285,** 11628–11637 (2010).
20. Tsubouchi, H. & Ogawa, H. Exo1 roles for repair of DNA double-strand breaks and meiotic crossing over in *Saccharomyces cerevisiae*. *Mol. Biol. Cell* **11,** 2221–2233 (2000).
21. Zakharyevich, K. *et al.* Temporally and biochemically distinct activities of Exo1 during meiosis: double-strand break resection and resolution of double holliday junctions. *Mol. Cell* **40,** 1001–1015 (2010).
22. Carballo, J. A., Johnson, A. L., Sedgwick, S. G. & Cha, R. S. Phosphorylation of the axial element protein Hop1 by Mec1/Tel1 ensures meiotic interhomolog recombination. *Cell* **132,** 758–770 (2008).
23. Usui, T., Ogawa, H. & Petrini, J. H. A. DNA damage response pathway controlled by Tel1 and the Mre11 complex. *Mol. Cell* **7,** 1255–1266 (2001).
24. Szankasi, P. & Smith, G. R. A. DNA exonuclease induced during meiosis of *Schizosaccharomyces pombe*. *J. Biol. Chem.* **267,** 3014–3023 (1992).
25. Paull, T. T. & Gellert, M. The 3′ to 5′ exonuclease activity of Mre11 facilitates repair of DNA double-strand breaks. *Mol. Cell* **1,** 969–979 (1998).
26. Pan, J. *et al.* A hierarchical combination of factors shapes the genome-wide topography of yeast meiotic recombination initiation. *Cell* **144,** 719–731 (2011).
27. Jazayeri, A., Balestrini, A., Garner, E., Haber, J. E. & Costanzo, V. Mre11–Rad50–Nbs1-dependent processing of DNA breaks generates oligonucleotides that stimulate ATM activity. *EMBO J.* **27,** 1953–1962 (2008).
28. Lange, J. *et al.* ATM controls meiotic double-strand-break formation. *Nature* doi:10.1038/nature10508 (this issue).
29. Hunter, N. & Kleckner, N. The single-end invasion: an asymmetric intermediate at the double-strand break to double-holliday junction transition of meiotic recombination. *Cell* **106,** 59–70 (2001).
30. Kim, K. P. *et al.* Sister cohesion and structural axis components mediate homolog bias of meiotic recombination. *Cell* **143,** 924–937 (2010).

Supplementary Information is linked to the online version of the paper at www.nature.com/nature.

Acknowledgements We thank R. Cha, E. Hoffmann, N. Hunter, S. Keeney and J. Nitiss for yeast strains; L. Symington for plasmids; F. Klein and J. Petrini for antisera. V.G. is supported by an MRC New Investigator Grant to M.J.N. M.J.N. is supported by a University Research Fellowship from the Royal Society and a Career Development Award from the Human Frontiers Science Program Organisation.

Author Contributions V.G. and M.J.N. designed the experiments and wrote the paper. V.G. and M.J.N. performed the experiments with technical support from S.E.L.P. and S.G.

Author Information Reprints and permissions information is available at www.nature.com/reprints. The authors declare no competing financial interests. Readers are welcome to comment on the online version of this article at www.nature.com/nature. Correspondence and requests for materials should be addressed to M.J.N. (m.neale@sussex.ac.uk).

METHODS

Yeast strains. Strains of *S. cerevisiae* were derived from SK1 using standard techniques. Spo11 protein is tagged by the HA3His6 epitope[15]. Mre11 mutations were introduced by pop-in/out using plasmids derived from pRS414-MRE11 (see below). *exo1*Δ, *tel1*Δ and *sae2*Δ are full replacements of the open reading frame (ORF) with kanMX4, hphNT2 and kanMX6, respectively. A full strain list is available on request.

Meiotic cultures. YPD cultures (1% yeast extract, 2% peptone, 2% glucose) were diluted 100-fold into YPA (1% yeast extract, 2% peptone, 1% K-acetate) and grown vigorously for 14 h at 30 °C. Cells were collected by centrifugation, washed once in water, resuspended in an equal volume of prewarmed 2% K-acetate containing diluted amino acid supplements, and shaken vigorously at 30 °C.

Construction of Mre11 nuclease mutant strains. The *mre11-H59S* mutant was constructed by site-directed mutagenesis PCR on the integrating plasmid pSM444 (pRS406::*mre11-D56N*), reversing the D56N mutation to wild type and introducing H59S (forward primer: GTACAGTCCGGTGATCTTTTTAGCGTG AATAAGCC; reverse primer: GGCTTATTCACGCTAAAAAGATCACCGG ACTGTAC). Integration plasmids containing *mre11-D56N* and *mre11-H125N* nuclease dead mutant alleles were provided by L. Symington (pSM444 and pSM438 respectively). To replace chromosomal *MRE11* with mutant alleles, the plasmid containing mutations in the nuclease domains of *MRE11* were linearized with SphI and transformed in the SK1 strain. Uracil-positive (Ura^+) transformants were inoculated in rich medium overnight and 20 µl of culture were spread onto medium containing 5-fluoroorotic acid (5-FOA) in order to select pop-out events. The presence of the *mre11-D56N* and *mre11-H125N* alleles in the resulting 5-FOA resistant cells was assessed by sensitivity to DNA damaging agent: cells from single 5-FOA resistant colonies were patched onto plates containing high concentration of CPT (30–50 µM) supplemented with phloxin B. Because the introduction of the *mre11-H59S* mutation also altered a PmlI restriction site, the presence of the *mre11-H59S* allele was tested by sensitivity of PCR reactions covering the mutated region to PmlI restriction. Replacement of wild-type *MRE11* by targeted mutations was confirmed by PCR amplification and sequencing.

Spot tests for DNA damage sensitivity. Cells were grown overnight in liquid YPD, diluted into fresh media and grown to log phase, adjusted to $OD_{600\,nm} = 0.2$, serially diluted tenfold, and 5 µl spotted onto control and drug-containing YPD plates.

Spo11–oligonucleotide assays. Spo11–oligonucleotide complexes were detected by immunoprecipitation and end labelling following established methods[15]. To reduce the co-precipitation of nonspecific genomic DNA, two rounds of immunoprecipitation were used. Specifically, 10–50 ml of sporulating culture was lysed in 10% ice-cold TCA using zirconia beads and a BioSpec 24. Precipitated material was dissolved in STE (2% SDS, 0.5 M Tris pH 8.1, 10 mM EDTA, 0.05% bromophenol blue), and boiled for 5 min. Extracts were diluted twofold in 2× IP buffer (2% Triton X-100, 300 mM NaCl, 30 mM Tris-HCl pH 8.1, 2 mM EDTA), centrifuged for 10 min at 16,000*g* at 4 °C, and supernatant was diluted a further twofold in 1× IP buffer. Anti-HA antibody (F-7; Santa Cruz Biotechnology) was added at 1 in 500, protein-G-agarose matrix (Roche) at 1 in 50, and then incubated with rotation for 4 h at 4 °C. Immune complexes were collected by low speed centrifugation, and washed three times with 1× IP buffer. Beads were boiled for 5 min in 250 µl STE, chilled on ice, and diluted twofold as above with 2× IP buffer, recentrifuged, and supernatant was dissolved further twofold in 1× IP buffer. Fresh antibody and beads were added at the above dilutions. The second immunoprecipitation was performed overnight at 4 °C, and then washed as above. Two additional washes in 1× TKAc (20 mM Tris-acetate pH 7.9, 50 mM K-acetate) were performed before incubation with 10–20 units TdT (Fermentas) and 5–10 µCi CoTP (cordycepin triphosphate; Perkin Elmer) in 1× TKAc, 0.25 mM $CoCl_2$ buffer at 37 °C for 1 h. Labelled complexes were washed twice with 1× IP buffer, and eluted in Laemmli loading buffer for direct analysis on 7.5% SDS–PAGE. For nucleotide resolution analysis of Spo11–oligonucleotide lengths, eluted complexes were mixed with 1 µg glycogen (Roche) and 10 volumes of 100% ethanol, and precipitated overnight at −20 °C. Precipitates were collected by centrifugation, dissolved in 15 µl of 10× TE containing 0.5 µg ml^{-1} proteinase K, and incubated at 50 °C for 30 min. Eluted oligonucleotides were mixed with 3 volumes of loading dye (95% formamide, 10 mM EDTA, 0.01% bromophenol blue, 0.01% xylene cyanol), and fractionated through a 28-cm tall, 0.5-mm thick 12% polyacrylamide (19:1), 6 M urea gel in 1× TBE running buffer at approx 1,200 V for 50–60 min. Gels were fixed in 10% methanol, 7% acetic acid and 5% glycerol, vacuum dried and exposed to phosphor screens for imaging.

DSB and crossover analysis. Genomic DNA was isolated from aliquots of synchronously sporulating cultures using standard methods. Briefly, spheroplasts were prepared in 1 M sorbitol, 0.1 M EDTA, 0.1 M $NaHPO_4$ pH 7.5, 1% BME and 200 µg ml^{-1} zymolyase 100T for 20–30 min at 37 °C, and lysed by adding SDS to 0.5% and proteinase K to 200 µg ml^{-1} with incubation for 60 min at 60 °C. Protein was removed by mixing with an equal volume of phenol:chloroform:isoamyl alcohol (25:24:1), and nucleic acids precipitated by adding one-tenth volume of 3 M NaAc pH 5.2 and an equal volume of 100% ethanol. Precipitates were washed in 70% ethanol and dissolved in 1× TE containing 100 µg ml^{-1} RNase, incubated for 60 min at 37 °C, reprecipitated with ethanol and NaAc and DNA pellets left to dissolve in 1× TE overnight at 4 °C. Genomic DNA was digested with restriction enzymes following the manufacturer's recommendations, fractionated on 0.6%, 0.7% or 0.9% agarose gels in 1× TAE or 1× TBE buffer and ethidium bromide (as required), and blotted under vacuum to zetaprobe membrane (BioRad) in 0.5 M NaOH, 1.5 M NaCl. Blots were equilibrated in hybridization solution (0.5 M $NaHPO_4$ pH 7.2, 7% SDS, 1 mM EDTA, 1% BSA) at 65 °C, and random primed radioactive probes (High Prime; Roche) prepared from gel-purified PCR products were then added. Blots were washed four times in 40 mM $NaHPO_4$, 1% SDS, 1 mM EDTA at 65 °C, then dried and exposed to phosphor screens for imaging.

Western blotting. TCA-denatured cell material dissolved in STE and 5% β-mercaptoethanol was fractionated in 7.5% or 10% SDS–PAGE, transferred to PVDF membrane (Millipore) in 1× CAPS buffer (10 mM CAPS-NaOH pH 11, 10% methanol), and incubated in TBST + 3% BSA with the requisite antibodies: phosphorylated H2Ax was detected using Ab17353 diluted 1/5,000 in TBST (Abcam) and Hop1 detected using anti-Hop1 antisera at a 1/4,000 dilution[31].

DAPI staining. Cells were fixed in 100% methanol, and aliquots mixed with 1 µg ml^{-1} DAPI in 75% glycerol. The number of cells with 0, 2 and 4 nuclei was scored under a fluorescence microscope. At least 200 cells were counted per time point. Sporulation efficiency was determined by observation of fixed tetrads (24 h into meiosis, on three independent time courses) under a Zeiss fluorescence microscope with both fluorescence and bright-field illumination. Samples were randomized and 150 to 300 cells were counted for each strain per time course. Sporulations were scored as abnormal when significant extranuclear material was detected by DAPI staining and the wall morphology of spores was abnormal under bright-field illumination. DAPI and DIC images were captured using a personalDV (DeltaVision) system (Applied Precision) using the softWoRx software.

Chromatin enrichment. Cell pellets corresponding to 100 ml meiotic cultures were resuspended in 30 ml Sphero/CoHex buffer (1 M sorbitol, 50 mM HEPES pH 7.5, 10 mM EDTA, 5 mM hexamine cobalt chloride) supplemented with 1% β-mercaptoethanol and zymolyase 100T to 50 µg ml^{-1}, and incubated for ~25min at 37 °C. Spheroplasts were transferred onto 10 ml sucrose cushion, spun for 5 min at 16,000*g* at 4 °C. Spheroplast pellets were resuspended in 1 ml sucrose buffer (1 M sucrose, 50 mM MES-NaOH, 50 mM NaCl, 1 mM EDTA, 0.5 mM $MgCl_2$, Roche protease inhibitors cocktail, AEBSF to 10 µg ml^{-1}), lysed in 30 ml lysis buffer (50 mM MES-NaOH, 1 mM $MgCl_2$, 5 mM EDTA, Roche protease inhibitors cocktail, AEBSF to 10 µg ml^{-1}), homogenized in a dounce homogenizer, and spun 5 min at 16,000*g* at 4 °C. Pellets were suspended in 30 ml lysis buffer and subcellular fractionation of cell contents was performed by centrifugation through a 10-ml sucrose cushion. Pellets were washed once in the same buffer, suspended in sucrose buffer, and 300 µl aliquots were stored at −20 °C . Aliquots were incubated at 25 °C with DNase I (NEB) in 50 mM HEPES, 50 mM NaCl, 5 mM $MgCl_2$ buffer supplemented with complete protease inhibitors tablet (Roche) and AEBSF. Reactions were split and processed for genomic DNA extraction or Spo11–oligonucleotide purification. As a positive control, parallel reactions included a 5′-labelled 55-base oligonucleotide (R1) that was detected on 1× TBE PAGE.

Recombinant protein purification. GST-Mre11 proteins were purified and reacted with DNA substrates as described[10]. Briefly, *MRE11* wild-type, *mre11-H59S* and *mre11-D56N* open reading frames (ORFs) were amplified by PCR, cloned with BamHI/SalI ends into pEG-KT plasmid and were transformed into the protease defective JEL1 *mre11*Δ strain (LSY1706; a gift from L. Symington). Galactose induction was performed as described in http://www.bio.brandeis.edu/haberlab/jehsite/protocol.html. Cells from a 100 ml culture were collected by centrifugation for 5 min at 3,000*g* at 4 °C, washed in cold lysis buffer (20 mM Tris-HCl pH 8, 1 mM EDTA, 500 mM NaCl, 0.1% Triton X-100, 10% glycerol), and lysed in 500 µl lysis buffer supplemented with 50 mM NaF, 10 µg ml^{-1} AEBSF and complete protease inhibitor tablet (Roche) using zirconia beads and a BioSpec 24 apparatus. Lysates were cleared by centrifugation for 10 min at 16,000*g* at 4 °C, and supernatants were incubated with 200 µl of Glutathione Sepharose beads slurry (pre-washed in lysis buffer) for 1 h at 4 °C. Beads were washed three times in lysis buffer and proteins were eluted over 30 min at 4 °C in elution buffer (50 mM Tris pH 8, 1 mM EDTA, 20 mM glutathione reduced, 40% glycerol, supplemented with protease inhibitors), and aliquots were frozen in liquid nitrogen and stored at −80 °C.

Oligonucleotide nicked substrate and exonuclease assay. The nicked, double-stranded substrate described in Fig. 2c was made by 5′-[^{32}P] end labelling of oligonucleotides F2: GACCTGGCACGTAGGACAGCATGGGATCTGGCCTG; and F3: TGTTACACAGTGCTACAGACatggt (lowercase indicates 3′ overhang) with PNK; and annealing to the unlabelled reverse complement, R1:

GTCTGTAGCACTGTGTAACACAGGCCAGATCCCATGCTGTCCTACGTGC CAGGT. Annealing was verified by migration on 1× TBE, 12% polyacrylamide gel. ~0.66 pmol of double-stranded nicked substrate was incubated with ~0.13 pmol of recombinant protein in nuclease buffer (25 mM MOPS pH 7, 60 mM KCl, 0.2% Triton X-100, 2 mM DTT, 50 mM $MnCl_2$) for the indicated length of time at 37 °C. Reactions were stopped by adding SDS to 0.3% and proteinase K to 0.5 mg ml^{-1} and incubated for 15 min at 37 °C. Reactions were denaturated in 2 volumes of formamide loading buffer (95% formamide, 10 mM EDTA, 0.005% bromophenol blue, 0.01% xylene cyanol) at 95 °C and separated on a 6 M urea, 12% polyacryamide gel in 1× TBE. Gels were exposed to a phosphor screen for imaging.

31. Panizza, S. *et al*. Spo11-accessory proteins link double-strand break sites to the chromosome axis in early meiotic recombination. *Cell* **146,** 372–383 (2011).

doi:10.1038/nature10515

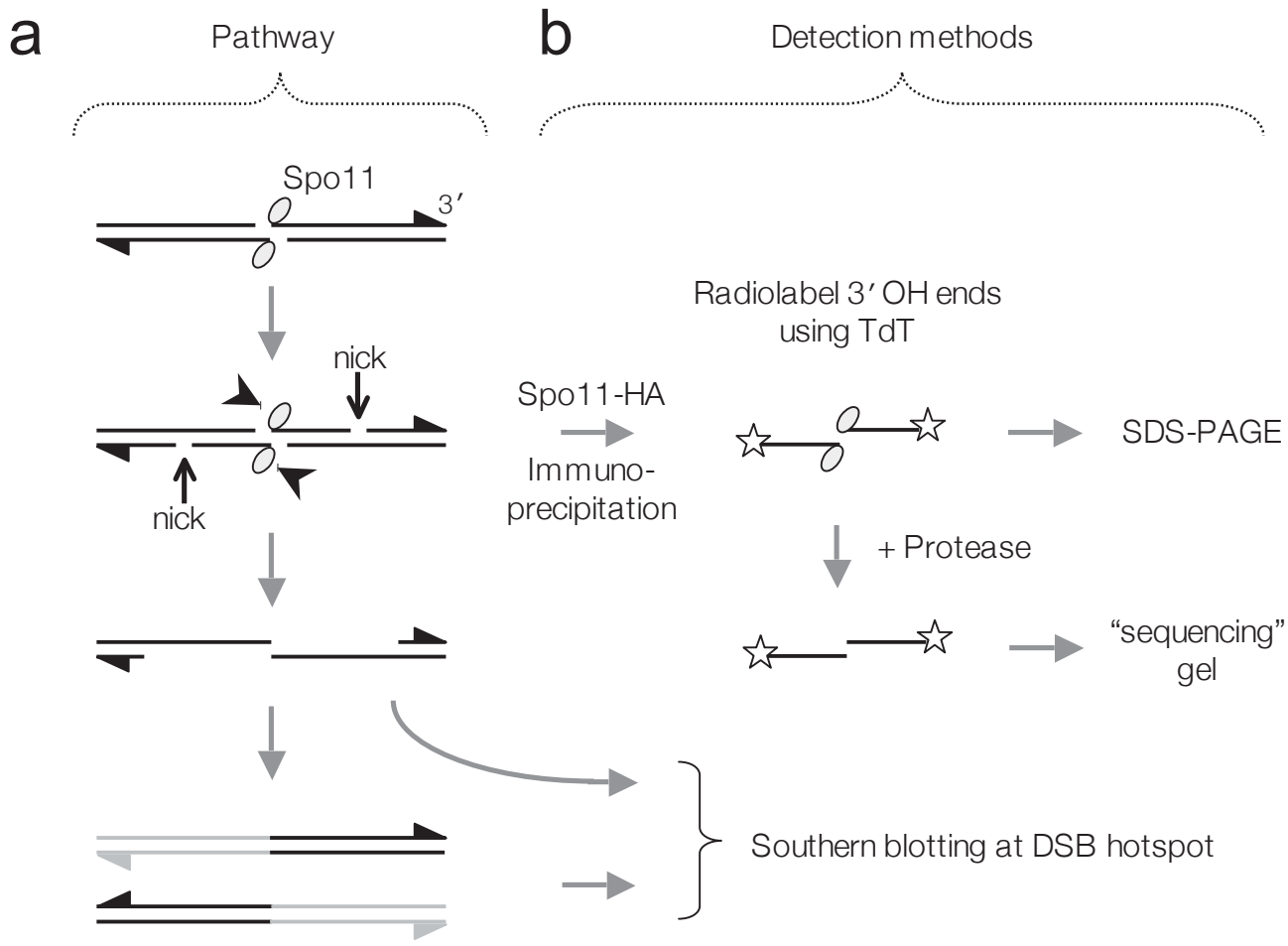

Figure S1. Overview of meiotic DSB end processing and detection methods used. **a,** Meiotic DSBs are created by a Spo11 dimer (grey ellipses), which becomes covalently attached to both 5' DSB ends. Mre11/Sae2-dependent nicking creates Spo11-oligonucleotide complexes (arrowheads), and permits ssDNA resection flanking the DSB. Resected DSBs are repaired as noncrossovers, or as crossovers (shown). Strand polarity is indicated with black triangles. **b,** Spo11 oligonucleotide complexes are purified from denatured cell extracts by immunoprecipitation against the HA-epitope, then 3'-end-labelled with ^{32}P-labelled chain-terminating nucleotide (stars) using terminal deoxynucleotide transferase (TdT). Labelled Spo11-oligo complexes are detected directly after fractionation on standard SDS-PAGE, or on a high-resolution denaturing urea/polyacrylamide "sequencing" gel after proteolytic removal of the Spo11 moiety (to measure more accurately the length of DNA attached to Spo11). Resected DSBs and crossovers are detected by Southern blotting and probing for a region close to a strong DSB hotspot (e.g. *HIS4*::*LEU2* or *ARE1*; see Figure S3 and S4 for details).

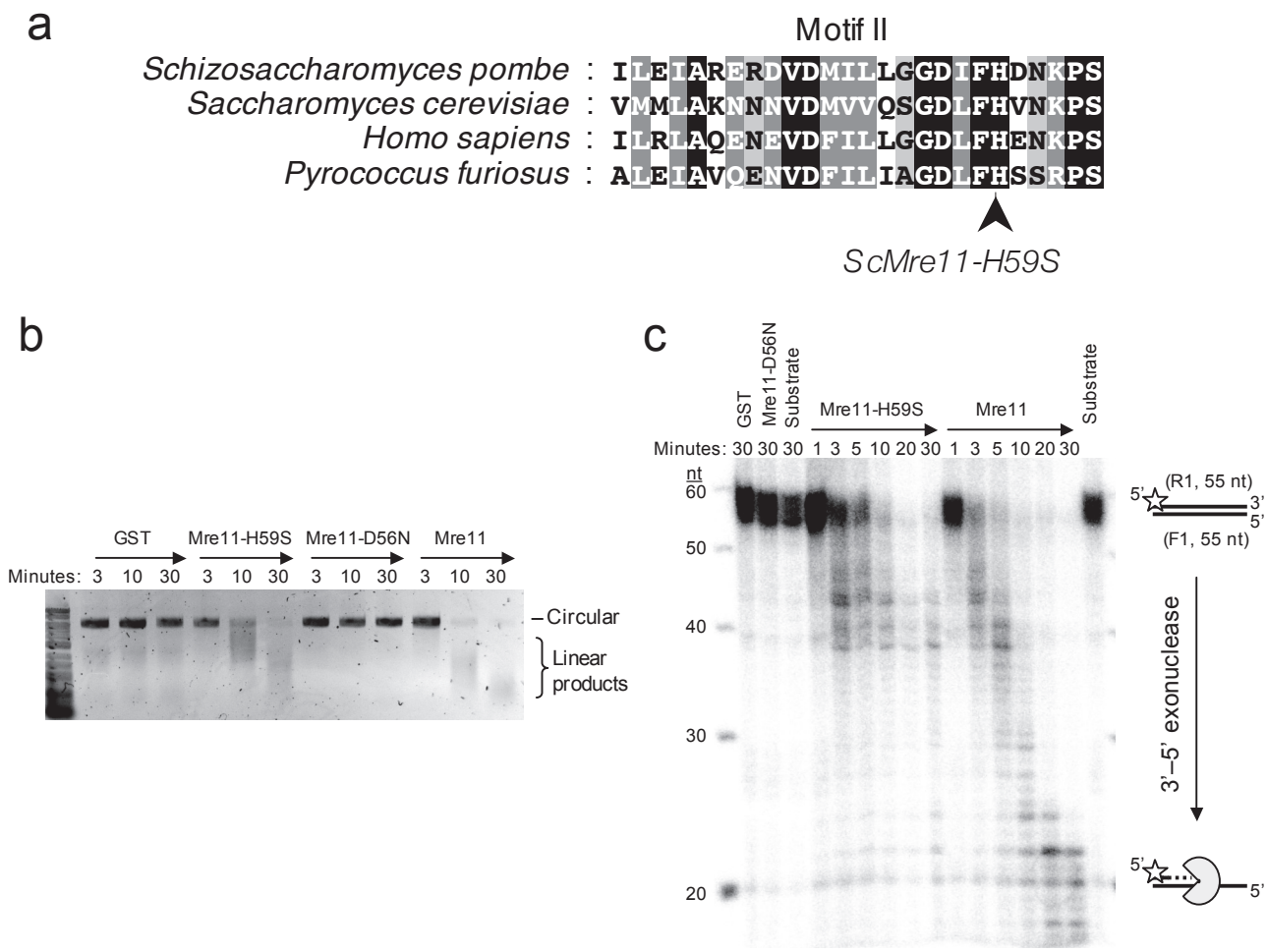

Figure S2. In vitro nuclease activity of Mre11 and Mre11-H59S.
a, Protein sequence alignment of Mre11 nuclease motif II in various species. The conserved *S.cerevisiae* histidine residue 59 mutated to serine in this study is indicated. Identical (black), conservative (dark grey), and semi-conservative (light grey) residues are indicated. **b,** ssDNA endonuclease activity. Circular single-stranded M13mp18 (0.05 pmoles; NEB) was incubated in 25 mM MOPS pH 7.0 / 60 mM KCl / 0.2 % Triton / 2 mM DTT / 5 mM MnCl2 at 37 ℃ for the indicated length of time with ~0.13 pmoles recombinant protein (GST only, GST-Mre11-H59S, GST-Mre11-D56N or GST-Mre11) overexpressed and prepared from yeast lysates of strain JEL1 (mre11Δ) bearing derivatives of plasmid pEGKT-MRE11[10]. Reactions were stopped by adding SDS to 0.3 % and Proteinase K to 0.5 mg/ml, and separated through 1 % agarose in 1x TAE stained with ethidium bromide. **c,** dsDNA 3'-5' exonuclease assay. A 55 bp dsDNA (2.8 pmol; 5'-labelled oligonucleotide R1: GTCTGTAGCACTGTGTAACACAGGCCAGATCCCATGCTGTCCTACGTGCCAGGTC annealed to its unlabelled reverse complement, F1) was incubated at 37 ℃ for the indicated length of time with ~0.13 pmoles of recombinant protein prepared as described in (b). Reactions were stopped as in (b), denatured by boiling with 2 volumes of loading dye (90 % formamide/ 10 mM EDTA / 0.01 % xylene cyanol / 0.005 % bromophenol blue), separated through 6 M urea / 12 % polyacrylamide in 1x TBE and imaged using a phosphor screen (Fuji). Cartoon depicts the exonuclease reaction being measured. Mre11-H59S exonuclease is less processive compared to wild-type Mre11.

Reference:

10. Moreau, S., Ferguson, J. R. & Symington, L. S. The nuclease activity of Mre11 is required for meiosis but not for mating type switching, end joining, or telomere maintenance. *Mol Cell Biol* **19,** 556-566 (1999).

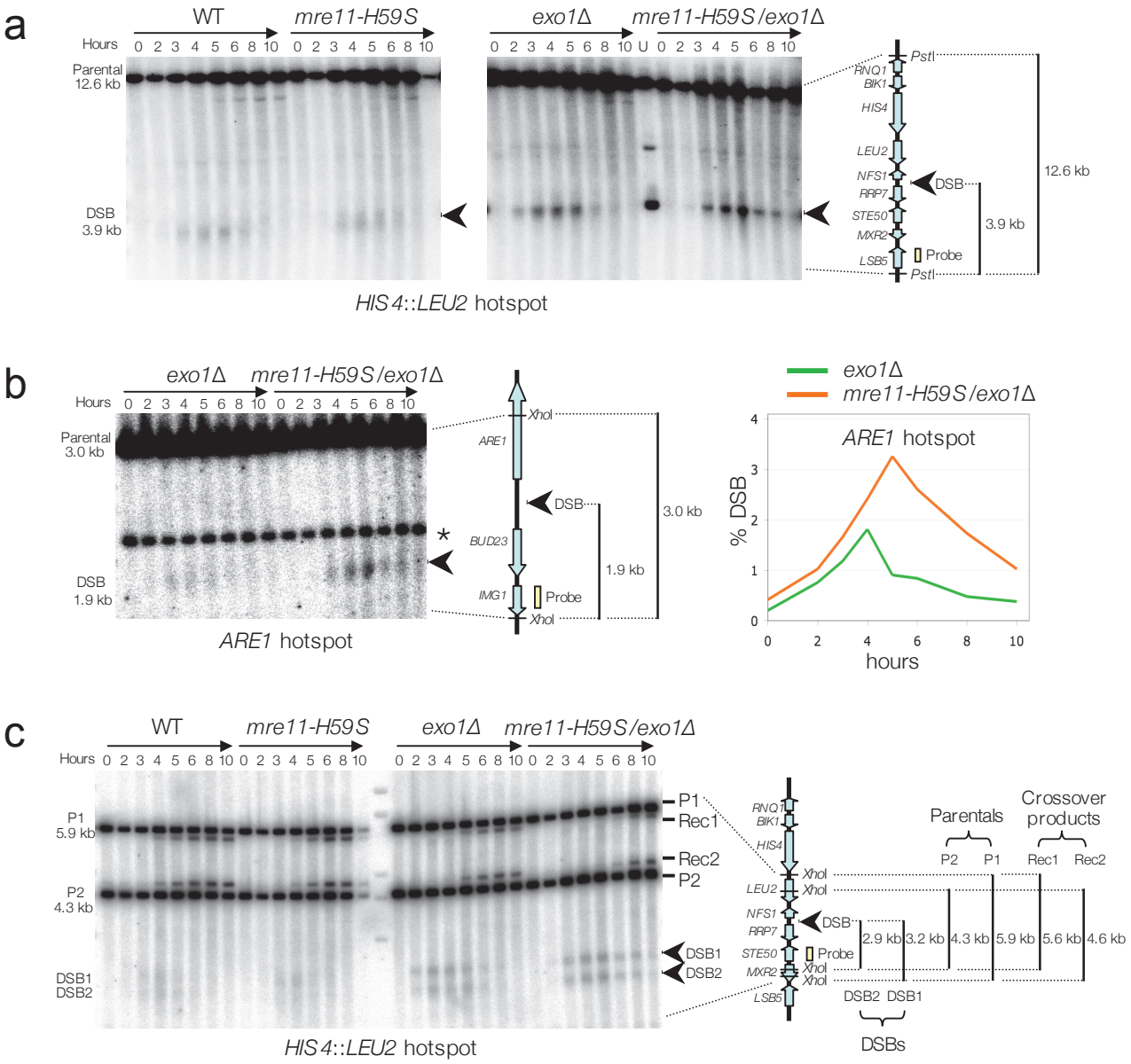

Figure S3. Southern blotting assays of meiotic DNA

Cartoons show restriction maps of relevant genomic regions. Cyan-coloured arrows indicate open reading frames. For all blots, DSB and crossover signals (expressed as a % of lane signal minus background) were quantified using Image Gauge software (Fuji). **a,** Detection of Spo11-DSBs at *HIS4*::*LEU2* recombination hotspot[29]. Genomic DNA isolated at the indicated times from synchronous meiotic timecourses of the indicated strains was digested with *Pst*I and separated through 0.7 % agarose in 1x TAE, blotted under vacuum to nylon membrane (Bio-Rad) in 0.5 M NaOH/1.5 M NaCl, and hybridised with a ^{32}P-labelled probe for the *LSB5* gene using standard conditions. (U, unresected control DNA from *sae2*Δ cells). **b,** Detection of Spo11-DSBs at *ARE1* recombination hotspot. As for (a), but DNA was digested with *Xho*I and separated through 0.6 % agarose in 1x TBE, and hybridised with a ^{32}P-labelled probe for the *IMG1* gene. **c**, Detection of crossover recombinants at *HIS4*::*LEU2* recombination hotspot[29]. As for (b), but DNA was hybridised with a ^{32}P-labelled probe for the *STE50* gene.

Reference:

29. Hunter, N. & Kleckner, N. The single-end invasion: an asymmetric intermediate at the double-strand break to double-holliday junction transition of meiotic recombination. *Cell* **106,** 59-70 (2001).

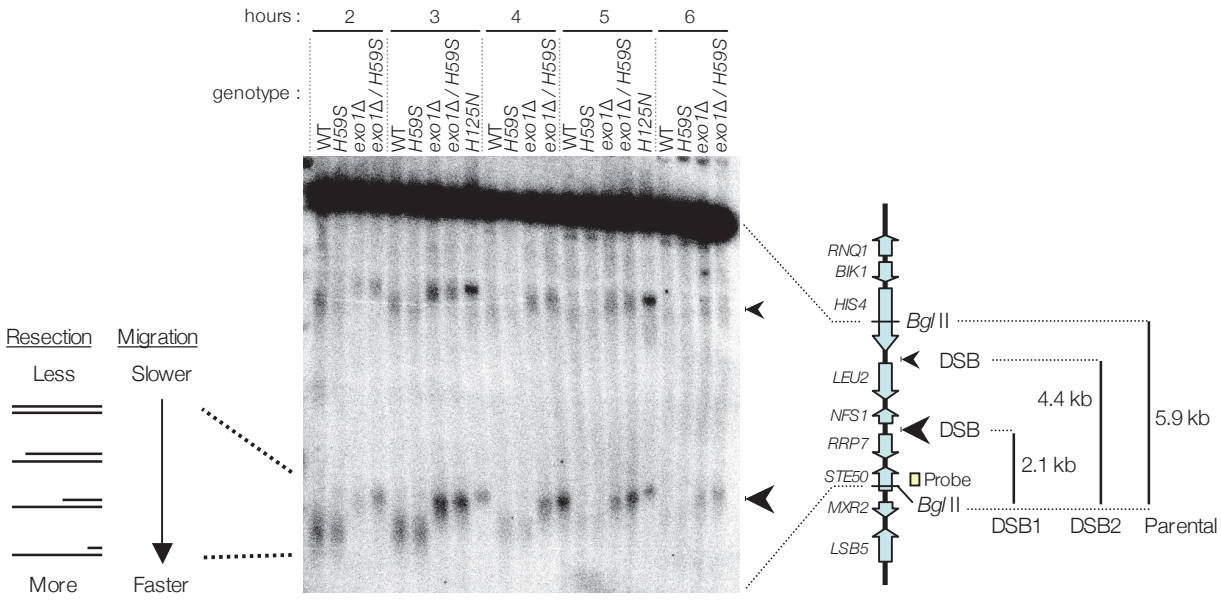

Figure S4. Detailed comparison of resection at *HIS4*::*LEU2* DSB hotspot in *mre11-H59S*

Genomic DNA isolated at the indicated times from synchronous meiotic timecourses of the indicated strains was digested with *Bgl*II and separated through 0.9 % agarose in 1x TAE, blotted under vacuum to nylon membrane (Bio-Rad) in 0.5 M NaOH/1.5 M NaCl, and hybridised with a ^{32}P-labelled probe for the *STE50* gene using standard conditions. DSBs were detected using an FLA5100 scanner and Image Gauge software (Fuji). Diagram on the left describes the relationship between the extent of resection and the rate of migration of the DSB fragments. Cartoon on the right depicts a map of *HIS4*::*LEU2* genomic region. Cyan-coloured arrows indicate open reading frames. *Bgl*II sites, probe (yellow box), and position of major and minor DSBs sites are indicated. At all timepoints, WT and *mre11-H59S* display very similar migration of DSB fragments, indicating very similar total resection profiles. Migration/resection is significantly reduced in *exo1*Δ, and reduced further in *exo1*Δ/ *mre11-H59S* double mutant, where DSB fragments migrate closer to that observed in *mre11-H125N* (where Spo11 protein is not removed and no ssDNA resection occurs).

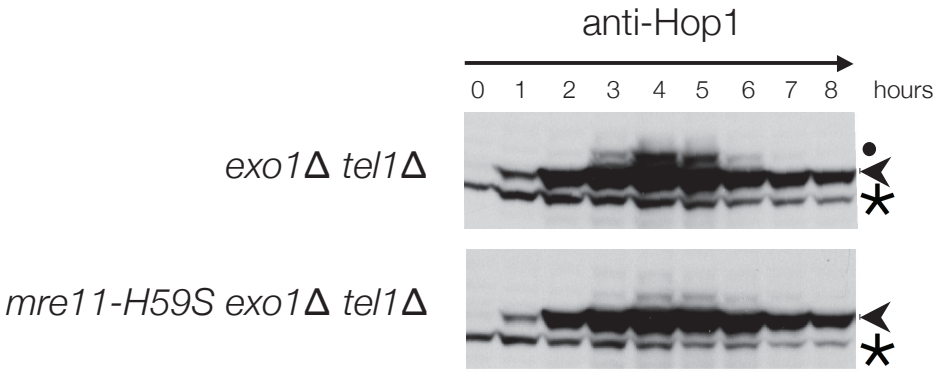

Figure S5. Tel1-independent Hop1 phosphorylation

Whole cell lysates were prepared at the indicated times from synchronous meiotic timecourses of the indicated strains, separated by 7.5 % SDS-PAGE, blotted to PVDF membrane and incubated with anti-Hop1 serum. Hop1 phosphorylation (dots) is reduced in *mre11-H59S*/e*xo1Δtel1Δ* compared to *exo1Δtel1Δ* indicating that in *exo1Δ* cells, Tel1-independent (Mec1) signalling requires the exonuclease activity of Mre11. Arrowhead is unmodified Hop1, asterisk is a cross-reacting band.

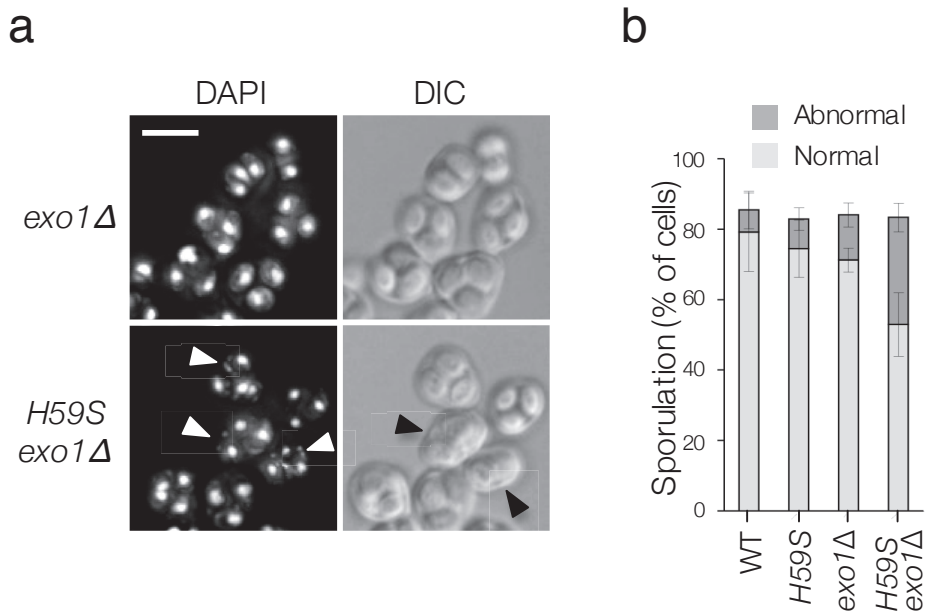

Figure S6. Frequency of abnormal tetrad formation is increased in *mre11-H59S/exo1*Δ

a, After 24 hours in sporulation conditions, the indicated strains were fixed with methanol and incubated with DAPI to stain DNA material. Abnormal sporulation (solid arrowheads) and fragmented chromosomes (open arrowheads) in *mre11-H59S/exo1*Δ are indicated. Scale bar is 5 μm. **b,** Chart shows sporulation frequencies as mean values ± s.d.

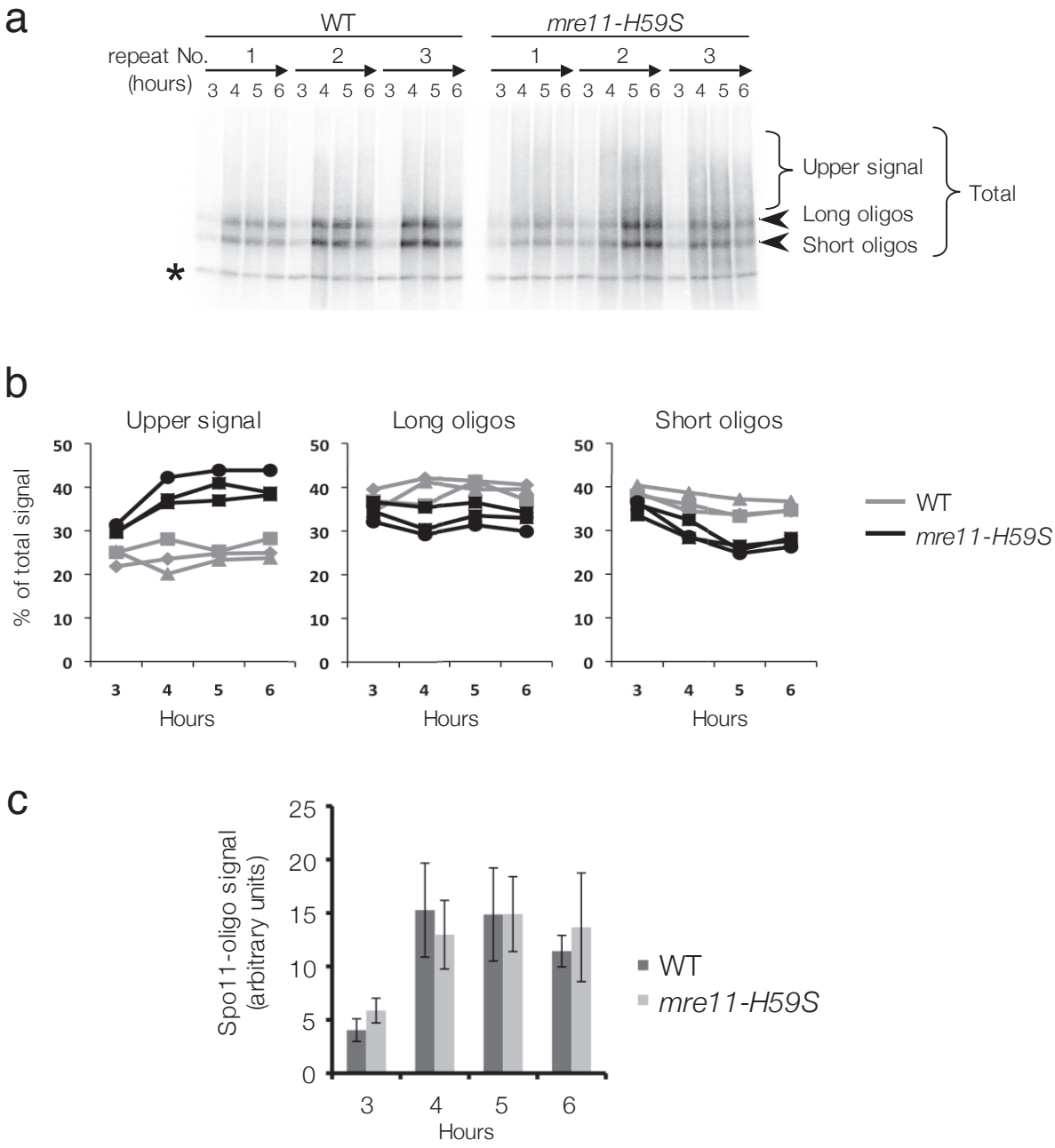

Figure S7. Identical timing of formation, but altered distribution, of Spo11-oligo complexes in WT and *mre11-H59S*

a, Spo11-oligo detection in wildtype (WT) and *mre11-H59S* during meiosis. Cultures were analysed in triplicate (1, 2 and 3), protein extracts prepared at the indicated times, and immunoprecipitated 3′-end labelled Spo11-complexes were fractionated by SDS-PAGE (see Methods). Asterisk marks an unrelated labeling artifact. **b,** Quantification of the proportion of signal present in the upper, long and short oligo species as a percentage of the total signal for the triplicate experiments shown in (a). **c,** Quantification of the total (upper+long+short) signal in (a). Quantifications were performed using ImageGauge software (Fuji). Bars in (c) show mean +/- S.D. No difference in the timing of total Spo11-oligo formation was observed between WT and *mre11-H59S*, whereas the distribution of molecules was reproducibly shifted towards longer molecules in *mre11-H59S*.

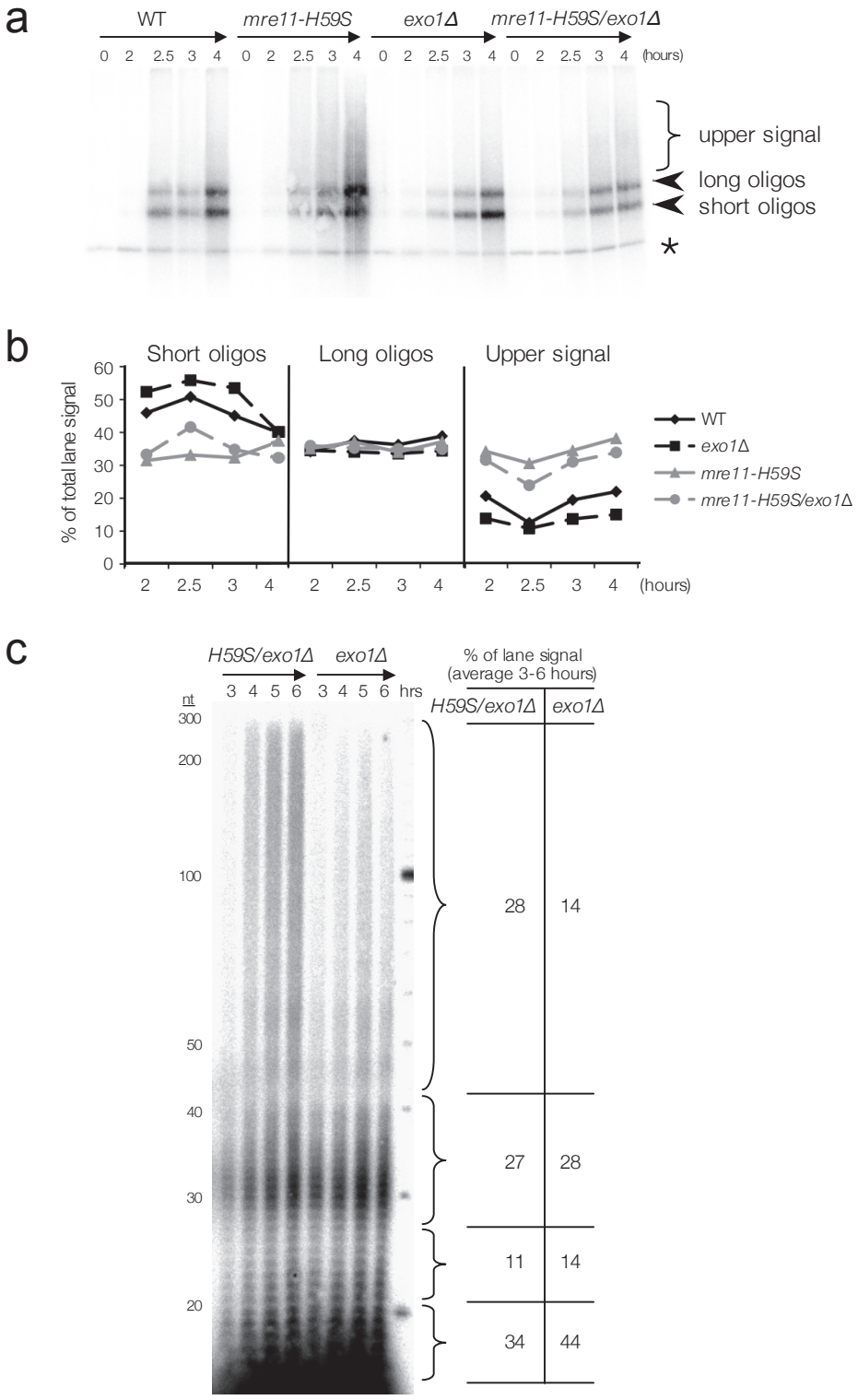

Figure S8. Altered distribution of Spo11-oligo length is independent of Exo1

a, Spo11-oligo detection in wildtype (WT), *mre11-H59S*, *exo1*Δ and *mre11-H59S/exo1*Δ during meiosis. Cell extracts were prepared at the indicated times and following 3'–end-labelling, Spo11-complexes were fractionated by SDS-PAGE. Asterisk marks an unrelated labeling artifact. **b,** Quantification of the percentage of: upper signal, long oligos, and short oligos (from a) was performed using ImageGauge software (Fuji). **c,** Nucleotide-resolution distribution of total deproteinised Spo11-oligonucleotides in *exo1*Δ and *mre11-H59S/exo1*Δ cells. Following 3'-end-labelling, Spo11-oligos were incubated with Proteinase K and fractionated by denaturing PAGE (see Methods for further details). The *mre11-H59S* mutation increases the abundance of Spo11-oligo signals 41-300 nt in length – and the effect is independent of Exo1.

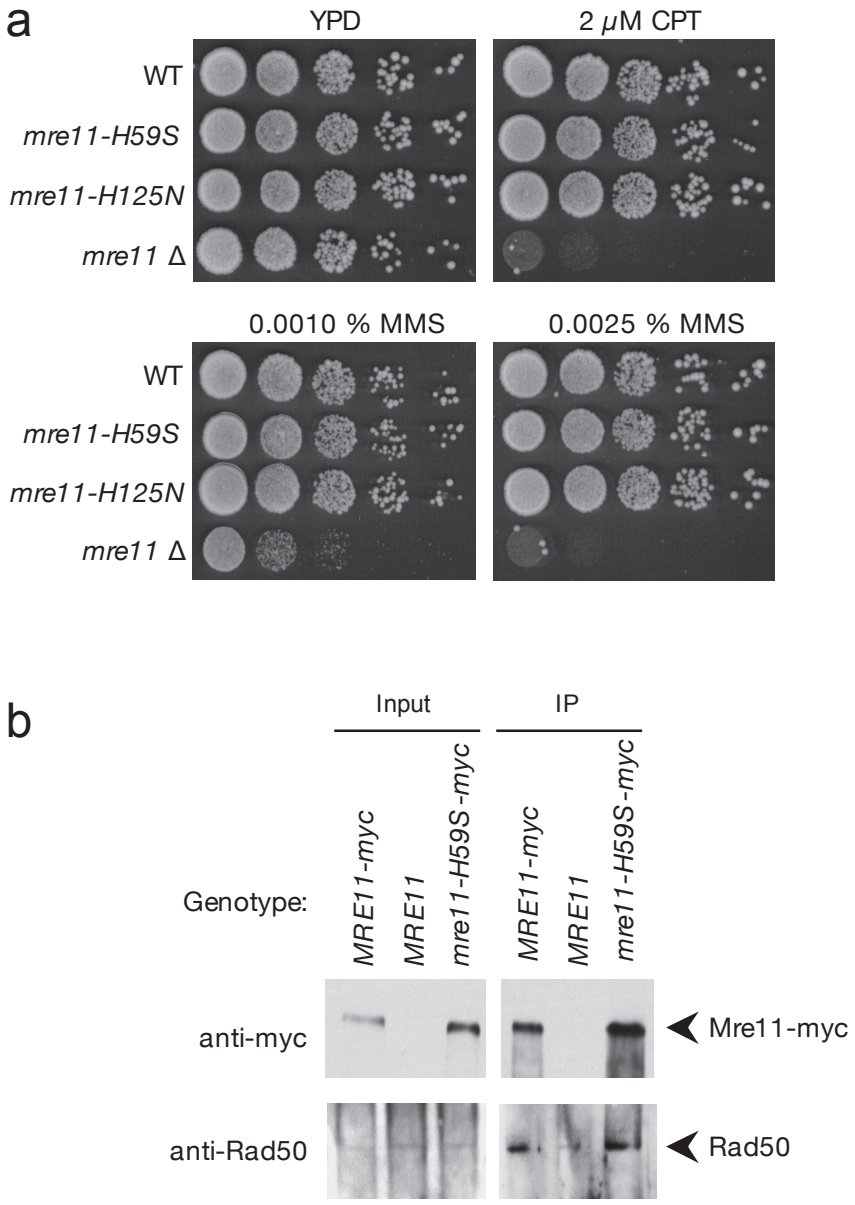

Figure S9. Mre11-complex formation in *mre11-H59S*

a, Ten-fold serial dilutions of the indicated strains were spotted onto solid media containing the indicated compounds and incubated for 2 days at 30°C. Like *mre11-H125N* (which is known to retain Mre11-complex formation[32]), *mre11-H59S* is not sensitive to low doses of DNA damage (CPT, camptothecin; MMS, methyl methanesulphonate). In addition, both mutants are far less sensitive compared to *mre11*Δ, strongly suggesting that other Mre11-complex functions are retained. **b,** Co-immunoprecipitation of Mre11 and Rad50. Protein extracts were prepared in 140 mm NaCl buffer from cells of the indicated genotype, immunoprecipitated (IP) with an anti-myc antibody (mouse monoclonal; 9E10 sc-40) and the western blot was probed with anti-myc (rabbit polyclonal; A14 sc-789) and anti-Rad50 antibody (a gift from J. Petrini).

Reference:

32. Krogh, Berit O, Bertrand Llorente, Alicia Lam, and Lorraine S Symington. "Mutations in Mre11 Phosphoesterase Motif I That Impair *Saccharomyces Cerevisiae* Mre11-Rad50-Xrs2 Complex Stability in Addition to Nuclease Activity." *Genetics* **171**, 1561-70 (2005)

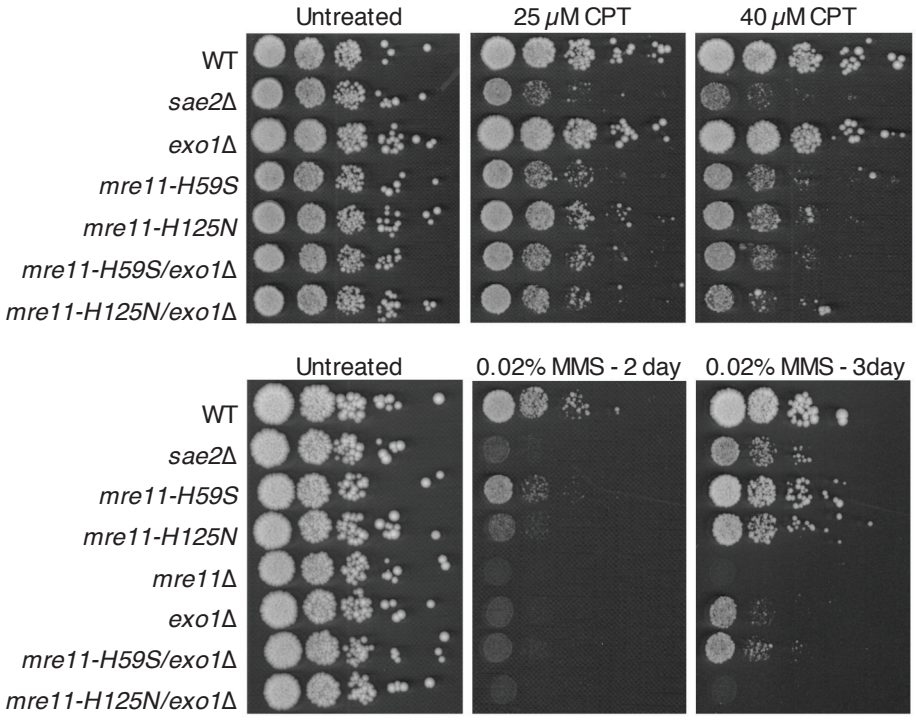

Figure S10. DNA damage sensitivity of *mre11* nuclease mutants in combination with *exo1*Δ

Ten-fold serial dilutions of the indicated strains were spotted onto solid media containing the indicated compounds and incubated for 2 or 3 days at 30°C (MMS, methyl methanesulphonate ; CPT, camptothecin). The nuclease mutants, *mre11-H59S* and *mre11-H125N* are slightly less sensitive to DNA damage than mutation of the accessory factor Sae2 (similar to human CtIP[33]). Combining *mre11-H59S* with a deletion of *EXO1* did not further sensitise cells to MMS, whereas *mre11-H125N/exo1*Δ was more sensitive than was either single mutant. This is consistent with Mre11 endonuclease activity (which is still present in *mre11-H59S*) permitting alternative exonuclease processing by the Sgs1-Dna2 complex[2,4,5]. This result, which is contrary to the synergistic effects seen in meiosis, is in fact expected because the Sgs1-Dna2 backup resection pathway does not function efficiently in meiosis[19,21]. No further sensitivity to camptothecin was observed in either double mutant consistent with factors other than Exo1 functioning to resolve topoisomerase I lesions (e.g. Tdp1).

References:

2. Mimitou, E. P. & Symington, L. S. Sae2, Exo1 and Sgs1 collaborate in DNA double-strand break processing. *Nature* **455,** 770-774 (2008).
4. Zhu, Z., Chung, W. H., Shim, E. Y., Lee, S. E. & Ira, G. Sgs1 helicase and two nucleases Dna2 and Exo1 resect DNA double-strand break ends. *Cell* **134,** 981-994 (2008).
5. Mimitou, E. P. & Symington, L. S. Ku prevents Exo1 and Sgs1-dependent resection of DNA ends in the absence of a functional MRX complex or Sae2. *EMBO J* **29,** 3358-3369 (2010).
19. Manfrini, N., Guerini, I., Citterio, A., Lucchini, G. & Longhese, M. P. Processing of meiotic DNA double-strand breaks requires cyclin-dependent kinase and multiple nucleases. *J Biol Chem* **285,** 11628-11637 (2010).
21. Zakharyevich, K., Ma, Y., Tang, S., Hwang, P. Y., *et al*. Temporally and Biochemically Distinct Activities of Exo1 during Meiosis: Double-Strand Break Resection and Resolution of Double Holliday Junctions. *Mol Cell* **40,** 1001-1015 (2010).
33. Sartori, A. A., Lukas, C., Coates, J., Mistrik, M., *et al*. Human CtIP promotes DNA end resection. *Nature* **450,** 509-514 (2007).